Numerical Approximation of Highly Oscillatory Integrals

Sheehan Olver

Trinity Hall

University of Cambridge

14 June 2008

This dissertation is submitted for the degree of Doctor of Philosophy

Abstract

The purpose of this thesis is the numerical integration of highly oscillatory functions, over both univariate and multivariate domains. Oscillatory integrals have many applications, including solving oscillatory differential equations and acoustics. Such integrals have an unwarranted reputation for being difficult to compute. We will demonstrate that high oscillation is in fact beneficial: the methods discussed improve with accuracy as the frequency of oscillations increases. The asymptotic expansion will provide a point of departure, allowing us to prove that other, convergent methods have the same asymptotic behaviour, up to arbitrarily high order. This includes Filon-type methods, which require moments and Levin-type methods, which do not require moments but are typically less accurate and are not available in certain situations. By combining these two methods, we will obtain a Moment-free Filon-type method for the case where the integral has a stationary point.

Though we initially focus on the exponential oscillator, we also demonstrate the effectiveness of these methods for other oscillators such as the Bessel and Airy functions. The methods are also applicable in certain cases where the integral is badly behaved; such as integrating over an infinite interval or when the integrand has an infinite number of oscillations. Finally we present a result that combines the asymptotic expansion with a least squares system, which appears to converge to the exact solution whilst retaining the asymptotic decay.

Declaration

This dissertation is the result of my own work and includes nothing which is the outcome of work done in collaboration except where specifically indicated in the text.

Sheehan Olver

Preface

After three years, I am pleased to have completed writing this thesis. I have found the topic of highly oscillatory quadrature to be incredibly fascinating, and I hope I have successfully relayed some of the intriguing phenomena of this area within the pages of this thesis.

I owe a great deal of thanks to my PhD supervisor, Arieh Iserles. He suggested the problem of oscillatory quadrature as a research topic, and has provided invaluable guidance throughout my time in Cambridge. It has been a pleasure to work alongside everyone in the numerical analysis group at Cambridge. In particular, I wish to express my appreciation to my office mates Alex Benton and Tanya Shingel, with whom I have had many stimulating (and distracting) conversations. The other members of the numerical analysis group—Ben Adcock, Brad Baxter, Anders Hansen, Marianna Khanamiryan, Mike Powell, Malcolm Sabin and Alexi Shadrin—have also been extraordinarily helpful. I would also like to thank everyone with whom I have collaborated and discussed my research with; including Chris Budd, Alfredo Deaño, Daan Huybrechs, David Levin and Nick Trefethen. Nick read through the first few chapters of this thesis, and provided extremely helpful comments and suggestions.

All of the members of my family have been very supportive, especially my fiancée Laurel Wooten. I had many interesting discussions on highly oscillatory quadrature with my parents, Peter Olver and Chehrzad Shakiban, and my grandfather, Frank Olver. I also cannot thank them enough for their advise on applying to Cambridge in the first place.

Last, but certainly not least, I thank the Gates Cambridge Trust, which funded the first three years of my PhD, and St John's College, Oxford, where I have spent the past two months completing my thesis while starting as a junior research fellow.

Oxford, November 2007
Sheehan Olver

Table of Contents

Introduction

In its most general form, we wish to find efficient numerical approximations for integrals of the form

$$I[f] = \int_\Omega f_\omega(x)\,\mathrm{d}V,$$

where f_ω is a function that oscillates rapidly, and the parameter ω determines the rate of oscillations. In practice, we separate the integral into a nonoscillatory function multiplied by an oscillatory kernel. In applications, the kernel can often be expressed in the form of an imaginary exponential function:

$$I[f] = \int_\Omega f(\boldsymbol{x})\,\mathrm{e}^{\mathrm{i}\omega g(\boldsymbol{x})}\,\mathrm{d}V,$$

where f and g are nonoscillatory functions, the frequency of oscillations ω is large and Ω is some piecewise smooth domain. By taking the real and imaginary parts of this integral, we obtain integrals with trigonometric kernels:

$$\mathrm{Re}\,I[f] = \int_\Omega f(\boldsymbol{x})\cos\omega g(\boldsymbol{x})\,\mathrm{d}V \qquad \text{and} \qquad \mathrm{Im}\,I[f] = \int_\Omega f(\boldsymbol{x})\sin\omega g(\boldsymbol{x})\,\mathrm{d}V.$$

If the integral cannot be written in this form, then for univariate integrals it typically can be expressed as

$$I[f] = \int_a^b \boldsymbol{f}(x)^\top \boldsymbol{y}_\omega(x)\,\mathrm{d}x,$$

where $\boldsymbol{f}$ is nonoscillatory and $\boldsymbol{y}_\omega$ is an oscillatory kernel which satisfies a differential equation. The aim of this thesis is the numerical approximation of such oscillatory integrals. Perhaps surprisingly, high oscillations make numerical quadrature easier: we will develop methods which actually improve with accuracy as the frequency ω increases.

Highly oscillatory integrals play a valuable role in applications. Using the *modified Magnus expansion* [**44**], highly oscillatory differential equations of the form $y'' + g(t)y = 0$, where $g(t) \to \infty$ while the derivatives of g are moderate, can be expressed in terms of an infinite sum of highly oscillatory integrals. Differential equations of this form appear in many areas, including special functions, e.g., the Airy function. From the field of acoustics, the boundary element method requires the evaluation of highly oscillatory integrals, in order to solve integral equations with oscillatory kernels [**39**]. *Modified Fourier series* use highly oscillatory integrals to obtain a function approximation scheme that converges faster than the standard Fourier series [**51**]. Other applications include fluid dynamics, image analysis and more. These applications are presented in Chapter 1.

We present an overview of prior research in Chapter 2. We begin with a quick review of nonoscillatory integration, and explain the reasons why traditional quadrature techniques are not effective in the presence of high oscillations. An enormous amount of research has been conducted on the asymptotics of such integrals, thus we present an overview of *asymptotic expansions* and the *methods of stationary phase and steepest descent*. We also investigate existing numerical quadrature schemes, in particular the *Filon method* and *Levin collocation method*. This thesis is mostly concerned with generalizing and improving these two methods.

With the groundwork in place, we consider in depth the univariate irregular exponential oscillator without *stationary points*—points where $g'(x)$ vanishes—in Chapter 3. We place the Filon method and Levin collocation method within an asymptotic framework, and generalize the two methods to obtain higher order asymptotic approximations. We also develop the *asymptotic basis*, where the terms of the asymptotic expansion are used in a collocation system. Finally, we find simple error bounds for the Filon method.

When the exponential oscillator contains stationary points the asymptotics of the integral is altered. As a result, Levin-type methods do not approximate such integrals accurately. Furthermore, complicated oscillators can make the construction of Filon-type methods impossible, though in some simple but important cases we are still able to find Filon-type methods. Thus to make a practical quadrature scheme, we will combine these two methods to obtain a *Moment-free Filon-type method* in Chapter 4. In the process, we also develop a new asymptotic expansion for such integrals, which is related to the method of stationary phase.

Having investigated these methods thoroughly for univariate integrals, we turn our attention to the more difficult problem of multivariate integrals in Chapter 5. A generalization of Filon-type methods to multivariate integrals is straightforward, and its asymptotic behaviour follows immediately from the asymptotic results of Chapter 2. Unfortunately, the domains and oscillators for which a Filon-type method is derivable are extremely limited. Thus we generalize Levin-type methods, which are applicable for integrals over complicated domains, and oscillators which satisfy a *nonresonance condition*: a multivariate version of requiring the absence of stationary points. Developing methods for when this condition is not satisfied is the topic of the last two sections of this chapter, including the initial development of a Moment-free Filon-type method for oscillatory integrals in which ∇g vanishes.

The Levin collocation method was generalized in [**62**] to oscillatory integrals with vector-valued kernels. In Chapter 6, we apply the new results from Chapter 3 to obtain Levin-type methods for such integrals. We first construct new asymptotic tools so that we can determine the asymptotic order of the approximation scheme. This will lead us to two Levin-type methods: the first collapses the vector-valued system to one collocation system, the second is a direct generalization of the Levin collocation method of [**62**]. Finally, we demonstrate that a vector-valued asymptotic basis can be constructed in order to obtain a high asymptotic order approximation.

We wrap up some loose ends for univariate quadrature in Chapter 7, where methods

are developed for oscillatory integrals which contain some sort of singularity. This includes integrals over an unbounded region, and integrals which contain an infinite number of oscillations within the integration interval. The methods used to tackle these problems will work for both exponential oscillators and integrals involving the Airy function. We can also use the methods to compute certain special functions from their integral representations, including the exponential, sine and cosine integrals, as well as the Airy function.

In Chapters 3, 5 and 6, the asymptotic basis allows us to capture the behaviour of the asymptotic expansion, whilst significantly improving the error. Indeed, it is observed that such a basis results in a quadrature scheme that appears to converge exponentially fast to the exact value of the integral. The motivation of Chapter 8 is to put this observation onto a firm theoretical grounding. We replace collocation with least squares, and are then able to compute the error of the approximation exactly, though convergence is not proved. We also utilize this method for solving oscillatory differential equations, using the Airy equation as a simple example.

Notation

Variables

x, y, z, t	Univariate integration dummy variables
i, j, k, ℓ	Summation dummy variables
$\boldsymbol{x}$	Multivariate integration dummy vector variable
d	Dimension
$\mathcal{G}$	Lie group
$\mathfrak{g}$	Lie algebra

Functions

$w(x)$	Integration weight function
ψ_k	Interpolation or collocation basis
$\boldsymbol{\psi}_k$	Vector-valued collocation basis
σ_k	Asymptotic expansion term
$\boldsymbol{\sigma}_k$	Multivariate asymptotic expansion term
$\boldsymbol{y}_\omega, \boldsymbol{y}$	Vector-valued oscillatory kernel

Spaces

$\mathbb{R}$	Space of real numbers
$\mathbb{N}$	Space of nonnegative integers
$L_p[a, b]$	Space of measurable functions f such that

$$\left(\int_a^b |f(x)|^p \, \mathrm{d}x \right)^{1/p} < \infty$$

$L_\infty[a, b]$	Space of measurable functions f such that

$$\sup_{a \le x \le b} |f(x)| < \infty$$

L_p	$L_p[a, b]$ where a and b are implied by context (and possibly infinite)
$C^r[a, b]$	Space of r-times differentiable functions

$C^\infty[a,b]$ Space of smooth functions

Products and norms

$\langle f,g\rangle$	Function inner product
$\langle f,g\rangle_2$	L_2 inner product $\int_a^b f\bar{g}\,\mathrm{d}x$
$[A,B]$	Lie group commutator
$\|f\|$	Function norm
$\|f\|_p$	L_p function norm: $\left(\int_a^b |f(x)|^p\,\mathrm{d}x\right)^{1/p}$
$\|f\|_\infty$	L_∞ function norm: $\sup_{a\le x\le b}|f(x)|$

Multidimensional domains

Ω	Multidimensional domain in $\mathbb{R}^d$
$\partial\Omega$	Boundary of Ω
Z_ℓ	Piecewise smooth component of $\partial\Omega$
T_ℓ	Parameterization map of Z_ℓ
Ω_ℓ	Domain in $\mathbb{R}^{d-1}$ mapped onto Z_ℓ by T_ℓ
$\boldsymbol{n}$	Vector orthogonal to $\partial\Omega$
S_d	d-dimensional simplex
H	Quarter disc
U	Half disc

Complex plane

$\bar{g}$	Complex conjugate
Re	Real part
Im	Imaginary part
ζ_k	Complex contour

Differential forms

$\mathcal{D}^{\boldsymbol{0}}$	The identity operator
$\mathcal{D}^m$	The mth derivative $\frac{\mathrm{d}^m}{\mathrm{d}^m x}$, for nonnegative integers $m\in\mathbb{N}$
$\mathcal{D}^{\boldsymbol{m}}$	The partial derivative $\frac{\partial^{\|\boldsymbol{m}\|_1}}{\partial x_1^{m_1}...\partial x_d^{m_d}}$ for $\boldsymbol{m}=(m_1,\cdots,m_d)^\top\in\mathbb{N}^d$
$\wedge$	Wedge product
$\mathrm{d}V$	Volume differential $\mathrm{d}\boldsymbol{x}=\mathrm{d}x_1\,\mathrm{d}x_2\cdots\mathrm{d}x_d=\mathrm{d}x_1\wedge\mathrm{d}x_2\wedge\cdots\wedge\mathrm{d}x_d$

$\mathrm{d}\boldsymbol{s}$ d-dimensional surface differential

$$\begin{pmatrix} \mathrm{d}x_2 \wedge \cdots \wedge \mathrm{d}x_d \\ -\mathrm{d}x_1 \wedge \mathrm{d}x_3 \wedge \cdots \wedge \mathrm{d}x_d \\ \vdots \\ (-1)^{d-1}\, \mathrm{d}x_1 \wedge \cdots \wedge \mathrm{d}x_{d-1} \end{pmatrix}$$

J_T Jacobian determinant of a map T

$J_T^{i_1,\dots,i_d}$ Jacobian determinant of a map T with respect to the indices $i_1, \dots, i_d$.

$\boldsymbol{J}_T^d(\boldsymbol{x})$ Vector of Jacobian determinants

$$\begin{pmatrix} J_T^{2,\dots,d}(\boldsymbol{x}) \\ -J_T^{1,3,\dots,d}(\boldsymbol{x}) \\ \vdots \\ (-1)^{d-1}J_T^{1,\dots,d-1}(\boldsymbol{x}) \end{pmatrix}$$

∇ Gradient operator

$\nabla\cdot$ Divergence operator

Δ Laplacian operator $\nabla^2 = \nabla \cdot \nabla$

Special functions

Ai, Bi Airy functions

J_ν, Y_ν, I_ν Bessel functions of order ν

$H_\nu^{(1)}, H_\nu^{(2)}$ Hankel functions of order ν

erf Error function

Γ Incomplete Gamma function

si Sine integral function

ci Cosine integral function

E_n Exponential integral function

$_pF_q$ Hypergeometric function

P_k kth Legendre polynomial

T_k kth Chebyshev polynomial

Vectors and matrices

$\sum \boldsymbol{m}$ The sum $\sum_{k=1}^d m_k$ for the vector $\boldsymbol{m}^\top = (m_1, \cdots, m_d)$

$\det A$ Determinant of the square matrix A

$\|A\|$ Norm of the matrix A

$(a_{ij})_{p \times q}$	The $p \times q$ matrix whose entry in the ith row and jth column is a_{ij}
I_p	The $p \times p$ identity matrix
I	I_p, where p is implied by context
$\mathbf{1}_{p \times q}$	The $p \times q$ matrix whose entries are all one: $(1)_{p \times q}$
$\mathbf{1}$	The matrix $\mathbf{1}_{p \times q}$, where p and q are implied by context
$\mathbf{1}^\top$	The row vector $\mathbf{1}_{1 \times q}$, where the dimension q is implied by context
$\lvert A \rvert$	For $A = (a_{ij})_{p \times q}$, the $p \times q$ matrix whose ijth entry is $\lvert a_{ij} \rvert$: $(\lvert a_{ij} \rvert)_{p \times q}$. Note the distinction between $\lvert A \rvert$, $\lVert A \rVert$ and $\det A$
A^{-1}	Matrix inverse
A^+	Matrix pseudoinverse

Asymptotics

$f \sim \sum_{k=0}^{\infty} \cdots$	Asymptotic expansion
$f(x) \sim g(x), x \to b$	f is asymptotically the same as g as x approaches b
$\mathcal{O}(\cdot)$	Big-O notation
$o(\cdot)$	Little-O notation
$\boldsymbol{\mathcal{O}}(\cdot)$	Function big-O notation: $f = \boldsymbol{\mathcal{O}}(g)$ if $\left\lVert f^{(k)} \right\rVert_\infty = \mathcal{O}(g)$ for $k = 0, 1, \dots$
$f \sim \mathcal{O}\!\left(\omega^{-s}\right)$	f has an asymptotic expansion whose first term decays like $\mathcal{O}\!\left(\omega^{-s}\right)$

Operators

$\mathcal{L}[v]$	Levin differential operator $v' + \mathrm{i}\omega g' v$
$\mathcal{L}[\boldsymbol{v}]$	Vector-valued Levin differential operator $\boldsymbol{v}' + A^\top \boldsymbol{v}$ or multivariate Levin differential operator $\nabla \cdot \boldsymbol{v} + \mathrm{i}\omega \nabla g \cdot \boldsymbol{v}$
$\mathcal{M}[y]$	Chung, Evans and Webster differential kernel operator
$\mathcal{M}^\star[z]$	Adjoint of $\mathcal{M}$
$Z[w, z]$	Bilinear concomitant
$\mathcal{P}[f]$	Vector of f applied to the nodes and multiplies of a collocation scheme

Oscillatory integrals

ω	Frequency of oscillations
f	Amplitude of oscillations
g	Oscillator

Ω	Domain of integration
a, b	Endpoints of integration interval
$I[f]$	Univariate oscillatory integral $\int_a^b f(x)\mathrm{e}^{\mathrm{i}\omega g(x)}\,\mathrm{d}x$
$I_g[f, \Omega]$	Multivariate oscillatory integral $\int_\Omega f(\boldsymbol{x})\mathrm{e}^{\mathrm{i}\omega g(\boldsymbol{x})}\,\mathrm{d}V$
$I[\boldsymbol{f}]$	Vector-valued kernel oscillatory integral $\int_a^b \boldsymbol{f}(x)^\top \boldsymbol{y}(x)\,\mathrm{d}x$
r	Order of stationary point
s	Asymptotic order of method

Oscillatory quadrature

$Q^F[f]$	Filon-type method
$Q_g^F[f, \Omega]$	Multivariate Filon-type method
$Q^L[f]$	Levin-type method
$Q_g^L[f, \Omega]$	Multivariate Levin-type method
$Q^B[f]$	Levin-type method with asymptotic basis
$\phi_{r,k}$	Moment-free Filon-type method basis
$\boldsymbol{\phi}_k$	Multivariate Moment-free Filon-type method basis

Chapter 1

Applications

Before delving into the details of approximating highly oscillatory integrals, we first motivate their utility by briefly describing some applications. We begin with the two applications that have reinvigorated the investigation of oscillatory quadrature: the modified Magnus expansion and acoustic integral equations. We begin with a description of the modified Magnus expansion in Section 1.1, which allows us to rewrite the solution to an oscillatory differential equation as an infinite sum of oscillatory integrals. Furthermore it has applications in geometric integration, as the approximation stays within the Lie group that the solution of the differential equation evolves in. Determining how an object scatters sound waves is accomplished via an integral equation with an oscillatory kernel. This naturally leads to the computation of oscillatory integrals, as described in Section 1.2.

Following these more recent applications, we review a couple of traditional applications. Many special functions have highly oscillatory integral representations, and in Section 1.3 we give an overview of several such functions. Finally, in Section 1.4 we look at function approximation with orthogonal series, which invariably have coefficients that are highly oscillatory integrals. We also see how oscillatory integrals play a role in spectral methods when such orthogonal series are used.

There are a plethora of other applications for oscillatory quadrature besides those discussed in this chapter. Indeed, wherever one finds waves—which are, of course, ubiquitous in physics—there is a good chance that oscillatory integrals require computation. These applications "...range from electromagnetics and nonlinear optics to fluid dynamics, plasma transport, computerized tomography, celestial mechanics, computation of Schrödinger spectra, Bose–Einstein condensates..." [45].

1.1. Modified Magnus expansion

The motivation behind the renewed interest by Iserles and Nørsett in approximating oscillatory integrals began due to new results in the field of geometric integration. Suppose we wish to solve the homogeneous matrix-valued linear ordinary differential equation

$$Y'(t) = A(t)Y(t), \qquad Y(0) = Y_0.$$

This has a solution of the form the form $Y(t) = \mathrm{e}^{M(t)}Y_0$, where M satisfies the differential

equation

$$M' = A - \frac{1}{2}[M, A] + \frac{1}{12}[M, [M, A]] - \frac{1}{720}[M, [M, [M, [M, A]]]] + \cdots, \qquad M(0) = 0, \quad (1.1.1)$$

cf. [46]. If the solution Y_0 lies in the Lie group $\mathcal{G}$ and the matrix $A(t)$ lies in the corresponding Lie algebra $\mathfrak{g}$ for all t, then Y evolves within $\mathcal{G}$. Numerically solving the differential equation for M, as opposed to the original differential equation for Y has the important property that the approximation preserves this group structure. Though $\mathcal{G}$ can be nonlinear, $\mathfrak{g}$ must be a linear space, and any numerical solver that utilizes only linear operations will remain within $\mathfrak{g}$. The Magnus expansion [69] gives us a solution to (1.1.1) in terms of only the matrix A:

$$\begin{aligned}
M(t) = {} & \int_0^t A(x)\,\mathrm{d}x - \frac{1}{2}\int_0^t \int_0^{x_1} [A(x_2), A(x_1)]\,\mathrm{d}x_2\,\mathrm{d}x_1 \\
& + \frac{1}{4}\int_0^t \int_0^{x_1} \int_0^{x_2} [[A(x_3), A(x_2)], A(x_1)]\,\mathrm{d}x_3\,\mathrm{d}x_2\,\mathrm{d}x_1 \qquad (1.1.2) \\
& + \frac{1}{12}\int_0^t \int_0^{x_1} \int_0^{x_1} [A(x_3), [A(x_2), A(x_1)]]\,\mathrm{d}x_3\,\mathrm{d}x_2\,\mathrm{d}x_1 + \cdots.
\end{aligned}$$

Truncating this sum and employing a suitable quadrature scheme for approximating the integrals gives us a powerful numerical method which preserves group structure [46].

We now turn our attention to highly oscillatory differential equations, where the matrix A has eigenvalues with large imaginary parts and nonpositive real parts. Our interest in the Magnus expansion stems not from its preservation of group structure, but rather another important property: the solution is written in terms of integrals. A great deal of cancellation occurs when integrating a highly oscillatory function, thus it stands to reason that the integral will be small in magnitude. Thus the modified Magnus expansion [43] consists of rewriting the original differential equation so that A itself encapsulates the oscillatory behaviour, resulting in the integrals in (1.1.2) becoming small in magnitude.

Suppose we have time stepped to t_n with step size h, to obtain an approximation $\boldsymbol{y}_n$ of the solution $\boldsymbol{y}(t_n)$. Define the function $\boldsymbol{v}$ so that

$$\boldsymbol{y}(t_n + \tau) = \mathrm{e}^{\tau \tilde{A}}\boldsymbol{v}(\tau),$$

where $\tilde{A} = A(t_n + \alpha h)$. Our approximation $\boldsymbol{y}_{n+1}$ of $\boldsymbol{y}(t_{n+1})$ would then be $\mathrm{e}^{h\tilde{A}}\boldsymbol{v}_1$, where $\boldsymbol{v}_1$ will be the approximation of $\boldsymbol{v}(h)$. We find that $\boldsymbol{v}$ satisfies the differential equation

$$\boldsymbol{v}' = B(\tau)\boldsymbol{v}, \qquad \boldsymbol{v}(0) = \boldsymbol{y}_n, \qquad \text{for} \qquad B(\tau) = \mathrm{e}^{-\tau \tilde{A}}\left[A(t_n + \tau) - \tilde{A}\right]\mathrm{e}^{\tau \tilde{A}}.$$

Because the imaginary parts of the eigenvalues of A are large, so are those of $\tilde{A}$, thus the exponentials within the definition of B are oscillatory functions. Thus the integrals in (1.1.2)—with B in place of A—are small, with higher dimensional integrals being even smaller in magnitude (this phenomenon will be explained in more detail in later chapters

of this thesis, though it follows from classical asymptotic theory). Furthermore, the more oscillatory the solution the faster the integrals decay. It is thus sensible to truncate this sum, and the accuracy of such a truncation amazingly *improves* as the frequency of oscillations increases. We are, however, left with the problem of approximating the resulting oscillatory integrals.

1.2. Acoustic integral equations

In the field of acoustics, the scattering of a sound wave off an object can be modelled by the solution to the Helmholtz equation over a domain Ω with a Dirichlet, Neumann or mixed boundary conditions, cf. [38]. In other words, we seek the solution to the equation

$$\Delta u(\boldsymbol{x}) + k^2 u(\boldsymbol{x}) = 0$$

with

$$u(\boldsymbol{x}) = f(\boldsymbol{x}), \qquad \boldsymbol{x} \in \partial\Omega_1 \qquad \text{and} \qquad \frac{\partial u}{\partial \boldsymbol{n}}(\boldsymbol{x}) = 0, \qquad \boldsymbol{x} \in \partial\Omega_2,$$

where $\partial\Omega = \partial\Omega_1 \cup \partial\Omega_2$. The solution to this partial differential equation can be written in terms of integral equations over the boundary of the domain. In certain cases, the problem can be reduced to solving integral equations of the form

$$\frac{\mathrm{i}}{4} \int_{\partial\Omega} H_0^{(1)}(k\, \|\boldsymbol{x} - \boldsymbol{y}\|)\, q(\boldsymbol{y})\, \mathrm{d}s_{\boldsymbol{y}} = u(\boldsymbol{x})$$

in $\mathbb{R}^2$, where H is the Hankel function [2], or

$$\frac{1}{4\pi} \int_{\partial\Omega} \frac{\mathrm{e}^{\mathrm{i}k\|\boldsymbol{x}-\boldsymbol{y}\|}}{\|\boldsymbol{x} - \boldsymbol{y}\|} q(\boldsymbol{y})\, \mathrm{d}s_{\boldsymbol{y}} = u(\boldsymbol{x})$$

in $\mathbb{R}^3$ [38].

Since the kernel of these integral equations are oscillatory, collocation and other Galerkin methods require solving oscillatory integrals, even when the basis itself is nonoscillatory. Furthermore, the frequency of oscillations is known, and thus we know for an incoming wave $u^i(\boldsymbol{x}) = u_s^i(\boldsymbol{x})\mathrm{e}^{\mathrm{i}k g^i(\boldsymbol{x})}$ that the solution has the form

$$q(\boldsymbol{x}) = q_s(\boldsymbol{x})\mathrm{e}^{\mathrm{i}k g^i(\boldsymbol{x})}, \qquad \boldsymbol{x} \in \partial\Omega,$$

where q_s is asymptotically a nonoscillatory function [15]. The knowledge of how the solution behaves asymptotically can be used in the construction of a collocation basis, giving us a hybrid high frequency boundary element method [42]. Suppose we approximate q_s by

$$q_c(\tau) = \sum c_k \psi_k(\tau),$$

3

where $\{\psi_k\}$ is a set of linearly independent basis functions. We determine the constants c_k by collocating at the points $\boldsymbol{x}_k = \kappa(t_k)$, where $\kappa : [0,1] \to \partial\Omega$ is a parameterization of the boundary. This requires solving integrals of the form (in two dimensions)

$$\frac{\mathrm{i}}{4} \int_0^1 H_0^{(1)}\big(k \, \|\kappa(t_n) - \kappa(\tau)\|\big) \, \mathrm{e}^{\mathrm{i}k\left[g^i(\kappa(\tau)) - g^i(\kappa(t_n))\right]} \, \|\nabla\kappa(\tau)\| \, \psi_k(\tau) \, \mathrm{d}\tau.$$

Hankel functions can be expressed asymptotically in terms of complex exponential, so at large frequencies this oscillatory integral behaves like an irregular Fourier oscillator. Thus being able to approximate oscillatory integrals allows us to derive an approximation to the solution of acoustic integral equations.

1.3. Special functions

Special functions play an extraordinarily important role in applied mathematics and physics, and how to compute such functions efficiently is an active area of research. Many special functions have integral representations that are oscillatory integrals. Some examples are:

- Airy functions

$$\mathrm{Ai}\,(x) = \frac{1}{\pi} \int_0^\infty \cos\left(\frac{t^3}{3} + xt\right) dt$$

- Bessel and Hankel functions

$$J_n(x) = \frac{1}{2\pi} \int_0^\pi \cos(nt - x\sin t)\, dt$$

$$Y_n(x) = \frac{1}{\pi} \int_0^\pi \sin(x\sin t - nt)\, dt - \frac{1}{\pi} \int_0^\infty \left[\mathrm{e}^{nt} + (-1)^n \mathrm{e}^{-nt}\right] \mathrm{e}^{-x\sinh t}\, dt$$

$$H_n^{(1)}(x) = J_n(x) + \mathrm{i}Y_n(x)$$

$$H_n^{(2)}(x) = J_n(x) - \mathrm{i}Y_n(x)$$

- Error function (for complex z)

$$\mathrm{erf}(z) = \frac{2}{\sqrt{\pi}} \int_0^z \mathrm{e}^{-t^2}\, dt$$

- Incomplete Gamma function (for complex z)

$$\Gamma(a, z) = \int_z^\infty t^{a-1} \mathrm{e}^{-t}\, dt$$

- Sine, cosine and exponential integrals

$$\mathrm{si}(x) = -\int_x^\infty \frac{\sin t}{t}\, dt$$

$$\mathrm{ci}(x) = -\int_x^\infty \frac{\cos t}{t}\, dt$$

$$\mathrm{E}_n(z) = \int_1^\infty \frac{\mathrm{e}^{-zt}}{t^n}\, dt$$

- Hypergeometric functions
- Basic hypergeometric functions

Basic hypergeometric functions are found in [**32**], all other functions are found in [**2**]. As described in more detail in Chapter 2, this is the application which existing research into approximating oscillatory functions has focused on most, especially with regards to asymptotics. The fact that each integral has a very specific form facilitates computation, particular when deforming the path of integration into the complex plane.

That being said, there is still room for improvement in the computation of special functions. Most computational implementations use the asymptotic expansion whenever it achieves the requested accuracy, whilst reverting to nonoscillatory methods otherwise. Furthermore, different regions in the complex plane have different asymptotic expansions, and—unless more sophisticated tools such as hyperasymptotics are utilized [**10**]—huge errors can result when near the border between expansions.

1.4. Orthogonal series

The higher order basis functions of orthogonal series invariably are oscillatory. The canonical example is the Fourier series, though polynomial orthogonal series also follow this pattern. The standard Fourier series over the interval $[-\pi, \pi]$, written in complex form, is

$$f(x) \sim \frac{1}{2\pi} \sum_{k=-\infty}^{\infty} \left\langle f, \mathrm{e}^{\mathrm{i}k\cdot} \right\rangle \mathrm{e}^{\mathrm{i}kx},$$

where $\langle \cdot, \cdot \rangle$ is the standard L_2 complex inner product:

$$\langle f, g \rangle = \int_{-\pi}^{\pi} f(t)\, \bar{g}(t)\, dt.$$

Thus the coefficients of the series are the oscillatory (for large k) integrals

$$\left\langle f, \mathrm{e}^{\mathrm{i}k\cdot} \right\rangle = \int_{-\pi}^{\pi} f(t)\, \mathrm{e}^{-\mathrm{i}kt}\, dt.$$

Of course, the coefficients of the series can be approximated in $\mathcal{O}(n \log n)$ operations via the fast Fourier transform (FFT), which in fact interpolates f at the chosen sample points. However, if interpolation is not required we can approximate the coefficients of this series using the methods developed in Chapter 3 with a fixed number of operations per coefficient, resulting in only $\mathcal{O}(n)$ complexity.

Other orthogonal series include the modified Fourier series of [51]. This series is constructed by replacing $\sin kx$ in the standard trigonometric Fourier series with $\sin(k - \frac{1}{2})x$, so that

$$f(x) \sim \frac{c_0}{2} + \sum_{k=1}^{\infty} c_k \cos kx + s_k \sin(k - \frac{1}{2})x.$$

This series converges at a faster rate than the standard Fourier series when f is not periodic. It was proved by this author (a result that will not appear in this thesis) that the partial sum of this series up to n approximates $f \in C^3[-\pi, \pi]$ with order $\mathcal{O}(n^{-2})$ in $(-\pi, \pi)$ and with order $\mathcal{O}(n^{-1})$ at the endpoints $\pm\pi$; indeed, when the function is smooth a full asymptotic expansion can be found in terms of Lerch transcendent functions [9] and the derivatives of f at the endpoints [79]. This compares to standard Fourier series' convergence rate of $\mathcal{O}(n^{-1})$ in the interior and lack of convergence at the boundary. Higher convergence rates can be achieved by using polyharmonic series [59], whose approximation properties were investigated in [52]. Furthermore, these results can be generalized for function approximation over multivariate domains [53]. In all of these cases the fast Fourier transform is not available, hence we must resort to computing the coefficients of the series using oscillatory quadrature.

Of greater importance—it is hard to beat approximation by orthogonal polynomials in the univariate case—is function approximation over multivariate domains. Suppose we are given a domain Ω and a linear self-adjoint operator $\mathcal{L}$. Then from standard spectral theory we know that, subject to suitable boundary conditions, the eigenfunctions of $\mathcal{L}$ form an orthogonal series. In all but the most exceptional cases, the FFT algorithm is no longer applicable, hence if we are to use an orthogonal system as a function approximation scheme, we must resort to quadrature methods.

Related to this subject are Galerkin methods, or in particular spectral methods. Suppose we wish to solve the linear differential equation

$$\mathcal{L}[u] = f,$$

with some boundary condition imposed. A Galerkin method approximates a weak solution to this equation by ensuring that the equality holds true on a subspace spanned by the basis $\{\psi_1, \ldots, \psi_n\}$. In other words, for some inner product $\langle \cdot, \cdot \rangle$, we approximate u by

$$v = \sum_{k=1}^{n} c_k \psi_k,$$

6

determining the coefficients c_k by solving the system

$$\langle \mathcal{L}[v], \psi_1 \rangle = \langle f, \psi_1 \rangle, \ldots, \langle \mathcal{L}[v], \psi_n \rangle = \langle f, \psi_n \rangle.$$

If ψ_k does not have compact support (e.g., finite elements), then it is typically an orthogonal series such as Fourier series. But then the inner products in the system become oscillatory integrals.

Chapter 2

History

In this chapter we review existing research into oscillatory integrals and their quadrature. Oscillatory quadrature's development and foundation differs greatly from nonoscillatory quadrature theory. Where traditional quadrature methods study the accuracy as the step size decreases or the number of sample points increases, oscillatory quadrature has focused primarily on the asymptotics as the frequency ω goes to infinity. Because of this, asymptotic expansions, complex analysis, partial integration and collocation take a central role, in place of the study of zeros of orthogonal polynomials and Taylor series.

In Section 2.1 we explain why approximating such integrals needs special attention: traditional quadrature methods are not accurate. We then turn our attention to a brief overview of existing research related to oscillatory quadrature. This can be divided into two groups: asymptotic theory and quadrature methods. The key difference between the two methodologies is that asymptotics is concerned with how the integrals behave as the frequency increases, whereas quadrature takes a more practical view by investigating convergent approximations for fixed frequencies. Section 2.2 derives the most basic asymptotic expansion via integration by parts, Section 2.3 looks at the method of stationary phase and Section 2.4 investigates the method of steepest descent, which deforms the path of integration into the complex plane in order to turn an oscillating integrand into an exponentially decreasing integrand, whose asymptotic expansion can then be determined. We then develop the counterpart for the asymptotic expansion for integrals over multivariate domains in Section 2.6, after reviewing multivariate integration theory in Section 2.5.

Oscillatory quadrature methods have not received as much attention as the asymptotic theory of oscillatory integrals. Indeed, it took over 75 years from the construction of the first of these methods—the Filon method [29]—until its asymptotic well-behavedness was realized [44]. In Section 2.7 we describe how the Filon method was initially constructed, forgoing its recent generalization until Chapter 3. This method is dependent on using the standard Fourier oscillator $e^{i\omega x}$, hence its generality is limited. In Section 2.8 we review the Levin collocation method, which applies to general oscillators. Chung, Evans and Webster extended the Levin collocation method to higher order oscillators, which is explained in Section 2.9. In Section 2.10 we look at how the method of steepest descent can be used as a quadrature method in addition to its use in asymptotics. Finally we give a very brief overview of other oscillatory quadrature methods in Section 2.11.

Remark: If the results were presented in their full detail, this chapter alone could easily span several volumes. So in the interest of brevity, we mostly forgo rigour in favour of formal derivation and intuitive arguments. Many of the results presented here are classical, and for those which are not we refer to other authors who have significantly more thorough treatments.

2.1. Nonoscillatory quadrature

To understand why we need special methods for oscillatory integrals, it is important to study where traditional quadrature methods fail. Most nonoscillatory quadrature methods approximate an integral by a weighted sum sampling the integrand at n discrete points $\{x_1, \ldots, x_n\}$, and averaging the samples with suitable weights $\{w_1, \ldots, w_n\}$:

$$\int_a^b w(x) f(x) \, \mathrm{d}x \approx \sum_{k=1}^n w_k f(x_k), \tag{2.1.1}$$

where w is some nonnegative weight function. The first definition of an integral one typically learns is the Riemann sum

$$\int_a^b f(x) \, \mathrm{d}x = \lim_{n \to \infty} \frac{1}{n} \sum_{k=0}^{n-1} f\left(\frac{k}{n}(b-a) + a\right).$$

Thus if we take n large enough the sum will approximate the value of the integral, and indeed falls into the framework of (2.1.1). This is equivalent to dividing the interval of integration into panels of size $1/n$ and approximating the integral in each panel by a rectangle of the same height as the function at the left endpoint. Though this does indeed work as an approximation scheme, its speed of convergence is very slow and it is not useful in practice.

This is the simplest example of a *composite Newton–Cotes formula*. Newton–Cotes formulæ consist of approximating the integrand f by a polynomial of degree n, which matches f at n evenly spaced points. A closed Newton–Cotes formula includes the endpoints of the interval, otherwise it is an open Newton–Cotes formula. Newton–Cotes methods do not necessarily converge as n goes to infinity [21], in particular convergence fails for the classic Runge example

$$\int_{-1}^1 \frac{1}{25x^2 + 1} \, \mathrm{d}x.$$

Thus a composite rule must be used, where the interval of integration is divided into equally spaced panels and a Newton–Cotes method is used within each panel.

The next composite Newton–Cotes method is the *trapezoidal rule*, where the function f is approximated by a trapezoid within each panel, or alternatively, f is approximated in each panel by an affine function and the resulting piecewise affine function is integrated in

closed form. This is equivalent to the weighted sum, for $h = (b - a)/n$:

$$\int_a^b f(x)\,\mathrm{d}x \approx \frac{h}{2}f(a) + h\sum_{k=1}^{n-1} f(x + kh) + \frac{h}{2}f(b).$$

In place of affine functions we could use higher order polynomials in each panel. Using a quadratic function results in *Simpson's rule*:

$$\int_a^b f(x)\,\mathrm{d}x \approx \frac{b - a}{6}\left[f(a) + 4f\left(\frac{a + b}{2}\right) + f(b)\right].$$

This is particularly important for the history of oscillatory quadrature, since the original Filon method is based on a composite Simpson's rule.

Like Newton–Cotes, most other quadrature schemes consist of choosing the weights so that (2.1.1) is exact when f is a polynomial of a certain degree, though not necessarily choosing evenly spaced nodes. The idea is that, if f can be approximated well by a polynomial, the quadrature error should be small. We can make the formula exact for polynomials of degree $n - 1$ if we fix the nodes x_k and determine the weights w_k by solving the system

$$\int_a^b w(x)\,\mathrm{d}x = \sum_{k=1}^n w_k \qquad \ldots \qquad \int_a^b w(x)x^{n-1}\,\mathrm{d}x = \sum_{k=1}^n w_k x_k^{n-1}. \qquad (2.1.2)$$

The most often used method in practice is *Gaussian quadrature*. The idea behind Gaussian quadrature is to choose the nodes and weights in order to to maximize the degree of polynomials for which (2.1.1) is exact. In (2.1.1) there are $2n$ unknowns, hence it might be possible to choose values for these unknowns so that polynomials up to degree $2n - 1$ are integrated exactly. It is well known that to achieve this goal, the sample points should be placed at the zeros of the associated orthogonal polynomials, and the weights can then be determined using (2.1.2), which is a linear system of equations.

Unless the integrand has a special form, the weight function is typically $w(x) \equiv 1$. The orthogonal polynomials with respect to a constant weight function are the well-known Legendre polynomials, leading us to the *Gauss–Legendre formulæ*. The first few of these polynomials are

$$P_0(x) = 1, P_1(x) = x, P_2(x) = \frac{1}{2}(3x^2 - 1), P_3(x) = \frac{1}{2}(5x^3 - 3x), \ldots.$$

The higher order polynomials can be computed via the recurrence relationship

$$(n + 1)P_{n+1} = (2n + 1)xP_n - nP_{n-1},$$

cf. [2]. The sample points $\{x_1, \ldots, x_n\}$ for an n point Gauss–Legendre rule are the zeros of the polynomial P_n, i.e.,

$$0 = P_n(x_1) = \cdots = P_n(x_n).$$
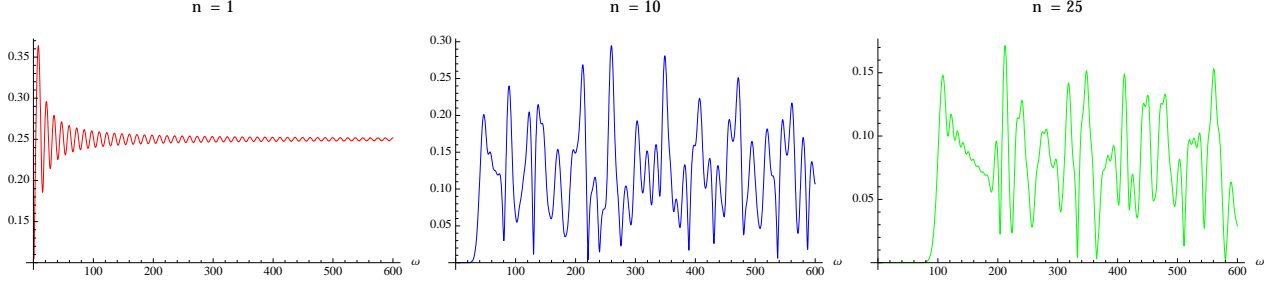
Figure 2.1:   The absolute error in approximating $\int_0^1 x^2 \mathrm{e}^{\mathrm{i}\omega x}\,\mathrm{d}x$ by an n-point Gauss–Legendre quadrature scheme, for $n = 1$, 10 and 25.

The weights are

$$w_i = \frac{2(1 - x_i^2)}{\left[nP_{n-1}(x_i)\right]^2},$$

cf. [**21**]. An efficient way of computing both the nodes and weights of a Gauss–Legendre rule was presented in [**36**], based on computing the eigenvalues and eigenvectors of a symmetric tridiagonal matrix.

The other Gaussian quadrature method of relevence to this thesis is Gauss–Laguerre quadrature, where the integral has the form

$$\int_0^\infty \mathrm{e}^{-x} f(x)\,\mathrm{d}x.$$

The associated orthogonal polynomials are the Laguerre polynomials.

Regardless of the particular method used, (2.1.1) fails as a quadrature scheme for high frequency oscillation when $w(x) \equiv 1$, unless n grows with ω. To see this, consider the integral

$$\int_a^b f(x) \sin \omega x\,\mathrm{d}x \approx \sum_{k=1}^n w_k f(x_k) \sin \omega x_k,$$

where n, w_k and x_k are all fixed for increasing ω. Assuming that this sum is not identically zero, it cannot decay as ω increases. This can be seen in Figure 2.1, for the integral

$$\int_0^1 x^2 \mathrm{e}^{\mathrm{i}\omega x}\,\mathrm{d}x.$$

A simple application of integration by parts—which will be investigated further in the next section—reveals that the integral itself decays like $\mathcal{O}\!\left(\omega^{-1}\right)$. Thus the error of any weighted sum is $\mathcal{O}(1)$, which compares to an error of order $\mathcal{O}\!\left(\omega^{-1}\right)$ if we simply approximate the integral by zero! It is safe to assume that a numerical method which is less accurate than equating the integral to zero is of little practical use. On the other hand, letting n be proportional to the frequency can result in considerable computational costs. This is magnified

11

significantly when we attempt to integrate over multivariate domains. Even nonoscillatory quadrature is computationally difficult for multivariate integrals, and high oscillations would only serve to further exasperate the situation. Thus we must look for alternative methods to approximate such integrals.

2.2. Asymptotic expansion

Whereas standard quadrature schemes are inefficient, a straightforward alternative exists in the form of asymptotic expansions. Unlike the preceding approximation, asymptotic expansions actually improve with accuracy as the frequency increases, and—assuming sufficient differentiability of f and g—to arbitrarily high order. Furthermore the number of operations required to produce such an expansion is independent of the frequency, and extraordinarily small. Even more surprising is that this is all obtained by only requiring knowledge of the function at the endpoints of the interval, as well as its derivatives at the endpoints if higher asymptotic orders are required. There is, however, one critical flaw which impedes their use as quadrature formulæ: asymptotic expansions do not in general converge when the frequency is fixed, hence their accuracy is limited.

Whenever g is free of stationary points—i.e., $g'(x) \neq 0$ within the interval of integration— we can derive an *asymptotic expansion* in a very straightforward manner by repeatedly applying integration by parts. The first term of the expansion is determined as follows:

$$I[f] = \int_a^b f(x)\mathrm{e}^{\mathrm{i}\omega g(x)}\,\mathrm{d}x = \frac{1}{\mathrm{i}\omega}\int_a^b \frac{f(x)}{g'(x)}\frac{\mathrm{d}}{\mathrm{d}x}\mathrm{e}^{\mathrm{i}\omega g(x)}\,\mathrm{d}x$$

$$= \frac{1}{\mathrm{i}\omega}\left[\frac{f(b)}{g'(b)}\mathrm{e}^{\mathrm{i}\omega g(b)} - \frac{f(a)}{g'(a)}\mathrm{e}^{\mathrm{i}\omega g(a)}\right] - \frac{1}{\mathrm{i}\omega}\int_a^b \frac{\mathrm{d}}{\mathrm{d}x}\left[\frac{f(x)}{g'(x)}\right]\mathrm{e}^{\mathrm{i}\omega g(x)}\,\mathrm{d}x.$$

The term

$$\frac{1}{\mathrm{i}\omega}\left[\frac{f(b)}{g'(b)}\mathrm{e}^{\mathrm{i}\omega g(b)} - \frac{f(a)}{g'(a)}\mathrm{e}^{\mathrm{i}\omega g(a)}\right] \tag{2.2.1}$$

approximates the integral $I[f]$ with an error

$$-\frac{1}{\mathrm{i}\omega}I\left[\frac{\mathrm{d}}{\mathrm{d}x}\left[\frac{f(x)}{g'(x)}\right]\right] = \mathcal{O}\!\left(\omega^{-2}\right),$$

using the fact that the integral decays like $\mathcal{O}\!\left(\omega^{-1}\right)$ [**85**]. Thus the more oscillatory the integrand, the more accurately (2.2.1) can approximate the integral, with a relative accuracy $\mathcal{O}\!\left(\omega^{-1}\right)$. Moreover the error term is itself an oscillatory integral, thus we can integrate by parts again to obtain an approximation with an absolute error $\mathcal{O}\!\left(\omega^{-3}\right)$. Iterating this procedure results in an asymptotic expansion:
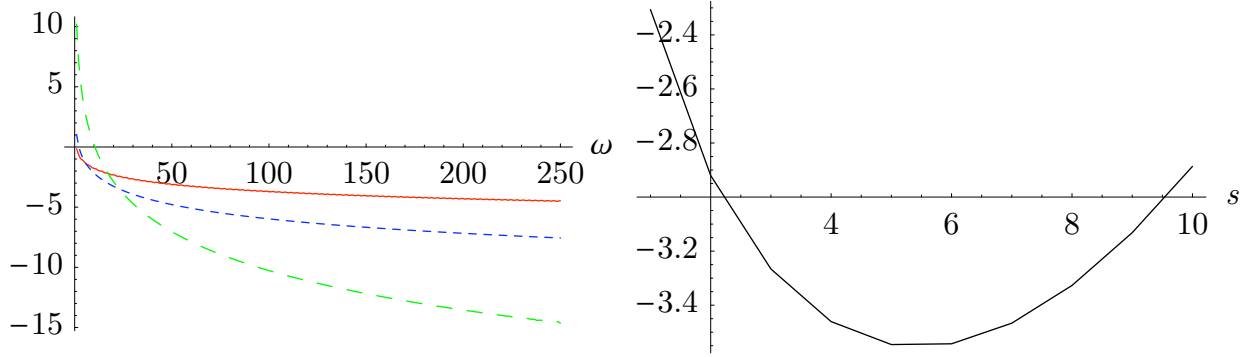
Figure 2.2: The base-10 logarithm of the error in approximating $\int_0^1 \cos x \, \mathrm{e}^{\mathrm{i}\omega(x^2+x)} \, \mathrm{d}x$. The left graph compares the one-term (solid line), three-term (dotted line) and ten-term (dashed line) asymptotic expansions. The right graph shows the error in the s-term asymptotic expansion for $\omega = 20$.

Theorem 2.2.1 *Suppose that $g' \neq 0$ in $[a, b]$. Then*

$$I[f] \sim -\sum_{k=1}^{\infty} \frac{1}{(-\mathrm{i}\omega)^k} \left\{ \sigma_k(b)\mathrm{e}^{\mathrm{i}\omega g(b)} - \sigma_k(a)\mathrm{e}^{\mathrm{i}\omega g(a)} \right\},$$

where

$$\sigma_1 = \frac{f}{g'}, \qquad \sigma_{k+1} = \frac{\sigma_k'}{g'}, \qquad k \geq 1.$$

We can find the error term for approximating $I[f]$ by the first s terms of this expansion:

$$I[f] = -\sum_{k=1}^{s} \frac{1}{(-\mathrm{i}\omega)^k} \left\{ \sigma_k(b)\mathrm{e}^{\mathrm{i}\omega g(b)} - \sigma_k(a)\mathrm{e}^{\mathrm{i}\omega g(a)} \right\} + \frac{1}{(-\mathrm{i}\omega)^s} I\left[\sigma_s'\right]$$

$$= -\sum_{k=1}^{s} \frac{1}{(-\mathrm{i}\omega)^k} \left\{ \sigma_k(b)\mathrm{e}^{\mathrm{i}\omega g(b)} - \sigma_k(a)\mathrm{e}^{\mathrm{i}\omega g(a)} \right\} + \frac{1}{(-\mathrm{i}\omega)^s} I\left[\sigma_{s+1}g'\right].$$

In Figure 2.2 we use the partial sums of the asymptotic expansion to approximate the integral

$$\int_0^1 \cos x \, \mathrm{e}^{\mathrm{i}\omega(x^2+x)} \, \mathrm{d}x.$$

We compare three partial sums of the asymptotic expansion in the left graph: s equal to one, three and ten. This graph demonstrates that increasing the number of terms used in the expansion does indeed increase the rate that the error in approximation goes to zero for increasing ω. However, at low frequencies adding terms to the expansion can actually cause the approximation to become worse. Thus higher order asymptotic series are only appropriate when the frequency is large enough. Furthermore for any given frequency the expansion reaches an optimal error, after which adding terms to the expansion actually

13
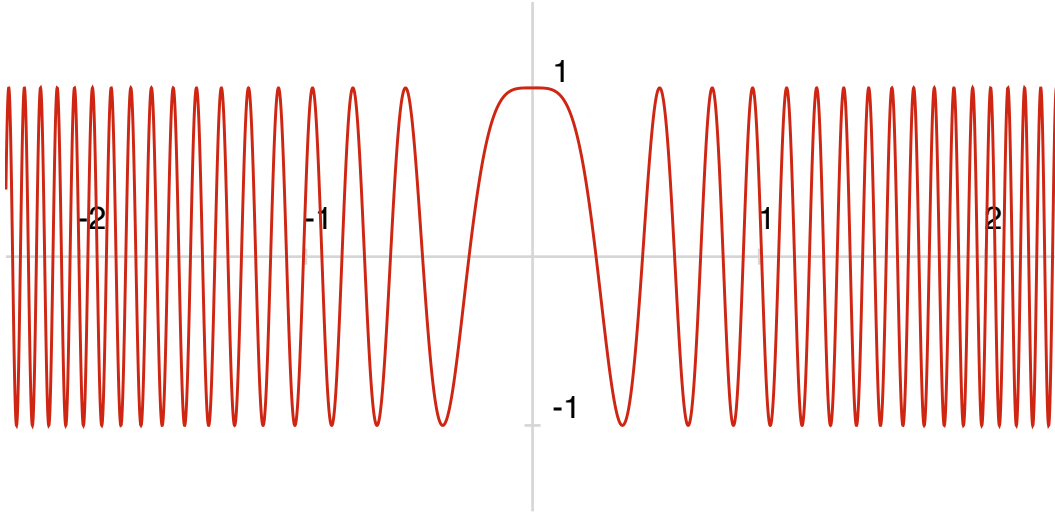
Figure 2.3: Plot of $\cos 20x^2$.

increases the error. This is shown in the right graph for ω fixed to be 20, in which case the optimal expansion consists of five terms.

2.3. Method of stationary phase

In the asymptotic expansion from the previous section, it is interesting to note that as the frequency increases, the behaviour of the integral is more and more dictated by the behaviour of the integrand at the endpoints of the interval. In fact, the behaviour within the interior of the interval is irrelevant as $\omega \to \infty$, and all integrals with the same boundary data begin to behave the same as the frequency increases. Though at first counterintuitive, this can be justified via a geometric argument. Consider for the moment the simple integral

$$\int_{-1}^{1} \cos \omega x \, \mathrm{d}x.$$

The integrand has extrema at the points

$$0, \pm \frac{\pi}{\omega}, \pm \frac{2\pi}{\omega}, \pm \frac{3\pi}{\omega} \dots .$$

Furthermore, due to cancellation, the integral between adjacent extrema is equal to zero. It thus follows that, if k is chosen to be the largest positive integer such that $\frac{k\pi}{\omega} \leq 1$, then

$$\int_{-1}^{1} \cos \omega x \, \mathrm{d}x = \int_{\frac{-k\pi}{\omega}}^{1} \cos \omega x \, \mathrm{d}x + \int_{-1}^{\frac{-k\pi}{\omega}} \cos \omega x \, \mathrm{d}x.$$

As ω becomes large, the intervals of integration become smaller, and the value of the integrand at the boundary becomes more significant. When we use a nontrivial amplitude function and an oscillator without stationary points, the same sort of cancellation occurs, albeit to a slightly lesser extent.

14

On the other hand, this cancellation does not occur wherever the oscillator g has a stationary point—a point ξ where $g'(\xi) = 0$. As can be seen in Figure 2.3, for the oscillator $g(x) = x^2$, the integrand becomes nonoscillatory in a small neighbourhood of the stationary point. Thus the asymptotics depends also on the behaviour at the stationary points, in addition to the behaviour at the endpoints of the interval.

We now determine how the stationary point contributes to the asymptotics of the integral, by utilizing the method of stationary phase. Consider for a moment the integral

$$\int_{-\infty}^{\infty} f(x)e^{i\omega g(x)} \, dx,$$

where $g(x)$ has a single stationary point of order $r - 1$ at zero:

$$0 = g'(0) = \cdots = g^{(r-1)}(0), \qquad g^{(r)}(0) \neq 0 \qquad \text{and} \qquad g'(x) \neq 0 \text{ whenever } x \neq 0.$$

Assume that this integral converges and that $f(x)$ is bounded. As ω increases, the value of the integral at the stationary point quickly dominates: the contribution from everywhere away from the stationary point is largely cancelled due to oscillations. Near the stationary point, $g(x)$ behaves like $g(0) + g_r x^r$, for some constant g_r, and $f(x)$ behaves like $f(0)$. Thus it stands to reason that

$$\int_{-\infty}^{\infty} f(x)e^{i\omega g(x)} \, dx \sim f(0)e^{i\omega g(0)} \int_{-\infty}^{\infty} e^{i\omega g_r x^r} \, dx = \frac{f(0)}{r}e^{\frac{i\pi}{2r}}\Gamma\left(\frac{1}{r}\right)\frac{e^{i\omega g(0)}}{(g_r\omega)^{\frac{1}{r}}}.$$

The asymptotic behaviour when the integral is taken over a finite interval is the same, since the contributions from the endpoints of the interval decay like $\mathcal{O}(\omega^{-1})$, whereas the stationary points contribution decays like $\mathcal{O}(\omega^{-\frac{1}{r}})$. For a proper proof and error bounds of this formula, see [74]. The stationary phase approximation can be extended to a full asymptotic expansion. We however prefer to utilize a new alternative derivation of this expansion developed in Chapter 4.

2.4. Method of steepest descent

Suppose that f and g are entire functions. In this case we can apply Cauchy's theorem and deform the integration path into the complex plane. The idea is to construct a path of integration $\zeta(t)$ so that the oscillations in the exponential kernel are removed. We then expand this new Laplace-type integral into its asymptotic expansion. In Section 2.10, we look at recent results that use the path of steepest descent to construct a quadrature scheme, rather than simply as an asymptotic tool. In this chapter, we determine the path of steepest descent for the specific oscillators $g(x) = x$ and $g(x) = x^2$ à la [38], referring the reader to more comprehensive treatments [1, 11, 74, 89] for more complicated oscillators.
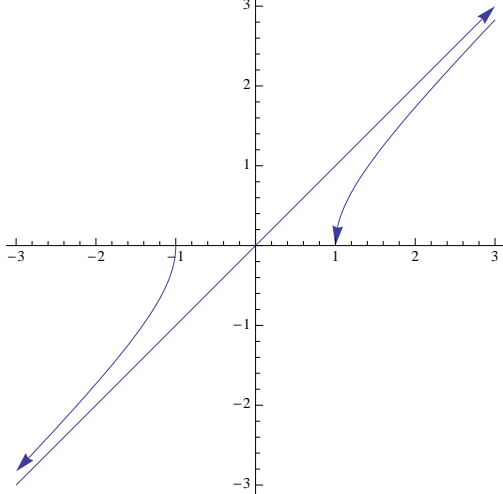
Figure 2.4: The path of steepest descent for the oscillator $g(z) = z^2$.

Writing $g(z)$ as $\mathrm{Re}\ g(z) + \mathrm{i}\,\mathrm{Im}\ g(z)$, we note that

$$\mathrm{e}^{\mathrm{i}\omega g(z)} = \mathrm{e}^{\mathrm{i}\omega\,\mathrm{Re}\ g(z)}\mathrm{e}^{-\omega\,\mathrm{Im}\ g(z)}.$$

Thus if $\mathrm{Im}\ g(z) > 0$, then the oscillator decays exponentially as $\omega \to \infty$. There is still an oscillatory component $\mathrm{e}^{\mathrm{i}\omega\mathrm{Re}\ g(z)}$, unless the path is deformed so that $\mathrm{Re}\ g(z) \equiv c$. If we have a Fourier integral

$$\int_a^b f(x)\mathrm{e}^{\mathrm{i}\omega x}\,\mathrm{d}x,$$

this is equivalent to choosing the path $\zeta_c(t) = c + \mathrm{i}t$, or in other words, the path of steepest descent from any point is directly perpendicular to the real axis. Thus we can use Cauchy's theorem to deform the path from a to b by integrating along ζ_a into the complex plane some distance N, cross over to the path ζ_b, then integrate along that path back to b:

$$\int_a^b f(x)\mathrm{e}^{\mathrm{i}\omega x}\,\mathrm{d}x = \mathrm{i}\mathrm{e}^{\mathrm{i}\omega a}\int_0^N f(\zeta_a(t))\mathrm{e}^{-\omega t}\,dt + \mathrm{e}^{-\omega N}\int_a^b f(t+\mathrm{i}N)\mathrm{e}^{\mathrm{i}\omega t}\,dt - \mathrm{i}\mathrm{e}^{\mathrm{i}\omega b}\int_0^N f(\zeta_b(t))\mathrm{e}^{-\omega t}\,dt.$$

Assuming that f only has exponential growth in the complex plane, the middle integral goes to zero when we let N go to infinity:

$$\int_a^b f(x)\mathrm{e}^{\mathrm{i}\omega x}\,\mathrm{d}x = \mathrm{i}\mathrm{e}^{\mathrm{i}\omega a}\int_0^\infty f(\zeta_a(t))\mathrm{e}^{-\omega t}\,dt - \mathrm{i}\mathrm{e}^{\mathrm{i}\omega b}\int_0^\infty f(\zeta_b(t))\mathrm{e}^{-\omega t}\,dt.$$

We have thus converted the Fourier integral into two Laplace integrals, which can be expanded into their asymptotic expansions. For the Fourier integral itself the method of steepest descent will give the very same asymptotic expansion as if we had simply integrated by parts, however with the extra requirement of analyticity and only exponential growth in the complex plane. This is not to say it does not have its uses as a quadrature scheme, as will be seen in Section 2.10.

16

When the oscillator is more complicated—say, with stationary points—the method of steepest descent is tremendously useful as an asymptotic tool. The method of stationary phase only gives the first term in the asymptotic expansion, and the method of steepest descent is needed to determine the higher order terms. The path of integration is now significantly more complicated, and must go through the stationary point. Consider the simplest oscillator with a stationary point: $g(z) = z^2$. Making the real part constant results in defining the path of steepest descent as $\pm\sqrt{c^2 + it}$, for $0 \leq t < \infty$. The choice in sign is determined by the sign of c. For the path out of the two endpoints we obtain

$$\zeta_{-1}(t) = -\sqrt{1 + it} \qquad \text{and} \qquad \zeta_1(t) = \sqrt{1 + it}.$$

These two paths do not connect, hence Cauchy's theorem is not yet applicable. To connect the paths we must cross the real axis at some point. In this case, $e^{i\omega z^2}$ exhibits exponential decay in the lower left and upper right quadrants, whilst it increases exponentially in the remaining two quadrants. Thus we wish to pass through the saddle point at $z = 0$ to avoid the areas of exponential increase. There are two paths through zero:

$$\zeta_0^{\pm}(t) = \pm\sqrt{it}.$$

We must integrate along both of these curves for the contour path to connect.

Figure 2.4 draws the resulting path of steepest descent for this particular integral. This corresponds to the following integral representation:

$$\int_{-1}^{1} f(x)e^{i\omega x^2} \, dx = \left(\int_{\zeta_{-1}} - \int_{\zeta_0^-} + \int_{\zeta_0^+} - \int_{\zeta_1} \right) f(x)e^{i\omega x^2} \, dx$$

$$= e^{i\omega} \int_0^{\infty} f(\zeta_{-1}(t))e^{-\omega t}\zeta_{-1}'(t) \, dt - \int_0^{\infty} f(\zeta_0^-(t))e^{-\omega t}\zeta_0^{-'}(t) \, dt \qquad (2.4.1)$$

$$+ \int_0^{\infty} f(\zeta_0^+(t))e^{-\omega t}\zeta_0^{+'}(t) \, dt - e^{i\omega} \int_0^{\infty} f(\zeta_1(t))e^{-\omega t}\zeta_1'(t) \, dt$$

Each of these integrals is a Laplace integral. Assuming that these integrals converge—in other words, f cannot increase faster than the exponential decay along the contour of integration—we can apply *Watson's lemma* to determine the asymptotic expansion:

Theorem 2.4.1 [**74**] *Suppose that q is analytic and*

$$q(t) \sim \sum_{k=0}^{\infty} a_k t^{\frac{k+\lambda-\mu}{\mu}}, \qquad t \to 0,$$

for Re $\lambda > 0$. *Then*

$$\int_0^{\infty} q(t)e^{-\omega t} \, dt \sim \sum_{k=0}^{\infty} \Gamma\left(\frac{k+\lambda}{\mu}\right) \frac{a_k}{\omega^{\frac{k+\lambda}{\mu}}}, \qquad \omega \to \infty,$$

whenever the abscissa of convergence is not infinite.

17

For the integrals along the paths $\zeta_{\pm 1}$ in (2.4.1), the integrand should be smooth at $t = 0$, so that $\lambda, \mu = 1$, and the contributions from the endpoints decay like $\mathcal{O}(\omega^{-1})$. A singularity is introduced because of $\zeta_0^{\pm \prime}$, and each integrand behaves like $\frac{1}{\sqrt{t}}$ at zero. Thus $\mu = 2$, and $\lambda = 1$, and the lemma predicts that these two integrals decay like $\mathcal{O}(\omega^{-\frac{1}{2}})$.

This technique of converting oscillatory integrals to Laplace integrals can be generalized to other oscillators, including oscillators with higher order stationary points, see [11]. The idea essentially remains the same: find the path of steepest descent, connecting disconnected paths through the stationary point. Once the integral is converted to a sum of Laplace integrals, Watson's lemma gives the asymptotic expansion. We will not actually utilize these asymptotic results extensively in this thesis: we will focus on methods which do not require deformation into the complex plane. We do however utilize the path of steepest descent again in Section 2.10, where a brief overview of a numerical quadrature scheme that obtains asymptotically accurate results via contour integration is presented.

2.5. Multivariate integration

We now turn our attention to multivariate asymptotics. We utilized integration by parts in the derivation of the univariate asymptotic expansion, which implicitly depended on the fundamental theorem of calculus. Thus in the construction of the multivariate asymptotic expansion, we need to use the multivariate version of the fundamental theorem of calculus: *Stokes' theorem*. In this section we restate this theorem, as well as defining key notation that will be used throughout this thesis.

Let $\mathrm{d}\boldsymbol{s}$ be the d-dimensional surface differential:

$$
\mathrm{d}\boldsymbol{s} = \begin{pmatrix} \mathrm{d}x_2 \wedge \cdots \wedge \mathrm{d}x_d \\ -\mathrm{d}x_1 \wedge \mathrm{d}x_3 \wedge \cdots \wedge \mathrm{d}x_d \\ \vdots \\ (-1)^{d-1}\mathrm{d}x_1 \wedge \cdots \wedge \mathrm{d}x_{d-1} \end{pmatrix}.
$$

The negative signs in the definition of this differential are chosen to simplify the notation of its exterior derivative. Stokes' theorem informs us, for some vector-valued function $\boldsymbol{v} : \mathbb{R}^d \to \mathbb{R}^d$ and piecewise smooth boundary Ω, that

$$
\int_{\partial \Omega} \boldsymbol{v} \cdot \mathrm{d}\boldsymbol{s} = \int_{\Omega} \mathrm{d}(\boldsymbol{v} \cdot \mathrm{d}\boldsymbol{s}) = \int_{\Omega} \nabla \cdot \boldsymbol{v} \, \mathrm{d}V.
$$

The definition of the *derivative matrix* of a vector-valued map $T : \mathbb{R}^d \to \mathbb{R}^n$, with component functions $T_1, \ldots, T_n$, is simply the $n \times d$ matrix

$$
T' = \begin{pmatrix} \mathcal{D}^{e_1} T_1 & \cdots & \mathcal{D}^{e_d} T_1 \\ \vdots & \ddots & \vdots \\ \mathcal{D}^{e_1} T_n & \cdots & \mathcal{D}^{e_d} T_n \end{pmatrix}.
$$

Note that $\nabla g^\top = g'$ when g is a scalar-valued function. The chain rule states that $(g \circ T)'(\boldsymbol{x}) = g'(T(\boldsymbol{x}))T'(\boldsymbol{x})$. The *Jacobian determinant* J_T of a map $T : \mathbb{R}^d \to \mathbb{R}^d$ is the determinant of its derivative matrix T'. For the case $T : \mathbb{R}^d \to \mathbb{R}^n$ with $n \geq d$ we define the Jacobian determinant of T for indices $i_1, \ldots, i_d$ as $J_T^{i_1, \ldots, i_d} = J_{\tilde{T}}$, where $\tilde{T} = (T_{i_1}, \cdots, T_{i_d})^\top$.

Suppose we know that a function T maps $Z \subset \mathbb{R}^{d-1}$ onto Ω. Then the definition of the integral of a differential form is

$$\int_\Omega \boldsymbol{f} \cdot \mathrm{d}\boldsymbol{s} = \int_Z \boldsymbol{f}(T(\boldsymbol{x})) \cdot \boldsymbol{J}_T^d(\boldsymbol{x}) \, \mathrm{d}V,$$

where $\boldsymbol{J}_T^d(\boldsymbol{x})$ is a vector of Jacobian determinants

$$\begin{pmatrix} J_T^{2,\ldots,d}(\boldsymbol{x}) \\ -J_T^{1,3,\ldots,d}(\boldsymbol{x}) \\ \vdots \\ (-1)^{d-1} J_T^{1,\ldots,d-1}(\boldsymbol{x}) \end{pmatrix}.$$

In the univariate asymptotic expansion, we exploited integration by parts to write an integral over an interval in terms of the integrands value at the endpoints of the interval and a smaller integral over the whole interval. This is essentially a rewritten form of the product rule for differentiation. For the multivariate case we proceed in the same manner: use the product rule for Stokes' theorem to rewrite the original integral as an integral along the boundary of the domain and a smaller integral within the domain. The product rule for a function $w : \mathbb{R}^d \to \mathbb{R}$ is:

$$\int_{\partial\Omega} w\boldsymbol{v} \cdot \mathrm{d}\boldsymbol{s} = \int_\Omega \nabla \cdot (w\boldsymbol{v}) \, \mathrm{d}V = \int_\Omega [\nabla w \cdot \boldsymbol{v} + w\nabla \cdot \boldsymbol{v}] \, \mathrm{d}V.$$

Reordering the terms in this equation, we obtain a partial integration formula:

$$\int_\Omega \nabla w \cdot \boldsymbol{v} \, \mathrm{d}V = \int_{\partial\Omega} w\boldsymbol{v} \cdot \mathrm{d}\boldsymbol{s} - \int_\Omega w\nabla \cdot \boldsymbol{v} \, \mathrm{d}V. \tag{2.5.1}$$

2.6. Multivariate asymptotic expansion

With a firm concept of how to derive a univariate asymptotic expansion and the multivariate tools of the preceding section, we now find the asymptotic expansion of higher dimensional integrals in the form

$$I[f] = I_g[f, \Omega] = \int_\Omega f(\boldsymbol{x}) \mathrm{e}^{\mathrm{i}\omega g(\boldsymbol{x})} \, \mathrm{d}V,$$

where the domain Ω has a piecewise smooth boundary. In this section we assume that the nonresonance condition is satisfied, which is somewhat similar in spirit to the condition that

g' is nonzero within the interval of integration. The *nonresonance condition* is satisfied if, for every point $\boldsymbol{x}$ on the boundary of Ω, $\nabla g(\boldsymbol{x})$ is not orthogonal to the boundary of Ω at $\boldsymbol{x}$. In addition, $\nabla g \neq 0$ in the closure of Ω, i.e., there are no stationary points. Note that the nonresonance condition does not hold true if g is linear and Ω has a completely smooth boundary, such as a circle, since ∇g must be orthogonal to at least one point in $\partial\Omega$.

Based on results from [**89**]—which were rediscovered in [**49**]—we derive the following asymptotic expansion. We also use the notion of a vertex of Ω, for which the definition may not be immediately obvious. Specifically, we define the *vertices* of Ω as:

- If Ω consists of a single point in $\mathbb{R}^d$, then that point is a vertex of Ω.

- Otherwise, let $\{Z_\ell\}$ be an enumeration of the smooth components of the boundary of Ω, where each Z_ℓ is of one dimension less than Ω, and has a piecewise smooth boundary itself. Then $\boldsymbol{v} \in \partial\Omega$ is a vertex of Ω if and only if $\boldsymbol{v}$ is a vertex of some Z_ℓ.

In other words, the vertices are the endpoints of all the smooth one-dimensional edges in the boundary of Ω. In two-dimensions, these are the points where the boundary is not smooth.

Theorem 2.6.1 *Suppose that Ω has a piecewise smooth boundary, and that the nonresonance condition is satisfied. Then, for $\omega \to \infty$,*

$$I_g[f, \Omega] \sim \sum_{k=0}^{\infty} \frac{1}{(-\mathrm{i}\omega)^{k+d}} \Theta_k[f],$$

where $\Theta_k[f]$ depends on $\mathcal{D}^{\boldsymbol{m}} f$ for $\sum \boldsymbol{m} \leq k$, evaluated at the vertices of Ω.

Proof:

In the partial integration formula (2.5.1), we choose $w = \frac{\mathrm{e}^{\mathrm{i}\omega g}}{\mathrm{i}\omega}$ and

$$\boldsymbol{v} = \frac{f \nabla g}{\|\nabla g\|^2}.$$

Because $\nabla g \neq 0$ within Ω, this is well defined and nonsingular. It follows that

$$\nabla \cdot w = \mathrm{e}^{\mathrm{i}\omega g} \nabla g,$$

thence

$$\int_\Omega f \mathrm{e}^{\mathrm{i}\omega g}\,\mathrm{d}V = \frac{1}{\mathrm{i}\omega} \int_{\partial\Omega} \frac{f}{\|\nabla g\|^2} \mathrm{e}^{\mathrm{i}\omega g} \nabla g \cdot \mathrm{d}\boldsymbol{s} - \frac{1}{\mathrm{i}\omega} \int_\Omega \nabla \cdot \left[\frac{f \nabla g}{\|\nabla g\|^2}\right] \mathrm{e}^{\mathrm{i}\omega g}\,\mathrm{d}V.$$

Iterating the process on the remainder term gives us the asymptotic expansion

$$I_g[f, \Omega] \sim -\sum_{k=1}^{s} \frac{1}{(-\mathrm{i}\omega)^k} \int_{\partial\Omega} \mathrm{e}^{\mathrm{i}\omega g} \boldsymbol{\sigma}_k \cdot \mathrm{d}\boldsymbol{s} + \frac{1}{(-\mathrm{i}\omega)^s} \int_\Omega \nabla \cdot \boldsymbol{\sigma}_s \mathrm{e}^{\mathrm{i}\omega g}\,\mathrm{d}V, \tag{2.6.1}$$

20

for

$$\boldsymbol{\sigma}_1 = f\frac{\nabla g}{\|\nabla g\|^2} \qquad \text{and} \qquad \boldsymbol{\sigma}_{k+1} = \nabla \cdot \boldsymbol{\sigma}_k\frac{\nabla g}{\|\nabla g\|^2}.$$

We now prove the theorem by expressing each of these integrals over the boundary in terms of its asymptotic expansion. Assume the theorem holds true for lower dimensions, where the univariate case follows from Theorem 2.2.1. For each ℓ, there exists a domain $\Omega_\ell \in \mathbb{R}^{d-1}$ and a smooth map $T_\ell : \Omega_\ell \to Z_\ell$ that parameterizes the ℓth smooth boundary component Z_ℓ by Ω_ℓ, where every vertex of Ω_ℓ corresponds to a vertex of Z_ℓ, and vice-versa. We can thus rewrite each surface integral as a sum of standard integrals:

$$\int_{\partial\Omega} \mathrm{e}^{\mathrm{i}\omega g}\boldsymbol{\sigma}_k \cdot \mathrm{d}\boldsymbol{s} = \sum_\ell \int_{Z_\ell} \mathrm{e}^{\mathrm{i}\omega g}\boldsymbol{\sigma}_k \cdot \mathrm{d}\boldsymbol{s} = \sum_\ell I_{g_\ell}\left[f_\ell, \Omega_\ell\right], \qquad (2.6.2)$$

where, for $\boldsymbol{y} \in \Omega_\ell$,

$$f_\ell(\boldsymbol{y}) = \boldsymbol{\sigma}_k(T_\ell(\boldsymbol{y})) \cdot \boldsymbol{J}_T^d(\boldsymbol{y}) \qquad \text{and} \qquad g_\ell(\boldsymbol{y}) = g(T_\ell(\boldsymbol{y})).$$

It follows from the definition of the nonresonance condition that the function g_ℓ satisfies the nonresonance condition in Ω_ℓ. This follows since if g_ℓ has a stationary point at $\boldsymbol{\xi}$ then

$$0 = \nabla g_\ell^\top(\boldsymbol{\xi}) = (g \circ T_\ell)'(\boldsymbol{\xi}) = \nabla g(T_\ell(\boldsymbol{\xi}))^\top T_\ell'(\boldsymbol{\xi}),$$

or in other words g is orthogonal to the boundary of Ω at the point $T_\ell(\boldsymbol{\xi})$.

Thus, by our assumption,

$$I_{g_\ell}\left[f_\ell, \Omega_\ell\right] \sim \sum_{i=0}^{\infty} \frac{1}{(-\mathrm{i}\omega)^{i+d-1}}\Theta_i[f_\ell],$$

where $\Theta_i\left[f_\ell\right]$ depends on $\mathcal{D}^{\boldsymbol{m}} f_\ell$ for $\sum \boldsymbol{m} \leq i$ applied at the vertices of Ω_ℓ. But $\mathcal{D}^{\boldsymbol{m}} f_\ell$ depends on $\mathcal{D}^{\boldsymbol{m}}\left[\boldsymbol{\sigma}_k \circ T_\ell\right]$ for $\sum \boldsymbol{m} \leq i$ applied at the vertices of Ω_ℓ, which in turn depends on $\mathcal{D}^{\boldsymbol{m}} f$ for $\sum \boldsymbol{m} \leq i + k$, now evaluated at the vertices of Z_ℓ, which are also vertices of Ω. The theorem follows from plugging these asymptotic expansions in place of the boundary integrals in (2.6.1).

<div align="right">Q.E.D.</div>

It is a significant challenge to find the coefficients of this asymptotic expansion explicitly, hence we use this theorem primarily to state that the asymptotics of a multivariate integral are dictated by the behaviour of f and its derivatives at the vertices of the domain of integration.

2.7. Filon method

Though the importance of asymptotic methods cannot be overstated, the lack of convergence forces us to look for alternative numerical schemes. In practice the frequency of
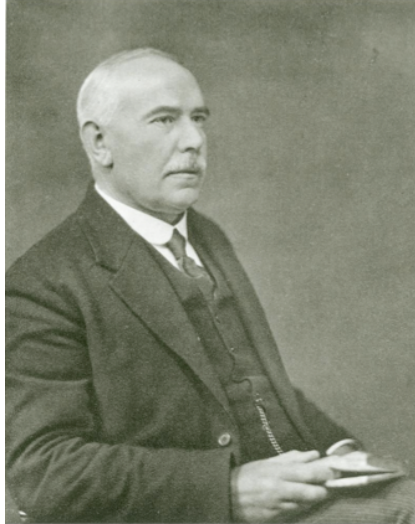
Figure 2.5: Louis Napoleon George Filon.

oscillations is fixed, and the fact that an approximation method is more accurate for higher frequency is irrelevant; all that matters is that the error for the given integral is small. Thus, though asymptotic expansions lie at the heart of oscillatory quadrature, they are not useful in and of themselves unless the frequency is extremely large. In a nutshell, the basic goal of this thesis, then, is to find and investigate methods which preserve the asymptotic properties of an asymptotic expansion, whilst allowing for arbitrarily high accuracy for a fixed frequency. Having been spoilt by the pleasures of asymptotic expansions, we also want methods such that the order of operations is independent of ω, and comparable in cost to the evaluation of the expansion. Fortunately, methods have been developed with these properties, in particular the Filon method and Levin collocation method.

The first known numerical quadrature scheme for oscillatory integrals was developed in 1928 by Louis Napoleon George Filon [54]. Filon presented a method for efficiently computing the Fourier integrals

$$\int_a^b f(x) \sin \omega x \, dx \qquad \text{and} \qquad \int_0^\infty \frac{f(x)}{x} \sin \omega x \, dx.$$

As originally constructed, the method consists of dividing the interval into $2n$ panels of size h, and applying a modified Simpson's rule on each panel. In other words, f is interpolated at the endpoints and midpoint of each panel by a quadratic. In each panel the integral becomes a polynomial multiplied by the oscillatory kernel $\sin \omega x$, which can be integrated in closed form. We determine the quadratic for the kth panel $v_k(x) = c_{k,0} + c_{k,1} x + c_{k,2} x^2$ by solving the system:

$$v_k(x_k) = f(x_k), v_k(x_{k+1}) = f(x_{k+1}), v_{k+2} = f(x_{k+2}).$$

22

We thus sum up the approximation on each subinterval:

$$\int_a^b f(x) \sin \omega x \, dx \approx \sum_{k=0}^{n-1} \int_{x_{2k}}^{x_{2k+2}} v_k(x) \sin \omega x \, dx. \qquad (2.7.1)$$

The moments

$$\int_a^b \left. \begin{matrix} 1 \\ x \\ x^2 \end{matrix} \right\} \sin \omega x \, dx$$

are all known trivially, thus we can compute (2.7.1) explicitly. The infinite integral was then computed using a series transformation. This method was generalized in [**68**] by using higher degree polynomials in each panel, again with evenly spaced nodes.

In the original paper by Filon, it is shown that the error of the Filon method is bounded by

$$C \sin \frac{h\omega}{2} \left(1 - \frac{1}{16} \sec \frac{h\omega}{4} \right).$$

This suggests that h must shrink as ω increases in order to maintain accuracy, a property which we have stated we are trying to avoid. Furthermore, Tukey [**87**]—which is referenced in Abramowitz and Stegun [**2**]—suggests that the Filon method cannot be accurate, due to problems with aliasing. This argument is fundamentally flawed, as aliasing does not exist when the number of sample points is allowed to increase. A related complaint was presented by Clendenin in [**19**], which says that, due to the use of evenly spaced nodes, at certain frequencies a nonzero integral is approximated by zero. Thus in order to achieve any relative accuracy the step size must decrease as the frequency increases. An earlier review of the Filon method [**58**], which Clendenin referenced, asserts that the error can not be worse than the error in interpolation by piecewise quadratics. Thus Clendenin's mistake was to focus on relative error: the Filon method's absolute error is still small at such frequencies.

What Filon failed to realize—and indeed apparently many other talented mathematicians who have used the Filon method since its inception—is the most important property of the Filon method: its accuracy actually improves as the frequency increases! Indeed, for a fixed step size the error decays like $\mathcal{O}(\omega^{-2})$. Thus h need not shrink as ω increases, rather, if anything, it should increase, thus reducing the required number of operations. This renders the existence of problem frequencies a nonissue: when ω is large, the issue Clendenin found will only surface at step sizes significantly smaller than necessary. Moreover, in Section 3.1 we will investigate Filon-type methods which use higher order polynomials, and avoid the problem of the integral vanishing completely.

Very little work on the Filon method was done for the remainder of the twentieth century, mostly consisting of investigating specific kernels similar in form to the Fourier oscillator. A Filon method for larger intervals is presented in [**30**], where a higher order rule is used for

each panel. This paper again makes the mistake of investigating asymptotic behaviour as $h\omega \to 0$. The paper [17] generalized the Filon method for integrals of the form

$$\int_a^b f(x)\,\mathrm{e}^{ax}\cos kx\,\mathrm{d}x.$$

More complicated methods based on the Filon method are explained in Section 2.11.

2.8. Levin collocation method

The computation of the Filon approximation rests on the ability to compute the moments

$$\int_a^b x^k \mathrm{e}^{\mathrm{i}\omega x}\,\mathrm{d}x.$$

For this particular oscillator the moments are computable in closed form, either through integration by parts or by the identity

$$\int_a^b x^k \mathrm{e}^{\mathrm{i}\omega x}\,\mathrm{d}x = \frac{1}{(-\mathrm{i}\omega)^{k+1}}\left[\Gamma(1+k,-\mathrm{i}\omega a) - \Gamma(1+k,-\mathrm{i}\omega b)\right],$$

where Γ is the incomplete Gamma function [2]. But often in applications we have irregular oscillators, giving us integrals of the form

$$\int_a^b f(x)\mathrm{e}^{\mathrm{i}\omega g(x)}\,\mathrm{d}x.$$

In this case knowledge of moments depends on the oscillator g. If we are fortunate, the moments are still known, and the Filon method is applicable. This is true if g is a polynomial of degree at most two or if $g(x) = x^r$. But we need not step too far outside the realm of these simple examples before explicit moment calculation falls apart: moments are not even known for $g(x) = x^3 - x$ nor $g(x) = \cos x$. Even when moments are known, they are typically known in terms of special functions, such as the incomplete Gamma function or more generally the hypergeometric function [2]. The former of these is efficiently computable [88]. The latter, on the other hand, are significantly harder to compute for the invariably large parameters needed, though some computational schemes exist [31, 73, 67]. Thus it is necessary that we find an alternative to the Filon method.

In 1982, David Levin developed the *Levin collocation method* [60], which approximates oscillatory integrals without using moments. A function F such that $\frac{\mathrm{d}}{\mathrm{d}x}\left[F\mathrm{e}^{\mathrm{i}\omega g}\right] = f\mathrm{e}^{\mathrm{i}\omega g}$ satisfies

$$I[f] = \int_a^b f\mathrm{e}^{\mathrm{i}\omega g}\,\mathrm{d}x = \int_a^b \frac{\mathrm{d}}{\mathrm{d}x}\left[F\mathrm{e}^{\mathrm{i}\omega g}\right]\,\mathrm{d}x = F(b)\mathrm{e}^{\mathrm{i}\omega g(b)} - F(a)\mathrm{e}^{\mathrm{i}\omega g(a)}.$$

By expanding out the derivatives, we can rewrite this condition as $\mathcal{L}[F] = f$ for the operator

$$\mathcal{L}[F] = F' + \mathrm{i}\omega g' F.$$

Note that we do not impose boundary conditions: since we are integrating, any particular solution to this differential equation is sufficient. If we can approximate the function F, then we can approximate $I[f]$ easily. In order to do so, we use collocation with the operator $\mathcal{L}$. Let $v = \sum_{k=1}^{\nu} c_k \psi_k$ for some *basis* $\{\psi_1, \ldots, \psi_\nu\}$. Given a sequence of collocation *nodes* $\{x_1, \ldots, x_\nu\}$, we determine the coefficents c_k by solving the collocation system

$$\mathcal{L}[v](x_1) = f(x_1), \ldots, \mathcal{L}[v](x_\nu) = f(x_\nu).$$

We can then define the approximation $Q^L[f]$ to be

$$Q^L[f] = \int_a^b \mathcal{L}[v]\, \mathrm{e}^{\mathrm{i}\omega g}\, \mathrm{d}x = \int_a^b \frac{\mathrm{d}}{\mathrm{d}x}\left[v\mathrm{e}^{\mathrm{i}\omega g} \right] \mathrm{d}x = v(b)\mathrm{e}^{\mathrm{i}\omega g(b)} - v(a)\mathrm{e}^{\mathrm{i}\omega g(a)}.$$

Levin was the first to note the asymptotic properties of these quadrature schemes, as well as the importance of endpoints in the collocation system. This method has an error $I[f] - Q^L[f] = \mathcal{O}\left(\omega^{-1}\right)$ when the endpoints of the interval are not included in the collocation nodes. When the endpoints are included, on the other hand, the asymptotic order increases to $I[f] - Q^L[f] = \mathcal{O}\left(\omega^{-2}\right)$. Though Filon failed to notice it, this property holds true for the Filon method as well, as discovered in [**44**]. This follows since the Levin collocation method with a polynomial basis is equivalent to a Filon method, whenever $g(x) = x$. In Chapter 3, we will see how this asymptotic behaviour relates to the asymptotic expansion, and exploit this relation in order to improve the asymptotic order further.

A Levin collocation method was also constructed for oscillatory integrals over a square. In this case a Levin differential operator was constructed by iterating the method for each dimension. Though we do investigate multivariate Levin-type methods in Chapter 5, we will not use this construction as it is limited to hypercubes.

Levin generalized his method for integrals whose vector-valued kernel satisfies a differential equation [**61**, **62**]. In other words, the method computes integrals of the form

$$\int_a^b \boldsymbol{f}(x)^\top \boldsymbol{y}(x)\, \mathrm{d}x,$$

such that

$$\boldsymbol{y}'(x) = A(x)\boldsymbol{y}(x).$$

The function $\boldsymbol{y}$ is oscillatory whenever A has eigenvalues with large imaginary components and nonpositive real components. The Levin collocation method can be used whenever the inverse of A and its derivatives are small. An example of such an integral is one involving Bessel functions [**2**], where we have the kernel

$$\boldsymbol{y}(x) = \begin{pmatrix} J_{m-1}(\omega x) \\ J_m(\omega x) \end{pmatrix}, \qquad A(x) = \begin{pmatrix} \frac{m-1}{x} & -\omega \\ \omega & -\frac{m}{x} \end{pmatrix}.$$

In this case

$$A^{-1}(x) = \frac{1}{\omega^2 x^2 - m^2 + m} \begin{pmatrix} -mx & \omega x^2 \\ -\omega x^2 & (m-1)x \end{pmatrix}.$$

The entries of this matrix, and its derivatives, are all $\mathcal{O}(\omega^{-1})$.

The collocation system is found in a similar manner as before. We wish to find a function $\boldsymbol{F}$ such that $(\boldsymbol{F}^\top \boldsymbol{y})' = \boldsymbol{f}^\top \boldsymbol{y}$. Expanding out derivatives gives us the new differential operator

$$\mathcal{L}[\boldsymbol{v}] = \boldsymbol{v}' + A^\top \boldsymbol{v}.$$

Thus, given a vector-valued basis $\{\boldsymbol{\psi}_k\}$, we approximate $\boldsymbol{F}$ by $\boldsymbol{v} = \sum_{k=1}^n c_k \boldsymbol{\psi}_k$, where $n = d\nu$ for d equal to the dimension of the kernel $\boldsymbol{y}$, and the coefficients c_k are determined by solving the system

$$\mathcal{L}[\boldsymbol{v}](x_1) = \boldsymbol{f}(x_1), \ldots, \mathcal{L}[\boldsymbol{v}](x_\nu) = \boldsymbol{f}(x_\nu).$$

We then obtain the Levin collocation method:

$$Q^L[\boldsymbol{f}] = \boldsymbol{v}(b)^\top \boldsymbol{y}(b) - \boldsymbol{v}(a)^\top \boldsymbol{y}(a).$$

Like the original Levin collocation method, the vector-valued version also improves with accuracy as the frequency increases.

Theorem 2.8.1 [**62**] *Let $B(x) = \omega A^{-1}(x)$ and assume that $x_1 = a$ and $x_\nu = b$. If B and its derivatives are bounded uniformly for all $\omega > \alpha$, then*

$$\left| I[\boldsymbol{f}] - Q^L[\boldsymbol{f}] \right| < C \frac{(b-a)^\nu}{\omega^2}$$

In Chapter 6 we will generalize this method to obtain higher asymptotic orders by deriving a vector-valued asymptotic expansion.

2.9. Chung, Evans and Webster method

Often methods represented as weighted sums, as in Section 2.1, are preferred. Though Filon and Levin collocation methods are extremely powerful, they do not fall into this framework. In [**26**], Evans and Webster construct such a method for irregular exponential oscillators, based on the Levin collocation method. We want to choose weights w_j and nodes x_j such that

$$\int_{-1}^{1} \phi_k(x) e^{i\omega g(x)} \, dx = \sum_{j=0}^{n} w_j \phi_k(x_j) \tag{2.9.1}$$

for some suitable basis ϕ_k. Unlike Gaussian quadrature, we do not choose ϕ_k to be polynomials. Instead, we choose them based on the Levin differential equation:

$$\phi_k = \mathcal{L}[T_k] = T_k' + i\omega g' T_k,$$

26

where T_k are the Chebyshev polynomials. The moments with respect to ϕ_k are computable in closed form:

$$\int_{-1}^{1} \phi_k(x) e^{i\omega g(x)} \, dx = T_k(1) e^{i\omega g(1)} - T_k(-1) e^{i\omega g(-1)}.$$

We can thus determine suitable weights and nodes to maximize the number of functions ϕ_k such that (2.9.1) holds. As this is a Levin-type method, it preserves the asymptotic niceties of the Levin collocation method.

This was generalized in [18, 24] for computation of the oscillatory integral

$$\int_{-1}^{1} f(x) y(x) \, dx,$$

where the oscillatory kernel y satisfies the differential equation

$$\mathcal{M}[y] = p_m y^{(m)} + \cdots + p_0 y = 0,$$

for some functions $\{p_0, \ldots, p_m\}$. As before, we want to choose nodes, weights and a basis so that

$$\int_{a}^{b} \phi_k(x) y(x) \, dx = \sum_{j=0}^{n} w_j \phi_k(x_j).$$

The adjoint of $\mathcal{M}$ is

$$\mathcal{M}^\star[z] = (-1)^m (p_m z)^{(m)} + (-1)^{m-1}(p_{m-1}z)^{(m-1)} + \cdots - (p_1 z)' + p_0 z.$$

The Lagrange identity then states that

$$z\mathcal{M}[y] - y\mathcal{M}^\star[z] = (Z[y, z])', \tag{2.9.2}$$

where Z is the bilinear concomitant

$$Z[y, z] = \sum_{r=1}^{m} \sum_{j+k=r-1} (-1)^k (p_r z)^{(k)} y^{(j)}.$$

Integrating (2.9.2) and using the fact that $\mathcal{M}[y] = 0$, we find that

$$\int_{a}^{b} \mathcal{M}^\star[z] \, y \, dx = Z[y, z](a) - Z[y, z](b). \tag{2.9.3}$$

We can thus choose our basis to be $\phi_k = \mathcal{M}^\star[T_k]$, in which case the moments are computable using (2.9.3), hence the nodes and weights can be determined by solving an algebraic equation. Numerical results for approximating the integral

$$\int_{\frac{1}{2}}^{1} e^x J_0(\omega \cos x) \, dx$$

suggest that the method improves with accuracy as the frequency increases. Using the method over infinite integration domains is explored in [25].

Remark: Based on the asymptotic expansion and many results in this thesis, it seems likely that imposing the condition

$$x_0 = a \qquad \text{and} \qquad x_n = b,$$

in the same vein as *Gauss–Lobatto quadrature*, should improve the asymptotic order of the method. As far as I am aware, this idea has not yet been explored.

2.10. Numerical steepest descent

The method of steepest descent, described briefly in Section 2.4, has an important feature that is neglected in its asymptotic form: the integrand along the path of integration does not oscillate, and thus can be approximated by using the nonoscillatory quadrature methods of Section 2.1. In this section we will give an overview of research based on this idea for oscillatory quadrature methods. Traditionally these techniques have been used in the computation of special functions, where f and g are fixed for any particular special function; however, recent research has investigated utilizing this technique for general f and g.

As described in Section 1.3, special functions often have highly oscillatory integral representations. Many methods for the computation of such special functions have been developed based on these integral representations and the method of steepest descent. Where in Section 2.4, the path of steepest descent was used merely to obtain the asymptotics of such integrals, in computation it can be used as an integration path, with nonoscillatory quadrature methods applied to the resulting integrals. Since the integral becomes exponentially decreasing, these methods can be extremely accurate. They have been used to compute Airy functions [34], Scorer functions [33] and an array of other special functions with integral representations [35]. Unfortunately they depend on the knowledge or computation of the path of steepest descent, which depends on the particular oscillator.

Contemporary with the work in this thesis is the investigation of numerical steepest descent for the general case by Daan Huybrechs and Stefan Vandewalle. In [40], they investigated univariate integrals, including those with stationary points. By employing Gauss–Laguerre quadrature along the path of steepest descent, high asymptotic order methods were obtained. In the case with no stationary points, if n quadrature points are used for each path (so $2n$ points total), the method has an error $\mathcal{O}\!\left(\omega^{-2n-1}\right)$, as $\omega \to \infty$. Furthermore, it is shown that the path of steepest descent can be computed using Newton's method. The method was also generalized for multivariate integrals in [41].

Though these methods are incredibly powerful, we will instead focus on Filon and Levin methods, due to several factors. The path of steepest descent goes to infinity and back again, thus the numerical steepest descent methods require the integrand of the oscillatory integral to be analytic throughout the entire complex plane, except perhaps at poles and branch points. The poles and branch points add difficulty to the computation of the steepest descent

path, as great care must be taken to stay on the same branch cut so that Cauchy's theorem remains valid. This is manageable for univariate integrals, but becomes an exhausting task for multivariate integrals, where there can be complicated poles and branch points for each variable. Furthermore, the amount of computation needed to obtain an approximation is significantly greater, due to the need of computing the path of steepest descent. Finally, the methods are less effective at low frequencies: an infinite integral with the kernel $e^{-\omega x}$ does not decay quickly when ω is close to zero.

An alternative complex plane method was used to solve the first problem of [12]. The idea is that a deformation into the complex plane does not necessarily have to be along the path of steepest descent. As long as it is deformed into the exponentially decreasing quadrant, the exponential decay will take over and only a small, manageable number of oscillations will remain, and standard quadrature methods become viable. Unfortunately, such a method does not achieve higher asymptotic orders; the error only decays at the same rate as the integral itself.

2.11.   Other numerical methods

There are assorted other numerical methods developed for approximating oscillatory integrals, typically specializing on particular oscillators. We will not investigate these methods in detail in this thesis, but they are mentioned here for completeness. Many methods exist for the Fourier oscillator, which were reviewed in [27]. They all are based on the fact that moments are computable, and hence are Filon-type methods. The *Bakhvalov and Vasil'eva method* [8] interpolates f by Legendre polynomials P_k, and uses the fact that the moments of such polynomials are known explicitly:

$$\int_{-1}^{1} P_k(x) e^{i\omega x}\, dx = i^k \left(\frac{2\pi}{\omega}\right)^{\frac{1}{2}} J_{k+\frac{1}{2}}(\omega), \tag{2.11.1}$$

where J_k is a Bessel function [2].

A method based on Clenshaw–Curtis quadrature was also devised, where f is interpolated by Chebyshev polynomials T_k. We do not have simple formulæ for the resulting moments, so the polynomials T_k are then expanded into Legendre polynomials and (2.11.1) is applied [80, 63]. An alternative from [3] is to express the moments in terms of the hypergeometric function $_0F_1$ [2]. Special functions can be avoided in both these methods by expanding the Legendre or Chebyshev polynomials into the standard polynomial basis x^k, whose moments can be found via partial integration [5]. This is not effective for large k due to significant cancellation in the expansions [27].

Though it was not observed in any of these papers, all of these Filon-type methods—methods based on interpolating f—have the same asymptotic behaviour as the Levin collocation method. If the endpoints of the interval are included in the interpolation nodes,

then error decays like $\mathcal{O}\left(\omega^{-2}\right)$; otherwise the error decays at the same rate as the integrand $\mathcal{O}\left(\omega^{-1}\right)$. This will be explored in more detail in the next chapter, as well as generalization in order to achieve even higher asymptotic orders. The importance of this observation cannot be over stressed: it means that high oscillation is beneficial, not a hindrance. Furthermore, it also means that the number of interpolation points required should actually decrease as the frequency of oscillations increases. Thus at high frequencies we never need to utilize large order polynomials in order to obtain accurate results.

There are several other methods not mentioned in [27]. Longman had a series of related papers [64, 65, 66] for integrals over infinite intervals, based on expressing the integral as an infinite sum and applying the Euler transformation. A method for irregular oscillatory integrals over infinite intervals based on series transformations is presented in [83]. In this case the Euler transformation is again utilized, as well as Aitken's Δ^2-process [13], Wynn's ϵ-algorithm [13] and Sidi's W-transformation [84].

Piessens developed a Gaussian quadrature formula with respect to the weight function $\sin x$ over the interval $[-\pi, \pi]$ [81]. It however relies on considering each period separately, thus still requires a large number of function evaluations to obtain accurate approximations. A similar method based on Gaussian quadrature was developed by Zamfirescu [92], and described in [44] (the original paper is in Romanian). We can rewrite the sine Fourier integral as

$$\int_0^1 f(x)\sin\omega x\,\mathrm{d}x = \int_0^1 f(x)(1+\sin\omega x)\,\mathrm{d}x - \int_0^1 f(x)\,\mathrm{d}x.$$

The second of these integrals is nonoscillatory, so the methods of Section 2.1 can be used to approximate its value. The first integral now has a nonnegative weight function, hence we can approximate it by a weighted sum. Since the moments with respect to the weight function are known, we can successfully compute the quadrature weights needed.

A very effective quadrature scheme is developed in [56] for the standard Fourier oscillator. The paper uses a weighted sum of the value of the function f and its first derivative at evenly spaced nodes, determining the weights so as to maximize the degree of polynomials integrated exactly. It is noted that, for a method of N points, the error behaves like $\mathcal{O}\left(\omega^{-N}\right)$. This is generalized to use higher order derivatives of f in [57], resulting in a significant decrease in error.

A method based on a minimax algorithm for oscillatory integrals of the form

$$\int_a^b f(x)\phi(x)\,\mathrm{d}x$$

is presented in [70]. It proves that the method is optimal-by-order. It then demonstrates

the method for the specific integrals

$$\int_a^b f(x) \begin{cases} \sin \omega x \\ \cos \omega x \end{cases} \mathrm{d}x,$$

in which case the method consists of approximating f by a spline v and integrating

$$\int_a^b v(x) \begin{cases} \sin \omega x \\ \cos \omega x \end{cases} \mathrm{d}x$$

explicitly. This is generalized to multivariate integrals over Cartesian products of intervals in [72, 71, 93]. In these papers, explicit quadrature formulæ are presented for the integrals

$$\int_a^b \int_c^d f(x,y) \begin{cases} \sin \omega x \sin \omega y \\ \cos \omega x \cos \omega y \end{cases} \mathrm{d}x.$$

In [6], local Fourier bases are used to approximate oscillatory integrals, with a generalization to multivariate rectangular domains in [7]. Unfortunately, though the resulting linear system is sparse, these methods require that the number of bases functions grows with the frequency, hence they are not competitive with other methods discussed in this thesis.

There is also a comparison of methods for irregular oscillators in [27]. In addition to the Levin collocation method and the Chung, Evans and Webster method already discussed, there is method developed by Evans in [22] where the transformation $y = g(x)$ is used to convert the irregular oscillator to a standard Fourier oscillator:

$$I[f] = \int_{g(a)}^{g(b)} \frac{f(g^{-1}(y))}{g'(g^{-1}(y))} \mathrm{e}^{\mathrm{i}\omega y} \, \mathrm{d}y. \tag{2.11.2}$$

Once the integral is in this form, a Filon-type method can be employed, in particular the method based on Clenshaw–Curtis quadrature. This technique is successful whenever the interval does not contain stationary points. Unfortunately it requires the computation of the inverse of g, albeit only at the interpolation points.

Another method for irregular oscillators is proposed by Evans in [23]. Instead of interpolating f by polynomials, we can interpolate $\frac{f(x)}{g'(x)}$ using a basis of the form

$$\sum c_k \psi_k(g(x)).$$

Then making the transformation $y = g(x)$, as in (2.11.2), does not require the computation of inverses of g. We must, however, be careful in the choice of the basis ψ_k. A related idea for integrals with stationary points will be presented in Chapter 4.

In [14], the problem of solving the acoustic equation of Section 1.2 was tackled. This method required the computation of oscillatory integrals, for which a new quadrature scheme was derived. As mentioned in Section 2.3, at high frequencies, univariate oscillatory integrals

are dominated by the contribution from the stationary points and endpoints (multivariate integrals are dominated by contributions from stationary points, resonance points and vertices). Thus we can obtain a high accuracy approximation by numerically integrating near these important points, and throwing away the contributions from the more oscillatory regions. This is accomplished by utilizing smooth windowing functions that focus on ϵ neighbourhoods of these important points. The part of the integral which we throw away decays exponentially fast as the frequency increases; though the error in the approximation only decays at the same rate as the integral due to quadrature error in each ϵ neighbourhood.

Chapter 3

Univariate Highly Oscillatory Integrals

Having reviewed the existing literature, we now begin developing the Filon and Levin collocation methods further. The basic idea is to put these two methods on the same framework as the asymptotic expansion, which will allow us to generalize the methods for higher asymptotic orders, whilst retaining their convergent properties. In this chapter we focus on the univariate highly oscillatory integral

$$I[f] = \int_a^b f(x) e^{i\omega g(x)} \, dx.$$

Until Chapter 4 we assume that g' does not vanish within $[a, b]$, in other words there are no stationary points. We also assume for simplicity that f and g are smooth, i.e., infinitely differentiable. Generalization of the results presented here to the case where $f, g \in C^r[a, b]$ is straightforward.

The key observation is that the asymptotic expansion only depends on the value and derivatives of f evaluated at the boundary points. Thus if we can write our approximation scheme as a highly oscillatory integral $I[v]$, then we can determine the asymptotic order of the error of the approximation by comparing f and v at the endpoints. The two primary numerical methods we investigated in the preceding chapter—the Filon method and Levin collocation method—both satisfy this property.

We begin with the development of Filon-type methods in Section 3.1, which is based on results in [**48**]. The idea is fairly straightforward: instead of dividing the interval into panels and performing a piecewise quadratic interpolation as in the original Filon method, we use Hermite interpolation over the entirety of the interval. This ensures that the derivatives of the interpolant match those of f up to a given order, and the approximation achieves a higher asymptotic order. Furthermore it retains the character of the original Filon method: adding additional sample points reduces the error further.

These new Filon-type methods require moments, which in certain applications are unavailable. Thus in Section 3.2 we look again at the Levin collocation method, using the ideas from the construction of Filon-type methods to derive Levin-type methods, which also obtain higher asymptotic order. This is accomplished in much the same manner; we use multiplicities in the collocation system. We also compare the Filon-type and Levin-type methods numerically. In their initial development, we use a polynomial basis in Levin-type methods. This is not strictly necessary, and in Section 3.3 we use information about f and

g to develop a more suitable collocation basis, which is based on the asymptotic expansion. This is exploited in Section 3.4, which investigates approximating integrals where f is badly behaved, in particular the Runge example.

In their initial construction, Filon-type and Levin-type methods require derivatives of f in order to achieve higher asymptotic orders. If f is at all complicated, computing its derivatives is a nontrivial task. In Section 3.5 we use an idea developed in [47] to achieve higher asymptotic orders without using derivatives, by choosing interpolation points that behave like finite difference formulæ as the frequency ω increases. Finally, in Section 3.6 we find some error bounds for a Filon-type method and a Filon–trapezoidal rule, where f is approximated by a piecewise affine function v which is integrated exactly.

Remark: Section 3.1 is based on results by Iserles and Nørsett in [48]. Sections 3.2 through 3.4 contain original research, first presented in [75]. Section 3.5 is based on results again by Iserles and Nørsett, from [47]. Section 3.6 consists of new research, derived with Daan Huybrechs.

3.1. Filon-type methods

The following corollary will be used in the proof of the order of error for Filon-type and Levin-type methods.

Corollary 3.1.1 *Allowing f to depend on ω, suppose for some $n \geq 0$ that $f = \mathcal{O}\!\left(\omega^{-n}\right)$, where $\mathcal{O}\!\left(\omega^{-n}\right)$ means that the $L^\infty[a,b]$ norm of f and its derivatives are all $\mathcal{O}\!\left(\omega^{-n}\right)$, cf. Notation. Furthermore, suppose that*

$$0 = f(a) = f'(a) = \cdots = f^{(s-1)}(a)\,,$$
$$0 = f(b) = f'(b) = \cdots = f^{(s-1)}(b)\,.$$

Then $I[f] \sim \mathcal{O}\!\left(\omega^{-n-s-1}\right)$, for $\omega \to \infty$.

Proof: Recall the asymptotic expansion from Section 2.2:

$$I[f] = -\sum_{k=1}^{s+1} \frac{1}{(-\mathrm{i}\omega)^k}\left\{\sigma_k(b)\mathrm{e}^{\mathrm{i}\omega g(b)} - \sigma_k(a)\mathrm{e}^{\mathrm{i}\omega g(a)}\right\} + \frac{1}{(-\mathrm{i}\omega)^{s+1}}\int_a^b g'\sigma_{s+2}\mathrm{e}^{\mathrm{i}\omega g}\,\mathrm{d}x,$$

where

$$\sigma_1 = \frac{f}{g'}\,, \qquad \sigma_{k+1} = \frac{\sigma_k'}{g'}\,, \qquad k \geq 1.$$

Each σ_k depends on f and its first $k-1$ derivatives, in the sense that it is a sum of terms independent of ω, each multiplied by some function in the set $\left\{f, \ldots, f^{(k-1)}\right\}$. Thus it follows

34

that $0 = \sigma_k(a) = \sigma_k(b)$ for all $k \leq s$, and the first s terms of the asymptotic expansion are identically zero. Thus we obtain

$$I[f] = -\frac{1}{(-\mathrm{i}\omega)^{s+1}} \left\{ \sigma_{s+1}(b)\mathrm{e}^{\mathrm{i}\omega g(b)} - \sigma_{s+1}(a)\mathrm{e}^{\mathrm{i}\omega g(a)} \right\} + \frac{1}{(-\mathrm{i}\omega)^{s+1}} \int_a^b g' \sigma_{s+2} \mathrm{e}^{\mathrm{i}\omega g} \, \mathrm{d}x.$$

From the properties of $\boldsymbol{\mathcal{O}}(\cdot)$ in Notation, we know that $\sigma_{s+1} = \boldsymbol{\mathcal{O}}(\omega^{-n})$. Thence $\sigma_{s+1}(b)$ and $\sigma_{s+1}(a)$ are $\mathcal{O}(\omega^{-n})$. Furthermore, the integral is also of order $\mathcal{O}(\omega^{-n})$, and all three terms are $\mathcal{O}(\omega^{-n-s-1})$.

<div align="right">Q.E.D.</div>

We could, of course, use the partial sums of the asymptotic expansion to approximate $I[f]$. The accuracy of this approximation would improve as the frequency of oscillations ω increased. Unfortunately, the expansion will typically not converge for fixed ω, thus there is a limit to the accuracy of an asymptotic expansion. Hence we derive a *Filon-type method*, a method which will provide convergent approximations whilst retaining the asymptotic behaviour of the expansion. Given some sequence of *nodes* $\{x_1, \ldots, x_\nu\}$ and *multiplicities* $\{m_1, \ldots, m_\nu\}$, the idea is to approximate f by a polynomial $v = \sum_{k=1}^n c_k x^{k-1}$ using Hermite interpolation, where $n = \sum m_k$. We thus determine the coefficients c_k by solving the system

$$v(x_k) = f(x_k) \, , v'(x_k) = f'(x_k) \, , \ldots, v^{(m_k-1)}(x_k) = f^{(m_k-1)}(x_k) \, , \qquad k = 1, \ldots, \nu.$$

We will assume for simplicity that $x_1 = a$ and $x_\nu = b$. If the moments of $\mathrm{e}^{\mathrm{i}\omega g}$ are available, then we can calculate $I[v]$ explicitly. We thus define a Filon-type method as

$$Q^F[f] = I[v] = \sum_{k=1}^n c_k I\left[x^{k-1}\right].$$

Because the accuracy of $Q^F[f]$ depends on the accuracy of v interpolating f, adding additional sample points and multiplicities will typically decrease the error. If v converges uniformly to f, then the approximation $Q^F[f]$ converges to the solution $I[f]$. We can easily prove the asymptotic order of this method:

Theorem 3.1.2 [48] *Let $s = \min\{m_1, m_\nu\}$. Then*

$$I[f] - Q^F[f] \sim \mathcal{O}(\omega^{-s-1}).$$

Proof: The order of error of this method follows immediately from Corollary 3.1.1:

$$I[f] - Q^F[f] = I[f] - I[v] = I[f - v] \sim \mathcal{O}(\omega^{-s-1})$$

as $\omega \to \infty$, since $f - v$ and its first $s - 1$ derivatives are zero at the endpoints.

<div align="right">Q.E.D.</div>
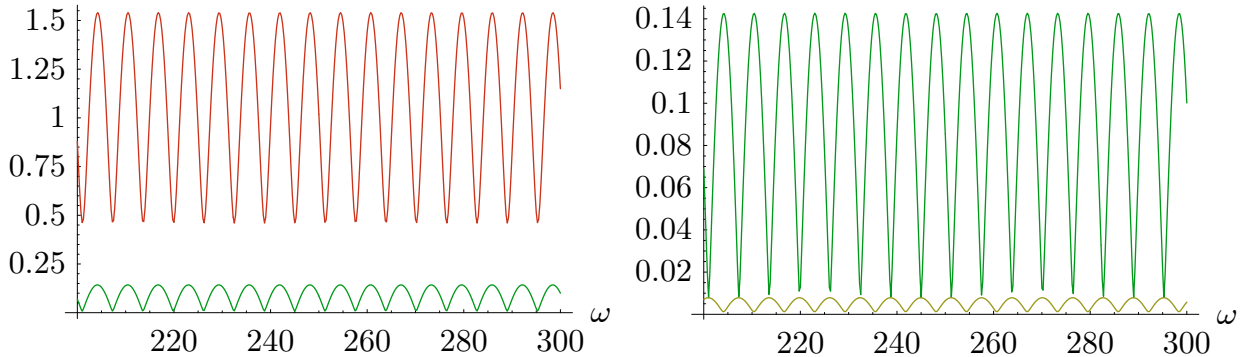
Figure 3.6: The error scaled by ω^3 of the asymptotic expansion (left graph, top), $Q^F[f]$ with only endpoints and multiplicities both two (left graph, bottom)/(right graph, top), and $Q^F[f]$ with nodes $\left\{0, \frac{1}{2}, 1\right\}$ and multiplicities $\{2, 1, 2\}$ (right graph, bottom) for $I[f] = \int_0^1 \cos x\, \mathrm{e}^{\mathrm{i}\omega x}\, \mathrm{d}x$.

We will now compare Filon-type methods to the asymptotic expansion numerically to show that we can indeed decrease the error by adding interpolation points. Consider the fairly simple integral

$$I[f] = \int_0^1 \cos x\, \mathrm{e}^{\mathrm{i}\omega x}\, \mathrm{d}x.$$

In Figure 3.6 we compare several methods of order three: the two-term asymptotic expansion, $Q^F[f]$ with nodes $\{0, 1\}$ and multiplicities $\{2, 2\}$, and $Q^F[f]$ with nodes $\left\{0, \frac{1}{2}, 1\right\}$ and multiplicities $\{2, 1, 2\}$. Even when sampling f only at the endpoints of the interval, the Filon-type method represents a significant improvement over the asymptotic expansion, having approximately one-twelfth the error, while using exactly the same information about the function f. Adding an additional interpolation point results in an error indistinguishable from zero in the graph. Adding additional node points continues to have a similar effect.

3.2. Univariate Levin-type methods

The major problem with using Filon-type methods is that they still require explicit formulæ for the moments $I\left[x^k\right]$, which are not known for general functions g. But we can employ the same idea of using multiplicities for the Levin collocation method, to obtain a *Levin-type method*. We still wish to find a particular solution to the differential equation

$$\mathcal{L}[v] = f \qquad \text{for} \qquad \mathcal{L}[v] = v' + \mathrm{i}\omega g' v.$$

For the given *nodes* $\{x_1, \ldots, x_\nu\}$ we associate a sequence of *multiplicities* $\{m_1, \ldots, m_\nu\}$. We then determine an approximate solution

$$v = \sum_{k=1}^n c_k \psi_k,$$

36

where $\{\psi_1, \ldots, \psi_n\}$ is a given *basis* and $n = \sum m_k$.

The unknown coefficients c_k are determined by solving the system:

$$\mathcal{L}[v](x_k) = f(x_k), \mathcal{L}[v]'(x_k) = f'(x_k), \ldots, \mathcal{L}[v]^{(m_k-1)}(x_k) = f^{(m_k-1)}(x_k), \qquad k = 1, \ldots, \nu.$$
(3.2.1)

The number of equations in this system is n, exactly the same as the number of unknowns in v. If every multiplicity m_k is one, then this is equivalent to the original Levin collocation method. We will prove that, as in a Filon-type method, if the multiplicities at the endpoint are greater than or equal to s, then $I[f] - Q^L[f] \sim \mathcal{O}(\omega^{-s-1})$. Thus we obtain the same asymptotic behaviour as a Filon-type method without requiring moments, and using exactly the same information about f and g. In order to prove the order of error, we require that the *regularity condition* is satisfied, which states that the set of functions $\{\psi_k\}$ can interpolate any function at the given nodes and multiplicities.

Theorem 3.2.1 *Suppose that the regularity condition is satisfied, and that $g' \neq 0$ within $[a, b]$. Then*

$$I[f] - Q^L[f] \sim \mathcal{O}(\omega^{-s-1}),$$

where $s = \min\{m_1, m_\nu\}$ and

$$Q^L[f] = v(b)\mathrm{e}^{\mathrm{i}\omega g(b)} - v(a)\mathrm{e}^{\mathrm{i}\omega g(a)}.$$

Proof: The error term of the approximation is $I[f] - Q^L[f] = I[f - \mathcal{L}[v]]$. In order to use Corollary 3.1.1 we need to show that $f - \mathcal{L}[v] = \mathcal{O}(1)$. Since f is independent of ω, we need only worry about $\mathcal{L}[v]$. Using Cramer's rule, we will show that each c_k is of order $\mathcal{O}(\omega^{-1})$. Define the operator $\mathcal{P}[f]$, written in partitioned form as

$$\mathcal{P}[f] = \begin{pmatrix} \rho_1[f] \\ \vdots \\ \rho_\nu[f] \end{pmatrix}, \qquad \text{where} \qquad \rho_k[f] = \begin{pmatrix} f(x_k) \\ \vdots \\ f^{(m_k-1)}(x_k) \end{pmatrix}.$$

Basically, $\mathcal{P}[f]$ maps f to the value of it and its derivatives at every node in $\{x_1, \ldots, x_\nu\}$ with multiplicities $\{m_1, \ldots, m_\nu\}$. Note that the system (3.2.1) can be written as $Ac = f$, for $c = (c_1, \cdots, c_n)^\top$ and

$$A = (\mathcal{P}[\mathcal{L}[\psi_1]], \cdots, \mathcal{P}[\mathcal{L}[\psi_n]]) = \left(\mathcal{P}[\psi_1'] + \mathrm{i}\omega \mathcal{P}[g'\psi_1], \cdots, \mathcal{P}[\psi_n'] + \mathrm{i}\omega \mathcal{P}[g'\psi_n]\right) = P + \mathrm{i}\omega G,$$

where

$$P = \left(\mathcal{P}[\psi_1'], \cdots, \mathcal{P}[\psi_n']\right), \qquad G = \left(\mathcal{P}[g'\psi_1], \cdots, \mathcal{P}[g'\psi_n]\right) \qquad \text{and} \qquad f = \mathcal{P}[f].$$

Solving the system $Gc = f$ is equivalent to interpolating f by $\{g'\psi_k\}$ at the given nodes and multiplicities. Thus the regularity condition ensures that $\det G \neq 0$. It follows that

37
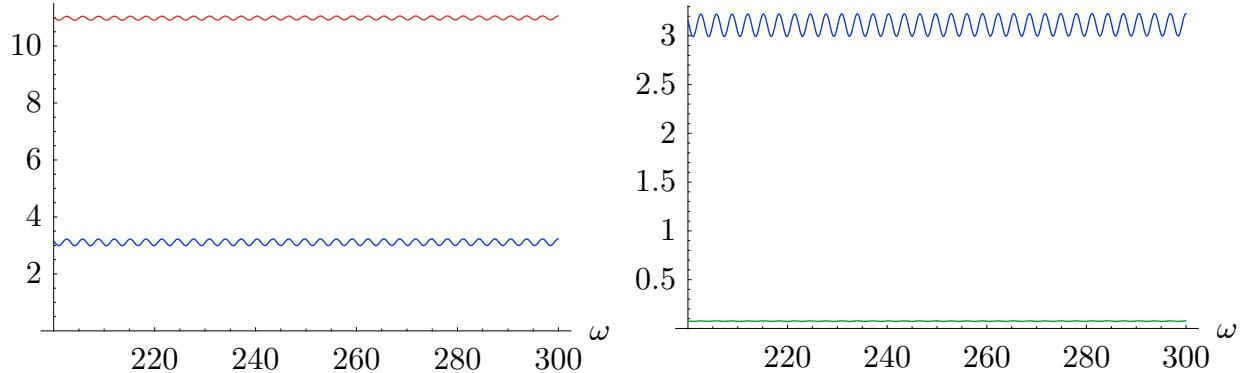
Figure 3.7: The error scaled by ω^3 of the two-term asymptotic expansion (left graph, top), $Q^L[f]$ (left graph, bottom)/(right graph, top) and $Q^F[f]$ (right graph, bottom) both with only endpoints and multiplicities two for $I[f] = \int_0^1 \cos x \, e^{i\omega(x^2+x)} \, dx$.

$\det A = (i\omega)^n \det G + \mathcal{O}(\omega^{n-1})$, hence large enough ω ensures that A is nonsingular and $(\det A)^{-1} = \mathcal{O}(\omega^{-n})$. Furthermore $\det A_k = \mathcal{O}(\omega^{n-1})$, for A_k defined as the matrix A with the kth column replaced by $\boldsymbol{f}$, since it has one less column of order $\mathcal{O}(\omega)$. Hence, by Cramer's rule,

$$c_k = \frac{\det A_k}{\det A} = \mathcal{O}(\omega^{-1}).$$

It follows that $v = \mathcal{O}(\omega^{-1})$; thus $\mathcal{L}[v] = \mathcal{O}(1)$, and the theorem follows.

Q.E.D.

Theorem 3.2.2 provides a simplified version of the regularity condition. It is especially helpful as it ensures that the standard polynomial basis can be used with a Levin-type method and any choice of nodes and multiplicities. Recall from [**82**] that a *Chebyshev set* is a basis of n functions that spans a set M that satisfies the *Haar condition*; in other words, that every function $u \in M$ has less than $n+1$ roots to the equation $u(x) = 0$ in the interval $[a, b]$. Equivalently, the basis can interpolate at any given sequence of n nodes.

Theorem 3.2.2 *Suppose that the basis $\{\psi_1, \ldots, \psi_n\}$ is a Chebyshev set. Then the regularity condition is satisfied for all choices of nodes and multiplicities.*

Figure 3.7 will demonstrate the effectiveness of this method. Consider the integral $\int_0^1 \cos(x) e^{i\omega(x^2+x)} \, dx$, in other words $f(x) = \cos x$ and $g(x) = x^2 + x$. We have no stationary points and moments are computable, hence all the methods discussed so far are applicable. We compare the asymptotic expansion with a Filon-type method and a Levin-type method, each with nodes $\{0, 1\}$ and multiplicities both two. For this choice of f and g,

38
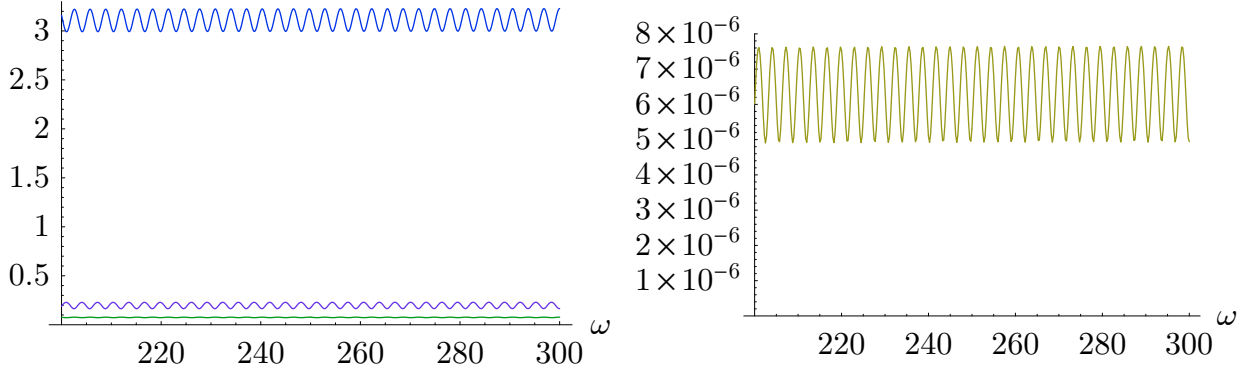
Figure 3.8: The error scaled by ω^3 of $Q^L[f]$ (left graph, top) and $Q^F[f]$ (left graph, bottom) both with only endpoints and multiplicities two compared to $Q^L[f]$ (left graph, middle) and $Q^F[f]$ (right graph) both with nodes $\left\{0, \frac{1}{4}, \frac{2}{3}, 1\right\}$ and multiplicities $\{2, 2, 1, 2\}$ for $I[f] = \int_0^1 \cos x \, \mathrm{e}^{\mathrm{i}\omega(x^2+x)} \, \mathrm{d}x$.

the Levin-type method is a significant improvement over the asymptotic expansion, whilst the Filon-type method is even more accurate.

Figure 3.8 compares the Levin-type method and the Filon-type method with the addition of two sample points. This graph helps emphasize the effectiveness of adding node points within the interval of integration. With just two additional node points, only one of which has multiplicity greater than one, the error of $Q^L[f]$ is less than a sixth of what it was. In fact it is fairly close to the former $Q^F[f]$ while still not requiring the knowledge of moments. On the other hand, adding the same node points and multiplicities to $Q^F[f]$ results in an error significantly smaller than the original $Q^L[f]$. It should be emphasized that even $Q^L[f]$ with only endpoints is still a very effective method, as all the values in this graph are divided by $\omega^3 \geq 200^3 = 8 \cdot 10^6$.

3.3. Asymptotic basis

For a Levin-type method we do not have to use polynomials for the collocation basis $\{\psi_k\}$. Not only can we greatly improve the accuracy of the approximation by choosing the basis wisely, but surprisingly we can even obtain higher asymptotic orders. The idea is to choose $\{\psi_k\}$ so that $\mathcal{L}[v]$ is qualitatively similar in shape to f within the interval of integration. We know the asymptotic expansion is very accurate at high frequencies, however it diverges in general, and is not very accurate in the low frequency regime. In this section we use the terms of the asymptotic expansion, however we throw away the coefficients of the expansion, determining them via a Levin collocation system. It turns out that we retain the asymptotic order of the expansion, whilst improving the accuracy significantly.

Theorem 3.3.1 *Define $Q^B[f]$ as a Levin-type method with the basis*

$$\psi_1 = \frac{f}{g'} \qquad and \qquad \psi_{k+1} = \frac{\psi'_k}{g'}.$$

If the regularity condition is satisfied then

$$Q^B[f] - I[f] = \mathcal{O}\left(\omega^{-n-s-1}\right),$$

where s is again the minimum endpoint multiplicity $s = \min\{m_1, m_\nu\}$.

Proof: We postpone a detailed proof of this theorem until Theorem 5.3.2, since it is a special case of the multivariate version. We however present a very brief sketch of the proof. Note that

$$\mathcal{L}[v] - f = \sum_{k=1}^{n} c_k \mathcal{L}[\psi_k] - f = \sum_{k=1}^{n} c_k \left(\psi'_k + i\omega g' \psi_k\right) - f$$

$$= \sum_{k=1}^{n} c_k \left(g' \psi_{k+1} + i\omega g' \psi_k\right) - g' \psi_1$$

$$= g' \left[(i\omega c_1 - 1)\psi_1 + \sum_{k=2}^{n} (c_{k-1} + i\omega c_k)\psi_k + c_n \psi_{n+1}\right]$$

$$= \frac{g'}{\det A} \left[(i\omega \det A_1 - \det A)\psi_1 + \sum_{k=2}^{n} (\det A_{k-1} + i\omega \det A_k)\psi_k + \det A_n \psi_{n+1}\right],$$

where A is again the matrix associated with the Levin collocation system and A_k is the matrix A with the kth row replaced by $\boldsymbol{f} = \mathcal{P}[f]$, as in Theorem 3.2.1. It is possible to show via determinant manipulations that each of the constants within the bracket are $\mathcal{O}(1)$, whilst we have already seen in the proof of Theorem 3.2.1 that $(\det A)^{-1} = \mathcal{O}\left(\omega^{-n}\right)$. Thus

$$\mathcal{L}[v] - f = \boldsymbol{\mathcal{O}}\left(\omega^{-n}\right),$$

and the proof follows from Corollary 3.1.1.

Q.E.D.

In the examples that follow, we include the constant function $\psi_1(x) \equiv 1$ in our collocation basis, in addition to the terms of the asymptotic basis. This does not affect the proof of the preceding theorem, other than that the error is now $\mathcal{O}\left(\omega^{-n-s}\right)$.

Consider the integral $\int_0^1 \log(x+1) \, e^{i\omega x} \, dx$. In Figure 3.9, we compare methods of order $\mathcal{O}\left(\omega^{-4}\right)$. This includes the three-term asymptotic exansion, $Q^F[f]$ (which is equivalent to $Q^L[f]$ with a polynomial basis) with nodes $\{0, 1\}$ and multiplicities both three, and $Q^B[f]$
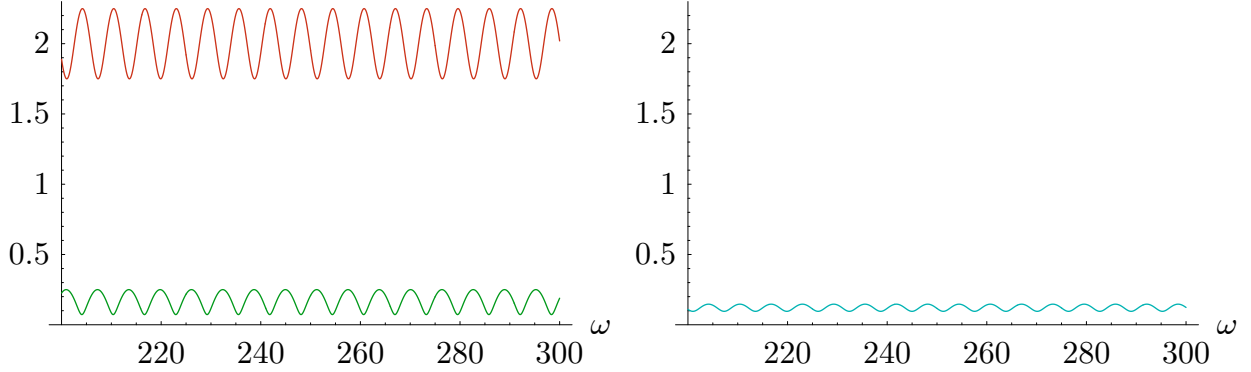
Figure 3.9: The error scaled by ω^4 of the three-term asymptotic expansion (left graph, top), $Q^F[f]$ with endpoints for nodes and multiplicities three (left graph, bottom), and $Q^B[f]$ in with nodes $\left\{0, \frac{1}{2}, 1\right\}$ and multiplicities one (right graph) for $I[f] = \int_0^1 \log(x+1)\, \mathrm{e}^{\mathrm{i}\omega x}\, \mathrm{d}x$.
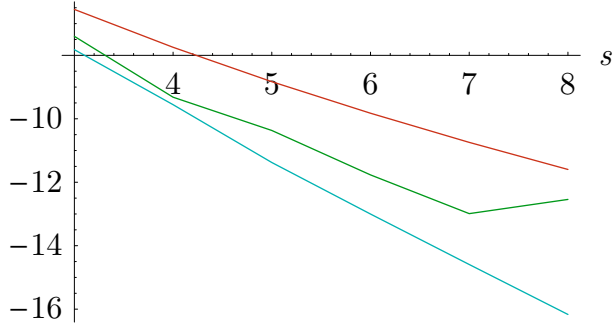
Figure 3.10: The base-10 logarithm of the error of the s-term asymptotic expansion (top), $Q^F[f]$ with endpoints for nodes and multiplicities s (middle), and $Q^B[f]$ with nodes $\{k/(s-1)\}_{k=0}^{s-1}$ and multiplicities all one (bottom) for $I[f] = \int_0^1 \log(x+1)\mathrm{e}^{\mathrm{i}\omega x}\, \mathrm{d}x$.

using nodes $\left\{0, \frac{1}{2}, 1\right\}$ and multiplicities all one. The results are decent, with $Q^B[f]$ being slightly more accurate than $Q^F[f]$ on average, though with a smaller collocation system.

The problem with the asymptotic expansion and $Q^F[f]$ with endpoints for nodes and multiplicities both s is that, in general, as $s \to \infty$ these methods diverge. Hence another worthwhile comparison is to see how $Q^B[f]$ compares to these two methods for fixed ω and increasing asymptotic order. Thus fix $\omega = 50$, chosen purposely relatively small since the larger ω, the longer it takes for increasing the asymptotic order to cause the approximations to diverge. This choice results in Figure 3.10, where we take the base-10 logarithm of the errors. This figure clearly shows the benefit of using $Q^B[f]$ for this particular case. Though at lower orders the errors of $Q^F[f]$ and $Q^B[f]$ are very similar, at higher orders they differ by orders of magnitude.
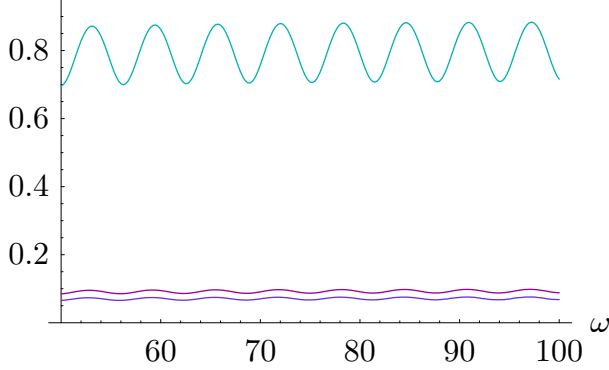
Figure 3.11: The error scaled by ω^6 of $Q^B[f]$ with nodes $\left\{0, \frac{1}{4}, \frac{1}{2}, \frac{3}{4}, 1\right\}$ and multiplicities all one (bottom), nodes $\left\{0, \frac{1}{2}, 1\right\}$ and multiplicities $\{1, 3, 1\}$ (middle), and nodes $\{0, 1\}$ and multiplicities both equal to two (top) for $I[f] = \int_0^1 \log(x+1)\mathrm{e}^{\mathrm{i}\omega x}\,\mathrm{d}x$.

We can also compare $Q^B[f]$ with itself under different choices of node points. Though we retain the same f and g, we compare different methods of order $\mathcal{O}(\omega^{-6})$ to increase the number of possible node choices. We consider three choices of nodes and multiplicities: nodes $\left\{0, \frac{1}{4}, \frac{1}{2}, \frac{3}{4}, 1\right\}$ and multiplicities all one, nodes $\left\{0, \frac{1}{2}, 1\right\}$ and multiplicities $\{1, 3, 1\}$, and nodes $\{0, 1\}$ and multiplicities both equal to two. This results in Figure 3.11. We take relatively mild values for ω as for any value significantly larger the accuracy reaches IEEE machine precision. It is not entirely suprising that the more concentrated the sampling the less accurate the approximation. Though they are not displayed in the preceding figure, for comparison the asymptotic expansion performed horribly, oscillating between 23 and 25, whilst $Q^F[f]$ with nodes $\{0, 1\}$ and multiplicities five performed roughly in the middle of the pack, oscillating between 0.2 and 0.8.

3.4. Runge's phenomenon

Unfortunately, it is not always true that the Filon-type method is more accurate than the asymptotic expansion. Take the case of the Fourier oscillator and $f(x) = \left(1 + 25x^2\right)^{-1}$, now over the interval $[-1, 1]$. This suffers from Runge's phenomenon, as described in [82], where certain nonoscillatory functions have oscillating interpolation polynomials. Since the Filon-type method is based on interpolation, it is logical that the accuracy of $Q^F[f]$ is directly related to the interpolation accuracy. In Figure 3.12 we see that adding additional nodes actually reduces the accuracy of $Q^F[f]$. It should be noted that in this example $Q^F[f]$ with only endpoints and the one-term asymptotic expansion are equivalent, which can be trivially proved by finding the explicit formula for $Q^F[f]$. Thus the asymptotic expansion is the best method of the three tried.
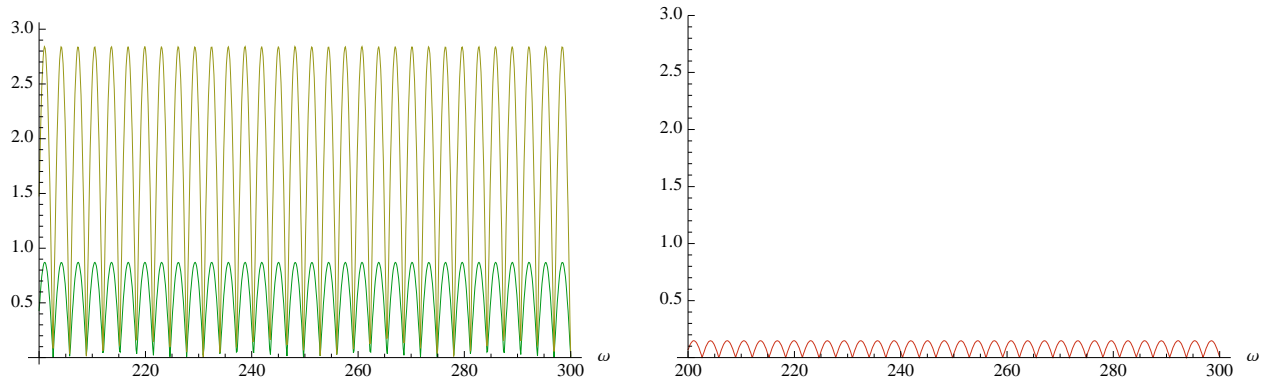
Figure 3.12: The error scaled by ω^2 of $Q^F[f]$ with only endpoints (right graph), endpoints and two additional evenly spaced points (left graph, bottom), and endpoints and four additional evenly spaced points (left graph, top), where all multiplicities are one for $I[f] = \int_{-1}^{1} \frac{1}{1+25x^2} e^{i\omega x} \, dx$.
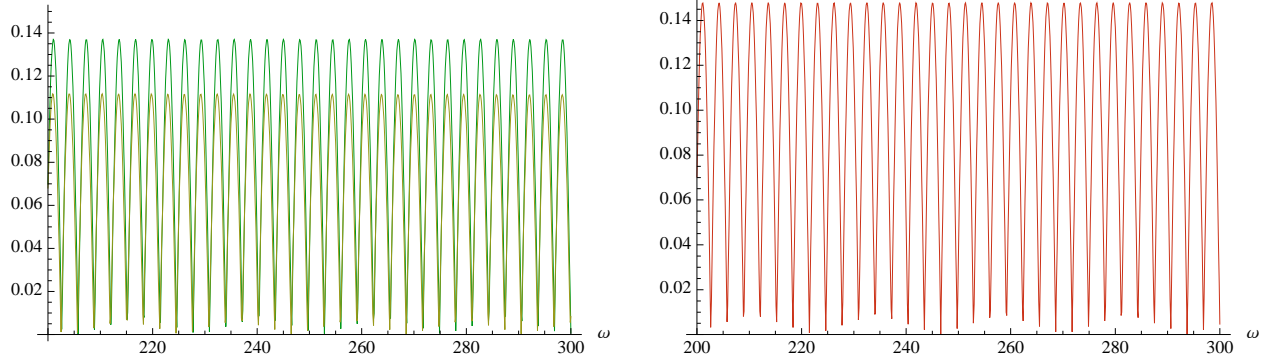

Figure 3.13: The error scaled by ω^2 of $Q^F[f]$ with only endpoints (right graph), endpoints and two additional Chebyshev interpolation points (left graph, top), and endpoints and four additional Chebyshev interpolation points (left graph, bottom), where all multiplicities are one for $I[f] = \int_{-1}^{1} \frac{1}{1+25x^2} e^{i\omega x} \, dx$.

We know that using Chebyshev interpolation points, also described in [82], eliminates Runge's phenomenon. Using this choice for nodes, along with the required endpoint nodes, results in the errors seen in Figure 3.13. Now adding additional node points results in a more accurate approximation. This certainly is a huge improvement over Figure 3.12, but Filon-type methods definitely do not have the same magnitude of improvement over the asymptotic expansion that they did in Figure 3.7.

Since $Q^B[f]$ is not polynomial interpolation, there is a good chance that Runge's phenomenon will not affect us in the same way. In fact, numerical tests show that $Q^B[f]$ has significantly less error than its polynomial counterparts. Direct computation shows that $\det A$ is a polynomial in ω of degree $n - 1$, not of degree n. Fortunately, the proof of The-

43
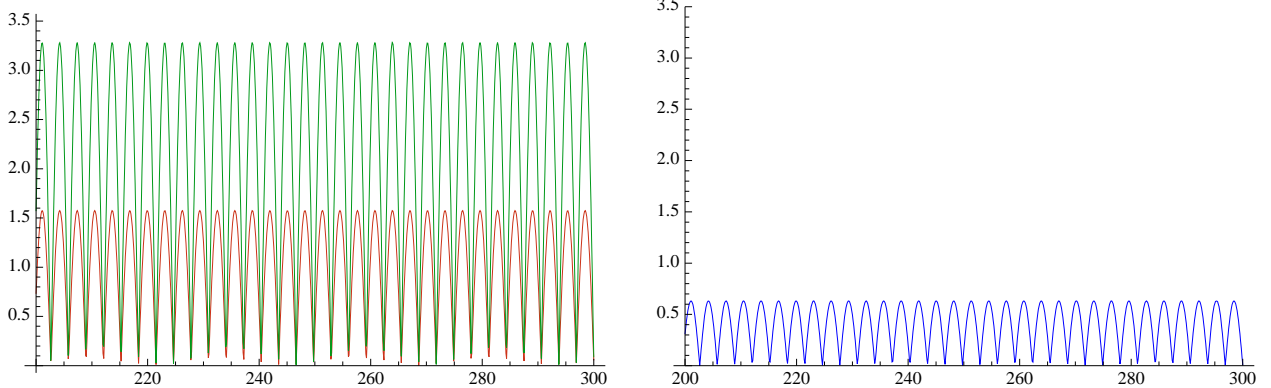
Figure 3.14:   The error scaled by ω^4 of the three-term asymptotic expansion (left graph, bottom), $Q^F[f]$ with only endpoints and multiplicities three (left graph, top), and $Q^B[f]$ with endpoints and two Chebyshev nodes, all with multiplicity one (right graph) for $I[f] = \int_{-1}^{1} \frac{1}{1+25x^2} e^{i\omega x}\, dx$.
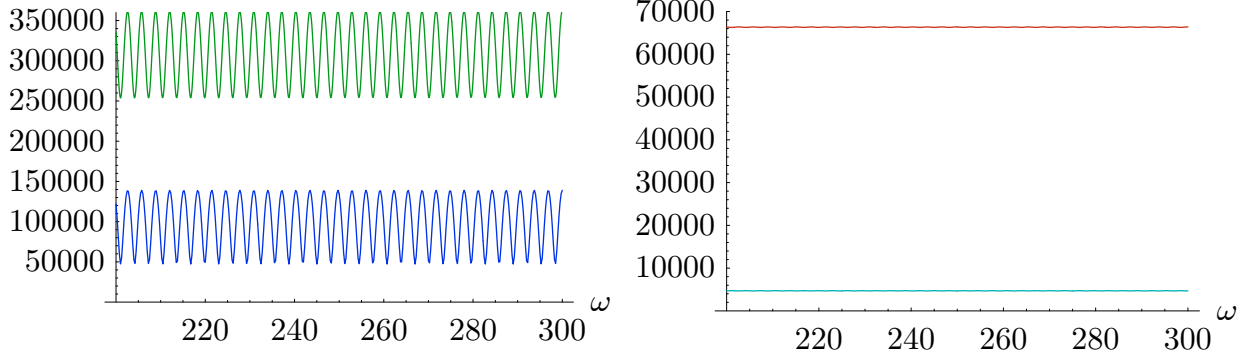

Figure 3.15:   The error scaled by ω^3 of $Q^F[f]$ with endpoints and multiplicities both two (left graph, top), $Q^L[f]$ with endpoints and multiplicities both two (left graph, bottom), the two-term asymptotic expansion (right graph, top) and $Q^B[f]$ with endpoints and multiplicities all one (right graph, bottom) for $I[f] = \int_{0}^{1} e^{10x} e^{i\omega(x^2+x)}\, dx$.

orem 3.3.1 holds as is, except that $Q^B[f]$ now has error of order $\mathcal{O}\!\left(\omega^{-n-s+1}\right)$. Again we compare methods of similar order in Figure 3.14, which shows that $Q^B[f]$ is the best of the three methods tried.

Remark: Another option, with regard to Runge's phenomenon, is to use cubic splines in place of interpolation. Unfortunately this suffers from the fact that a cubic spline can only match the function and its first two derivatives at the endpoints, hence the order is at most $\mathcal{O}\!\left(\omega^{-4}\right)$ in the present framework, though higher order splines can achieve higher asymptotic orders. In Section 3.6 we investigate using the simplest "spline" approximation, namely piecewise affine functions.

s	Asym. expan.	$Q^F[f]$	$Q^L[f]$	$Q^B[f]$
2	0.0083	0.042	0.015	0.00059
3	0.00011	0.0016	0.00043	$2.8 \cdot 10^{-6}$
5	$1.7 \cdot 10^{-8}$	$1.3 \cdot 10^{-6}$	$3 \cdot 10^{-7}$	$9.9 \cdot 10^{-12}$

Table 3.1: The absolute value of the errors for $\omega = 200$ of the following methods of order $\mathcal{O}(\omega^{-s-1})$: the s-term asymptotic expansion, $Q^F[f]$ and $Q^L[f]$ with endpoints and multiplicities both s, and $Q^B[f]$ with nodes $\{k/(s-1)\}_{k=0}^{s-1}$ and multiplicities all one for $I[f] = \int_0^1 \mathrm{e}^{10x} \mathrm{e}^{200\mathrm{i}(x^2+x)} \, \mathrm{d}x$.

Similar to Runge's phenomenon is the situation when f increases much too fast to be accurately approximated by polynomials. Let $f(x) = \mathrm{e}^{10x}$ and $g(x) = x^2 + x$. Note that this appears to be a ludicrously difficult example—not only do we have high oscillations but f exceeds $22,000$ in the interval of integration! Amazingly, we will see that the methods described are still very accurate, especially a Levin-type method with asymptotic basis. We compare $Q^B[f]$ which has only endpoints for nodes and multiplicities all one to the two-term asymptotic expansion and $Q^F[f]$ with only endpoints for nodes and multiplicities both two in Figure 3.15. We omit the proof that the regularity condition for $Q^B[f]$ is satisfied, as it is a simple exercise in linear algebra.

In this example $Q^F[f]$ produces a tremendously bad approximation, due to the difficulty in interpolating an exponential by a polynomial. As seen in Table 3.1, the actual error for $\omega = 200$ is about 0.042. On the other hand, the asymptotic expansion performed significantly better than the Filon-type method, though still not spectacularly, with an error of approximately 0.0083 for $\omega = 200$. The star of this show is clearly $Q^B[f]$, where the actual error for $\omega = 200$ is about 0.000585; less than a tenth of the error of the asymptotic expansion.

Adding additional nodes to $Q^B[f]$ increases the accuracy further. For example, again with $\omega = 200$, adding a single node at the midpoint decreases the error to $2.79 \cdot 10^{-6}$ while adding nodes at $\frac{1}{4}$, the midpoint, and $\frac{3}{4}$ further decreases the error to the astoundingly small $9.93 \cdot 10^{-12}$. This example demonstrates just how powerful these quadrature techniques are compared to Gauss–Legendre quadrature: even with $100,000$ points Gauss–Legendre quadrature had an error of 0.11, not even close to the accuracy of the Filon-type method, to say nothing of $Q^B[f]$.

3.5. Derivative-free methods

One issue with the Filon-type and Levin-type methods is that they ostensibly require derivatives in order to achieve higher asymptotic orders. If the function f is even moderately complicated, the task of determining its derivatives can be unmanageable. Approximating

the value of the derivatives—say by finite differences—might also not be feasible. But we are concerned with asymptotic orders, hence we only require an accurate approximation to the derivative at high frequencies. This leads us to the idea for Filon-type methods, originating in [**47**], to interpolate at the points $a, a + \frac{1}{\omega}$ and $b - \frac{1}{\omega}, b$, so that v approximates the first derivative at the endpoint with an error $\mathcal{O}\left(\omega^{-2}\right)$ as ω increases. Adding additional points that depend on ω allows us to approximate higher derivatives. We use the following lemma to prove the order of error:

Lemma 3.5.1 *Suppose that*

$$f(a), f(b) = \mathcal{O}\left(\omega^{-s}\right), \qquad f'(a), f'(b) = \mathcal{O}\left(\omega^{-s+1}\right), \qquad \cdots, \qquad f^{(s)}(a), f^{(s)}(b) = \mathcal{O}(1)$$

and

$$f(x), f'(x), \ldots, f^{(s+1)}(x) = \mathcal{O}(1), \qquad a \leq x \leq b.$$

Then

$$I[f] \sim \mathcal{O}\left(\omega^{-s-1}\right).$$

Proof: The theorem follows immediately from the asymptotic expansion. Since σ_k, which was defined in Theorem 2.2.1, is a combination of f and its first $k - 1$ derivatives, it follows that $\sigma_k(a), \sigma_k(b) = \mathcal{O}\left(\omega^{-s-1+k}\right)$ and $\sigma_k(x) = \mathcal{O}(1)$. Thus the terms in the s-term expansion are all $\mathcal{O}\left(\omega^{-s-1}\right)$ while the error integral is

$$\frac{1}{(-\mathrm{i}\omega)^s} I\left[\sigma_{s+1} g'\right] = \mathcal{O}\left(\omega^{-s-1}\right).$$

Q.E.D.

Theorem 3.5.2 [**47**] *Suppose that we interpolate at the points*

$$x_k, x_k + \frac{\gamma_{k,1}}{\omega}, \ldots, x_k + (m_k - 1)\frac{\gamma_{k,m_k}}{\omega}, \qquad k = 1, \ldots, \nu,$$

where $\left\{\gamma_{1,1}, \ldots, \gamma_{k,m_k}\right\}$ *are constants. Then*

$$I[f] - Q^F[f] = \mathcal{O}\left(\omega^{-s-1}\right),$$

where $s = \min\left\{m_1, m_\nu\right\}$.

Proof: Let v_ω be the interpolation of f at the given points, where the dependence on ω is written explicitly. From the Taylor expansion we know that

$$\begin{aligned} f^{(k)}(a) - v_\omega^{(k)}(a) &= \mathcal{O}\left(\omega^{-m_1+k}\right) \\ f^{(k)}(b) - v_\omega^{(k)}(b) &= \mathcal{O}\left(\omega^{-m_\nu+k}\right) \end{aligned} \qquad \text{for} \qquad k = 1, \ldots, s.$$

46
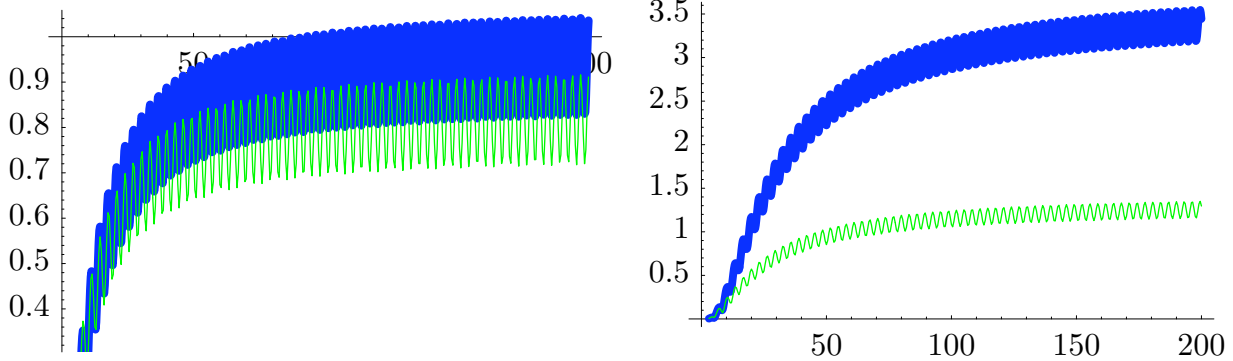
Figure 3.16: The errors in approximating $\int_0^1 \frac{x+1}{x-2} e^{i\omega(x^2+x)} \, dx$ for an adaptive Filon-type method (solid line) and an adaptive Levin-type method (thick line). In the left graph, both methods have nodes $\left\{0, \frac{1}{\omega}, 1 - \frac{1}{\omega}, 1\right\}$ and the error is scaled by ω^3. In the right graph, both methods have nodes $\left\{0, \frac{1}{\omega}, \frac{2}{\omega}, 1 - \frac{2}{\omega}, 1 - \frac{1}{\omega}, 1\right\}$ and the error is scaled by ω^4.

Furthermore, as $\omega \to \infty$, $v_\omega^{(k)} \to \tilde{v}^{(k)}$, where $\tilde{v}$ is the Hermite interpolation polynomial with nodes $\{x_1, \ldots, x_\nu\}$ and multiplicities $\{m_1, \ldots, m_\nu\}$. Thus

$$f^{(k)} - v_\omega^{(k)} \sim f^{(k)} - \tilde{v}^{(k)} = \boldsymbol{\mathcal{O}}(1).$$

The theorem then follows from Lemma 3.5.1.

Q.E.D.

We refer to such an approximation as an *adaptive Filon-type method*. We can construct an *adaptive Levin-type method* similarly.

As an example, we compare adaptive Filon-type methods and adaptive Levin-type methods in Figure 3.16 for the integral

$$\int_0^1 \frac{x+1}{x-2} e^{i\omega(x^2+x)} \, dx.$$

We look at both methods with nodes $\left\{0, \frac{1}{\omega}, 1 - \frac{1}{\omega}, 1\right\}$, which do indeed achieve an asymptotic order of $\mathcal{O}\left(\omega^{-3}\right)$. Adding the additional points $\frac{2}{\omega}$ and $1 - \frac{2}{\omega}$ increases the asymptotic order to $\mathcal{O}\left(\omega^{-4}\right)$. As in previous examples, Filon-type methods are more accurate than Levin-type methods.

3.6. Error bounds and the Filon–trapezoidal rule

This section is based on as-of-yet unpublished joint work with Daan Huybrechs. We will present error bounds for both Filon-type methods and composite Filon methods. We focus on the Fourier oscillator $g(x) = x$, though most of the results can be generalized in a

47

straightforward manner to other Filon-type methods via the change of variables $u = g(x)$. We choose the simplicity of the Fourier oscillator, however, partly due to the lack of significant other oscillators for which a Filon-type method is computable.

Though the asymptotic properties of Filon-type and Levin-type methods are excellent, in implementation one typically has a fixed frequency and the behaviour of the error for larger frequencies is irrelevant. Thus we wish to find a bound on the error. The most trivial error bound for a Filon-type method is

$$\left| I[f] - Q^F[f] \right| = \left| I[f - v] \right| \leq (b - a) \left\| f - v \right\|_\infty .$$

The quadrature error must be less than the error in interpolation, and must converge whenever interpolation converges uniformly. It follows that if we use Chebyshev interpolation points—or better yet, Lobatto points to ensure that the endpoints are included and we achieve $\mathcal{O}(\omega^{-2})$ asymptotic decay—the approximation is guaranteed to converge. Unfortunately, this bound does not decay as ω increases, hence it is not particularly sharp at large frequencies. We can, however, integrate by parts to obtain a second error bound, assuming that the endpoints are included in the interpolation points:

$$\left| I[f] - Q^F[f] \right| = \left| \frac{1}{i\omega} I[f' - v'] \right| \leq \frac{(b - a)}{\omega} \left\| f' - v' \right\| .$$

Iterating this procedure results in the following theorem:

Theorem 3.6.1 *Let $s = \min \{m_1, m_\nu\}$. Then*

$$\left| I[f] - Q^F[f] \right| \leq \min \begin{cases} (b - a) \left\| f - v \right\|_\infty \\ \frac{b-a}{\omega} \left\| f' - v' \right\|_\infty \\ \vdots \\ \frac{b-a}{\omega^s} \left\| f^{(s)} - v^{(s)} \right\|_\infty \\ \frac{1}{\omega^{s+1}} \left[2 \left\| f^{(s)} - v^{(s)} \right\|_\infty + (b - a) \left\| f^{(s+1)} - v^{(s+1)} \right\|_\infty \right] \end{cases} .$$

The L_∞ norms could be expressed in terms of bounds related to Hermite interpolation. We however leave them as is for clarity.

In Figure 3.17, we compare the error bound determined by Theorem 3.6.1 to the actual error, for the integral $\int_0^1 \cos x \, e^{i\omega x} \, dx$. We do so for two Filon-type methods: the first with only endpoints for nodes and multiplicities both one, the second with nodes $\left\{ 0, \frac{1}{2}, 1 \right\}$ and multiplicities $\{2, 1, 2\}$. This bound does indeed capture the asymptotic decay of the approximation, though there definitely is room for improvement.

An alternative to adding interpolation points is to apply a composite scheme: divide the interval into panels and use a Filon-type method on each panel. This is closely related to the original Filon method, except with the possibility of interpolating f by something other
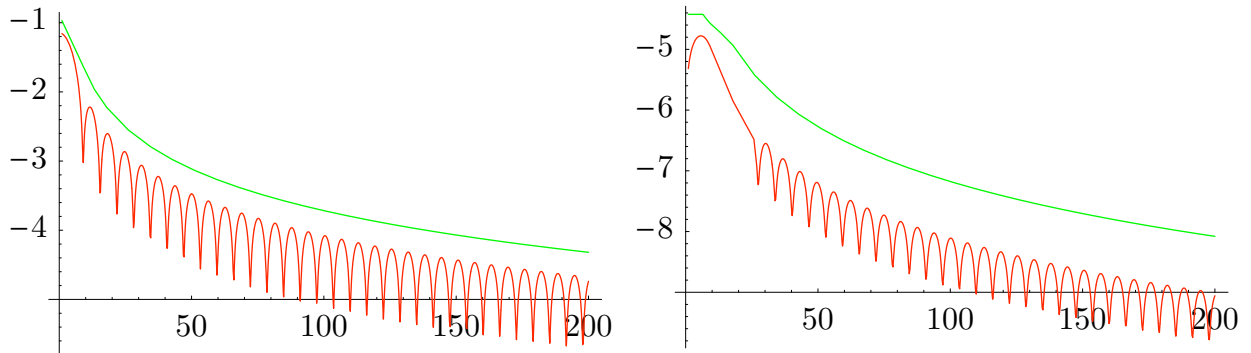
Figure 3.17: The base-10 logarithm of the error and bound in approximating $\int_0^1 \cos x \, \mathrm{e}^{\mathrm{i}\omega x} \, \mathrm{d}x$, for the Filon-type method with endpoints for nodes and multiplicities both one (left graph) and the Filon-type method with nodes $\left\{0, \frac{1}{2}, 1\right\}$ and multiplicities $\{2, 1, 2\}$ (right graph).

than a quadratic. We choose to focus on a *Filon–trapezoidal rule*, where we approximate f by a piecewise affine function with panels of the same size. This idea was suggested in [21]. We wish to find the rate that the error decays as the panel size h approaches zero. Let v_n be the piecewise affine function, so that (for $h = \frac{(b-a)}{n}$)

$$v_n(a) = f(a), v_n(a + h) = f(a + h), \ldots, v_n(b - h) = f(b - h), v_n(b) = f(b).$$

By applying Theorem 3.6.1 on each panel, combined with the facts that $|v(x) - f(x)| = \mathcal{O}\!\left(h^2\right)$ and $|v'(x) - f'(x)| = \mathcal{O}(h)$, we immediately know that the error is both $\mathcal{O}\!\left(h^2\right)$ and $\mathcal{O}\!\left(\frac{h}{\omega}\right)$ as $h \to 0$. However, numerical results suggest that the error is actually of a smaller magnitude, behaving like $\mathcal{O}\!\left(\frac{h^2}{\omega}\right)$. The following is a proof of this observation:

Theorem 3.6.2

$$\lim_{n \to \infty} n^2 \int_0^1 [f(x) - v_n(x)] \, \mathrm{e}^{\mathrm{i}\omega x} \, \mathrm{d}x = \mathcal{O}\!\left(\omega^{-1}\right).$$

Proof: Let $e_n = f - v_n$. Note that

$$\int_0^1 e_n(x) \mathrm{e}^{\mathrm{i}\omega x} \, \mathrm{d}x = \sum_{i=0}^{n-1} \int_{x_i}^{x_{i+1}} e_n(x) \mathrm{e}^{\mathrm{i}\omega x} \, \mathrm{d}x,$$

49

where $x_i = a + ih$. For $x_i \leq x \leq x_{i+1}$,

$$e_n(x) = f(x) + \frac{f(x_i) - f(x_{i+1})}{x_{i+1} - x_i}(x - x_i) - f(x_i)$$

$$= f'(x_i)(x - x_i) + \frac{f''(x_i)}{2}(x - x_i)^2 + \mathcal{O}(x - x_i)^3$$

$$- \left[f'(x_i) + \frac{f''(x_i)}{2}(x_{i+1} - x_i) + \mathcal{O}(h^2) \right](x - x_i)$$

$$= \frac{f''(x_i)}{2}(x - x_i)(x - x_{i+1}) + \mathcal{O}(x - x_i)^3 - \mathcal{O}(h^2)(x - x_i).$$

Note that

$$\lim_{n \to \infty} n^3 \int_{x_{i+1}}^{x_i} \mathcal{O}(x - x_i)^3 \, e^{i\omega x} \, dx = \lim_{n \to \infty} n^3 \mathcal{O}(h^4) = 0.$$

Likewise

$$\lim_{n \to \infty} n^3 \mathcal{O}(h^2) \int_{x_{i+1}}^{x_i} (x - x_i) e^{i\omega x} \, dx = \lim_{n \to \infty} n^3 \mathcal{O}(h^4) = 0.$$

Thus we need not worry about higher order terms. Thus we focus on the error term

$$\frac{f''(x_i)}{2} \int_{x_i}^{x_{i+1}} (x - x_i)(x - x_{i+1}) e^{i\omega x} \, dx = \frac{f''(x_i) e^{i\omega x_i}}{2\omega^3} \left[-2i + h\omega + e^{i\omega h}(2i + h\omega) \right].$$

Summing up we obtain:

$$\lim_{n \to \infty} n^2 \frac{-2i + h\omega + e^{i\omega h}(2i + h\omega)}{h2\omega^3} \sum_{i=1}^{n-1} h f''(x_i) e^{i\omega x_i}$$

$$= \frac{1}{2\omega^3} \int_0^1 f''(x) e^{i\omega x} \, dx \lim_{h \to 0} \frac{-2i + h\omega + e^{i\omega h}(2i + h\omega)}{h^3}.$$

We can compute this limit with L'Hôpital's rule:

$$\lim_{h \to 0} \frac{-2i + h\omega + e^{i\omega h}(2i + h\omega)}{h^3} = \omega \lim_{h \to 0} \frac{1 + e^{i\omega h}(i h\omega - 1)}{3h^2} = \omega^3 \lim_{h \to 0} \frac{-h e^{i\omega h}}{6h} = -\frac{\omega^3}{6}.$$

Thus

$$\lim_{n \to \infty} n^2 \int_0^1 e_h(x) e^{i\omega x} \, dx = -\frac{1}{12} \int_0^1 f''(x) e^{i\omega x} \, dx = \mathcal{O}(\omega^{-1}).$$

Q.E.D.

Note that this theorem is in fact a generalization of the standard Euler–Maclaurin formula. The last line of the proof, $-\frac{1}{12} \int_0^1 f''(x) e^{i\omega x} \, dx$, becomes $-\frac{1}{12} [f'(1) - f'(0)]$ when we
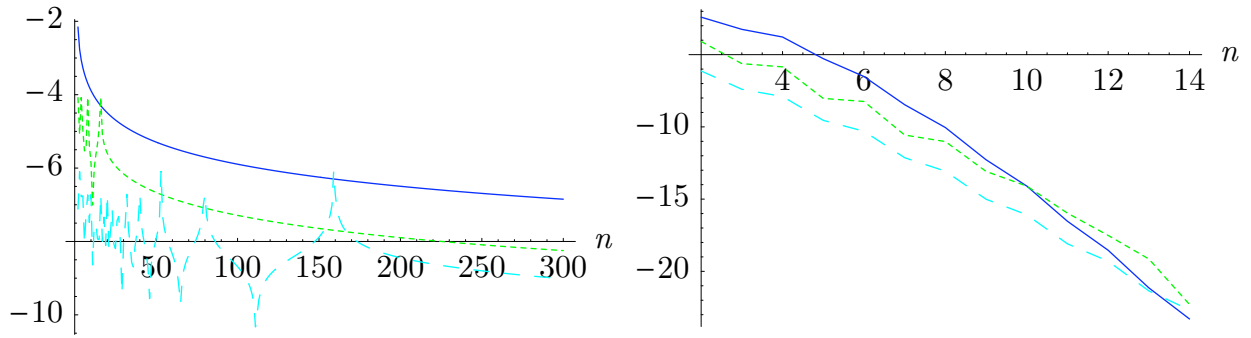
Figure 3.18: The base-10 errors scaled by n^2 in approximating $\int_0^1 \cos x\, e^{i\omega x}\, dx$ by the Filon–trapezoidal rule (left) and Filon-type method with Lobatto quadrature points (right), for $\omega = 10$ (solid line), 100 (dotted line) and 1000 (dashed line).

let $\omega \to 0$. We can obtain higher terms in this expansion, however, since the terms are highly oscillatory integrals themselves, the usefulness of such an exercise is unclear.

As an example, consider again the integral

$$\int_0^1 \cos x\, e^{i\omega x}\, dx.$$

In Figure 3.18 we compare the error of the Filon–trapezoidal rule for three choices of ω. Note how the rate of decay for each value of ω is the same, $\mathcal{O}(n^{-2})$, however increasing ω causes the actual error to decrease. However, n needs to scale in proportion to ω in order to achieve this decay rate. This is not to suggest that we need n to increase as ω increases in order to achieve the requisite accuracy: we always have the error bound that the quadrature cannot do any worse than interpolation error, which is independent of ω. In the right graph, we can see a comparison with a Filon-type method using Lobatto quadrature points. As can be seen, using Hermite interpolation instead of a composite rule results in the approximation converging at a faster rate to the exact integral.

Chapter 4

Stationary Points

In the preceding chapter, we assumed that the oscillatory integrals have no stationary points, in other words, $g'(x) \neq 0$ within the interval of integration. Of course integrals with stationary points are important in applications. For simplicity we assume the integral has a single stationary point at $x = 0$, and that we are integrating over the interval $[-1, 1]$. In other words, we want to approximate the integral

$$I[f] = \int_{-1}^{1} f(x) e^{i\omega g(x)} \, dx,$$

where ω is large and g has a single stationary point of order $r - 1$ at zero. This means that

$$0 = g(0) = g'(0) = \cdots = g^{(r-1)}(0), \qquad g^{(r)}(0) > 0,$$

and $g'(x) \neq 0$ for $0 < |x| \leq 1$. If $g(0) \neq 0$ then we transform the integral into the required form as follows:

$$\int_{-1}^{1} f(x) e^{i\omega g(x)} \, dx = e^{i\omega g(0)} \int_{-1}^{1} f(x) e^{i\omega[g(x) - g(0)]} \, dx.$$

The condition that $g^{(r)}(0) > 0$ implies that $g(x) > 0$ for $0 < x \leq 1$, and $(-1)^r g(x) > 0$ for $-1 \leq x < 0$. This condition can be relaxed, at the expense of complicating the proofs. The more general case of integrals over $[a, b]$ with multiple stationary points can easily be transformed into several integrals of this form, as long as the number of stationary points is finite.

The methods of stationary phase and steepest descent, cf. Section 2.3 and Section 2.4, provide only asymptotic results; for fixed frequency the accuracy of the approximation is limited. It is possible to compute the integrals by moving to the complex plane and integrating along the path of steepest descent with nonoscillatory quadrature methods, as mentioned briefly in Section 2.10. Unfortunately, both f and g must be analytic in order to deform the integration path, and the path of steepest descent must be known or computed. In addition, greater care is needed when the oscillator has branch points in the complex plane, as the path must remain on the correct branch cut.

In this chapter we will present methods based on Filon-type quadrature for approximating such integrals. We begin in Section 4.1 with the development of the recently discovered Iserles and Nørsett asymptotic expansion. With this expansion in hand, we can successfully determine the asymptotic order of a Filon-type method in Section 4.2. Both the Iserles

and Nørsett expansion and Filon-type methods require moments, hence we construct a new asymptotic expansion that does not require moments in Section 4.3. From this asymptotic expansion we can find a basis for a Filon-type method which can be integrated explicitly in closed form, which is done in Section 4.4. Finally, we demonstrate how these methods can be generalized for oscillators that behave like x^r near zero, where r is not an integer, in Section 4.5.

Remark: Sections 4.1 and 4.2 are based on results by Iserles and Nørsett in [48]. The rest of the chapter contains original research, first presented in [78].

4.1. The Iserles and Nørsett asymptotic expansion

Until Section 4.5, we assume that f and g are in $C^\infty[-1, 1]$. Asymptotic expansions are invaluable tools for high frequency integration. For the integral in question, there are two existing asymptotic expansions: the Iserles and Nørsett expansion [48] and the well-known *method of stationary phase* [74]. The former of these requires knowledge of the moments $I[1],...,I\left[x^{r-1}\right]$ but leads us to the more powerful numerical approximation of Filon-type methods [48]. Stationary phase does not require moments, unfortunately it only provides an asymptotic result, hence its usefulness as a numerical quadrature scheme is limited.

The standard technique of deriving asymptotic expansions for integrals without stationary points, namely integration by parts, fails due to the introduction of a singularity at the stationary point. But we can make the singularity removable (here we assume $r = 2$):

$$I[f] = I[f - f(0)] + f(0)I[1] = \frac{1}{i\omega} \int_{-1}^{1} \frac{f(x) - f(0)}{g'(x)} \frac{d}{dx} e^{i\omega g(x)} \, dx + f(0)I[1]$$

$$= \frac{1}{i\omega} \left[\frac{f(1) - f(0)}{g'(1)} e^{i\omega g(1)} - \frac{f(-1) - f(0)}{g'(-1)} e^{i\omega g(-1)} \right] - \frac{1}{i\omega} I \left[\frac{d}{dx} \left[\frac{f(x) - f(0)}{g'(x)} \right] \right] \quad (4.1.1)$$

$$+ f(0)I[1].$$

Iterating this procedure on the error term $I\left[\frac{d}{dx}\left[\frac{f(x)-f(0)}{g'(x)}\right]\right]$ results in an asymptotic expansion. If there are higher order stationary points, we can subtract out a polynomial to ensure both the function value and necessary derivatives of the integrand vanish in order to make the singularity removable. We thus obtain the following theorem, whose proof is very similar to the asymptotic expansion we will develop in Theorem 4.3.3.

Theorem 4.1.1 [48] *Define* $\mu[f] = \sum_{k=0}^{r-2} \frac{f^{(k)}(0)}{k!} \mu_k(x)$, *where* $\mathcal{L}[\mu_k](x) = x^k$ *for* $\mathcal{L}[v] = v' + i\omega g'v$. *Furthermore, let*

$$\sigma_0(x) = f(x), \qquad \sigma_{k+1}(x) = \frac{d}{dx} \frac{\sigma_k(x) - \mathcal{L}[\mu[\sigma_k]](x)}{g'(x)}.$$

53

Then

$$I[f] \sim \sum_{k=0}^{\infty} \frac{1}{(-\mathrm{i}\omega)^k} \left\{ \mu[\sigma_k](1)\mathrm{e}^{\mathrm{i}\omega g(1)} - \mu[\sigma_k](-1)\mathrm{e}^{\mathrm{i}\omega g(-1)} \right\}$$

$$- \sum_{k=0}^{\infty} \frac{1}{(-\mathrm{i}\omega)^{k+1}} \left\{ \frac{\sigma_k(1) - \mathcal{L}[\mu[\sigma_k]](1)}{g'(1)}\mathrm{e}^{\mathrm{i}\omega g(1)} - \frac{\sigma_k(-1) - \mathcal{L}[\mu[\sigma_k]](-1)}{g'(-1)}\mathrm{e}^{\mathrm{i}\omega g(-1)} \right\}.$$

The following corollary, originally stated in [**48**] and the analogue of Corollary 4.1.2 for stationary points, follows from this asymptotic expansion. It is used in the proof of the asymptotic order of Filon-type methods.

Corollary 4.1.2 [**48**] *Suppose that*

$$0 = f(-1) = \cdots = f^{(s-1)}(-1),$$
$$0 = f(0) = \cdots = f^{(rs-2)}(0),$$
$$0 = f(1) = \cdots = f^{(s-1)}(1).$$

Then

$$I[f] \sim \mathcal{O}\left(\omega^{-s-1/r}\right), \qquad \omega \to \infty.$$

Proof: Note that σ_k depends on f and its first k derivatives, hence the requirement at the boundary points. We prove the requirement on the number of derivatives at the stationary point by induction. The case where $s = 1$ is clear: we need f and its first $r - 2$ derivatives to be zero in order for $\mu[\sigma_0] = \mu[f] = 0$. The corollary thus follows from L'Hôpital's rule, and the fact that g' has a zero of order $r - 1$.

<div align="right">*Q.E.D.*</div>

The asymptotic order now depends on the stationary point, in addition to the endpoints.

4.2. Filon-type methods

Recall from Section 3.1 that a *Filon-type method* is constructed by interpolating the function f by another function v, using a set of *basis functions* $\{\psi_k\}$, at a sequence of *nodes* $\{x_1, \ldots, x_\nu\}$ and *multiplicities* $\{m_1, \ldots, m_\nu\}$. Then $I[f]$ is approximately equal to $I[v]$. This definition holds as is when there are stationary points, the only complication being that the moments $I[\psi_k]$ must be known.

The following theorem is from [**48**]. It states that the asymptotic behaviour of a Filon-type method depends on the number of derivatives interpolated at the stationary point and the endpoints of the interval. As before, unlike an asymptotic expansion, we can add additional interpolation points within the interval to reduce the error further.
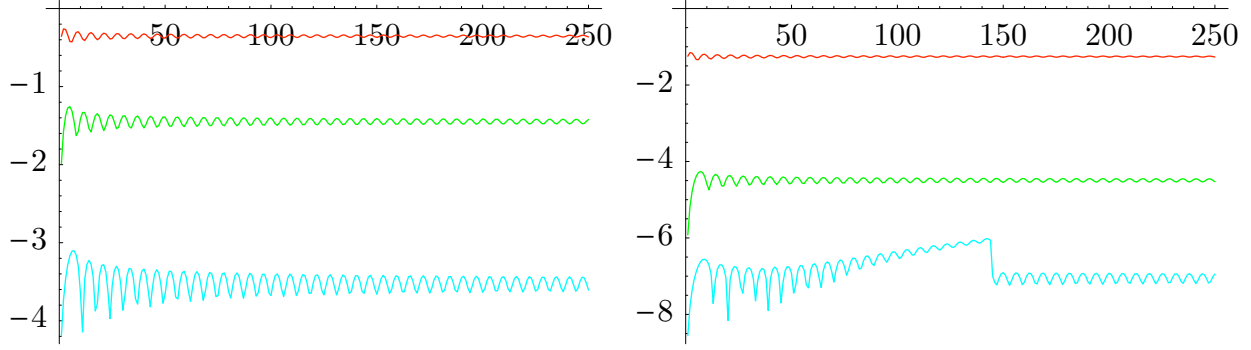
Figure 4.19: The base-10 logarithm of the error in approximating $\int_{-1}^{1} \cos x \, e^{i\omega x^2} \, dx$. In the left graph, we scale the error by $\omega^{3/2}$ for the one-term asymptotic expansion (top) and two Filon-type methods with multiplicities all one: nodes $\{-1, 0, 1\}$ (middle) and nodes $\left\{-1, -\frac{1}{2}, 0, \frac{1}{2}, 1\right\}$ (bottom). In the right graph, we scale the error by $\omega^{5/2}$ for the two-term asymptotic expansion (top), Filon-type method with nodes $\{-1, 0, 1\}$ and multiplicities $\{2, 3, 2\}$ (middle) and nodes $\left\{-1, -\frac{1}{2}, 0, \frac{1}{2}, 1\right\}$ and multiplicities $\{2, 1, 3, 1, 2\}$ (bottom).

Theorem 4.2.1 [48] *Let* $v(x) = \sum_{k=1}^{n} c_k \psi_k(x)$, *where* ψ_k *is independent of* ω *and* $n = \sum_{k=1}^{\nu} m_k$. *Assume that* $x_1 = -1$, $x_\eta = 0$ *and* $x_\nu = 1$. *The coefficients* c_k *are determined by solving the system*

$$v(x_k) = f(x_k), \ldots, v^{(m_k-1)}(x_k) = f^{(m_k-1)}(x_k), \qquad k = 1, 2, \ldots, \nu.$$

If this system is nonsingular, $m_1, m_\nu \geq s$ *and* $m_\eta \geq rs - 1$, *then*

$$I[f] - Q^F[f] \sim \mathcal{O}\left(\omega^{-s-1/r}\right),$$

where

$$Q^F[f] = I[v] = \sum_{k=1}^{n} c_k I[\psi_k].$$

Proof: The theorem follows as a direct consequence of Corollary 4.1.2:

$$I[f] - Q^F[f] = I[f - v] \sim \mathcal{O}\left(\omega^{-s-1/r}\right).$$

Q.E.D.

In practice—as in the case without stationary points, cf. Theorem 3.1.2—$\psi_k(x)$ is typically defined to be x^{k-1}, i.e., we use standard polynomial interpolation. The reasons are two-fold: polynomial interpolation is well-understood and guaranteed to interpolate at the given nodes and multiplicities, and the simplicity of the integrand suggests that the moments $I\left[x^k\right]$ are likely to be known. However, when the moments are unknown, Filon-type methods with the polynomial basis cannot provide an approximation.

As a simple example of Theorem 4.2.1, consider the integral

$$\int_{-1}^{1} \cos x \, e^{i\omega x^2} \, dx.$$

In the left graph of Figure 4.19 we compare three approximations of order $\mathcal{O}\left(\omega^{-3/2}\right)$: the one-term asymptotic expansion versus two Filon-type methods with multiplicities all one, one with nodes $\{-1, 0, 1\}$ and the other with nodes $\left\{-1, -\frac{1}{2}, 0, \frac{1}{2}, 1\right\}$. As can be seen, all methods have the predicted asymptotic order. The Filon-type methods are considerably more accurate than the asymptotic expansion, the first of which uses the exact same information about f and its derivatives. Adding interpolation points does indeed decrease the error further. The right graph compares three similar methods that are of asymptotic order $\mathcal{O}\left(\omega^{-5/2}\right)$, demonstrating that higher order methods are computable.

4.3. Moment-free asymptotic expansion

We now use the preceding two sections as a jumping off point in the derivation of moment-free methods, beginning first with an asymptotic expansion. The idea behind the new expansion is to note that we do not necessarily need to subtract a polynomial in (4.1.1), it is only necessary that the function we subtract can interpolate f and sufficient derivatives of f at the stationary point. Hence we can replace the moments $I\left[x^k\right]$, which may not be computable in closed form, with $I[\psi_k]$, where ψ_k is constructed in such a way that the integral is guaranteed to be computable. In order to do this, we first look at the canonical case of $g(x) = x^r$. In a similar manner to Section 2.8, suppose there exists a function F such that

$$\frac{d}{dx}\left[F(x)e^{i\omega g(x)}\right] = x^k e^{i\omega g(x)}.$$

We can expand out the left side to obtain the following differential equation, where $\mathcal{L}[F]$ is defined to be $F' + i\omega g' F$:

$$\mathcal{L}[F](x) = F'(x) + i\omega g'(x)F(x) = x^k.$$

Replacing $g'(x)$ with rx^{r-1} we obtain the equation $F'(x) + ri\omega x^{r-1}F(x) = x^k$. In the Levin collocation method, Section 2.8, and Levin-type methods, Section 3.2, a solution to an equation of this form was numerically approximated using collocation; but neither of these methods are accurate when stationary points are present. In this particular case, however, a solution is known in closed form:

$$F(x) = \frac{\omega^{-\frac{1+k}{r}}}{r}e^{-i\omega x^r + \frac{1+k}{2r}i\pi}\left[\Gamma\left(\frac{1+k}{r}, -i\omega x^r\right) - \Gamma\left(\frac{1+k}{r}, 0\right)\right], \qquad x \geq 0,$$

where Γ is the incomplete Gamma function [2]. Incomplete Gamma functions are well-understood, and can be computed efficiently [20]. In fact, modern mathematical programming packages, such as MAPLE, MATHEMATICA and MATLAB (via the `mfun` function) have very efficient built-in numerical implementations.

Intuition suggests that if we replace x^r with $g(x)$, then $\mathcal{L}[F]$ will give us the ψ_k we are looking for, hopefully independent of ω. The following lemma shows that our intuition is indeed correct, subject to a minor alteration to ensure smoothness around $x = 0$:

Lemma 4.3.1 *Let*

$$\phi_{r,k}(x) = D_{r,k}(\operatorname{sgn} x)\frac{\omega^{-\frac{k+1}{r}}}{r}\mathrm{e}^{-\mathrm{i}\omega g(x)+\frac{1+k}{2r}\mathrm{i}\pi}\left[\Gamma\left(\frac{1+k}{r}, -\mathrm{i}\omega g(x)\right) - \Gamma\left(\frac{1+k}{r}, 0\right)\right],$$

where

$$D_{r,k}(\operatorname{sgn} x) = \begin{cases} (-1)^k & \operatorname{sgn} x < 0 \text{ and } r \text{ even,} \\ (-1)^k\mathrm{e}^{-\frac{1+k}{r}\mathrm{i}\pi} & \operatorname{sgn} x < 0 \text{ and } r \text{ odd,} \\ -1 & \text{otherwise.} \end{cases}$$

Then $\phi_{r,k} \in C^\infty[-1,1]$ and, for $\mathcal{L}[F] = F' + \mathrm{i}\omega g' F$,

$$\mathcal{L}\Big[\phi_{r,k}\Big](x) = \operatorname{sgn}(x)^{r+k+1}\frac{|g(x)|^{\frac{k+1}{r}-1}\,g'(x)}{r}.$$

Furthermore, $\mathcal{L}\Big[\phi_{r,k}\Big] \in C^\infty[-1,1]$. Finally,

$$I\Big[\mathcal{L}\Big[\phi_{r,k}\Big]\Big] = \phi_{r,k}(1)\mathrm{e}^{\mathrm{i}\omega g(1)} - \phi_{r,k}(-1)\mathrm{e}^{\mathrm{i}\omega g(-1)}.$$

Proof:

The form of $\mathcal{L}\Big[\phi_{r,k}\Big]$ away from the stationary point follows immediately from the equation for the derivative of the incomplete Gamma function [2]. The smoothness of $\mathcal{L}\Big[\phi_{r,k}\Big]$ follows from the fact that

$$\mathcal{L}\Big[\phi_{r,k}\Big](x) = \frac{\mathrm{d}}{\mathrm{d}x}\left[\operatorname{sgn}(x)^{k+1}\frac{1}{1+k}\,|g(x)|^{\frac{1+k}{r}}\right], \qquad x \neq 0.$$

The antiderivative of $\mathcal{L}\Big[\phi_{r,k}\Big]$ is clearly smooth away from zero, while its limit at zero is also infinitely differentiable:

$$\operatorname{sgn}(x)^{k+1}\,|g(x)|^{\frac{1+k}{r}} = \operatorname{sgn}(x)^{k+1}\left|\frac{g^{(r)}(0)}{r!}x^r + \mathcal{O}\left(x^{r+1}\right)\right|^{\frac{1+k}{r}}$$

$$= \left(\frac{g^{(r)}(0)}{r!}\right)^{\frac{k+1}{r}}x^{k+1}(1+\mathcal{O}(x))^{\frac{k+1}{r}}.$$

57

Combining the smoothness of $\mathcal{L}\left[\phi_{r,k}\right]$ with the fact that $\phi_{r,k}$ is continuous ensures that $\phi_{r,k} \in C^{\infty}[-1,1]$. The value of the final integral thus follows from the fundamental theorem of calculus.

<div align="right">Q.E.D.</div>

Remark: The use of sgn and the case statement in the preceding lemma are merely to choose the branch cut so that $(x^r)^{1/r} = x$ for both positive and negative x.

We can also prove that $\left\{\mathcal{L}\left[\phi_{r,k}\right]\right\}$ is a Chebyshev set [82], hence can interpolate at any given sequence of sample points.

Lemma 4.3.2 *The basis $\left\{\mathcal{L}\left[\phi_{r,k}\right]\right\}$ is a Chebyshev set.*

Proof: Let $u = \operatorname{sgn}(x)\,|g(x)|^{1/r}$, so that u ranges monotonically from $-|g(-1)|^{1/r}$ to $|g(1)|^{1/r}$. Let $g_+^{-1}(u)$ equal $x \geq 0$ such that $g(x) = u$, and $g_-^{-1}(u)$ equal to $x < 0$ such that $g(x) = u$. When r is odd then $g_\pm^{-1} = g^{-1}$. Note that $\operatorname{sgn} x = \operatorname{sgn} u$, hence $x = g_{\operatorname{sgn} u}^{-1}(u^r)$. Thus we obtain

$$\sum c_k \mathcal{L}\left[\phi_{r,k}\right](x) = \operatorname{sgn}(x)^{r+1}\frac{g'(x)\,|g(x)|^{\frac{1}{r}-1}}{r}\sum c_k \operatorname{sgn}(x)^k\,|g(x)|^{\frac{k}{r}} = \frac{g'(x)u^{1-r}}{r}\sum c_k u^k.$$

It follows that interpolating f by $\mathcal{L}\left[\phi_{r,k}\right]$ is equivalent to interpolating

$$\frac{ru^{r-1}f(x)}{g'(x)}$$

by the polynomial $\sum c_k u^k$. This function is clearly well-defined for $u \neq 0$, hence we must show that it is also well-defined for $u = x = 0$. But this follows since

$$\frac{u^{r-1}}{g'(x)} = \frac{\operatorname{sgn}(x)^{r+1}\,|g(x)|^{1-1/r}}{g'(x)} = \frac{\operatorname{sgn}(x)g(x)}{|g(x)|^{1/r}\,g'(x)}$$

$$= \frac{g_r x^r + \mathcal{O}\left(x^{r+1}\right)}{x^r(g_r + \mathcal{O}(x))^{1/r}(rg_r + \mathcal{O}(x^r))} = \frac{g_r + \mathcal{O}\left(x^{r+1}\right)}{(g_r + \mathcal{O}(x))^{1/r}(rg_r + \mathcal{O}(x^r))}.$$

The limit of this as x goes to zero, hence also as u goes to zero, is $\frac{1}{rg_r^{1/r}}$. Thus $\mathcal{L}\left[\phi_{r,k}\right]$ is a Chebyshev set.

<div align="right">Q.E.D.</div>

Though we have only shown that the basis $\left\{\mathcal{L}\left[\phi_{r,k}\right]\right\}$ can interpolate at a sequence of sample points, the fact that it can interpolate with multiplicities as well follows from a trivial

limiting argument, since every $\mathcal{L}\left[\phi_{r,k}\right]$ is smooth. Using $\mathcal{L}\left[\phi_{r,k}\right]$ in place of x^k, we can derive an alternative to the asymptotic expansion in Section 4.1, which does not depend on any moments:

Theorem 4.3.3 *Define* $\mu[f] = \sum_{k=0}^{r-2} c_k \phi_{r,k}$ *so that*

$$\mathcal{L}[\mu[f]](0) = f(0), \dots, \mathcal{L}[\mu[f]]^{(r-2)}(0) = f^{(r-2)}(0).$$

Furthermore, let

$$\sigma_0(x) = f(x), \qquad \sigma_{k+1}(x) = \frac{\mathrm{d}}{\mathrm{d}x} \frac{\sigma_k(x) - \mathcal{L}[\mu[\sigma_k]](x)}{g'(x)}.$$

Then

$$I[f] \sim \sum_{k=0}^{\infty} \frac{1}{(-\mathrm{i}\omega)^k} \left\{ \mu[\sigma_k](1)\mathrm{e}^{\mathrm{i}\omega g(1)} - \mu[\sigma_k](-1)\mathrm{e}^{\mathrm{i}\omega g(-1)} \right\}$$

$$- \sum_{k=0}^{\infty} \frac{1}{(-\mathrm{i}\omega)^{k+1}} \left\{ \frac{\sigma_k(1) - \mathcal{L}[\mu[\sigma_k]](1)}{g'(1)} \mathrm{e}^{\mathrm{i}\omega g(1)} - \frac{\sigma_k(-1) - \mathcal{L}[\mu[\sigma_k]](-1)}{g'(-1)} \mathrm{e}^{\mathrm{i}\omega g(-1)} \right\}.$$

Proof: This proof is roughly based on the proof of Theorem 3.2 in [**48**]. Note that the existence of such a μ follows from Lemma 4.3.2. We find that $\sigma_k \in C^{\infty}[-1, 1]$, since

$$\frac{\sigma_k(x) - \mathcal{L}[\mu[\sigma_k]](x)}{g'(x)} = \frac{\mathcal{O}\left(x^{r-1}\right)}{\frac{g^{(r)}(0)}{(r-1)!}x^{r-1} + \mathcal{O}(x^r)} = \frac{\mathcal{O}(1)}{\frac{g^{(r)}(0)}{(r-1)!} + \mathcal{O}(x)}$$

is in $C^{\infty}[-1, 1]$. Then

$$I[\sigma_k] = I[\sigma_k - \mathcal{L}[\mu[\sigma_k]]] + I[\mathcal{L}[\mu[\sigma_k]]]$$

$$= \frac{1}{\mathrm{i}\omega} \int_{-1}^{1} \frac{\sigma_k - \mathcal{L}[\mu[\sigma_k]]}{g'} \frac{\mathrm{d}}{\mathrm{d}x} \mathrm{e}^{\mathrm{i}\omega g} \, \mathrm{d}x + \left\{ \mu[\sigma_k](1)\mathrm{e}^{\mathrm{i}\omega g(1)} - \mu[\sigma_k](-1)\mathrm{e}^{\mathrm{i}\omega g(-1)} \right\}$$

$$= \frac{1}{\mathrm{i}\omega} \left\{ \frac{\sigma_k(1) - \mathcal{L}[\mu[\sigma_k]](1)}{g'(1)} \mathrm{e}^{\mathrm{i}\omega g(1)} - \frac{\sigma_k(-1) - \mathcal{L}[\mu[\sigma_k]](-1)}{g'(-1)} \mathrm{e}^{\mathrm{i}\omega g(-1)} \right\}$$

$$+ \left\{ \mu[\sigma_k](1)\mathrm{e}^{\mathrm{i}\omega g(1)} - \mu[\sigma_k](-1)\mathrm{e}^{\mathrm{i}\omega g(-1)} \right\} - \frac{1}{\mathrm{i}\omega} I[\sigma_{k+1}].$$

The theorem follows by induction.

Q.E.D.

The method of stationary phase can be derived as a consequence of Theorem 4.3.3. Consider the case of r equal to two. Then $\mu[f](x) = \sqrt{\frac{2}{g''(0)}} f(0)\phi_{2,0}(x)$, since $\mathcal{L}[\phi_{2,0}](0) = \sqrt{\frac{g''(0)}{2}}$. If we assume that $|g(x)|$ grows at least quadratically as $x \to \pm\infty$, then $\int_{\pm 1}^{\pm\infty} f\mathrm{e}^{\mathrm{i}\omega g} \, \mathrm{d}x =$
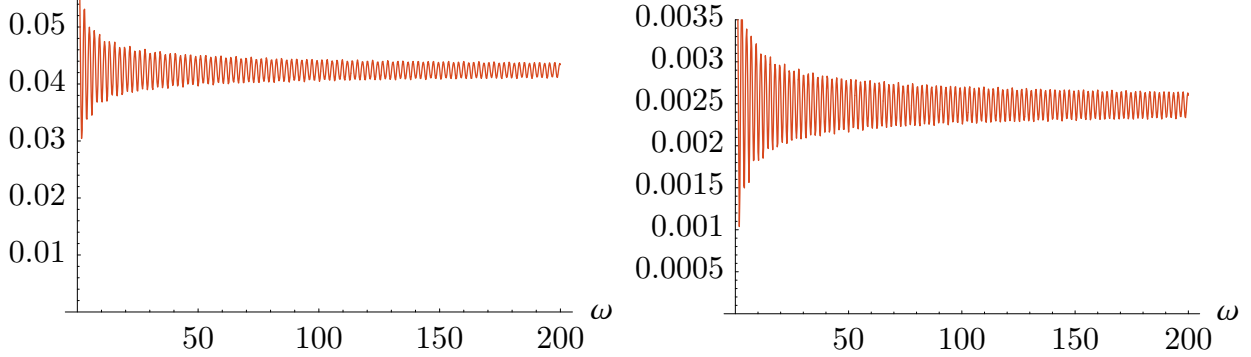
Figure 4.20: The error scaled by $\omega^{3/2}$ of the one-term asymptotic expansion (left graph), versus the error scaled by $\omega^{5/2}$ of the two-term asymptotic expansion (right graph), for the integral $\int_{-1}^{1} \cos x \, \mathrm{e}^{\mathrm{i}\omega(4x^2+x^3)} \, \mathrm{d}x$.

$\mathcal{O}\!\left(\omega^{-1}\right)$ [74]. If we assume that a function which vanishes at the stationary point has a higher asymptotic order, then formally we obtain

$$
I[f] = \int_{-\infty}^{\infty} f\mathrm{e}^{\mathrm{i}\omega g} \, \mathrm{d}x + \mathcal{O}\!\left(\omega^{-1}\right) = \int_{-\infty}^{\infty} (f - \mathcal{L}[\mu[f]])\mathrm{e}^{\mathrm{i}\omega g} \, \mathrm{d}x + \int_{-\infty}^{\infty} \mathcal{L}[\mu[f]] \, \mathrm{e}^{\mathrm{i}\omega g} \, \mathrm{d}x + \mathcal{O}\!\left(\omega^{-1}\right)
$$

$$
= \frac{\mathrm{e}^{\frac{\mathrm{i}\pi}{4}}}{2\sqrt{\omega}}\sqrt{\frac{2}{g''(0)}} f(0) \left\{ \left[\lim_{x\to\infty} \Gamma\!\left(\frac{1}{2}, -\mathrm{i}\omega g(x)\right) - \Gamma\!\left(\frac{1}{2}, 0\right) \right] \right.
$$

$$
\left. - \left[\lim_{x\to-\infty} \Gamma\!\left(\frac{1}{2}, -\mathrm{i}\omega g(x)\right) - \Gamma\!\left(\frac{1}{2}, 0\right) \right] \right\} + \mathcal{O}\!\left(\omega^{-1}\right)
$$

$$
= \mathrm{e}^{\frac{\mathrm{i}\pi}{4}}\sqrt{\frac{2\pi}{\omega g''(0)}} f(0) + \mathcal{O}\!\left(\omega^{-1}\right).
$$

This is equivalent to the stationary phase contribution found in Section 2.3.

We now demonstrate this asymptotic expansion in action. Note that $\mu[\sigma_k](\pm 1) = \mathcal{O}\!\left(\omega^{-1/r}\right)$, thus the partial sum up to $s-1$ of the asymptotic expansion has an asymptotic order $\mathcal{O}\!\left(\omega^{-s-1/r}\right)$. Consider the case where $f(x) = \cos x$ with the polynomial oscillator $g(x) = 4x^2 + x^3$. The moments cannot be integrated in closed form, hence the Iserles and Nørsett expansion is not applicable to this integral. On the other hand, Figure 4.20 demonstrates numerically that Theorem 4.3.3 does indeed give an asymptotic expansion. For a more complicated example, consider the integral where $f(x) = (x+2)^{-1}$ with the oscillator $g(x) = 1 - \cos x - \frac{1}{2}x^2 + x^3$. Figure 4.21 demonstrates that the expansion works with higher order stationary points—in this case $r = 3$—and with nonpolynomial oscillators.
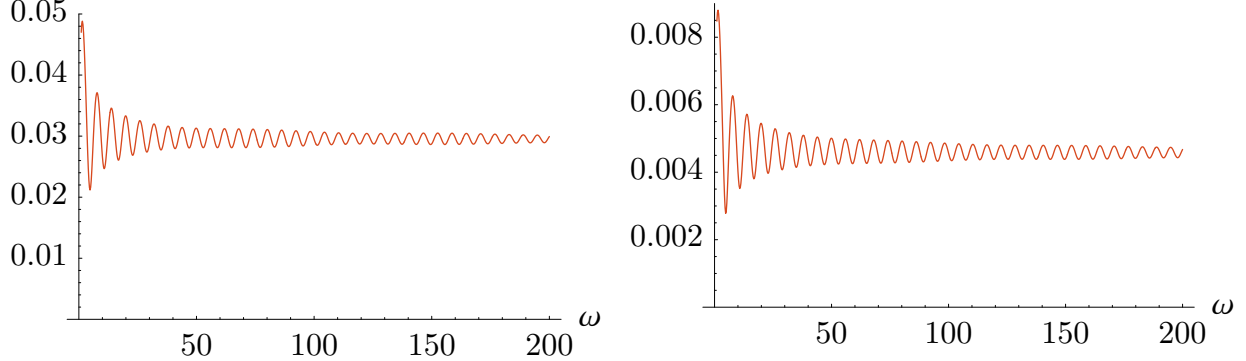
Figure 4.21: The error scaled by $\omega^{4/3}$ of the one-term asymptotic expansion (left graph), versus the error scaled by $\omega^{7/3}$ of the two-term asymptotic expansion (right graph), for the integral $\int_{-1}^{1} \frac{1}{x+2} e^{i\omega(1-\cos x - \frac{1}{2}x^2 + x^3)} \, dx$.

4.4. Moment-free Filon-type methods

In Lemma 4.3.1, we determined a basis of functions such that the moments are guaranteed to be known, hence it makes sense to choose $\psi_k = \mathcal{L}[\phi_{r,k-1}]$ in a Filon-type method. Moreover, it was proved in Lemma 4.3.2 that ψ_k is a Chebyshev set, hence we know that it can interpolate at the given nodes and multiplicities. Using this basis we obtain a Moment-free Filon-type method, resulting in the following theorem:

Theorem 4.4.1 Let $\psi_k = \mathcal{L}[\phi_{r,k-1}]$. Assume that $x_1 = -1$, $x_\eta = 0$ and $x_\nu = 1$. If $m_1, m_\nu \geq s$ and $m_\eta \geq rs - 1$, then

$$I[f] - Q^F[f] \sim \mathcal{O}\left(\omega^{-s-1/r}\right),$$

where

$$Q^F[f] = \sum_{k=1}^{n} c_k \left[\phi_{r,k-1}(1)e^{i\omega g(1)} - \phi_{r,k-1}(-1)e^{i\omega g(-1)}\right].$$

When the integral does not contain stationary points—i.e., $r = 1$—then this method is equivalent to the Moment-free Filon-type method constructed in [**91**].

Figure 4.22 demonstrates the power of a Moment-free Filon-type method with the same integral as in Figure 4.20. Note that the errors in the left graph are of the same asymptotic order as the left graph of Figure 4.20, however the error is significantly less. This is despite the fact that we are using exactly the same information about f as we are in the asymptotic expansion. Furthermore, this figure demonstrates how adding interpolation points can further reduce the error. The right graph shows how adding sufficient multiplicities to a Filon-type method does indeed increase the asymptotic order, and compares the resulting quadrature with the equivalent asymptotic expansion. We obtain similar results for the integral with a higher-order stationary point found in Figure 4.21, as seen in Figure 4.23.
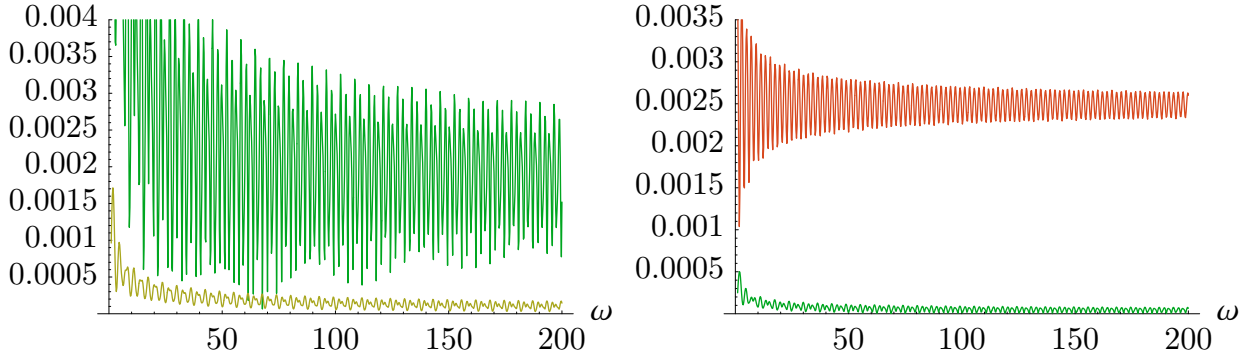
Figure 4.22: Errors in approximating $I[f] = \int_{-1}^{1} \cos x \, e^{i\omega(4x^2+x^3)} \, dx$. In the left graph, the error scaled by $\omega^{3/2}$ of a Filon-type method with nodes $\{-1, 0, 1\}$ and multiplicities all one (top) versus a Filon-type method with nodes $\left\{-1, -\frac{1}{2}, 0, \frac{1}{2}, 1\right\}$ and multiplicities all one (bottom). In the right graph, the error scaled by $\omega^{5/2}$ of the two-term asymptotic expansion (top) versus a Filon-type method with nodes $\{-1, 0, 1\}$ and multiplicities $\{2, 3, 2\}$ (bottom).
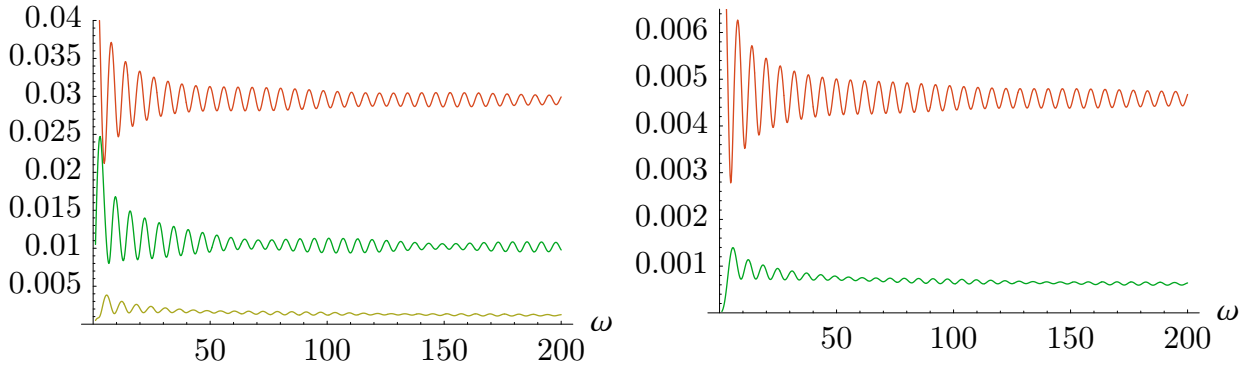
Figure 4.23: Errors in approximating $I[f] = \int_{-1}^{1} \frac{1}{x+2} e^{i\omega(1-\cos x - \frac{1}{2}x^2+x^3)} \, dx$. In the left graph, the error scaled by $\omega^{4/3}$ of the one-term asymptotic expansion (top), a Filon-type method interpolating at the nodes $\{-1, 0, 1\}$ and multiplicities $\{1, 2, 1\}$ (middle) and a Filon-type method with nodes $\left\{-1, -\frac{1}{2}, 0, \frac{1}{2}, 1\right\}$ and multiplicities $\{1, 1, 2, 1, 1\}$ (bottom). In the right graph, the error scaled by $\omega^{7/3}$ of the two-term asymptotic expansion (top) and a Filon-type method with nodes $\{-1, 0, 1\}$ and multiplicities $\{2, 5, 2\}$ (bottom).

Remark: We purposely chose oscillators such that $g''(x) \neq 0$ for $0 < |x| < 1$. Without this, $g'(x)$ would no longer be monotone away from zero and the basis $\mathcal{L}\left[\phi_{r,k}\right]$ would differ greatly in behaviour from the polynomial basis. Though the theorems remain valid, numerical results suggest that $\mathcal{L}\left[\phi_{r,k}\right]$ becomes much less accurate for interpolation, hence a significant amount of sample points would be required. A simple workaround is to choose a sufficiently small neighbourhood around zero such that this condition is satisfied, and use a Moment-

free Filon-type method within this neighbourhood. We could then approximate the integral outside this neighbourhood using a Levin-type method, which is not affected numerically by g'' vanishing.

Remark: In Lemma 4.3.2, we showed that under a change of variables, interpolation by $\mathcal{L}\left[\phi_{r,k}\right]$ is equivalent to interpolation of a function by polynomials. It might be possible to use this fact to determine the equivalent of Chebyshev points, in order to determine where the interpolation points should be. Alternatively, it might also be possible to construct a Gauss-like quadrature rule by choosing points and weights to maximize the order of $\mathcal{L}\left[\phi_{r,k}\right]$ which are integrated exactly.

4.5. Fractional powers

We finally consider the case where $g(x) \sim g_r x^r$ at zero and r is no longer an integer. To avoid the issue of choosing the correct branch cut, we restrict our attention to positive x:

$$\int_0^1 f(x)\mathrm{e}^{\mathrm{i}\omega g(x)}\,\mathrm{d}x.$$

In fact, $g(x)$ is typically imaginary otherwise, and therefore either exponentially increasing or decreasing in the interval $[-1, 0)$. Restricting our attention to positive x simplifies the functions $\phi_{r,k}$ from Lemma 4.3.1:

$$\phi_{r,k}(x) = -\frac{\omega^{-\frac{k+1}{r}}}{r}\mathrm{e}^{-\mathrm{i}\omega g(x)+\frac{1+k}{2r}\mathrm{i}\pi}\left[\Gamma\left(\frac{1+k}{r}, -\mathrm{i}\omega g(x)\right) - \Gamma\left(\frac{1+k}{r}, 0\right)\right]$$

and

$$\mathcal{L}\left[\phi_{r,k}\right](x) = \frac{g(x)^{\frac{k+1}{r}-1}g'(x)}{r}.$$

An unfortunate consequence of having a stationary point on the boundary is that the asymptotic expansion now depends on one more derivative of f. The derivation of the asymptotic expansion is significantly more difficult since it is not true that each σ_k is smooth. Thus we will not derive an equivalent to Theorem 4.3.3; instead we generalize Corollary 4.1.2:

Theorem 4.5.1 *Suppose that*

$$0 = f(0) = \cdots = f^{(\lceil sr \rceil - 1)}(0),$$
$$0 = f(1) = \cdots = f^{(s-1)}(1).$$

Furthermore, assume that $g(x) \sim g_r x^r$ as $x \to 0$, and that the $\sim$ relationship is differentiable $s + 1$ times (i.e., $g^{(k)}(x) \sim \frac{r!}{(r-k)!}x^{r-k}$ for $k = 0, 1, \ldots, s + 1$). If $r \geq 2$ or $\lceil sr \rceil - sr + 1 < r$,

then

$$I[f] \sim \mathcal{O}\left(\omega^{-s-\frac{\lceil sr \rceil - sr + 1}{r}}\right), \qquad \omega \to \infty.$$

Otherwise,

$$I[f] \sim \mathcal{O}\left(\omega^{-s-1}\right), \qquad \omega \to \infty.$$

Proof: Since f is smooth, we know that $f(x) \sim \mathcal{O}\left(x^{\lceil sr \rceil}\right)$ as $x \to 0$ and $f(x) \sim \mathcal{O}((1-x)^s)$ as $x \to 1$, where both relationships are differentiable. Thus at zero $\sigma_0(x) = f(x) \sim \mathcal{O}\left(x^{\lceil sr \rceil}\right)$. Define

$$\sigma_{k+1} = \frac{\mathrm{d}}{\mathrm{d}x}\frac{\sigma_k}{g'}.$$

It is easy to see that $\sigma_k(x) \sim \mathcal{O}\left(x^{\lceil sr \rceil - kr}\right)$ as x goes to zero and $\sigma_k(x) \sim \mathcal{O}\left((1-x)^{s-k}\right)$ as x goes to one.

For $k \leq s-1$, we have $\lim_{x \to 0} \frac{\sigma_k(x)}{g'(x)} = \lim_{x \to 0} \mathcal{O}\left(x^{\lceil sr \rceil - (k+1)r + 1}\right) = 0$, and likewise $\frac{\sigma_k(1)}{g'(1)} = 0$. Thus

$$I[\sigma_k] = \frac{1}{\mathrm{i}\omega} \int_0^1 \frac{\sigma_k}{g'} \frac{\mathrm{d}}{\mathrm{d}x} \mathrm{e}^{\mathrm{i}\omega g}\,\mathrm{d}x = \frac{1}{\mathrm{i}\omega}\left\{\frac{\sigma_k(1)}{g'(1)}\mathrm{e}^{\mathrm{i}\omega g(1)} - \lim_{x\to 0}\frac{\sigma_k(x)}{g'(x)}\right\} - \frac{1}{\mathrm{i}\omega}I[\sigma_{k+1}]$$

$$= -\frac{1}{\mathrm{i}\omega}I[\sigma_{k+1}].$$

It follows by induction that $I[f] = (-\mathrm{i}\omega)^{-s}I[\sigma_s]$. Since $\sigma_s(x) \sim \mathcal{O}\left(x^{\lceil sr \rceil - sr}\right)$ and is differentiable away from zero, the theorem follows from Theorem 13.1 and Theorem 13.2 in [**74**].

<div align="right">Q.E.D.</div>

As in the integer power case, if $g(x) = x^r$ then $\mathcal{L}\left[\phi_{r,k}\right](x) = x^k$, hence we obtain a standard Filon-type method. On the other hand, consider the example $g(x) = x^{\frac{3}{2}} + x^3$. Obtaining high asymptotic order in a Filon-type method depends on taking derivatives of the interpolation basis at the endpoint and stationary point, hence the smoothness of $\mathcal{L}\left[\phi_{r,k}\right]$ is important. However, for this particular g we obtain (with $r = 3/2$):

$$g(x)^{\frac{1+k}{r}} = x^{k+1}(1 + x^{\frac{3}{2}})^{\frac{2}{3}(1+k)}.$$

This is not a $C^\infty[0,1]$ function, instead it is only in $C^{k+2}[0,1]$, and

$$L[\phi_{r,k}] = \frac{1}{1+k}\frac{\mathrm{d}}{\mathrm{d}x}g(x)^{\frac{1+k}{r}}$$
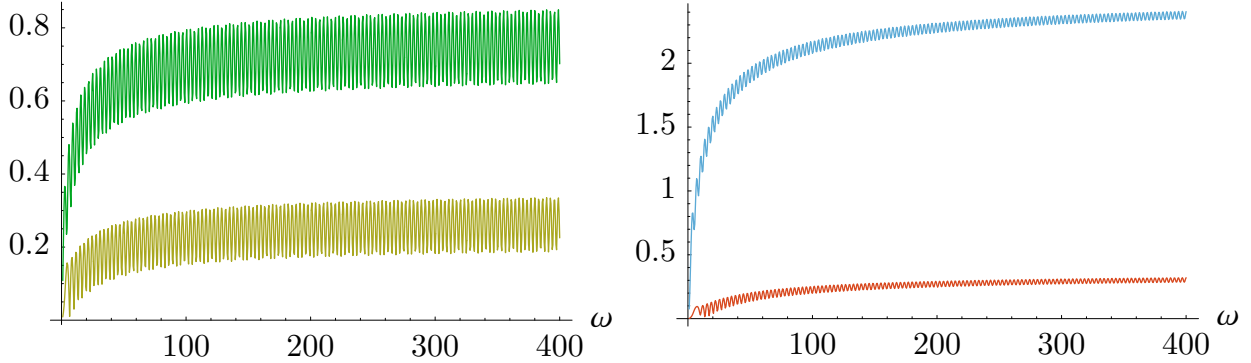
Figure 4.24: Errors in approximating $\int_0^1 e^x e^{i\omega(x^{3/2}+x^{5/2})}\,dx$. In the left graph the error scaled by ω^2 of a Filon-type method with nodes $\{0,1\}$ and multiplicities $\{2,1\}$ (top) versus a Filon-type method with nodes $\left\{0,\frac{1}{3},\frac{2}{3},1\right\}$ and multiplicities $\{2,1,1,1\}$ (bottom). In the right graph the error scaled by $\omega^{8/3}$ of a Filon-type method with nodes $\{0,1\}$ and multiplicities $\{3,2\}$ (top) versus a Filon-type method with nodes $\left\{0,\frac{1}{3},\frac{2}{3},1\right\}$ and multiplicities $\{3,2,2,2\}$ (bottom).

is only in $C^{k+1}[0,1]$. On the other hand, consider the oscillator $g(x) = x^r h(x)$, where h is in $C^\infty[0,1]$ and is nonzero at $x=0$. Then

$$g(x)^{\frac{1+k}{r}} = x^{k+1} h(x)^{\frac{1+k}{r}},$$

which is smooth. A suitably altered Lemma 4.3.2 demonstrates that this basis still forms a Chebyshev set. We thus focus on oscillators of this form, though a Moment-free Filon-type method should work in the previous case, with a restriction on the asymptotic orders achievable and no guarantee of interpolation.

As an example, consider the integral $\int_0^1 e^x e^{i\omega(x^{3/2}+x^{5/2})}\,dx$. In Figure 4.24 we compare four Moment-free Filon-type methods. In the two Filon-type methods in the left graph s is equal to one, therefore $\lceil r \rceil - r + 1 = \frac{3}{2} = r$ and we obtain an asymptotic decay of $\mathcal{O}(\omega^{-2})$. In the right graph we compare two Filon-type methods with $s=2$, hence the asymptotic order is increased to $\mathcal{O}(\omega^{\frac{8}{3}})$.

65

<div align="center">

Chapter 5

Multivariate Highly Oscillatory Integrals

</div>

We now turn our attention to the multivariate integral

$$I_g[f, \Omega] = \int_\Omega f(\boldsymbol{x}) \mathrm{e}^{\mathrm{i}\omega g(\boldsymbol{x})} \, \mathrm{d}V,$$

where Ω is a piecewise smooth boundary in $\mathbb{R}^d$ and $\boldsymbol{x} = (x_1, \ldots, x_d)^\top \in \mathbb{R}^d$. We emphasize the dependence of the integral on its domain and oscillator, as the approximation methods we will construct will be in terms of oscillatory integrals over lower dimensional domains and with different oscillators. The construction of quadrature schemes proceeds much as it did in the univariate case: we write the methods as oscillatory integrals and use the asymptotic expansion to determine the asymptotic order of the methods. Interestingly, and unexpectedly, we find that oscillatory integration is significantly easier than nonoscillatory integration: we can obtain extraordinarily accurate approximations at large frequencies using only function values at the vertices of the domain.

In analogue to Theorem 2.6.1, we will initially require the nonresonance condition. Recall that this requires that $\nabla g(\boldsymbol{x})$ is not orthogonal to the boundary of Ω at every point $\boldsymbol{x}$ on the boundary of Ω. Also, there cannot be stationary points, thus $\nabla g \neq 0$ within the closure of Ω. In Section 5.1 we develop the multivariate version of Filon-type methods. This is almost identical to their univariate construction, the only snag being difficulties associated with standard polynomial interpolation. However, they still require moments, which now depend on both the integration domain Ω and the oscillator g. These are known if g is an affine oscillator and Ω is a simplex or a disc, or if $g(\boldsymbol{x}) = g_1(x_1) + \cdots + g_d(x_d)$ is separable, the univariate moments of each g_k are known and Ω is a rectangular domain. Besides these examples, moments could possibly be computable—say, by symbolic algebra—in only extraordinary cases.

Because of these issues, Levin-type methods are of increased importance for multivariate integrals. We present a generalization of Levin-type methods over domains for which a boundary parameterization is known in Section 5.2. This is based on Stokes' theorem, in place of the fundamental theorem of calculus used in the univariate case. We then generalize the asymptotic basis in Section 5.3, which as before allows us to increase the asymptotic order without increasing the size of the Levin collocation system.

Requiring the nonresonance condition prohibits many important integrals from being evaluated. The last two sections of this chapter are concerned with alleviating this issue.

<div align="center">

66

</div>

The requirement that ∇g is not orthogonal to the boundary corresponds to a stationary point in an integral over the boundary of the domain. Thus we will see in Section 5.4 that a Levin-type method only fails when trying to compute such boundary integrals, and we need only concern ourselves with handling stationary points where ∇g vanishes. The univariate case was handled in Chapter 4, hence we can already handle bivariate integrals with resonance points. In Section 5.5 we explore generalizing the Moment-free Filon-type methods to multivariate integrals with stationary points. This will result in requiring the computation of oscillatory integrals involving incomplete Gamma functions over the boundary, which we leave as an open problem.

Remark: Section 5.1 is based on results by Iserles and Nørsett in [**49**]. The rest of the chapter consists of original research. Sections 5.2 and 5.3, and parts of Section 5.4, were first presented in [**76**].

5.1. Multivariate Filon-type methods

Recall the asymptotic expansion derived in Section 2.6. Though it was possible, we chose not to find the terms in the expansion $\Theta_k[f]$ explicitly. The issue is that it is a significant logistical task in large dimensions, versus the simplicity of the Filon-type methods and Levin-type methods we develop. Thus we only use this asymptotic expansion for error analysis, not as a means of approximation. The following corollary serves the same purpose as Corollary 3.1.1: it will be used to prove the order of error for multivariate Filon-type and Levin-type methods.

Corollary 5.1.1 *Let V be the set of all vertices of a domain Ω, cf. Section 2.6 for the definition of a vertex. Suppose that $f = \mathcal{O}(\omega^{-n})$. Suppose further that*

$$0 = \mathcal{D}^m f(\boldsymbol{v})$$

for all $\boldsymbol{v} \in V$ and $\boldsymbol{m} \in \mathbb{N}^d$ such that $0 \leq \sum \boldsymbol{m} \leq s - 1$. If the nonresonance condition is satisfied, then

$$I_g[f, \Omega] \sim \mathcal{O}(\omega^{-n-s-d}).$$

Proof: We prove this corollary by induction on the dimension d, with the univariate case following from Corollary 3.1.1. We begin by showing that the sum in (2.6.1) (up to $s + d$) is

$$\sum_{k=1}^{s+d} \frac{1}{(\mathrm{i}\omega)^k} \int_{\partial\Omega} \mathrm{e}^{\mathrm{i}\omega g} \boldsymbol{\sigma}_k \cdot \mathrm{d}\boldsymbol{s} = \mathcal{O}(\omega^{-n-s-d}), \tag{5.1.1}$$

for

$$\boldsymbol{\sigma}_1 = f \frac{\nabla g}{\|\nabla g\|^2} \qquad \text{and} \qquad \boldsymbol{\sigma}_{k+1} = \boldsymbol{\sigma}_{k+1} = \nabla \cdot \boldsymbol{\sigma}_k \frac{\nabla g}{\|\nabla g\|^2}.$$

67

Since every $\boldsymbol{\sigma}_k$ depends on f and its partial derivatives, it follows that $\boldsymbol{\sigma}_k = \mathcal{O}(\omega^{-n}\mathbf{1})$. Furthermore, $0 = \mathcal{D}^m\boldsymbol{\sigma}_k(\boldsymbol{v})$ for all $\boldsymbol{v} \in V$ and every $\sum \boldsymbol{m} \le s - k$, where $1 \le k \le s$. Employing the definition of the integral of a differential form, cf. Section 2.5, we determine from the induction hypothesis that (2.6.2) is of order $\mathcal{O}(\omega^{-n-(s-k)-(d-1)})$ for all $1 \le k \le s$. For $k > s$, we know that (2.6.2) is at least of order $\mathcal{O}(\omega^{-n-(d-1)})$. Since each (2.6.2) is multiplied by $(-\mathrm{i}\omega)^{-k-1}$ in the construction of (5.1.1), it follows that this sum is $\mathcal{O}(\omega^{-n-s-d})$. Finally, the remainder term in (2.6.1)

$$\frac{1}{(-\mathrm{i}\omega)^{-s-d}}I_g[\nabla \cdot \boldsymbol{\sigma}_{s+d}, \Omega] = \mathcal{O}(\omega^{-s-n-d}),$$

since $\|\boldsymbol{\sigma}_{s+d}\|_\infty = \mathcal{O}(\omega^{-n})$. Thus $I_g[f, \Omega] \sim \mathcal{O}(\omega^{-s-n-d})$.

<div align="right">Q.E.D.</div>

We find a generalization of Filon-type methods for multivariate integrals in [**49**]. As in the univariate case, the function f is interpolated by a multivariate polynomial v, and moments are assumed to be available. Define

$$Q_g^F[f, \Omega] = I_g[v, \Omega],$$

where v is the Hermite interpolation polynomial of f at a given set of nodes $\{\boldsymbol{x}_1, \ldots, \boldsymbol{x}_\nu\}$ with multiplicities $\{m_1, \ldots, m_\nu\}$, obtained by solving the system

$$\mathcal{D}^m v(\boldsymbol{x}_k) = \mathcal{D}^m f(\boldsymbol{x}_k), \qquad 0 \le \sum \boldsymbol{m} \le m_k - 1, \qquad k = 1, \ldots, \nu.$$

Assuming a solution to this system exists, it is clear from Corollary 5.1.1 that

$$Q_g^F[f, \Omega] - I_g[f, \Omega] = \mathcal{O}(\omega^{-s-d}),$$

where s is the minimum multiplicity associated with a vertex.

Moments are known whenever g is affine and Ω is a simplex. Consider the integral over the bivariate simplex:

$$\int_0^1 \int_0^{1-x} x^p y^q \mathrm{e}^{\mathrm{i}\omega(k_1 x + k_2 y)} \,\mathrm{d}y\,\mathrm{d}x.$$

The interior integral can be integrated explicitely:

$$\int_0^{1-x} x^p y^q \mathrm{e}^{\mathrm{i}\omega(k_1 x + k_2 y)} \,\mathrm{d}y = x^p \mathrm{e}^{\mathrm{i}\omega k_1 x} \int_0^{1-x} y^q \mathrm{e}^{\mathrm{i}\omega k_2 y} \,\mathrm{d}y$$

$$= x^p v(1-x)\mathrm{e}^{\mathrm{i}\omega[k_1 x + k_2(1-x)]} - x^p v(0)\mathrm{e}^{\mathrm{i}\omega[k_1 x + k_2]},$$

where v is a polynomial of degree q determined via a simple application of integration by parts. But taking the integral of this over $(0, 1)$ is simply a sum of moments with respect
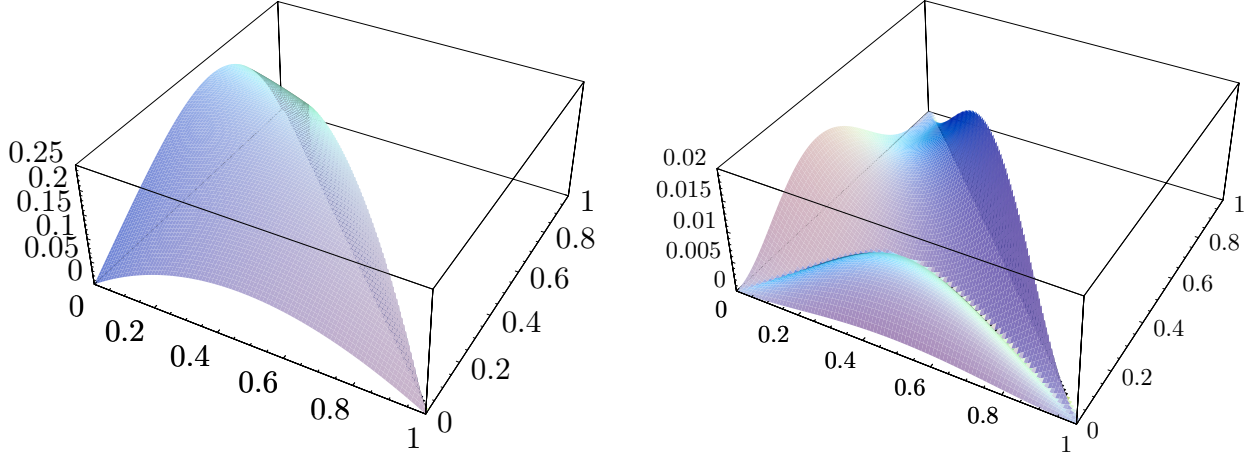
Figure 5.25: The Hermite interpolation error for $\cos(x + y^2)$. In the left graph, we interpolate at the vertices $\{(0,0), (1,0), (0,1)\}$ with multiplicities all one. In the right graph, we interpolate at the nodes $\left\{(0,0), (1,0), (0,1), \left(\frac{1}{3}, \frac{1}{3}\right)\right\}$ with multiplicities $\{2, 2, 2, 1\}$.

to an affine oscillator: this is also known in closed form. Similar logic holds for higher dimensional simplices. If we attempted to solve the same integral over another domain, for example $\int_0^1 \int_0^{T(x)}$ where T is not affine, we would need to integrate the term

$$x^p v(T(t)) e^{i\omega[k_1 x + k_2 T(t)]}.$$

Both the amplitude and oscillator functions are no longer polynomial, and unless we are hit by a stroke of serendipity, this cannot be integrated in closed form. However as long as the oscillator is affine, we could triangulate the domain by a simplicial complex, for which we can integrate over. This adds significant amount of computational complexity to the quadrature scheme, thus we prefer utilizing Levin-type methods in this situation.

As a simple example, consider the integral over the 2-dimensional simplex

$$\int_{S_2} \cos(x + y^2) \, e^{i\omega(x-y)} \, dV.$$

We consider two Filon-type methods: one interpolating at vertices $\{(0,0), (1,0), (0,1)\}$ with multiplicities all one, the other interpolating at $\left\{(0,0), (1,0), (0,1), \left(\frac{1}{3}, \frac{1}{3}\right)\right\}$ with multiplicities $\{2, 2, 2, 1\}$. In Figure 5.25 we plot the interpolation error: the quadrature error thus must be bounded in the first case by 0.125 and the second case by 0.01, though both of these bounds neglect the asymptotic properties of Filon-type methods. In Figure 5.26 we compare the error in quadrature. As can be seen, the methods reach their predicted asymptotic order: the first decays like $\mathcal{O}(\omega^{-3})$ whilst interpolating derivatives in the second approximation increases the asymptotic order to $\mathcal{O}(\omega^{-4})$.

69
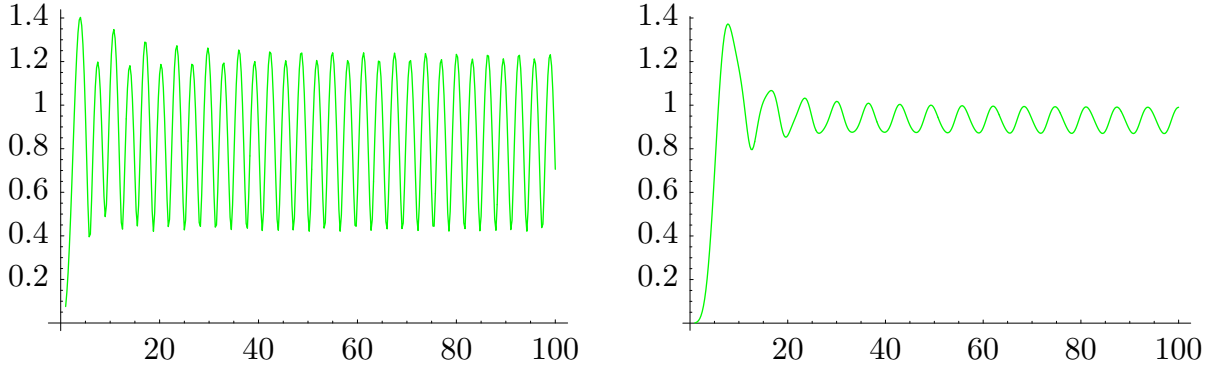
Figure 5.26:　The error scaled by ω^3 of $Q_g^F[f, S_2]$ interpolating only at the vertices with multiplicities all one (left graph), and the error scaled by ω^4 with vertex multiplicities all two and an additional point at $\left(\frac{1}{3}, \frac{1}{3}\right)$ with multiplicity one (right graph), for approximating $\int_{S_2} \cos(x + y^2)\, \mathrm{e}^{\mathrm{i}\omega(x-y)}\, \mathrm{d}V$.
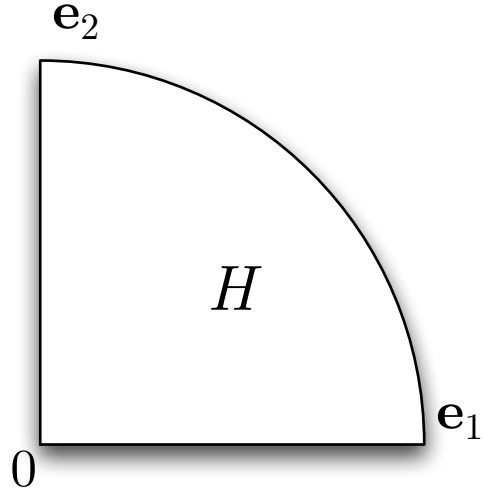

Figure 5.27:　A unit quarter disc H, where $\boldsymbol{e}_1 = (1, 0)$ and $\boldsymbol{e}_2 = (0, 1)$.

5.2.　Multivariate Levin-type methods

In this section we will derive a Levin-type method for the multivariate highly oscillatory integral $I_g[f, \Omega]$. As in the univariate case, we will not require moments. This enables the approximation of highly oscillatory integrals with more complicated oscillators and over more complicated domains than was possible with a Filon-type method. We begin by demonstrating how to derive a multivariate Levin-type method on a specific two-dimensional domain, namely a quarter unit disc H as seen in Figure 5.27. Afterwards, we generalize the technique to higher dimensional and more general domains.

In the univariate case, we determined the collocation operator $\mathcal{L}[v]$ using the fundamental

theorem of calculus. We mimic this by using Stokes' theorem. Suppose we have a bivariate function $\boldsymbol{F}(x,y) = (F_1(x,y), F_2(x,y))^\top$ such that

$$I[f] = \int_{\partial H} \mathrm{e}^{\mathrm{i}\omega g} \boldsymbol{F} \cdot \mathrm{d}\boldsymbol{s} = \int_{\partial H} \mathrm{e}^{\mathrm{i}\omega g}(F_1 \, \mathrm{d}y - F_2 \, \mathrm{d}x), \qquad (5.2.1)$$

where $\mathrm{d}\boldsymbol{s} = (\,\mathrm{d}y, -\,\mathrm{d}x)^\top$ is the surface differential. We can express the integrand as the differential form $\rho = \mathrm{e}^{\mathrm{i}\omega g(x,y)} \boldsymbol{F}(x,y) \cdot \mathrm{d}\boldsymbol{s}$. Then

$$\begin{aligned} \mathrm{d}\rho &= (F_{1,x} + \mathrm{i}\omega g_x F_1)\mathrm{e}^{\mathrm{i}\omega g} \, \mathrm{d}x \wedge \mathrm{d}y - (F_{2,y} + \mathrm{i}\omega g_y F_2)\mathrm{e}^{\mathrm{i}\omega g} \, \mathrm{d}y \wedge \mathrm{d}x \qquad (5.2.2) \\ &= (F_{1,x} + F_{2,y} + \mathrm{i}\omega(g_x F_1 + g_y F_2))\mathrm{e}^{\mathrm{i}\omega g} \, \mathrm{d}x \wedge \mathrm{d}y \\ &= (\nabla \cdot \boldsymbol{F} + \mathrm{i}\omega \nabla g \cdot \boldsymbol{F})\mathrm{e}^{\mathrm{i}\omega g} \, \mathrm{d}x \wedge \mathrm{d}y \\ &= \mathcal{L}[\boldsymbol{F}]\,\mathrm{e}^{\mathrm{i}\omega g} \, \mathrm{d}V, \end{aligned}$$

where $\mathcal{L}[\boldsymbol{F}] = \nabla \cdot \boldsymbol{F} + \mathrm{i}\omega \nabla g \cdot \boldsymbol{F}$. We can rewrite the condition (5.2.1) as $\mathcal{L}[\boldsymbol{F}] = f$.

We now use the operator $\mathcal{L}[\boldsymbol{F}]$ to collocate f. Let $\boldsymbol{v}(x,y) = \sum_{k=1}^{n} c_k \boldsymbol{\psi}_k(x,y)$, for some basis $\{\boldsymbol{\psi}_k\}$, where $\boldsymbol{\psi}_k : \mathbb{R}^2 \to \mathbb{R}^2$. Given a sequence of nodes $\{\boldsymbol{x}_1, \ldots, \boldsymbol{x}_\nu\} \subset \mathbb{R}^2$ and multiplicities $\{m_1, \ldots, m_\nu\}$, we determine the coefficients c_k by solving the system

$$\mathcal{D}^{\boldsymbol{m}}\mathcal{L}[\boldsymbol{v}]\,(\boldsymbol{x}_k) = \mathcal{D}^{\boldsymbol{m}} f(\boldsymbol{x}_k), \qquad 0 \le \sum \boldsymbol{m} \le m_k - 1, \qquad k = 1, \ldots, \nu,$$

where again $\boldsymbol{m} \in \mathbb{N}^d$ and $\sum \boldsymbol{m}$ is the sum of the entries of the vector $\boldsymbol{m}$. We then obtain, using $T_1(t) = (\cos t, \sin t)^\top$, $T_2(t) = (0, 1-t)^\top$ and $T_3(t) = (t, 0)^\top$ as the positively oriented boundary,

$$\begin{aligned} I_g[f, H] \approx I_g[\mathcal{L}[\boldsymbol{v}], H] &= \iint_H \mathcal{L}[\boldsymbol{v}]\,\mathrm{e}^{\mathrm{i}\omega g} \, \mathrm{d}x \wedge \mathrm{d}y = \iint_H \mathrm{d}\rho = \oint_{\partial H} \rho = \oint_{\partial H} \mathrm{e}^{\mathrm{i}\omega g} \boldsymbol{v} \cdot \mathrm{d}\boldsymbol{s} \\ &= \int_0^{\frac{\pi}{2}} \mathrm{e}^{\mathrm{i}\omega g(T_1(t))} \boldsymbol{v}(T_1(t)) \cdot T_1'(t)\,dt + \int_0^1 \mathrm{e}^{\mathrm{i}\omega g(T_2(t))} \boldsymbol{v}(T_2(t)) \cdot T_2'(t)\,dt+ \\ &\qquad \int_0^1 \mathrm{e}^{\mathrm{i}\omega g(T_3(t))} \boldsymbol{v}(T_3(t)) \cdot T_3'(t)\,dt \\ &= \int_0^{\frac{\pi}{2}} \mathrm{e}^{\mathrm{i}\omega g(\cos t, \sin t)} \left[v_2(\cos t, \sin t)\cos t - v_1(\cos t, \sin t)\sin t\right]\,dt- \\ &\qquad \int_0^1 v_2(0, 1-t)\mathrm{e}^{\mathrm{i}\omega g(0, 1-t)}\,dt + \int_0^1 v_1(t, 0)\mathrm{e}^{\mathrm{i}\omega g(t, 0)}\,dt. \end{aligned}$$

This is a sum of three univariate highly oscillatory integrals, with oscillators $\mathrm{e}^{\mathrm{i}\omega g(\cos t, \sin t)}$, $\mathrm{e}^{\mathrm{i}\omega g(0, 1-t)}$ and $\mathrm{e}^{\mathrm{i}\omega g(t, 0)}$. If we assume that these three oscillators have no stationary points, which can be shown to be equivalent to the nonresonance condition, then we can approximate each of these integrals with a univariate Levin-type method, as described in Section 3.2.

Hence we define:

$$Q_g^L[f, H] = Q_{g_1}^L \left[f_1, \left(0, \frac{\pi}{2} \right) \right] + Q_{g_2}^L \left[f_2, (0, 1) \right] + Q_{g_3}^L \left[f_3, (0, 1) \right],$$

for $f_1(t) = v_2(\cos t, \sin t) \cos t - v_1(\cos t, \sin t) \sin t$, $g_1(t) = g(\cos t, \sin t)$, $f_2(t) = -v_2(0, 1-t)$, $g_2(t) = g(0, 1-t)$, $f_3(t) = v_1(t, 0)$ and $g_3(t) = g(t, 0)$.

We approach the general case in a similar manner. Suppose we are given a sequence of nodes $\{\boldsymbol{x}_1, \ldots, \boldsymbol{x}_\nu\}$ in $\Omega \subset \mathbb{R}^d$, multiplicities $\{m_1, \ldots, m_\nu\}$ and basis functions $\{\boldsymbol{\psi}_1, \boldsymbol{\psi}_2, \ldots\}$, where $\boldsymbol{\psi}_k : \mathbb{R}^d \to \mathbb{R}^d$. Assume further that we are given a positive-oriented boundary of Ω defined by a set of functions $T_\ell : \Omega_\ell \to \mathbb{R}^d$, where $\Omega_\ell \subset \mathbb{R}^{d-1}$ is again a domain with piecewise smooth boundary and the ℓth boundary component Z_ℓ is the image of T_ℓ. Furthermore, assume we have the same information—nodes, multiplicities, basis and boundary parameterization—for each Ω_ℓ, recursively down to the one-dimensional edges. We define a Levin-type method $Q_g^L[f, \Omega]$ recursively as follows:

- If $\Omega = (a, b) \subset \mathbb{R}$, then $Q_g^L[f, \Omega]$ is equivalent to a univariate Levin-type method, á la Section 3.2.

- If $\Omega \subset \mathbb{R}^d$, the definition of $\mathcal{L}[\boldsymbol{v}]$ remains

$$\mathcal{L}[\boldsymbol{v}] = \nabla \cdot \boldsymbol{v} + i\omega \nabla g \cdot \boldsymbol{v}.$$

Define $\boldsymbol{v} = \sum_{k=1}^n c_k \boldsymbol{\psi}_k$, where n will be the number of equations in the system (5.2.3). We then determine the coefficients c_k by solving the collocation system

$$\mathcal{D}^m \mathcal{L}[\boldsymbol{v}] (\boldsymbol{x}_k) = \mathcal{D}^m f(\boldsymbol{x}_k), \qquad 0 \leq \sum \boldsymbol{m} \leq m_k - 1, \qquad k = 1, \ldots, \nu. \qquad (5.2.3)$$

We now define

$$Q_g^L[f, \Omega] = \sum_\ell Q_{g_\ell}^L \left[f_\ell, \Omega_\ell \right], \qquad (5.2.4)$$

where $g_\ell(\boldsymbol{x}) = g(T_\ell(\boldsymbol{x}))$ and $f_\ell = \boldsymbol{v}(T_\ell(\boldsymbol{x})) \cdot \boldsymbol{J}_{T_\ell}^d(\boldsymbol{x})$, cf. Notation for the definition of $\boldsymbol{J}_{T_\ell}^d(\boldsymbol{x})$. Assume that the nodes and multiplicities for each Levin-type method $Q_{g_\ell}^L [f_\ell, \Omega_\ell]$ contain the vertices of Ω_ℓ with the same multiplicity as the associated vertex of Ω. In other words, if $\boldsymbol{x}_j = T_\ell(\boldsymbol{u})$ is a vertex of Ω, then $\boldsymbol{u}$ has a multiplicity of m_j.

The *regularity condition* for the multivariate case is defined by the following two conditions:

- The basis $\{\nabla g \cdot \boldsymbol{\psi}_k\}$ can interpolate at the given nodes and multiplicities.

- The regularity condition is satisfied for each Levin-type method in the right side of (5.2.4).

We thus derive the following theorem:

72

Theorem 5.2.1 *Suppose that both the nonresonance and regularity condition are satisfied. Suppose further that $\{\boldsymbol{x}_1, \ldots, \boldsymbol{x}_\nu\}$ contains all the vertices of Ω, namely, $\{\boldsymbol{x}_{i_1}, \cdots, \boldsymbol{x}_{i_\nu}\}$. Then*

$$I[f] - Q^L[f] \sim \mathcal{O}\left(\omega^{-s-d}\right),$$

where $s = \min\{m_{i_1}, \cdots, m_{i_\nu}\}$.

Proof: Assume the theorem holds for all dimensions less than d. The univariate case was proved in Theorem 3.2.1. We begin by showing that

$$I_g[f, \Omega] - I_g[\mathcal{L}[\boldsymbol{v}], \Omega] = I_g[f - \mathcal{L}[\boldsymbol{v}], \Omega] = \mathcal{O}\left(\omega^{-s-d}\right).$$

This will follow if $\mathcal{L}[\boldsymbol{v}] = \boldsymbol{\mathcal{O}}(1)$. Let

$$\mathcal{P}[f] = \begin{pmatrix} \rho_1[f] \\ \vdots \\ \rho_\nu[f] \end{pmatrix}, \qquad \text{for} \qquad \rho_k[f] = \begin{pmatrix} \mathcal{D}^{\boldsymbol{p}_{k,1}} f(\boldsymbol{x}_k) \\ \vdots \\ \mathcal{D}^{\boldsymbol{p}_{k,n_k}} f(\boldsymbol{x}_k) \end{pmatrix}, \qquad k = 1, \ldots, \nu,$$

where $\boldsymbol{p}_{k,1}, \ldots, \boldsymbol{p}_{k,n_k} \in \mathbb{N}^d$, $n_k = \frac{1}{2}m_k(m_k + 1)$, are the lexicographically ordered vectors such that $\sum \boldsymbol{p}_{k,i} \le m_k - 1$. As in the proof of Theorem 3.2.1, $\mathcal{P}[f]$ maps f to itself evaluated at the given nodes and multiplicities. The system (5.2.3) has the form $A\boldsymbol{c} = \boldsymbol{f}$, where

$$A = (\mathcal{P}[\mathcal{L}[\boldsymbol{\psi}_1]], \cdots, \mathcal{P}[\mathcal{L}[\boldsymbol{\psi}_n]]) = (\mathcal{P}[\nabla \cdot \boldsymbol{\psi}_1] + \mathrm{i}\omega\mathcal{P}[\nabla g \cdot \boldsymbol{\psi}_1], \cdots, \mathcal{P}[\nabla \cdot \boldsymbol{\psi}_n] + \mathrm{i}\omega\mathcal{P}[\nabla g \cdot \boldsymbol{\psi}_n])$$
$$= P + \mathrm{i}\omega G,$$

for

$$P = (\mathcal{P}[\nabla \cdot \boldsymbol{\psi}_1], \cdots, \mathcal{P}[\nabla \cdot \boldsymbol{\psi}_n]), \quad G = (\mathcal{P}[\nabla g \cdot \boldsymbol{\psi}_1], \cdots, \mathcal{P}[\nabla g \cdot \boldsymbol{\psi}_n]) \quad \text{and} \quad \boldsymbol{f} = \mathcal{P}[f].$$

Note that G is the matrix associated with the system resulting from the basis $\{\nabla g \cdot \boldsymbol{\psi}_k\}$ interpolating at the given nodes and multiplicities, hence the regularity condition ensures that $\det G$ is nonsingular. By the same logic as in Theorem 3.2.1, it follows that the A is nonsingular for large ω and $c_k = \mathcal{O}\left(\omega^{-1}\right)$. Thus $\mathcal{L}[\boldsymbol{v}] = \boldsymbol{\mathcal{O}}(1)$, and Corollary 5.1.1 states that $I_g[f, \Omega] - I_g[\mathcal{L}[\boldsymbol{v}], \Omega] = \mathcal{O}\left(\omega^{-s-d}\right)$.

We now show that

$$Q_g^L[f, \Omega] - I_g[\mathcal{L}[\boldsymbol{v}], \Omega] = \mathcal{O}\left(\omega^{-s-d}\right).$$

Define the differential form $\rho = \mathrm{e}^{\mathrm{i}\omega g}\boldsymbol{v} \cdot \mathrm{d}\boldsymbol{s}$, where $\mathrm{d}\boldsymbol{s}$ is again the surface differential, cf. Notation. It can easily be seen that $\mathrm{d}\rho = \mathcal{L}[\boldsymbol{v}]\,\mathrm{e}^{\mathrm{i}\omega g}\,\mathrm{d}V$, see (5.2.2). Thus

$$I_g[\mathcal{L}[\boldsymbol{v}], \Omega] = \int_\Omega \mathrm{d}\rho = \int_{\partial\Omega} \rho = \sum_\ell \int_{Z_\ell} \rho,$$

where $Z_\ell = T_\ell(\Omega_\ell)$. Furthermore, using the definition of the integral of differential form:

$$\int_{Z_\ell} \rho = \int_{Z_\ell} \mathrm{e}^{\mathrm{i}\omega g} \boldsymbol{v} \cdot \mathrm{d}\boldsymbol{s} = \int_{\Omega_\ell} \mathrm{e}^{\mathrm{i}\omega g(T_\ell(\boldsymbol{x}))} \boldsymbol{v}(T_\ell(\boldsymbol{x})) \cdot \boldsymbol{J}_{T_\ell}^d(\boldsymbol{x})\, \mathrm{d}V$$

$$= \sum_{j=1}^{n} c_j \int_{\Omega_\ell} \mathrm{e}^{\mathrm{i}\omega g(T_\ell(\boldsymbol{x}))} \boldsymbol{\psi}_j(T_\ell(\boldsymbol{x})) \cdot \boldsymbol{J}_{T_\ell}^d(\boldsymbol{x})\, \mathrm{d}V$$

$$= \sum_{j=1}^{n} c_j I_{g_\ell}\left[f_{\ell,j}, \Omega_\ell\right],$$

for $f_{\ell,j}(\boldsymbol{x}) = \boldsymbol{\psi}_j(T_\ell(\boldsymbol{x})) \cdot \boldsymbol{J}_{T_\ell}^d(\boldsymbol{x})$. By assumption, since the nonresonance and regularity conditions are satisfied, $Q_{g_\ell}^L\left[f_{\ell,j}, \Omega_\ell\right] - I_{g_\ell}\left[f_{\ell,j}, \Omega_\ell\right] = \mathcal{O}\left(\omega^{-s-d+1}\right)$, where this Levin-type method has the same nodes and multiplicities as $Q_{g_\ell}^L[f_\ell, \Omega_\ell]$ in (5.2.4). Due to the linearity of Q^L, $Q_{g_\ell}^L[f_\ell, \Omega_\ell] = \sum_{j=1}^{n} c_j Q_{g_\ell}^L\left[f_{\ell,j}, \Omega_\ell\right]$. Thus

$$Q_g^L[f, \Omega] - I_g[\mathcal{L}[\boldsymbol{v}], \Omega] = \sum_\ell \left(Q_{g_\ell}^L\left[f_\ell, \Omega_\ell\right] - \int_{Z_\ell} \rho\right)$$

$$= \sum_\ell \sum_{j=1}^{n} c_j \left(Q_{g_\ell}^L\left[f_{\ell,j}, \Omega_\ell\right] - I_{g_\ell}\left[f_{\ell,j}, \Omega_\ell\right]\right) \qquad (5.2.5)$$

$$= \sum_\ell \sum_{j=1}^{n} \mathcal{O}\left(\omega^{-1}\right) \mathcal{O}\left(\omega^{-s-d+1}\right) = \mathcal{O}\left(\omega^{-s-d}\right).$$

Putting both parts together we obtain that $I_g[f, \Omega] - Q_g^L[f, \Omega] = \mathcal{O}\left(\omega^{-s-d}\right)$.

Q.E.D.

Admittedly the regularity condition seems strict, however, it typically holds in practice.

There is no equivalent to a Chebyshev set in higher dimensions [**16**], so we cannot generalize Theorem 3.2.2. We can, however, under certain circumstances show that the regularity condition is satisfied whenever the standard polynomial basis can interpolate at the given nodes and multiplicities. The following corollary states, for simplicial domains and affine g, that a Levin-type method is equivalent to a Filon-type method with the standard polynomial basis. This is the main problem domain where Filon-type methods are effective, so in essence Levin-type methods are an extension of Filon-type methods.

Corollary 5.2.2 *If g is affine, then $I_g[\mathcal{L}[\boldsymbol{v}], \Omega] = Q_g^F[f, \Omega]$ whenever $\boldsymbol{\psi}_k = \psi_k\, \boldsymbol{t}$, where ψ_k is the standard polynomial basis and $\boldsymbol{t} \in \mathbb{R}^d$ is chosen so that $\boldsymbol{t} \cdot \nabla g \neq 0$. Furthermore, if Ω is the d-dimensional simplex S_d, then $Q_g^L[f, S_d]$ is equal to $Q_g^F[f, S_d]$ whenever a sufficient number of sample points are taken.*

Proof: Note that solving a Levin-type method collocation system is equivalent to interpolating with the basis $\tilde{\psi}_j = \mathcal{L}[\boldsymbol{\psi}_j] = \boldsymbol{t} \cdot \nabla \psi_j + i\omega \psi_j \boldsymbol{t} \cdot \nabla g$. We begin by showing that $\tilde{\psi}_k$ and ψ_k are equivalent. Assume that $\{\tilde{\psi}_1, \ldots, \tilde{\psi}_{j-1}\}$ has equivalent span to $\{\psi_1, \ldots, \psi_{j-1}\}$. This is true for the case $\psi_1 \equiv 1$ since $\mathcal{L}[\boldsymbol{t}] = i\omega \boldsymbol{t} \cdot \nabla g = C$, where $C \neq 0$ by hypothesis. Note that $\psi_j(x_1, \ldots, x_d) = x_1^{p_1} \ldots x_d^{p_d}$ for some nonnegative integers p_k. Then, for $\boldsymbol{t} = (t_1, \cdots, t_d)^\top$,

$$\tilde{\psi}_j = i\omega \psi_j \boldsymbol{t} \cdot \nabla g + \boldsymbol{t} \cdot \nabla \psi_j = C\psi_j + \sum_{k=1}^{d} t_k \mathcal{D}^{e_k} \psi_j$$

$$= C\psi_j + \sum_{k=1}^{d} t_k p_k x_1^{p_1} \ldots x_{k-1}^{p_{k-1}} x_k^{p_k - 1} x_{k+1}^{p_{k+1}} \ldots x_d^{p_d}.$$

The sum is a polynomial of degree less than the degree of ψ_j, hence it lies in the span of $\{\psi_1, \ldots, \psi_{j-1}\}$. Thus ψ_j lies in the span of $\{\tilde{\psi}_1, \ldots, \tilde{\psi}_j\}$. It follows that interpolation by each of these two bases is equivalent, or in other words $I_g[\mathcal{L}[\boldsymbol{v}], \Omega] = Q_g^F[f, \Omega]$.

We prove the second part of the theorem by induction, where the case of $\Omega = S_1$ holds true by the definition $Q_g^L[f, S_1] = I_g[\mathcal{L}[\boldsymbol{v}], S_1]$. Now assume it is true for each dimension less than d. Since g is affine and each boundary T_ℓ of the simplex is affine we know that each g_ℓ is affine. Furthermore we know that the Jacobian determinants of T_ℓ are constants, hence each f_ℓ is a polynomial. Thus $Q_{g_\ell}^L[f_\ell, S_{d-1}] = Q_{g_\ell}^F[f_\ell, S_{d-1}] = I_{g_\ell}[f_\ell, S_{d-1}]$, as long as enough sample points are taken so that f_ℓ lies in the span of the interpolation basis. Hence $Q_g^L[f, S_d] = I_g[\mathcal{L}[\boldsymbol{v}], S_d] = Q_g^F[f, S_d]$.

<div align="right">*Q.E.D.*</div>

An important consequence of this corollary is that, in the two-dimensional case, a Levin-type method provides an approximation whenever the standard polynomial basis can interpolate f at the given nodes and multiplicities, assuming that g is affine and the nonresonance condition is satisfied in Ω.

We can now demonstrate the effectiveness of this method with several numerical examples. For simplicity, we take $\boldsymbol{\psi}_k = \psi_k \boldsymbol{1}$, where ψ_k is the d-dimensional polynomial basis and $\boldsymbol{1}$ is the d-dimensional vector of all ones $(1, \ldots, 1)^\top$. Note that this attaches an artificial orientation to this approximation scheme, however, this will not affect the asymptotics of the method. We begin with the case of integrating over a simplex, which Corollary 5.2.2 showed is equivalent to a Filon-type method. Let $f(x, y, z, t) = x^2$, $g(x, y, z, t) = x - 2y + 3z - 4t$ and approximate $I_g[f, S_4]$ by $Q_g^L[f, S_4]$ collocating only at the vertices with multiplicities all one. As expected, we obtain an error of order $\mathcal{O}(\omega^{-5})$, as seen in Figure 5.28. Because this Levin-type method is equivalent to a Filon-type method, it would have solved this integral exactly had we increased the number of node points so that $\psi_k(x, y, z, t) = x^2$ was included
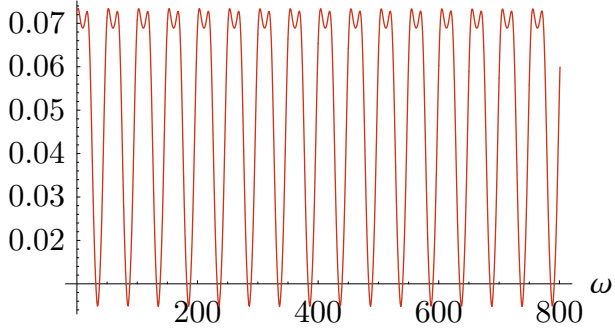
Figure 5.28: The error scaled by ω^5 of $Q_g^L[f, S_4]$ collocating only at the vertices with multiplicities all one, for $I_g[f, S_4] = \int_{S_4} x^2 e^{i\omega(x-2y+3z-4t)}\, dV$.
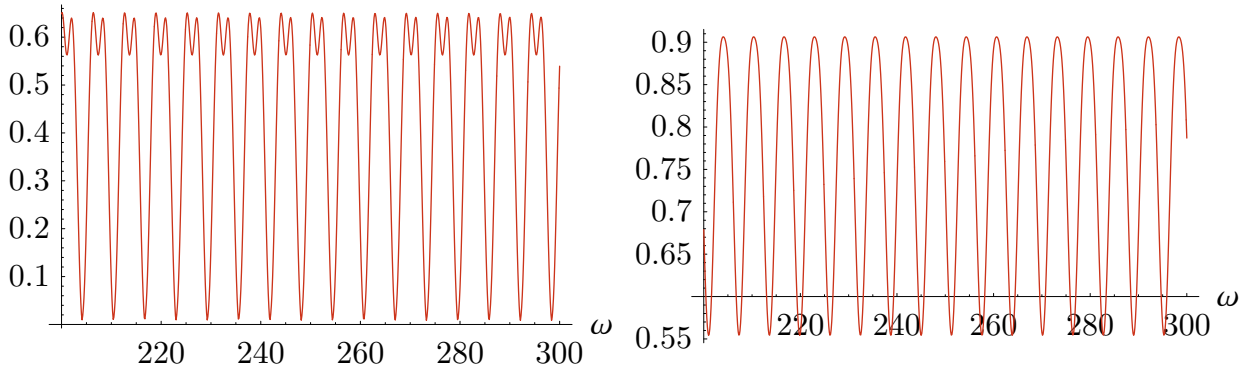

Figure 5.29: The error scaled by ω^3 of $Q_g^L[f, S_2]$ collocating only at the vertices with multiplicities all one (left graph), and the error scaled by ω^4 with vertex multiplicities all two and an additional point at $\left(\frac{1}{3}, \frac{1}{3}\right)$ with multiplicity one (right graph), for $I_g[f, S_2] = \int_{S_2} \left(\frac{1}{x+1} + \frac{2}{y+1}\right) e^{i\omega(2x-y)}\, dV$.

as a basis vector.

Now consider the more complicated function $f(x, y) = \frac{1}{x+1} + \frac{2}{y+1}$ with oscillator $g(x, y) = 2x - y$, approximated by $Q_g^L[f, S_2]$, again only sampling at the vertices with multiplicities all one. As expected we obtain an order of error of $\mathcal{O}(\omega^{-3})$. By adding an additional multiplicity to each vertex, as well as the sample point $\left(\frac{1}{3}, \frac{1}{3}\right)$ with multiplicity one to ensure that we have ten equations in our system as required by polynomial interpolation, we increase the asymptotic order by one to $\mathcal{O}(\omega^{-4})$. Both of these cases can be seen in Figure 5.29. Note that the different scale factor means that the right graph is in fact much more accurate, as it has about $1/\omega$th the error. Finally we demonstrate an integral over a three-dimensional simplex. Let $f(x, y) = x^2 - y + z^3$ and $g(x, y) = 3x + 4y - z$. Figure 5.30 shows the error of $Q_g^L[f, S_3]$, sampling only at the vertices, multiplied by ω^4.

76
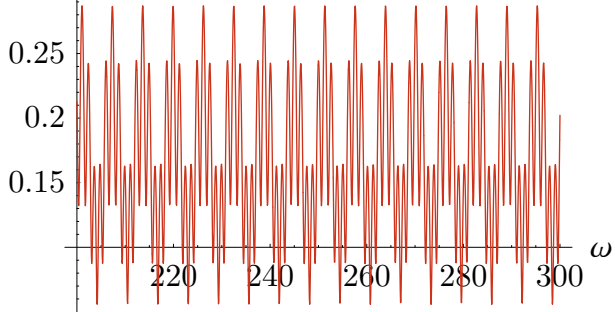
Figure 5.30: The error scaled by ω^4 of $Q_g^L[f, S_3]$ collocating only at the vertices with multiplicities all one, for $I_g[f, S_3] = \int_{S_3}(x^2 - y + z^3)\mathrm{e}^{\mathrm{i}\omega(3x+4y-z)}\,\mathrm{d}V$.
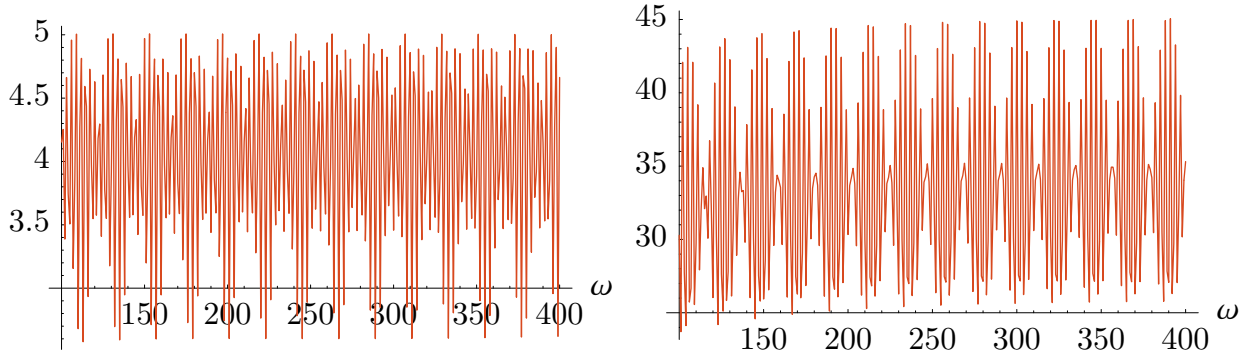
Figure 5.31: The error scaled by ω^3 of $Q_g^L[f, H]$ collocating only at the vertices with multiplicities all one (left graph), and the error scaled by ω^4 with vertex multiplicities all two and an additional point at $\left(\frac{1}{3}, \frac{1}{3}\right)$ with multiplicity one (right graph), for $I_g[f, H] = \int_H \mathrm{e}^x \cos xy\, \mathrm{e}^{\mathrm{i}\omega(x^2+x-y^2-y)}\,\mathrm{d}V$.

Because Levin-type methods do not require moments, they allow us to integrate over more complicated domains that satisfy the nonresonance condition, without resorting to tessellation. For example, we return to the case of the quarter unit disc H. Let $f(x, y) = \mathrm{e}^x \cos xy$, $g(x, y) = x^2 + x - y^2 - y$, and choose vertices for nodes with multiplicities all one. Note that g is nonlinear, in addition to the domain not being a simplex. Despite these difficulties, $Q_g^L[f, H]$ still attains an order of error $\mathcal{O}(\omega^{-3})$, as seen in the left hand side of Figure 5.31. If we increase the multiplicities at the vertices to two, adding an additional node at $\left(\frac{1}{3}, \frac{1}{3}\right)$ with multiplicity one, we obtain an error of order $\mathcal{O}(\omega^{-4})$. This can be seen in the right side of Figure 5.31. This example is significant since, due to the unavailability of moments, Filon-type methods fail to provide approximations in a quarter disc, let alone with nonlinear g. Were g linear, we could have tessellated H to obtain a polytope, but that would have resulted in an unnecessarily large number of calculations. With nonlinear g we

77

do not even have this option, hence Filon-type methods are completely unsuitable.

5.3. Asymptotic basis condition

It is important to note that, for a Levin-type method, we do not necessarily need to use polynomials for $\{\psi_k\}$. Not only can we greatly improve the accuracy of the approximation by choosing the basis wisely, but surprisingly we can even obtain a higher asymptotic order. The *asymptotic basis condition* is satisfied if the basis $\{\psi_1, \ldots, \psi_n\}$ satisfies the following conditions:

$$\nabla g \cdot \psi_1 = f, \qquad \nabla g \cdot \psi_{k+1} = \nabla \cdot \psi_k, \qquad k = 1, 2, \ldots.$$

For the univariate case, this condition becomes the asymptotic basis of Section 3.3:

$$\psi_1 = \frac{f}{g'}, \qquad \psi_{k+1} = \frac{\psi_k'}{g'}, \qquad k = 1, 2, \ldots.$$

We will use $Q^B[f]$ to denote a Levin-type method whose basis satisfies the asymptotic basis condition.

Surprisingly, this choice of basis increases the asymptotic order of $Q^B[f]$ to $\mathcal{O}\left(\omega^{-\tilde{n}-s-d}\right)$, where s is again the minimum vertex multiplicity and $\tilde{n}$ is equal to the minimum of the number of equations in every collocation system (5.2.3) solved for in the definition of Q^L, recursively down to the univariate integrals. It follows that if $\Omega \subset \mathbb{R}$, then $\tilde{n} = n$. As an example, if we are collocating on a two-dimensional simplex at only the three vertices with multiplicities all one, then the initial collocation system has three equations, whilst each boundary collocation system has only two equations. Thus $\tilde{n} = \min\{3, 2, 2, 2\} = 2$, and the order is $\mathcal{O}\left(\omega^{-2-1-2}\right) = \mathcal{O}\left(\omega^{-5}\right)$.

The following lemma is used extensively in the proof of the asymptotic order:

Lemma 5.3.1 *Suppose $\{\psi_k\}$ satisfies the asymptotic basis condition. Then, for $k \geq 1$,*

$$\det\left(\boldsymbol{g}_k, \boldsymbol{a}_k, \cdots, \boldsymbol{a}_{k+j}, B\right) = \det\left(\boldsymbol{g}_k, \boldsymbol{g}_{k+1}, \cdots, \boldsymbol{g}_{k+j+1}, B\right),$$

where B represents all remaining columns that render the matrices square and $\boldsymbol{a}_k = \boldsymbol{p}_k + \mathrm{i}\omega\boldsymbol{g}_k$, for

$$\boldsymbol{p}_k = \mathcal{P}[\nabla \cdot \psi_k], \qquad \boldsymbol{g}_k = \mathcal{P}[\nabla g \cdot \psi_k].$$

Proof: We know that $\boldsymbol{p}_k = \mathcal{P}[\nabla \cdot \psi_k] = \mathcal{P}[\nabla g \cdot \psi_{k+1}] = \boldsymbol{g}_{k+1}$. Thus we can multiply the first column by $\mathrm{i}\omega$ and subtract it from the second to obtain

$$\det\left(\boldsymbol{g}_k, \boldsymbol{p}_k + \mathrm{i}\omega\boldsymbol{g}_k, \cdots, \boldsymbol{a}_{k+j}, B\right) = \det\left(\boldsymbol{g}_k, \boldsymbol{g}_{k+1}, \boldsymbol{a}_{k+1}, \cdots, \boldsymbol{a}_{k+j}, B\right).$$

The lemma follows by repeating this process on the remaining columns.

<div align="right">*Q.E.D.*</div>

This lemma holds for any column interchange on both sides of the determinant. We can now prove the theorem:

Theorem 5.3.2 *Suppose every basis $\{\psi_k\}$ in a Levin-type method satisfies the asymptotic basis condition. Then*

$$Q_g^B[f, \Omega] - I_g[f, \Omega] \sim \mathcal{O}\left(\omega^{-\tilde{n}-s-d}\right).$$

Proof: We begin by showing that $\mathcal{L}[\boldsymbol{v}] - f = \mathcal{O}\left(\omega^{-n}\right)$. Note that

$$\mathcal{L}[\boldsymbol{v}] - f = \sum_{k=1}^{n} c_k \mathcal{L}[\boldsymbol{\psi}_k] - f = \sum_{k=1}^{n} c_k \left(\nabla \cdot \boldsymbol{\psi}_k + i\omega \nabla g \cdot \boldsymbol{\psi}_k\right) - f$$

$$= \sum_{k=1}^{n} c_k \left(\nabla g \cdot \boldsymbol{\psi}_{k+1} + i\omega \nabla g \cdot \boldsymbol{\psi}_k\right) - \nabla g \cdot \boldsymbol{\psi}_1$$

$$= \nabla g \cdot \left[(i\omega c_1 - 1)\boldsymbol{\psi}_1 + \sum_{k=2}^{n} (c_{k-1} + i\omega c_k)\boldsymbol{\psi}_k + c_n \boldsymbol{\psi}_{n+1}\right]$$

$$= \frac{\nabla g}{\det A} \cdot \left[(i\omega \det A_1 - \det A)\boldsymbol{\psi}_1 + \sum_{k=2}^{n} (\det A_{k-1} + i\omega \det A_k)\boldsymbol{\psi}_k + \det A_n \boldsymbol{\psi}_{n+1}\right],$$

where again A_k is the matrix A with the kth column replaced by $\boldsymbol{f}$. Since the regularity condition is satisfied, we know that $(\det A)^{-1} = \mathcal{O}\left(\omega^{-n}\right)$, cf. Theorem 3.2.1, thus it remains to be shown that each term in the preceding equation is $\mathcal{O}(1)$. This boils down to showing that each of the following terms are $\mathcal{O}(1)$: $i\omega \det A_1 - \det A$, $\det A_{k-1} + i\omega \det A_k$ for $2 \leq k \leq n$ and finally $\det A_n$. The first case follows from Lemma 5.3.1 after rewriting the determinants as

$$i\omega \det A_1 - \det A = i\omega \det A_1 - \det \left(\boldsymbol{p}_1 + i\omega \boldsymbol{g}_1, \boldsymbol{a}_2, \cdots, \boldsymbol{a}_n\right)$$

$$= i\omega \det A_1 - i\omega \det \left(\boldsymbol{g}_1, \boldsymbol{a}_2, \cdots, \boldsymbol{a}_n\right) - \det \left(\boldsymbol{p}_1, \boldsymbol{a}_2, \cdots, \boldsymbol{a}_n\right)$$

$$= -\det \left(\boldsymbol{g}_2, \boldsymbol{a}_2, \cdots, \boldsymbol{a}_n\right) = \mathcal{O}(1),$$

where we used the facts that $\boldsymbol{p}_1 = \boldsymbol{g}_2$ and $\boldsymbol{f} = \boldsymbol{g}_1$. Similarly,

$$\det A_{k-1} + i\omega \det A_k = \det \left(\boldsymbol{a}_1, \cdots, \boldsymbol{a}_{k-2}, \boldsymbol{g}_1, \boldsymbol{p}_k + i\omega \boldsymbol{g}_k, \boldsymbol{a}_{k+1}, \cdots, \boldsymbol{a}_n\right)$$

$$+ i\omega \det \left(\boldsymbol{a}_1, \cdots, \boldsymbol{a}_{k-2}, \boldsymbol{p}_{k-1} + i\omega \boldsymbol{g}_{k-1}, \boldsymbol{g}_1, \boldsymbol{a}_{k+1}, \cdots, \boldsymbol{a}_n\right)$$

$$= \det \left(\boldsymbol{a}_1, \cdots, \boldsymbol{a}_{k-2}, \boldsymbol{g}_1, \boldsymbol{p}_k, \boldsymbol{a}_{k+1}, \cdots, \boldsymbol{a}_n\right)$$

$$+ i\omega \det \left(\boldsymbol{a}_1, \cdots, \boldsymbol{a}_{k-2}, \boldsymbol{g}_1, \boldsymbol{g}_k, \boldsymbol{a}_{k+1}, \cdots, \boldsymbol{a}_n\right)$$

$$+ i\omega \det \left(\boldsymbol{a}_1, \cdots, \boldsymbol{a}_{k-2}, \boldsymbol{g}_k, \boldsymbol{g}_1, \boldsymbol{a}_{k+1}, \cdots, \boldsymbol{a}_n\right)$$

$$- \omega^2 \det \left(\boldsymbol{a}_1, \cdots, \boldsymbol{a}_{k-2}, \boldsymbol{g}_{k-1}, \boldsymbol{g}_1, \boldsymbol{a}_{k+1}, \cdots, \boldsymbol{a}_n\right)$$

$$= \det \left(\boldsymbol{a}_1, \cdots, \boldsymbol{a}_{k-2}, \boldsymbol{g}_1, \boldsymbol{p}_k, \boldsymbol{a}_{k+1}, \cdots, \boldsymbol{a}_n\right)$$

$$- \omega^2 \det \left(\boldsymbol{a}_1, \cdots, \boldsymbol{a}_{k-2}, \boldsymbol{g}_{k-1}, \boldsymbol{g}_1, \boldsymbol{a}_{k+1}, \cdots, \boldsymbol{a}_n\right).$$
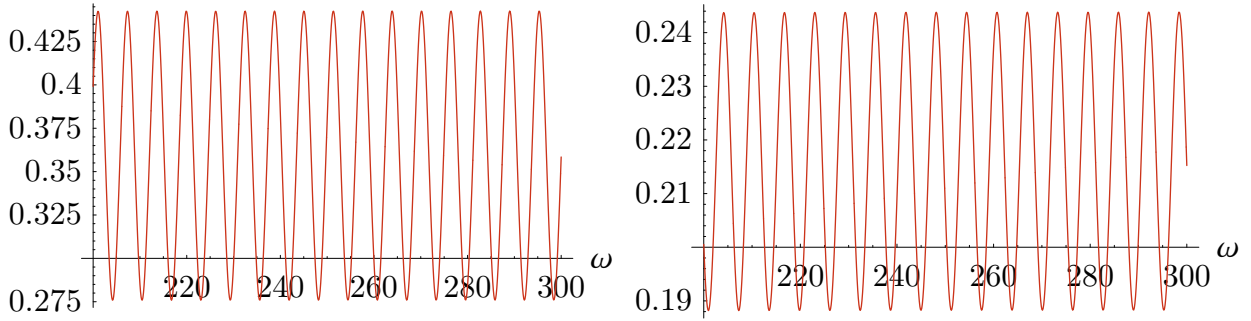
Figure 5.32: The error scaled by ω^4 of $Q_g^B[f, S_2]$ collocating only at the vertices with multiplicities all one (left graph), and the error scaled by ω^5 collocating at the vertices as well as each of the boundary midpoints $\{(1/2, 0), (0, 1/2), (1/2, 1/2)\}$ with multiplicities all one (right graph), for $\int_{S_2} \left(\frac{1}{x+1} + \frac{2}{y+1}\right) e^{i\omega(2x-y)} \, \mathrm{d}V$.

Using Lemma 5.3.1 the first of these determinants is $\mathcal{O}(1)$, whilst the second determinant has two columns equal to $\boldsymbol{g}_{k-1}$, hence is equal to zero. The last determinant $\det A_n$ is also $\mathcal{O}(1)$, due to Lemma 5.3.1. Thus we have shown that $\mathcal{L}[\boldsymbol{v}] - f = \mathcal{O}(\omega^{-n})$.

From Corollary 5.1.1, it follows that

$$I_g[f, \Omega] - I_g[\mathcal{L}[v], \Omega] = \mathcal{O}(\omega^{-n-s-d}) = \mathcal{O}(\omega^{-\tilde{n}-s-d}).$$

For the univariate case the lemma has been proved, since $Q_g^B[f, (a, b)] = I_g[\mathcal{L}[v], (a, b)]$. By induction, $Q_{g_\ell}^B\left[f_{\ell,j}, \Omega_\ell\right] - I_{g_\ell}\left[f_{\ell,j}, \Omega_\ell\right] = \mathcal{O}(\omega^{-\tilde{n}-s-(d-1)})$ in (5.2.5). It follows that

$$I_g[f, \Omega] - Q_g^B[f, \Omega] = \left(I_g[f, \Omega] - I_g[\mathcal{L}[v], \Omega]\right) - \left(Q_g^B[f, \Omega] - I_g[\mathcal{L}[v], \Omega]\right)$$
$$= \mathcal{O}(\omega^{-\tilde{n}-s-d}).$$

Q.E.D.

The derivatives required to find each $\boldsymbol{\psi}_k$ can quickly become unmanageable when either f or g is even moderately complicated. This issue can be mitigated since it is possible to show that including j other basis functions, for example the first j polynomials, and using a basis which satisfies the asymptotic basis condition for the remaining basis functions results in an error of order $\mathcal{O}(\omega^{-\tilde{n}-s-d+j})$. With this in mind, in all the examples we include the constant function 1 in our basis. This results in errors on the order $\mathcal{O}(\omega^{-\tilde{n}-s-d+1})$.

For the remainder of this section we will use the basis $\boldsymbol{\psi}_k = (\psi_k, -\psi_k)^\top$, where

$$\psi_1 = \frac{f}{g_x - g_y}, \qquad \psi_{k+1} = \frac{\psi_{k,x} - \psi_{k,y}}{g_x - g_y}, \qquad k = 1, 2, \ldots.$$

80
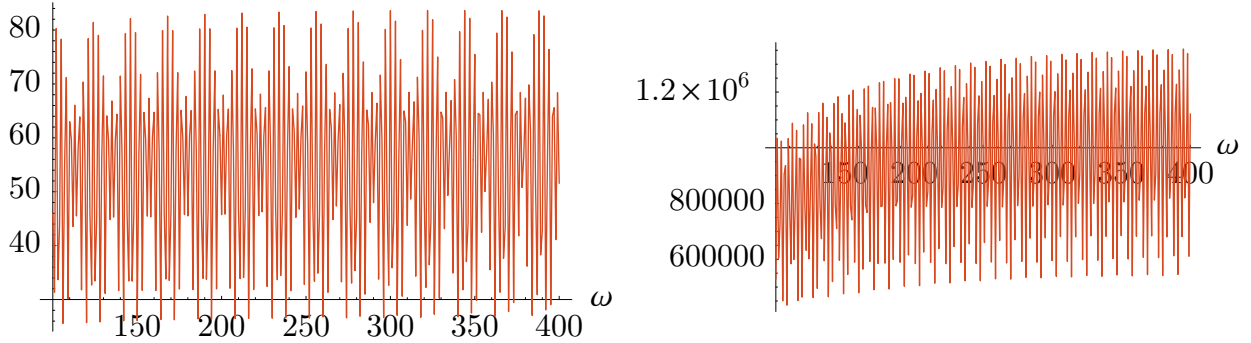
Figure 5.33: The error scaled by ω^4 of $Q_g^B[f, H]$ collocating only at the vertices with multiplicities all one (left graph), and the error scaled by ω^7 of $Q_g^B[f, H]$ collocating only at the vertices with multiplicities all two (right graph), for $I_g[f, H] = \int_H e^x \cos xy \; e^{i\omega(x^2+x-y^2-y)} \, dV$.

This satisfies the asymptotic basis condition, since

$$\nabla g \cdot \boldsymbol{\psi}_1 = \frac{f}{g_x - g_y} \nabla g \cdot (1, -1)^\top = f,$$

$$\nabla g \cdot \boldsymbol{\psi}_{k+1} = \frac{\psi_{k,x} - \psi_{k,y}}{g_x - g_y} \nabla g \cdot (1, -1)^\top = \psi_{k,x} - \psi_{k,y} = \nabla \cdot \boldsymbol{\psi}_k.$$

Recall the example where $f(x, y) = \frac{1}{x+1} + \frac{2}{y+1}$ with oscillator $g(x, y) = 2x - y$ over the simplex S_2. We now use $Q_g^B[f, S_2]$ in place of $Q_g^L[f, S_2]$, collocating only at the vertices. Since this results in each univariate boundary collocation having two node points, we know that $\tilde{n} = 2$. Hence we now scale the error by ω^4, i.e., we have increased the order by one, as seen in Figure 5.32. Since the initial two-dimensional system has three node points, adding the midpoint to the sample points of each univariate integral should increase the order again by one to $\mathcal{O}(\omega^{-5})$. This can be seen in the right side of Figure 5.32.

There is nothing special about a simplex or linear g: the asymptotic basis works equally well on other domains with nonlinear g, assuming that the regularity and nonresonance conditions are satisfied. Recall the example with $f(x, y) = e^x \cos xy$ and $g(x, y) = x^2 + x - y^2 - y$ on the quarter disc H. As in the simplex case, $Q_g^B[f, H]$ collocating only at vertices with multiplicities all one results in an error of $\mathcal{O}(\omega^{-4})$, as seen in the left side of Figure 5.33. Note that increasing multiplicities not only increases s, but also $\tilde{n}$. If we increase the multiplicities to two, then $s = 2$ and $\tilde{n} = 4$, and the order increases to $\mathcal{O}(\omega^{-7})$, as seen in the right side of Figure 5.33. It should be emphasized that, though the scale is large in the graph, the error is being divided by $\omega^7 \geq 100^7 = 10^{14}$. As a result, the errors for the right graph are in fact less than the errors in the left graph.

81
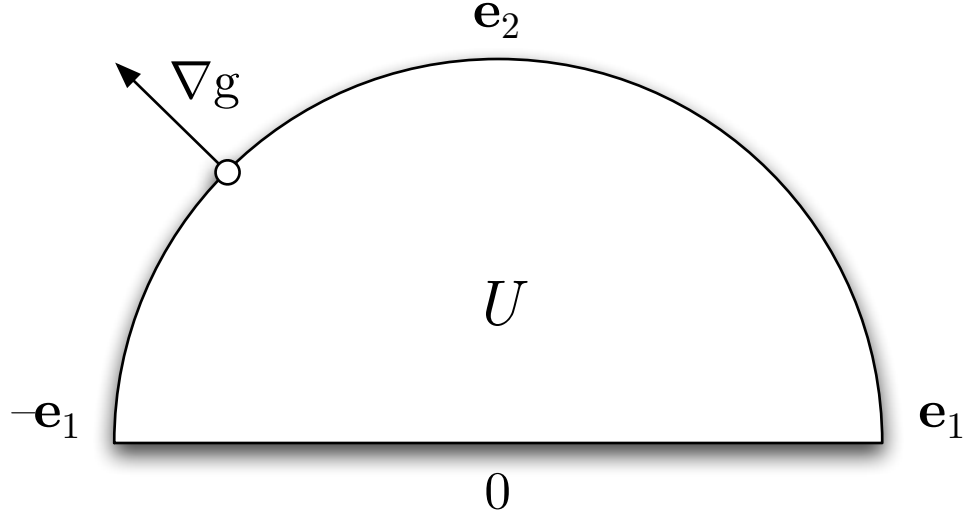
Figure 5.34: Depiction of a half disc U, where the vector ∇g represents the direction of the gradient of $g(x, y) = y - x$, highlighting where it is orthogonal to the boundary of U.

5.4. Resonance points

Up until this point we have avoided computing highly oscillatory integrals that do not satisfy the nonresonance condition. But we know that a large class of integrals fail this condition: for example if g is linear then any Ω with a completely smooth boundary must have at least two point of resonance. In this section we investigate such integrals, and see where Levin-type methods fail.

Suppose that ∇g is orthogonal to the boundary of $\Omega \subset \mathbb{R}^d$ at a single point $\boldsymbol{u}$. Let us analyse what happens at this point when we push the integral to the boundary, as in a Levin-type method. If T_ℓ is the map that defines the boundary component Z_ℓ containing $\boldsymbol{u}$, then the statement of orthogonality is equivalent to

$$\nabla g(T_\ell(\boldsymbol{\xi}))^\top T_\ell'(\boldsymbol{\xi}) = \mathbf{0},$$

where $\boldsymbol{\xi} \in \Omega_\ell$, $\boldsymbol{u} = T_\ell(\boldsymbol{\xi})$ and T_ℓ' is the derivative matrix of T_ℓ. After pushing the integral to the boundary we now have the oscillator $g_\ell = g \circ T_\ell$. But it follows that

$$\nabla g_\ell(\boldsymbol{\xi})^\top = (g \circ T_\ell)'(\boldsymbol{\xi}) = \nabla g(T_\ell(\boldsymbol{\xi}))^\top T_\ell'(\boldsymbol{\xi}) = \mathbf{0}.$$

In other words the resonance point has become a stationary point. An asymptotic expansion in [50] states that a Filon-type method must sample at a stationary point in order to obtain a higher asymptotic order than that of the integral, hence, by the same logic, a Levin-type method must also sample at a stationary point. It follows that a Levin-type method cannot be used because the regularity condition can never be satisfied, since $\nabla g_\ell(\boldsymbol{\xi})^\top \boldsymbol{\psi}_k(\boldsymbol{\xi}) = 0$. Moreover, in general each g_ℓ is a fairly complicated function and no moments are available, thus Filon-type methods are not feasible.
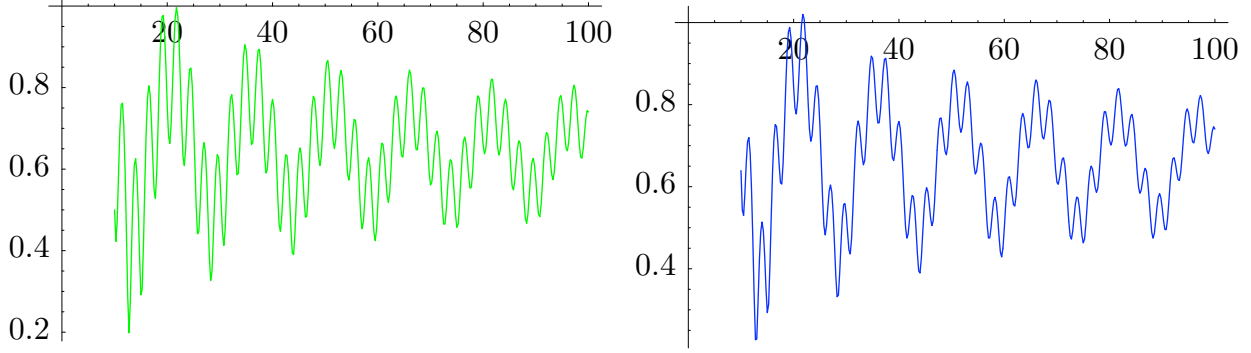
Figure 5.35: The error scaled by $\omega^{5/2}$ in approximating $I_g[f,U] = \iint_U \cos x \cos y \, e^{i\omega(y-x)} \, dV$. The left graph approximates the integral by $I_g[\mathcal{L}[\boldsymbol{v}],U]$, where $\mathcal{L}[\boldsymbol{v}]$ is determined by collocation at the two vertices and the resonance point, all with multiplicities one. The right graph approximates $I_g[\mathcal{L}[\boldsymbol{v}],U]$ by three Moment-free Filon-type methods.

As a concrete example, consider the unit *half disc* U, with $g(x,y) = y - x$, as seen in Figure 5.34. The boundary curve which exhibits the problem is defined for $\Omega_1 = (0,\pi)$ as $T_1(t) = (\cos t, \sin t)^\top$. We find that ∇g is orthogonal to the boundary at the point $T_1\left(\frac{3\pi}{4}\right) = \left(-\frac{\sqrt{2}}{2}, \frac{\sqrt{2}}{2}\right)^\top$, since $\nabla g\left(T_1\left(\frac{3\pi}{4}\right)\right)^\top T_1'\left(\frac{3\pi}{4}\right) = (-1,1)\left(-\sin\frac{3\pi}{4}, \cos\frac{3\pi}{4}\right)^\top = 0$. Combining Theorem 2.6.1 and [50], we assert that in order to obtain an order of error $\mathcal{O}\left(\omega^{-s-\frac{3}{2}}\right)$ our collocation points must include $(-1,0)$ and $(1,0)$ with multiplicity s, as well as the point of resonance $\left(-\frac{\sqrt{2}}{2}, \frac{\sqrt{2}}{2}\right)$ with multiplicity $2s-1$. We assume that the resulting system is in fact solvable. When we push the integral to the boundary, we obtain two line integrals:

$$\int_U f e^{i\omega g} \approx \int_U \mathcal{L}[\boldsymbol{v}] \, e^{i\omega g} = \int_{Z_1} e^{i\omega g}\boldsymbol{v} \cdot d\boldsymbol{s} + \int_{Z_2} e^{i\omega g}\boldsymbol{v} \cdot d\boldsymbol{s}$$
$$= I_{g_1}[f_1,(0,\pi)] + I_{g_2}[f_2,(-1,1)],$$

where Z_2 corresponds to the boundary of U on the x-axis, while

$$f_1(t) = (-\sin t, \cos t)^\top \cdot \boldsymbol{v}(\cos t, \sin t), \qquad\qquad g_1(t) = g(\cos t, \sin t) = \sin t - \cos t,$$

$$f_2(t) = v_1(t,0) \qquad\qquad \text{and} \qquad g_2(t) = g(t,0) = -t.$$

We see that $I_g[f,U] - I_{g_1}[f_1,(0,\pi)] - I_{g_2}[f_2,(-1,1)]$ does indeed appear to have an order of error $\mathcal{O}\left(\omega^{-5/2}\right)$ in the left graph of Figure 5.35, where the univariate integrals are computed numerically using MATHEMATICA. It follows that, if we can approximate these univariate integrals with the appropriate error, then we can derive an equivalent to Theorem 5.2.1 for when the nonresonance condition is not satisfied.

Note that $I_{g_1}[f_1,(0,\pi)]$ is a one-dimensional integral with oscillator $g_1(t) = \sin t - \cos t$.

But $g_1'\left(\frac{1}{2}\right) = -\cos\frac{3\pi}{4} + \sin\frac{3\pi}{4} = 0$, meaning that we have a stationary point. Unfortunately none of the moments of g_1 are elementary, including the zeroth moment. Thus neither a standard Filon-type method nor the Iserles and Nørsett expansion from Chapter 4 are applicable. However, we can employ a Moment-free Filon-type method to approximate these integrals successfully. To avoid issues with g_1'' vanishing, we write the integral as

$$I_{g_1}\left[f_1,\left(0,\frac{\pi}{2}\right)\right] + I_{g_1}\left[f_1,\left(\frac{\pi}{2},\pi\right)\right] + I_{g_2}\left[f_2,(-1,1)\right].$$

The first integral has no stationary points, thus we utilizing a Moment-free Filon-type method with nodes $\left\{0,\frac{\pi}{2}\right\}$ and multiplicities both one. The second integral has a single stationary point at $\frac{3\pi}{4}$, thus we use the nodes $\left\{\frac{\pi}{2},\frac{3\pi}{4},\pi\right\}$ again with multiplicities all one. The last integral is simply a constant times the zeroth moment of the Fourier oscillator, thus either Filon-type methods will compute it exactly. The right graph of Figure 5.35 shows the resulting error, which is almost indistinguishable from the left graph which computes the univariate integral exactly. Thus the error is dominated by the initial bivariate collocation system.

5.5. Stationary points

The conclusion of the previous section—which can be confirmed by analysing the proof of Theorem 5.2.1—is that resonance points do not present a problem; in themselves they only affect the approximation in the lower dimensional boundary integrals. Thus if we are able to compute integrals with stationary points then we can handle resonance points as well. In Chapter 4, we obtained a method for univariate oscillatory integrals with stationary points via incomplete Gamma functions. In this section we attempt to generalize this result for bivariate integrals. As this is a work in progress, we restrict our attention to a simple particular integral:

$$\iint_{S_2} f(x,y)e^{i\omega(x^2+y^2)}\,dV,$$

where S_2 is again the two-dimensional simplex. We however compute this integral in a way that allows for generalization. This integral has a single stationary point at zero.

In Lemma 4.3.1, we determined the basis for a univariate Moment-free Filon-type method to be

$$\phi_{r,k}(x) = \frac{\omega^{-\frac{k+1}{r}}}{r}e^{-i\omega g(x)}\Gamma\left(\frac{1+k}{r},-i\omega g(x)\right), \qquad x \geq 0,$$

where we drop the constant $D_{r,k}$ since we restrict our attention to positive x. This suggests an ansatz for the first basis function in the multivariate case:

$$\boldsymbol{\phi}_0(x,y) = \omega^{-\frac{1}{2}}\left(e^{-i\omega q_1(x,y)}\Gamma\left(\frac{1}{2},-i\omega q_1(x,y)\right), e^{-i\omega q_2(x,y)}\Gamma\left(\frac{1}{2},-i\omega q_2(x,y)\right)\right)^{\top},$$

where q_1 and q_2 have not yet been determined. The choice of constant in front will become clear later. Plugging this function into the operator

$$\mathcal{L}[\boldsymbol{v}] = \nabla \cdot \boldsymbol{v} + \mathrm{i}\omega \nabla g \cdot \boldsymbol{v}$$

gives us

$$\mathcal{L}[\boldsymbol{\phi}_0] = \mathrm{i}\sqrt{\omega}\mathrm{e}^{-\mathrm{i}\omega q_1}\Gamma\left(\frac{1}{2}, -\mathrm{i}\omega q_1\right)\frac{\partial}{\partial x}(g - q_1) + \mathrm{i}\sqrt{\omega}\mathrm{e}^{-\mathrm{i}\omega q_2}\Gamma\left(\frac{1}{2}, -\mathrm{i}\omega q_2\right)\frac{\partial}{\partial y}(g - q_2)$$

$$- \frac{\partial q_1}{\partial x}\frac{\mathrm{e}^{\frac{-\mathrm{i}\pi}{4}}}{\sqrt{q_1}} - \frac{\partial q_2}{\partial y}\frac{\mathrm{e}^{\frac{-\mathrm{i}\pi}{4}}}{\sqrt{q_2}}.$$

For this to be nonoscillatory we must eliminate the terms involving incomplete Gamma functions, thus we require q_1 and q_2 to solve

$$\frac{\partial g}{\partial x} = \frac{\partial q_1}{\partial x} \qquad \text{and} \qquad \frac{\partial g}{\partial y} = \frac{\partial q_2}{\partial y}. \tag{5.5.1}$$

At first glance one might be tempted to set $q_1, q_2 = g$, unfortunately, this causes $\mathcal{L}[\boldsymbol{\phi}_0]$ to be no longer smooth at zero:

$$\mathcal{L}[\boldsymbol{\phi}_0] = \frac{\mathrm{e}^{\frac{-\mathrm{i}\pi}{4}}}{\sqrt{g}}\nabla \cdot g = \frac{\mathrm{e}^{\frac{-\mathrm{i}\pi}{4}}}{\sqrt{x^2 + y^2}}(x + y).$$

Thus we have the additional requirement that

$$\frac{\partial q_1}{\partial x}\frac{1}{\sqrt{q_1}} \qquad \text{and} \qquad \frac{\partial q_2}{\partial y}\frac{1}{\sqrt{q_2}} \tag{5.5.2}$$

are smooth. For the oscillator $g(x, y) = x^2 + y^2$ inspection reveals that $q_1(x, y) = x^2$ and $q_2(x, y) = y^2$ satisfy both conditions (though this is not the only possible solution: $q_1(x, y) = q_2(x, y) = \frac{(x+y)^2}{2}$ works as well). In this case

$$\mathcal{L}[\boldsymbol{\phi}_0] = -4\mathrm{e}^{-\mathrm{i}\frac{\pi}{4}},$$

hence we can scale $\boldsymbol{\phi}_0$ by $-\frac{1}{4}\mathrm{e}^{\mathrm{i}\frac{\pi}{4}}$, giving us

$$\boldsymbol{\phi}_0(x, y) = -\frac{1}{4}\mathrm{e}^{\mathrm{i}\frac{\pi}{4}}\omega^{-\frac{1}{2}}\left(\mathrm{e}^{-\mathrm{i}\omega x^2}\Gamma\left(\frac{1}{2}, -\mathrm{i}\omega x^2\right), \mathrm{e}^{-\mathrm{i}\omega y^2}\Gamma\left(\frac{1}{2}, -\mathrm{i}\omega y^2\right)\right)^{\top}.$$

The next two terms are much more straightforward:

$$\boldsymbol{\phi}_1(x, y) = \frac{1}{2\mathrm{i}\omega}(1, 0)^{\top} \qquad \Rightarrow \qquad \mathcal{L}[\boldsymbol{\phi}_1](x, y) = x,$$

$$\boldsymbol{\phi}_2(x, y) = \frac{1}{2\mathrm{i}\omega}(0, 1)^{\top} \qquad \Rightarrow \qquad \mathcal{L}[\boldsymbol{\phi}_2](x, y) = y.$$
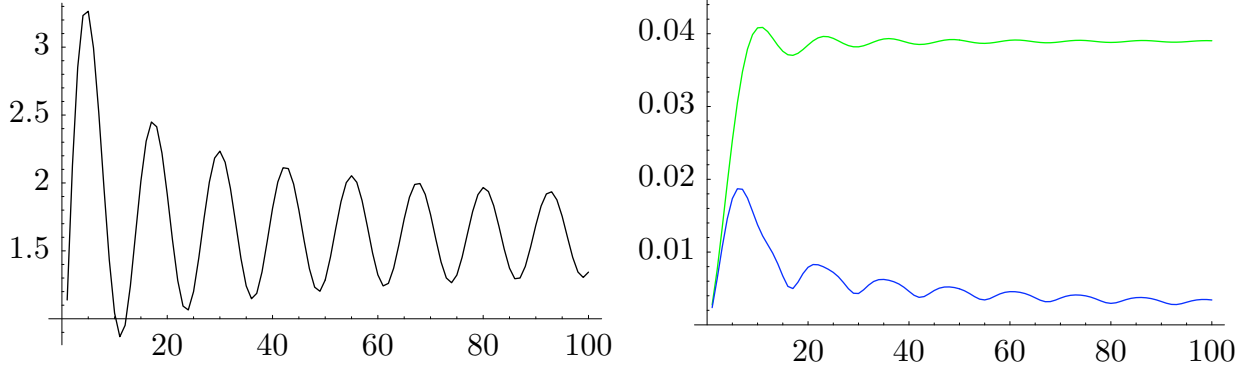
Figure 5.36:   In the left graph, we depict the integral $\iint_{S_2} (\cos xy + y + 1)\, e^{i\omega(x^2+y^2)}\, dV$ scaled by ω. In the right graph, we depict the error scaled by $\omega^{3/2}$ in approximating the integral by interpolating at the nodes $\{(0,0),(1,0),(0,1)\}$ and with nodes $\left\{(0,0),(1,0),(0,1),\left(\frac{1}{2},0\right),\left(0,\frac{1}{2}\right),\left(\frac{1}{2},\frac{1}{2}\right)\right\}$.

Higher order terms can be found without too much difficulty. The quadratic terms are

$$\boldsymbol{\phi}_3(x,y) = \frac{1}{2i\omega}\left[(x,0)^\top - \boldsymbol{\phi}_0(x,y)\right] \qquad \Rightarrow \qquad \mathcal{L}[\boldsymbol{\phi}_1](x,y) = x^2,$$

$$\boldsymbol{\phi}_4(x,y) = \frac{1}{4i\omega}(y,x)^\top \qquad \Rightarrow \qquad \mathcal{L}[\boldsymbol{\phi}_2](x,y) = xy,\,.$$

$$\boldsymbol{\phi}_5(x,y) = \frac{1}{2i\omega}\left[(0,y)^\top - \boldsymbol{\phi}_0(x,y)\right] \qquad \Rightarrow \qquad \mathcal{L}[\boldsymbol{\phi}_1](x,y) = y^2.$$

This process can be continued, giving us a representation of all the moments as integrals along the boundary of our domain. This holds true over any domain, though we focus on the simplex. In Figure 5.36 we compare approximation methods for the integral

$$\iint_{S_2} (\cos xy + y + 1)\, e^{i\omega(x^2+y^2)}\, dV.$$

In Figure 5.36, we approximate this integral with two methods: the first method interpolates at the vertices $\{(0,0),(1,0),(0,1)\}$; the second method again interpolates at the vertices, as well as three additional interpolation nodes at $\left\{\left(\frac{1}{2},0\right),\left(0,\frac{1}{2}\right),\left(\frac{1}{2},\frac{1}{2}\right)\right\}$. In both methods, we integrate the resulting boundary integrals exactly. The first method appears to have an asymptotic order of $\mathcal{O}\left(\omega^{-3/2}\right)$, while the second method has an asymptotic order of $\mathcal{O}\left(\omega^{-2}\right)$. This is due to a resonance point at $\left(\frac{1}{2},\frac{1}{2}\right)$, which contributes to the asymptotic order of the method. These errors are compared to the integral itself, which decays like $\mathcal{O}\left(\omega^{-1}\right)$.

The problem we have not yet dealt with is how to integrate the resulting boundary integrals. We have several different kernels which must be integrated over the boundary of the domain. Suppose we parameterize the boundary as $T(t) = (T_1(t), T_2(t))^\top$. The kernels

for the terms associated with ϕ_1 and ϕ_2 are irregular exponential kernels:

$$e^{i\omega\left[T_1(t)^2+T_2(t)^2\right]}.$$

If we integrate over a circle, we obtain a nonoscillatory integral; otherwise the results of Chapter 3 and Chapter 4 should accurately approximate the integrals. The kernels associated with the basis function ϕ_0—and all basis functions that depend on ϕ_0—depend on the incomplete Gamma function. An example of such a kernel is

$$e^{i\omega T_2(t)^2}\Gamma\left(\frac{1}{2}, -i\omega T_1(t)^2\right).$$

This is no longer strictly an exponential kernel, and the incomplete Gamma function does not satisfy a differential equation of the form of Chapter 6. Thus we require the development of new quadrature methods for such kernels before the results of this section form a useable quadrature scheme.

Extending this method to other oscillators requires finding q_1 and q_2 which satisfy the requirements (5.5.1) and (5.5.2). Here are some examples where this task is straightforward:

- If $g(x, y) = g_1(x) + g_2(y)$, $g_1(x) = \mathcal{O}\left(x^2\right)$, $g_2(y) = \mathcal{O}\left(y^2\right)$ and g_1 and g_2 are nonzero away from zero, then $q_1(x, y) = g_1(x)$ and $q_2(x, y) = g_2(y)$.

- If $g(x, y) = \tilde{g}(x, y)^2$, then $q_1(x, y) = q_2(x, y) = \tilde{g}(x, y)$.

How to choose q_1 and q_2 for other kernels requires further investigation, as does the analysis of the resulting basis $\mathcal{L}[\phi_k]$ when it is no longer a standard polynomial basis. For example, though we cannot prove an equivalent to Lemma 4.3.2, we may be able to prove that the basis is dense, and find interpolation points where convergence is guaranteed.

Chapter 6

Higher Order Oscillators

In this chapter, we are concerned with numerically approximating the integral

$$I[\boldsymbol{f}] = \int_a^b \boldsymbol{f}(x)^\top \boldsymbol{y}(x)\, \mathrm{d}x,$$

where $\boldsymbol{f} : \mathbb{R} \to \mathbb{R}^d$ is a smooth vector-valued function and $\boldsymbol{y} : \mathbb{R} \to \mathbb{R}^d$ is a smooth, highly oscillatory vector-valued function. We assume that $\boldsymbol{y}$ depends on a parameter ω that determines the frequency of oscillations. We also assume that $\boldsymbol{y}$ satisfies the differential equation

$$\boldsymbol{y}'(x) = A(x)\boldsymbol{y}(x),$$

where A is a $d \times d$ matrix-valued function that depends on ω and has no turning points: $A(x)$ is nonsingular for every x in $[a, b]$. Some common examples are

$$y(x) = \mathrm{e}^{\mathrm{i}\omega g(x)}, \qquad\qquad A(x) = \mathrm{i}\omega g'(x),$$

$$\boldsymbol{y}(x) = \begin{pmatrix} J_{m-1}(\omega x) \\ J_m(\omega x) \end{pmatrix}, \qquad A(x) = \begin{pmatrix} \frac{m-1}{x} & -\omega \\ \omega & -\frac{m}{x} \end{pmatrix},$$

$$\boldsymbol{y}(x) = \begin{pmatrix} \mathrm{Ai}\,(-\omega x) \\ -\omega \mathrm{Ai}\,'(-\omega x) \end{pmatrix}, \quad A(x) = \begin{pmatrix} 0 & 1 \\ -\omega^3 x & 0 \end{pmatrix},$$

where Ai is an Airy function and J_m is a Bessel function [74].

Due to similar logic as in Section 2.1, for large values of ω, traditional quadrature techniques fail to approximate $I[f]$ efficiently. Unless the number of sample points is sufficiently greater than the frequency of oscillations, the relative error of Gauss–Legendre quadrature increases drastically as the frequency becomes large.

The goal of this chapter is to generalize the Levin collocation method of Section 2.8 to obtain higher asymptotic orders. This will be accomplished in a similar vein to the Levin-type method from Section 3.2, which generalized the original Levin collocation method for the exponential oscillatory kernel $y = \mathrm{e}^{\mathrm{i}\omega g}$. The asymptotic expansion was used to determine the asymptotic behaviour of the error of a Levin-type method. Thus our first task is to derive a vector-valued kernel version of the asymptotic expansion. This is accomplished in Section 6.2, using the asymptotic tools developed in Section 6.1. With an asymptotic expansion in hand, we can successfully find the order of error for a Levin-type method.

Two such constructions are presented: Section 6.3 reduces the vector-valued problem to a single differential equation, while Section 6.4 solves a vector-valued collocation system. In Sections 3.3 and 5.3, it was noted that choosing a particular basis for a Levin-type method causes the asymptotic order to increase without the need for nontrivial multiplicities (though still using derivatives). In Section 6.5, we construct a vector-valued version of such a basis, allowing us to obtain higher asymptotic orders with significantly smaller systems.

Remark: The entirety of this chapter consists of original research, though contemporary research by Shuhang Xiang obtained similar results to Theorem 6.2.1 and Theorem 6.4.1 with a polynomial basis. Xiang's work is unpublished as of the submission of this thesis. Every section other than Section 6.3 was first presented in [**77**].

6.1. Matrix and function asymptotics

In this section we present notation for the asymptotic behaviour of matrices and functions that depend on ω as a parameter. For the entirety of the chapter, all norms are L^∞ norms, for vectors, matrices and functions. The norm of a function is taken over the interval $[a, b]$. See Notation for the matrix and vector notation used.

We now define the big-O and little-o notation for matrices. Let $A = (a_{ij})_{p \times q}$ and $\tilde{A} = (\tilde{a}_{ij})_{p \times q}$ be two $p \times q$ matrices which depend on a real parameter ω, such that the entries of $\tilde{A}$ are always nonnegative. We write $A = \mathcal{O}(\tilde{A})$ for $\omega \to \infty$ if it is true componentwise: $a_{ij} = \mathcal{O}(\tilde{a}_{ij})$. This operator has several important properties, where $B = (b_{ij})_{q \times r}$, $\tilde{B} = (\tilde{b}_{ij})_{q \times r}$ with nonnegative entries and $\boldsymbol{\varphi}$ is a p-dimensional vector:

- $A = \mathcal{O}(\mathbf{1})$ implies that all the components of A are bounded for increasing ω, where $\mathbf{1}$ is the $p \times q$ matrix whose entries are all one (cf. Notation).

- Multiplication works as expected: $AB = \mathcal{O}(\tilde{A}\tilde{B})$.

- $\mathcal{O}(\mathbf{1}\tilde{A})$ is not necessarily equivalent to $\mathcal{O}(\tilde{A})$, but $\tilde{A} = \mathcal{O}(\mathbf{1}\tilde{A})$ and $\tilde{A} = \mathcal{O}(\tilde{A}\mathbf{1})$.

- $\|A\|$ and $\|A^\top\|$ have the same asymptotic order: $\|A\| = \mathcal{O}(\|A^\top\|)$ and $\|A^\top\| = \mathcal{O}(\|A\|)$.

- $\|\boldsymbol{\varphi}\|$ is of the same asymptotic order as $|\boldsymbol{\varphi}|^\top \mathbf{1}_{p \times 1} = \mathbf{1}^\top |\boldsymbol{\varphi}|$.

- If A is square and $\mathcal{O}(\mathbf{1})$, then $\det A = \mathcal{O}(1)$.

The definition and properties of the little-o notation $o(A)$ are essentially the same, with all occurrences of O replaced with o.

We can find the asymptotic behaviour of A^{-1} under certain assumptions, which will be necessary for the proof of Theorem 6.4.1.

Theorem 6.1.1 *Suppose that $A = P + G$ is a square matrix. If $P = o(\mathbf{1})$ and G is invertible with $G^{-1} = \mathcal{O}(\mathbf{1})$, then A is nonsingular when ω is large and $A^{-1} = \mathcal{O}(\mathbf{1})$.*

Proof: Note that $A = (PG^{-1} + I)G = (I - M)G$ for $M = -PG^{-1}$. Since $G^{-1} = \mathcal{O}(\mathbf{1})$, it follows that $M = o(\mathbf{1})$ and large ω ensures that $\|M\| < 1$. We thus know that the inverse of $I - M$ exists, and furthermore

$$(I - M)^{-1} = I + M(I - M)^{-1} = I + o(\mathbf{1})\,(I - M)^{-1}.$$

If $(I - M)^{-1}$ was not $\mathcal{O}(\mathbf{1})$, we would obtain a contradiction, since the right side of the equality could not be of the same asymptotic order. It follows that $(I - M)^{-1} = \mathcal{O}(\mathbf{1})$, and we can write

$$A^{-1} = G^{-1}(I - M)^{-1} = \mathcal{O}(\mathbf{1})\,.$$

Q.E.D.

In practice G is typically independent of ω, in which case it is only necessary to show that G is nonsingular.

We now turn our attention to functions which depend on ω as a parameter, for example $f(x) = \omega x$. Let f be a function that depends on ω, and $\tilde{f}$ a nonnegative constant that depends on ω. We write $f = \mathcal{O}\big(\tilde{f}\big)$ if the norm of f and its derivatives are all of order $\mathcal{O}\big(\tilde{f}\big)$ as $\omega \to \infty$. In other words,

$$\left\| f^{(m)} \right\| = \mathcal{O}\big(\tilde{f}\big)\,, \qquad m = 0, 1, \dots\,.$$

The most common usage is $f = \mathcal{O}(1)$, which states that f and its derivatives are bounded in $[a, b]$ for increasing ω. We also use this notation for vector-valued and matrix-valued functions in a componentwise manner. Let $A(x) = (a_{ij}(x))_{p \times q}$ be a matrix-valued function that depends on ω, and let $\tilde{A} = (\tilde{a}_{ij})_{p \times q}$ be a matrix with nonnegative components, which also depends on ω. We write $A = \mathcal{O}\big(\tilde{A}\big)$ if it is true componentwise: $a_{ij} = \mathcal{O}(\tilde{a}_{ij})$ for $\omega \to \infty$.

Note that this class of functions has the following properties, where $A = \mathcal{O}\big(\tilde{A}\big)$ and $B = \mathcal{O}\big(\tilde{B}\big)$ are matrix-valued functions:

- For every $x \in [a, b]$, $A(x) = \mathcal{O}\big(\tilde{A}\big)$.

- All derivatives of A belong to the same class: $A^{(m)} = \mathcal{O}\big(\tilde{A}\big)$ for every nonnegative integer m.

- If A and B are both $p \times q$ matrix-valued functions, then $A + B = \mathcal{O}\big(\tilde{A} + \tilde{B}\big) = \mathcal{O}((\max\{\tilde{a}_{ij}, \tilde{b}_{ij}\})_{p \times q})$.

- If the dimensions of A and B are compatible, then $AB = \mathcal{O}\big(\tilde{A}\tilde{B}\big)$.

- Scalar multiplication works as expected: if $c = \mathcal{O}(\tilde{c})$ then $cA = \mathcal{O}\big(\tilde{c}\tilde{A}\big)$.

- Integration is of the same order as A itself: $\int_a^b A(x)\,\mathrm{d}x = \mathcal{O}\big(\tilde{A}\big)$.

6.2. Asymptotic expansion

An asymptotic expansion is a valuable tool in the analysis of integrals, and for large ω will provide a fairly accurate numerical approximation to $I[\boldsymbol{f}]$. Consider for a moment the one-dimensional oscillator $y = \mathrm{e}^{\mathrm{i}\omega g}$ analysed in Chapter 3. In the derivation of its asymptotic expansion in Section 2.2, we used the fact that y satisfies the differential equation

$$y'(x) = \mathrm{i}\omega g'(x)y(x) = A(x)y(x).$$

The asymptotic expansion follows from writing y as $A^{-1}y'$, assuming that $A(x) \neq 0$ in the interval of integration, and integrating by parts:

$$\int_a^b fy\,\mathrm{d}x = \int_a^b fA^{-1}y'\,\mathrm{d}x = \left[fA^{-1}y\right]_a^b - \int_a^b (fA^{-1})'y\,\mathrm{d}x$$

$$= \frac{1}{\mathrm{i}\omega}\left[\frac{f(b)}{g'(b)}y(b) - \frac{f(a)}{g'(a)}y(a)\right] - \frac{1}{\mathrm{i}\omega}\int_a^b \left(\frac{f}{g'}\right)'y\,\mathrm{d}x.$$

Throughout this chapter the notation A^{-1} means matrix (or scalar) inverse, not function inverse. As ω becomes large, the term

$$\frac{1}{\mathrm{i}\omega}\left[\frac{f(b)}{g'(b)}y(b) - \frac{f(a)}{g'(a)}y(a)\right]$$

approximates the integral with an error of order $\mathcal{O}\big(\omega^{-2}\big)$, since $\int_a^b \left(\frac{f}{g'}\right)'y\,\mathrm{d}x = \mathcal{O}\big(\omega^{-1}\big)$ [85]. Furthermore, the error term is itself a highly oscillatory integral, thus we can iterate the process to obtain a full asymptotic expansion.

We obtain a vector-valued version of the asymptotic expansion by using integration by parts in a similar manner:

Theorem 6.2.1 *Suppose that $\boldsymbol{y}$ satisfies the differential equation*

$$\boldsymbol{y}'(x) = A(x)\boldsymbol{y}(x),$$

in the interval $[a, b]$, for some invertible matrix-valued function A such that $A^{-1} = \mathcal{O}\big(\hat{A}\big)$, for $\omega \to \infty$. Define

$$Q_s^A[\boldsymbol{f}] = \sum_{k=0}^{s-1}(-1)^k\left[\boldsymbol{\sigma}_k(b)^\top A^{-1}(b)\boldsymbol{y}(b) - \boldsymbol{\sigma}_k(a)^\top A^{-1}(a)\boldsymbol{y}(a)\right],$$

where

$$\boldsymbol{\sigma}_0 \equiv \boldsymbol{f}, \qquad \boldsymbol{\sigma}_{k+1} = (A^{-\top}\boldsymbol{\sigma}_k)', \qquad k = 0, 1, \ldots.$$

If $\boldsymbol{f} = \mathcal{O}(\tilde{\boldsymbol{f}})$ and $\boldsymbol{y}(x) = \mathcal{O}(\tilde{\boldsymbol{y}})$ for $a \le x \le b$, then

$$I[\boldsymbol{f}] - Q_s^A[\boldsymbol{f}] = (-1)^s \int_a^b \boldsymbol{\sigma}_s^\top \boldsymbol{y}\, \mathrm{d}x = \mathcal{O}\left(\tilde{\boldsymbol{f}}^\top \hat{A}^{s+1}\tilde{\boldsymbol{y}}\right), \qquad \omega \to \infty.$$

Proof: Note that

$$\int_a^b \boldsymbol{\sigma}_k^\top \boldsymbol{y}\, \mathrm{d}x = \int_a^b \boldsymbol{\sigma}_k^\top A^{-1}\boldsymbol{y}'\, \mathrm{d}x = \left[\boldsymbol{\sigma}_k^\top A^{-1}\boldsymbol{y}\right]_a^b - \int_a^b (\boldsymbol{\sigma}_k^\top A^{-1})'\boldsymbol{y}\, \mathrm{d}x$$

$$= \left[\boldsymbol{\sigma}_k^\top A^{-1}\boldsymbol{y}\right]_a^b - \int_a^b \boldsymbol{\sigma}_{k+1}^\top \boldsymbol{y}\, \mathrm{d}x.$$

Thus, by induction, the first equality holds. We now show that $\boldsymbol{\sigma}_k^\top = \mathcal{O}\left(\tilde{\boldsymbol{f}}^\top \hat{A}^k\right)$. This is obvious when $k = 0$ from the definition of $\boldsymbol{\sigma}_0$. Otherwise, assume it is true for $\boldsymbol{\sigma}_k$, and we will prove it for $\boldsymbol{\sigma}_{k+1}$:

$$\boldsymbol{\sigma}_{k+1}^\top = \boldsymbol{\sigma}_k^{\top'} A^{-1} + \boldsymbol{\sigma}_k^\top A^{-1'} = \mathcal{O}\left(\tilde{\boldsymbol{f}}^\top \hat{A}^k\right)\mathcal{O}\left(\hat{A}\right) + \mathcal{O}\left(\tilde{\boldsymbol{f}}^\top \hat{A}^k\right)\mathcal{O}\left(\hat{A}\right)$$

$$= \mathcal{O}\left(\tilde{\boldsymbol{f}}^\top \hat{A}^{k+1}\right).$$

The theorem now follows since

$$\int_a^b \boldsymbol{\sigma}_s^\top \boldsymbol{y}\, \mathrm{d}x = \left[\boldsymbol{\sigma}_s^\top A^{-1}\boldsymbol{y}\right]_a^b - \int_a^b \boldsymbol{\sigma}_{s+1}^\top \boldsymbol{y}\, \mathrm{d}x = \mathcal{O}\left(\tilde{\boldsymbol{f}}^\top \hat{A}^{s+1}\tilde{\boldsymbol{y}}\right) + \mathcal{O}\left(\tilde{\boldsymbol{f}}^\top \hat{A}^{s+1}\tilde{\boldsymbol{y}}\right)$$

$$= \mathcal{O}\left(\tilde{\boldsymbol{f}}^\top \hat{A}^{s+1}\tilde{\boldsymbol{y}}\right).$$

Q.E.D.

Corollary 6.2.2 follows immediately from Theorem 6.2.1, and will be used in the proof of Theorem 6.3.1 and Theorem 6.4.1. It is a generalization of Corollary 3.1.1, and states that the asymptotic behaviour of an integral depends only on the value of $\boldsymbol{f}$ and its derivatives at the endpoints of the integration interval.

Corollary 6.2.2 *Suppose that*

$$\boldsymbol{0} = \boldsymbol{f}(a) = \boldsymbol{f}(b) = \boldsymbol{f}'(a) = \boldsymbol{f}'(b) = \cdots = \boldsymbol{f}^{(s-1)}(a) = \boldsymbol{f}^{(s-1)}(b).$$

Then

$$I[\boldsymbol{f}] = \mathcal{O}\left(\tilde{\boldsymbol{f}}^\top \hat{A}^{s+1}\tilde{\boldsymbol{y}}\right).$$

The asymptotic expansion for $y(x) = \mathrm{e}^{\mathrm{i}\omega g(x)}$ follows immediately when $g' \neq 0$ within the interval of integration, in which case $A^{-1}(x) = 1/(\mathrm{i}\omega g(x)) = \mathcal{O}\left(\omega^{-1}\right)$. Thus $Q_s^A[f]$
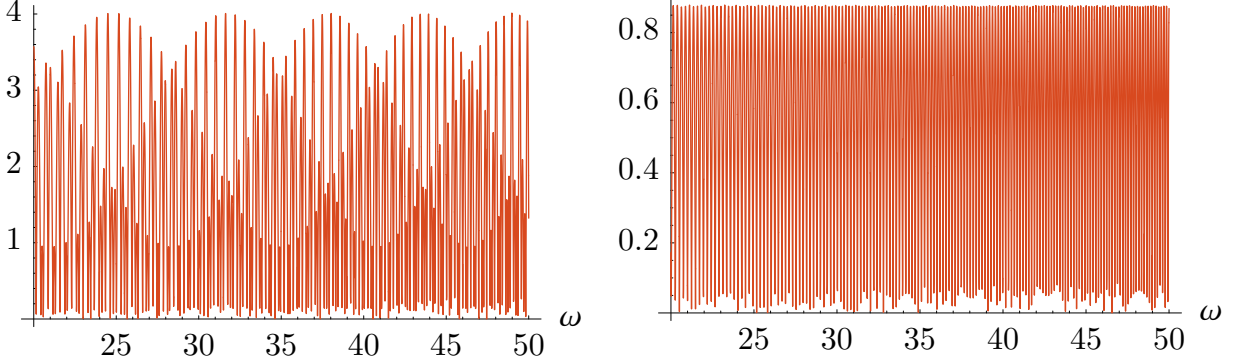
Figure 6.37: The error of $Q_1^A[\boldsymbol{f}]$ scaled by $\omega^{7/4}$ (left graph), compared to the error of $Q_2^A[\boldsymbol{f}]$ scaled by $\omega^{13/4}$ (right graph), for $I[f] = \int_1^2 \left[\cos x \, \mathrm{Ai}\,(-\omega x) - \omega\, \mathrm{e}^x \mathrm{Ai}\,'(-\omega x)\right]\,\mathrm{d}x$.

approximates $I[f]$ with an error $\mathcal{O}\!\left(\omega^{-s-1}\right)$. For the other two examples, assuming that $0 < a < b$,

$$\boldsymbol{y}(x) = \begin{pmatrix} J_{m-1}(\omega x) \\ J_m(\omega x) \end{pmatrix} = \mathcal{O}\!\left(\omega^{-1/2}\mathbf{1}\right), \qquad A^{-1} = \mathcal{O}\!\begin{pmatrix} \omega^{-2} & \omega^{-1} \\ \omega^{-1} & \omega^{-2} \end{pmatrix} = \mathcal{O}\!\left(\omega^{-1}\mathbf{1}\right),$$

$$\boldsymbol{y}(x) = \begin{pmatrix} \mathrm{Ai}\,(-\omega x) \\ -\omega\,\mathrm{Ai}\,'(-\omega x) \end{pmatrix} = \mathcal{O}\!\begin{pmatrix} \omega^{-1/4} \\ \omega^{5/4} \end{pmatrix}, \qquad A^{-1} = \mathcal{O}\!\begin{pmatrix} 0 & \omega^{-3} \\ 1 & 0 \end{pmatrix},$$

where the asymptotics of the Bessel and Airy functions can be found in [**2**]. In the Bessel case, each component of A^{-1} is $\mathcal{O}\!\left(\omega^{-1}\right)$, hence, if $\boldsymbol{f} = \mathcal{O}(\mathbf{1})$, then we have an error of order

$$\tilde{\boldsymbol{f}}^\top \hat{A}^{s+1}\tilde{\boldsymbol{y}} = \mathcal{O}\!\left(\left\|\hat{A}^{s+1}\right\| \|\tilde{\boldsymbol{y}}\|\right) = \mathcal{O}\!\left(\omega^{-s-\frac{3}{2}}\right).$$

In the Airy case, we know that

$$\hat{A}^{2k}\tilde{\boldsymbol{y}} = \begin{pmatrix} \omega^{-3k} & 0 \\ 0 & \omega^{-3k} \end{pmatrix}\tilde{\boldsymbol{y}} = \begin{pmatrix} \omega^{-3k-1/4} \\ \omega^{-3k+5/4} \end{pmatrix},$$

$$\hat{A}^{2k+1}\tilde{\boldsymbol{y}} = \begin{pmatrix} 0 & \omega^{-3(k+1)} \\ \omega^{-3k} & 0 \end{pmatrix}\tilde{\boldsymbol{y}} = \begin{pmatrix} \omega^{-3k-7/4} \\ \omega^{-3k-1/4} \end{pmatrix}.$$

Thus, if $\tilde{\boldsymbol{f}} = \mathbf{1}$,

$$\tilde{\boldsymbol{f}}^\top \hat{A}^{s+1}\tilde{\boldsymbol{y}} = \mathcal{O}\!\left(\omega^{-\frac{3}{2}s-\frac{1}{4}}\right).$$

On the other hand, if $\tilde{\boldsymbol{f}} = (1,0)^\top$, then

$$\tilde{\boldsymbol{f}}^\top \hat{A}^{s+1}\tilde{\boldsymbol{y}} = \mathcal{O}\!\left(\omega^{-\frac{3}{2}s-\frac{7}{4}}\right).$$

93

As a simple example, consider the integral

$$\int_1^2 \boldsymbol{f}^\top \boldsymbol{y} \, \mathrm{d}x = \int_1^2 \left[\cos x \, \mathrm{Ai}\left(-\omega x\right) - \omega \, \mathrm{e}^x \mathrm{Ai}'(-\omega x) \right] \mathrm{d}x.$$

In this case $\boldsymbol{f}(x) = \left(\cos x, \mathrm{e}^x\right)^\top$ and $\boldsymbol{y}(x) = \left(\mathrm{Ai}\left(-\omega x\right), -\omega \mathrm{Ai}'(-\omega x)\right)^\top$. Figure 6.37 compares the one-term and two-term expansions. As can be seen, adding an additional term does indeed increase the asymptotic order by $3/2$. In this example, as well as in all other examples, the approximation is compared to a Gauss–Legendre quadrature approximation with sufficient data points and working precision to ensure machine precision accuracy.

6.3. High order Levin-type methods

As with the exponential oscillator, the fundamental problem with using an asymptotic expansion as a numerical approximation is that for fixed ω the accuracy is limited: the sum $Q_s^A[\boldsymbol{f}]$ does not typically converge as $s \to \infty$. To combat this issue, we will derive a Levin-type method that has the same asymptotic behaviour as the asymptotic expansion, whilst providing the ability to decrease error further. In Section 6.4, we generalize the vector-valued kernel version of the Levin collocation method developed in [62], and described in Section 2.8. Before we do so, we will present an alternative for the case when $d = 2$, which results in smaller systems and increased accuracy than the usual vector-valued kernel Levin-type methods.

Consider the integral

$$I[\boldsymbol{f}] = \int_a^b \boldsymbol{f}^\top \boldsymbol{y} \, \mathrm{d}x = \int_a^b f_1 y + f_2 y' \, \mathrm{d}x,$$

where y satisfies the differential equation

$$y''(x) + q(x)y'(x) + \omega r(x)y(x) = 0.$$

As an ansatz, we write the antiderivative of the integrand as

$$\boldsymbol{v}^\top \boldsymbol{y} = v_1 y + v_2 y'.$$

Taking this ansatz's derivative, we obtain the differential operator:

$$v_1' y + v_1 y' + v_2' y' + v_2 y'' = (v_1' - \omega r v_2)y + (v_1 + v_2' - q v_2)y'. \tag{6.3.1}$$

Thus we want v_1 and v_2 to satisfy

$$v_1' - \omega r v_2 = f_1 \qquad \text{and} \qquad v_1 + v_2' - q v_2 = f_2.$$

Let $v = v_2$ and define $v_1 = f_2 - v' + qv$. Plugging these values into (6.3.1) results in a differential equation with only one unknown function:

$$\tilde{\mathcal{L}}[v] = v'' - q'v - qv' + \omega r v = f_2' - f_1.$$

A particular solution v to this differential equation can be approximated via collocation, as in the Levin-type method constructed in Section 3.2. We then approximate $I[\boldsymbol{f}]$ by

$$Q^L[\boldsymbol{f}] = \boldsymbol{v}(b)^\top \boldsymbol{y}(b) - \boldsymbol{v}(a)^\top \boldsymbol{y}(a)$$
$$= \left[f_2(b) - v'(b) + q(b)v(b) \right] y(b) + v(b)y'(b)$$
$$- \left[f_2(a) - v'(a) + q(a)v(a) \right] y(a) - v(a)y'(a).$$

Consider specifically an integral involving the Airy function:

$$I[f] = \int_1^2 f(x)\mathrm{Ai}\left(-\omega x\right)\,\mathrm{d}x.$$

In this case, we have the simplified collocation operator

$$\tilde{\mathcal{L}}[v] = v'' + \omega^3 x v.$$

This is almost exactly the same as the Levin differential operator $v' + \mathrm{i}\omega g'v$; the only difference is a second derivative v'' in place of v'. Thus we obtain the following theorem:

Theorem 6.3.1 *Assume that $0 < a < b$, $x_1 = a$ and $x_2 = b$. Let $v = \sum c_k \psi_k$ be the solution to the collocation system*

$$\tilde{\mathcal{L}}[v]\left(x_k\right) = f(x_k), \cdots, \tilde{\mathcal{L}}[v]^{(m_k-1)}\left(x_k\right) = f^{(m_k-1)}(x_k), \qquad k = 1, \ldots, \nu.$$

If $\{\psi_1, \ldots, \psi_n\}$ can interpolate at a given sequence of nodes $\{x_1, \ldots, x_\nu\}$ with multiplicities $\{m_1, \ldots, m_\nu\}$, then

$$\int_a^b f(x)\mathrm{Ai}\left(-\omega x\right)\,\mathrm{d}x - Q^L[f] \sim \mathcal{O}\left(\omega^{-\frac{3}{2}s-\frac{7}{4}}\right),$$

where
$$Q^L[f] = -v'(b)y(b) + v(b)y'(b) + v'(a)y(a) - v(a)y'(a)$$

and $s = \min\{m_1, m_\nu\}$.

Proof: The proof that $\tilde{\mathcal{L}}[v]$ and its derivatives are bounded for increasing ω is virtually identical to the proof of Theorem 3.2.1. Let $\boldsymbol{f} = (f, 0)^\top$, $\boldsymbol{v} = (-v', v)^\top$ and $\boldsymbol{y}(x) = \left(\mathrm{Ai}\left(-\omega x\right), -\omega \mathrm{Ai}'(-\omega x)\right)^\top$. Then

$$I[f] - Q^L[f] = \int_a^b (f - \tilde{\mathcal{L}}[v])\mathrm{Ai}\left(-\omega x\right)\,\mathrm{d}x = \int_a^b (\boldsymbol{f} - \mathcal{L}[\boldsymbol{v}])^\top \boldsymbol{y}\,\mathrm{d}x.$$

The theorem follows from Corollary 6.2.2.

<div align="right">*Q.E.D.*</div>
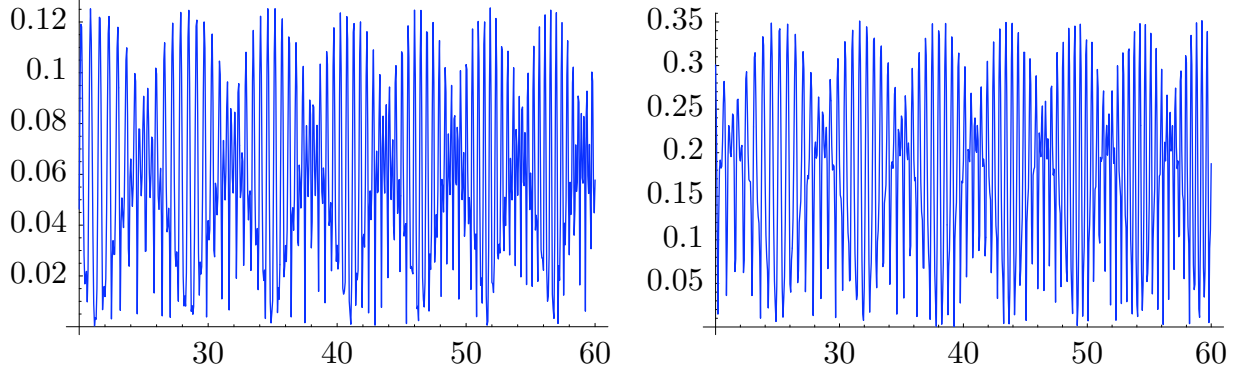
Figure 6.38: The error in approximating $\int_1^2 \cos x \, \mathrm{Ai}\,(-\omega x)\,\mathrm{d}x$, scaled by $\omega^{13/4}$ for a Levin-type method with nodes $\left\{1, \frac{3}{2}, 2\right\}$ and multiplicities all one (left graph), and scaled by $\omega^{19/4}$ for a Levin-type method with nodes $\{1, 2\}$ and multiplicities both two (right graph).

Similar theorems can be derived for other oscillators in a very straightforward manner, but we focus on the Airy kernel for simplicity.

In Figure 6.38 we use this new method to approximate the integral

$$\int_1^2 \cos x \, \mathrm{Ai}\,(-\omega x)\,\mathrm{d}x.$$

In the left graph we use three nodes—the two endpoints of the interval and the midpoint—which achieves an asymptotic order $\mathcal{O}\!\left(\omega^{\frac{-13}{4}}\right)$. In the second graph we demonstrate that using multiplicities successfully increases the asymptotic order: the error now decays like $\mathcal{O}\!\left(\omega^{\frac{-19}{4}}\right)$.

Remark: There is probably a relationship between this construction and the Chung, Evans and Webster method of Section 2.9. Indeed, it is quite possible that this method can be extended to oscillators which satisfy higher order differential equations by utilizing the adjoint representation and Lagrange identity, though we leave this as an open problem.

6.4. Vector-valued kernel Levin-type methods

In Section 2.8, a method was developed to compute integrals using a collocation system. This method was generalized to include multiplicities in Section 3.2, for the specific oscillator $\mathrm{e}^{\mathrm{i}\omega g}$. By adding multiplicities to the endpoints, we obtained a method with higher asymptotic order. In this section, we complete the generalization for vector-valued kernels. Unlike the preceding section, we leave everything in a vector form: we do not collapse the problem into a single differential equation. This simplifies the construction of the method for more complicated oscillators. We will use the asymptotic expansion to determine the asymptotic order of the resulting Levin-type methods. Note that we include cases that were not analysed

in Theorem 2.8.1, such as the Airy function case where $\left\| A^{-1} \right\|$ does not decay. When a Levin-type method is equivalent to the original Levin collocation method, we obtain the asymptotic bound derived in [**90**], which is more accurate than the original bound found in [**62**].

Had we known a vector-valued function $\boldsymbol{F}$ such that

$$\left(\boldsymbol{F}^\top \boldsymbol{y}\right)' = \boldsymbol{f}^\top \boldsymbol{y},$$

then computing the integral $I[\boldsymbol{f}]$ would have been trivial: $I[\boldsymbol{f}] = \left[\boldsymbol{F}^\top \boldsymbol{y}\right]_a^b$. We can rewrite this condition as

$$\mathcal{L}[\boldsymbol{F}] = \boldsymbol{f} \qquad \text{for} \qquad \mathcal{L}[\boldsymbol{F}] = \boldsymbol{F}' + A^\top \boldsymbol{F}.$$

Finding $\boldsymbol{F}$ explicitly is in general impossible. However, we can approximate this function using collocation. Suppose we are given a sequence of *nodes* $\{x_1, \ldots, x_\nu\}$, *multiplicities* $\{m_1, \ldots, m_\nu\}$ and *basis functions* $\{\psi_1, \ldots, \psi_n\}$, where $\boldsymbol{\psi}_k : \mathbb{R} \to \mathbb{R}^d$ for d again equal to the dimension of $\boldsymbol{y}(x)$. Let $\boldsymbol{v}(x) = \sum_{k=1}^n c_k \boldsymbol{\psi}_k(x)$ for $n = d \sum m_k$. We determine the coefficients c_k by equating the function value and derivatives of $\mathcal{L}[\boldsymbol{v}]$ and $\boldsymbol{f}$ at the given nodes, up to the given multiplicities. This is equivalent to solving the system

$$\mathcal{L}[\boldsymbol{v}](x_k) = \boldsymbol{f}(x_k), \ldots, \mathcal{L}[\boldsymbol{v}]^{(m_k-1)}(x_k) = \boldsymbol{f}^{(m_k-1)}(x_k), \quad k = 1, 2, \ldots, \nu. \tag{6.4.1}$$

The number of equations in this system is n, which equals the number of unknowns c_k. We then define a Levin-type method as

$$Q^L[\boldsymbol{f}] = \int_a^b \mathcal{L}[\boldsymbol{v}](x)^\top \boldsymbol{y}(x) \, \mathrm{d}x = \boldsymbol{v}(b)^\top \boldsymbol{y}(b) - \boldsymbol{v}(a)^\top \boldsymbol{y}(a).$$

The following theorem proves the asymptotic order of a Levin-type method, assuming that $A^{-1} = \mathrm{o}(\boldsymbol{1})$.

Theorem 6.4.1 *Assume that the following conditions are met:*

(1) $\boldsymbol{f} = \mathcal{O}(\tilde{\boldsymbol{f}})$, $A = \mathcal{O}(\tilde{A})$ and $\boldsymbol{y}(x) = \mathcal{O}(\tilde{\boldsymbol{y}})$.

(2) $A(x)$ is invertible for $x \in [a, b]$ and $A^{-1} = \mathcal{O}(\hat{A})$, where $\tilde{A}\hat{A} = \mathcal{O}(\boldsymbol{1})$ and $\hat{A} = \mathrm{o}(\boldsymbol{1})$.

(3)   *The basis* $\{\psi_1, \ldots, \psi_n\}$ *is independent of* ω.

(4)   *The basis* $\{\psi_1, \ldots, \psi_n\}$ *can interpolate at the given nodes and multiplicities.*

Then for large ω $Q^L[\boldsymbol{f}]$ *is well-defined and*

$$I[\boldsymbol{f}] - Q^L[\boldsymbol{f}] = \mathcal{O}\left(\tilde{\boldsymbol{f}}^\top \hat{A} \boldsymbol{1} \hat{A}^s \tilde{\boldsymbol{y}}\right),$$

where $s = \min\{m_1, m_\nu\}$.

Proof:

We will prove the order of error by applying Corollary 6.2.2 to the integral

$$I[\boldsymbol{f}] - Q^L[\boldsymbol{f}] = \int_a^b (\boldsymbol{f} - \mathcal{L}[\boldsymbol{v}])^\top \boldsymbol{y} \, \mathrm{d}x.$$

The theorem will follow from this corollary if we can show that both $\boldsymbol{f}$ and $\mathcal{L}[\boldsymbol{v}]$ are of order $\mathcal{O}(\tilde{A}^\top \mathbf{1} \hat{A}^\top \tilde{\boldsymbol{f}})$. This is true for $\boldsymbol{f}$ since

$$\boldsymbol{f} = A^\top A^{-\top} \boldsymbol{f} = \mathcal{O}(\tilde{A}^\top \hat{A}^\top \tilde{\boldsymbol{f}}) = \mathcal{O}(\tilde{A}^\top \mathbf{1} \hat{A}^\top \tilde{\boldsymbol{f}}).$$

The remainder of the theorem consists of proving the order of $\mathcal{L}[\boldsymbol{v}]$. Let $\mathcal{P}[\boldsymbol{g}]$ be the n-dimensional vector consisting of the function $\boldsymbol{g} : \mathbb{R} \to \mathbb{R}^d$ evaluated at each node and multiplicity, written in partitioned form as

$$\mathcal{P}[\boldsymbol{g}] = \begin{pmatrix} \boldsymbol{g}(x_1) \\ \vdots \\ \boldsymbol{g}^{(m_1-1)}(x_1) \\ \vdots \\ \boldsymbol{g}(x_\nu) \\ \vdots \\ \boldsymbol{g}^{(m_\nu-1)}(x_\nu) \end{pmatrix}.$$

Furthermore, let Ψ be the $d \times n$ matrix-valued function such that the kth column of $\Psi(x)$ equals $\boldsymbol{\psi}_k(x)$:

$$\Psi(x) = (\boldsymbol{\psi}_1(x), \ldots, \boldsymbol{\psi}_n(x)).$$

Then we can write the system (6.4.1) as $B\boldsymbol{c} = \boldsymbol{\varphi}$, where $\boldsymbol{c} = (c_1, \ldots, c_n)^\top$,

$$B = \mathcal{P}[\mathcal{L}[\Psi]] = (\mathcal{P}[\mathcal{L}[\boldsymbol{\psi}_1]], \ldots, \mathcal{P}[\mathcal{L}[\boldsymbol{\psi}_n]]), \qquad \boldsymbol{\varphi} = \mathcal{P}[\boldsymbol{f}] \tag{6.4.2}$$

and $\boldsymbol{v} = \Psi \boldsymbol{c}$.

Collocating $\boldsymbol{f}$ by $\boldsymbol{v}' + A^\top \boldsymbol{v}$ is equivalent to collocating $A^{-\top} \boldsymbol{f}$ by $A^{-\top} \boldsymbol{v}' + \boldsymbol{v}$, or in other words,

$$\mathcal{P}[A^{-\top} \Psi' + \Psi] \boldsymbol{c} = \mathcal{P}[A^{-\top} \boldsymbol{f}].$$

Note that $A^{-\top} \Psi' = \mathcal{O}(\hat{A}^\top \mathbf{1}_{d \times n}) = \mathrm{o}(\mathbf{1}_{d \times n})$. Furthermore $\mathcal{P}[\Psi]$ consists of the basis functions evaluated at the given nodes and multiplicities, thus by hypothesis is nonsingular. It follows that the alternate collocation matrix $\mathcal{P}[A^{-\top} \Psi' + \Psi] = \mathcal{P}[A^{-\top} \Psi'] + \mathcal{P}[\Psi]$ satisfies the conditions of Theorem 6.1.1, hence its inverse exists and is $\mathcal{O}(\mathbf{1})$ when ω is large and

$$\boldsymbol{c} = \mathcal{P}[A^{-\top} \Psi' + \Psi]^{-1} \mathcal{P}[A^{-\top} \boldsymbol{f}] = \mathcal{O}\left(\mathbf{1}_{n \times n} \begin{pmatrix} \hat{A}^\top \tilde{\boldsymbol{f}} \\ \vdots \\ \hat{A}^{\dot{\top}} \tilde{\boldsymbol{f}} \end{pmatrix}\right).$$

We thus find that

$$\mathcal{L}[\boldsymbol{v}] = \mathcal{L}[\Psi\boldsymbol{c}] = A^\top(A^{-\top}\Psi' + \Psi)\boldsymbol{c} = \mathcal{O}\left(\tilde{A}^\top \mathbf{1}_{d\times n}\begin{pmatrix}\hat{A}^\top\tilde{\boldsymbol{f}}\\ \vdots\\ \hat{A}^\dagger\tilde{\boldsymbol{f}}\end{pmatrix}\right).$$

The theorem follows since

$$\mathbf{1}_{d\times n}\begin{pmatrix}\hat{A}^\top\tilde{\boldsymbol{f}}\\ \vdots\\ \hat{A}^\dagger\tilde{\boldsymbol{f}}\end{pmatrix} = (\mathbf{1}_{d\times d}, \ldots, \mathbf{1}_{d\times d})\begin{pmatrix}\hat{A}^\top\tilde{\boldsymbol{f}}\\ \vdots\\ \hat{A}^\dagger\tilde{\boldsymbol{f}}\end{pmatrix} = \frac{n}{d}\mathbf{1}_{d\times d}\hat{A}^\top\tilde{\boldsymbol{f}}.$$

<div align="right">Q.E.D.</div>

The following corollary shows, under fairly general conditions, that a polynomial basis will always obtain the desired order of error in a Levin-type method. It proves this order of error for cases which were not included in the preceding theorem, such as integrals with an Airy kernel.

Corollary 6.4.2 *Suppose that $A(x) = C^{-1}K(x)C$ for some nonsingular matrix K such that $K^{-1} = \mathcal{O}\left(\hat{K}\right)$ for $\hat{K} = \mathrm{o}(\mathbf{1})$. Then a Levin-type method with the standard polynomial basis has an order of error*

$$Q^L[\boldsymbol{f}] - I[\boldsymbol{f}] = \mathcal{O}\left(\tilde{\boldsymbol{f}}^\top \left|C^{-1}\right|\hat{K}\mathbf{1}\hat{K}^s\tilde{\boldsymbol{y}}\right).$$

Proof:

The standard polynomial basis is equivalent to taking

$$\Psi(x) = \left(I_d, xI_d, \ldots, x^{n/d}I_d\right).$$

Suppose that $C = I_d$, hence $A = K$. In this case $\mathcal{P}[\Psi]$ is a block confluent Vandermonde matrix, where the confluent Vandermonde matrix is the matrix associated with Hermite interpolation. Thus $\mathcal{P}[\Psi]$ is nonsingular, and this corollary follows from Theorem 6.4.1.

Now suppose that $C \neq I_d$. The remainder of the proof of this corollary consists of showing that the Levin-type method we have constructed is equivalent to a Levin-type method with the matrix K in place of A, hence both methods have exactly the same error. Note that $\boldsymbol{y}_2 = C\boldsymbol{y}$ satisfies the differential equation $\boldsymbol{y}_2' = K\boldsymbol{y}_2$. Furthermore

$$I[\boldsymbol{f}] = \int_a^b \boldsymbol{f}^\top\boldsymbol{y}\,\mathrm{d}x = \int_a^b \boldsymbol{f}^\top C^{-1}\boldsymbol{y}_2\,\mathrm{d}x = \int_a^b \boldsymbol{f}_2^\top\boldsymbol{y}_2\,\mathrm{d}x,$$

for $\boldsymbol{f}_2 = C^{-\top}\boldsymbol{f}$. We have just shown that a Levin-type method for the oscillator $\boldsymbol{y}_2$ has the requisite order of error. Let $\boldsymbol{v}_2$ be the collocation function associated with the Levin-type method with $\boldsymbol{y}_2$. We will show that

$$\boldsymbol{v}^\top\boldsymbol{y} = \boldsymbol{v}_2^\top\boldsymbol{y}_2 = \boldsymbol{v}_2^\top C\boldsymbol{y}.$$

Let

$$\bar{C} = \begin{pmatrix} C & & \\ & \ddots & \\ & & C \end{pmatrix}.$$

For the $\boldsymbol{y}_2$ collocation system, we solve the system $B_2 \boldsymbol{c}_2 = \boldsymbol{\varphi}_2$, where

$$B_2 = \mathcal{P}\big[\Psi'\big] + \mathcal{P}\big[K^\top \Psi\big] \qquad \text{and} \qquad \boldsymbol{\varphi}_2 = \mathcal{P}[\boldsymbol{f}_2] = \mathcal{P}\big[C^{-\top}\boldsymbol{f}\big] = \bar{C}^{-\top}\boldsymbol{\varphi}.$$

Because of the block diagonal structure of Ψ, $C^\top \Psi = \Psi \bar{C}^\top$. Thus we find that

$$\mathcal{P}\big[K^\top \Psi\big] = \mathcal{P}\big[C^{-\top}A^\top C^\top \Psi\big] = \mathcal{P}\big[C^{-\top}A^\top \Psi \bar{C}^\top\big] = \bar{C}^{-\top}\mathcal{P}\big[A^\top \Psi\big]\bar{C}^\top.$$

Because of this, and the fact that $\mathcal{P}[\Psi']$ commutes with $\bar{C}^\top$,

$$\bar{C}^\top B_2 \bar{C}^{-\top} = \bar{C}^\top (\mathcal{P}\big[\Psi'\big] + \mathcal{P}\big[K^\top \Psi\big])\bar{C}^{-\top} = \bar{C}^\top (\mathcal{P}\big[\Psi'\big] + \bar{C}^{-\top}\mathcal{P}\big[A^\top \Psi\big]\bar{C}^\top)\bar{C}^{-\top}$$

$$= \mathcal{P}\big[\Psi'\big] + \mathcal{P}\big[A^\top \Psi\big] = B.$$

It follows that

$$C^\top \boldsymbol{v}_2 = C^\top \Psi B_2^{-1}\boldsymbol{\varphi}_2 = \Psi \bar{C}^\top B_2^{-1}\bar{C}^{-\top}\boldsymbol{\varphi} = \Psi B^{-1}\boldsymbol{\varphi} = \boldsymbol{v}.$$

<div align="right">Q.E.D.</div>

The Bessel kernel satisfies the conditions of this corollary with $C = I$. For the Airy kernel, we take $C = \mathrm{diag}\,(\omega^{3/2}, 1)$, in which case

$$K(x) = CA(x)C^{-1} = \begin{pmatrix} 0 & \omega^{3/2} \\ -\omega^{3/2}x & 0 \end{pmatrix}.$$

Then

$$K^{-1}(x) = \begin{pmatrix} 0 & -\frac{1}{\omega^{3/2}x} \\ \frac{1}{\omega^{3/2}} & 0 \end{pmatrix} = \mathrm{o}(\mathbf{1}),$$

and the requisite hypothesis is satisfied. The asymptotic order of error predicted by the preceding corollary is equivalent to that of the asymptotic expansion for both the case where $\tilde{\boldsymbol{f}} = \mathbf{1}$ and $\tilde{\boldsymbol{f}} = (1, 0)^\top$.

Returning to the example of Figure 6.37, we now approximate the same integral,

$$I[f] = \int_1^2 \Big[\cos x \mathrm{Ai}\,(-\omega x) - \omega\, \mathrm{e}^x \mathrm{Ai}\,'(-\omega x)\Big]\, \mathrm{d}x,$$

using a Levin-type method with polynomial basis in Figure 6.39. Using exactly the same information as the asymptotic expansion, we reduce the error by a factor of two. Unlike an asymptotic expansion, we also have the ability to reduce the error further by adding nodes
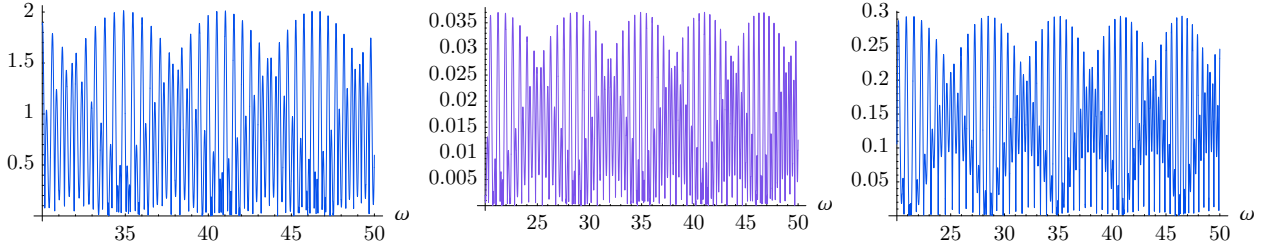
Figure 6.39: The error scaled by $\omega^{7/4}$ of $Q^L[\boldsymbol{f}]$ with endpoints for nodes and multiplicities both one (left graph) and $Q^L[\boldsymbol{f}]$ with nodes $\{1, 4/3, 5/3, 2\}$ and multiplicities all one (middle graph), and the error scaled by $\omega^{13/4}$ of $Q^L[\boldsymbol{f}]$ with endpoints for nodes and multiplicities both two (right graph), for $I[f] = \int_1^2 [\cos x \operatorname{Ai}(-\omega x) - \omega\, e^x \operatorname{Ai}'(-\omega x)]\, dx$.
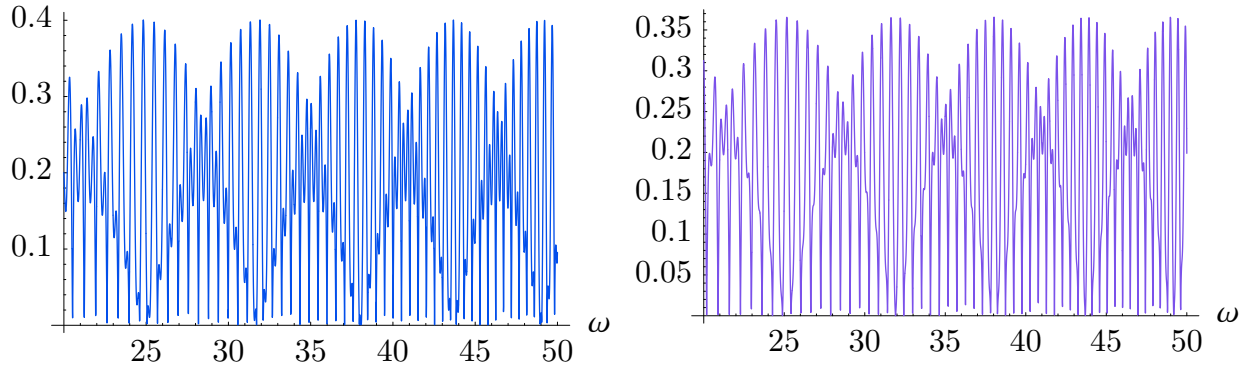
Figure 6.40: The error scaled by $\omega^{13/4}$ of $Q^L[\boldsymbol{f}]$ with endpoints for nodes and multiplicities both one (left graph), compared to the error scaled by $\omega^{19/4}$ of $Q^L[\boldsymbol{f}]$ with endpoints for nodes and multiplicities both two (right graph), for $I[f] = \int_1^2 \operatorname{Ai}(-\omega x)\, dx$.

within the interior of the interval. Adding just two nodes, one at $4/3$ and one at $5/3$, reduces the error by a factor of 100. This figure also demonstrates that adding multiplicities to the endpoints does indeed increase the asymptotic order.

As another example, consider the computation of the zeroth moment of the Airy function Ai, in particular $\int_1^2 \operatorname{Ai}(-\omega x)\, dx$. In this case, $\boldsymbol{y}$ remains the same, while we take $\boldsymbol{f} = (1, 0)^\top$. As predicted, Figure 6.40 shows that the approximation has an error of order $\omega^{-13/4}$ with multiplicities both one, which increases to $\omega^{-19/4}$ with the addition of multiplicities. This is indeed a higher asymptotic order than the previous integral involving Airy functions.

Remark: With this approximation in hand we can immediately approximate any of the higher moments, using the integral relation

$$\int x^{k+3}\operatorname{Ai}(x)\, dx = x^{k+2}\operatorname{Ai}'(x) - (k+2)x^{k+1}\operatorname{Ai}(x) + (k+1)(k+2)\int x^k \operatorname{Ai}(x)\, dx,$$

cf. [2]. This presents the possibility of constructing a Filon-type method, where we approx-
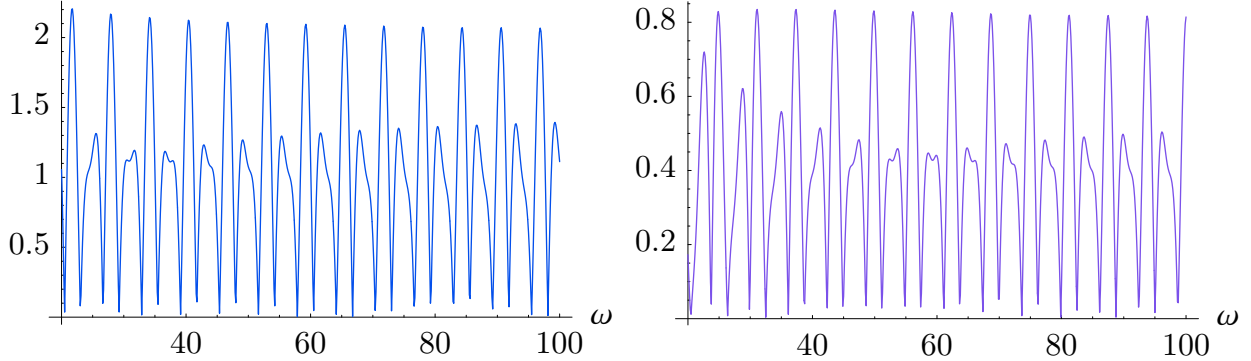
Figure 6.41: The error scaled by $\omega^{7/2}$ of $Q^L[\boldsymbol{f}]$ with endpoints for nodes and multiplicities both two (left graph), compared to $Q^L[\boldsymbol{f}]$ with nodes $\{1, 3/2, 2\}$ and multiplicities $\{2, 1, 2\}$ (right graph), for $I[f] = \int_1^2 \left[x^{-2} J_2(\omega x) + x^3 J_3(\omega x) \right] \, \mathrm{d}x$.

imate the integral $\int_a^b f(x) \mathrm{Ai}(-\omega x) \, \mathrm{d}x$ by interpolating f by a polynomial v, and using the formulæ for the moments to compute $\int_a^b v(x) \mathrm{Ai}(-\omega x) \, \mathrm{d}x$. As this idea is tangential to the topic of this chapter, we will not investigate it further.

Finally, consider the integral $\int_1^2 \left[x^{-2} J_2(\omega x) + x^3 J_3(\omega x) \right] \, \mathrm{d}x$. In Figure 6.41 we compare two methods of order $\mathcal{O}(\omega^{-7/2})$: the first with endpoints for nodes and multiplicities both equal to two, and the second with an additional node at $3/2$ with multiplicity one. We obtain the expected order of error and adding an additional interpolation point further decreases the error.

6.5. Asymptotic basis

One key—and easily overlooked—degree of freedom in a Levin-type method is in the choice of basis. Though the obvious choice of using polynomials does indeed provide good approximation, it ignores the wealth of information known about $\boldsymbol{f}$ and A which could be used to make $\mathcal{L}[\boldsymbol{v}]$ close to $\boldsymbol{f}$. In Section 3.3 it was noted that for the $\mathrm{e}^{\mathrm{i}\omega g}$ oscillator, using the functions σ_k from the asymptotic expansion as a basis caused the order of the resulting Levin-type method to increase with each additional node point. In this section we show that this carries over to vector-valued kernels as well. This observation is of considerably more importance for the vector-valued case, since it allows us to derive a high asymptotic order approximation with a significantly smaller system. Note, however, that we still require the same number of derivatives for $\boldsymbol{f}$ and A as in the asymptotic expansion.

Define the *asymptotic basis* as

$$\boldsymbol{\psi}_1 = A^{-\top} \boldsymbol{f}, \qquad \boldsymbol{\psi}_{k+1} = A^{-\top} \boldsymbol{\psi}_k', \qquad k = 1, 2, \dots.$$

As in Theorem 6.4.1, suppose that $\boldsymbol{f} = \mathcal{O}(\tilde{\boldsymbol{f}})$, $A = \mathcal{O}(\tilde{A})$ and $A^{-1} = \mathcal{O}(\hat{A})$, where $\tilde{A}\hat{A} = \mathcal{O}(\boldsymbol{1})$. Thus $\boldsymbol{\psi}_k = \mathcal{O}(\hat{A}^{k\top}\tilde{\boldsymbol{f}})$. Let

$$W = \operatorname{diag}\left(1, \|\hat{A}\|, \ldots, \|\hat{A}^{n-1}\|\right).$$

If $\boldsymbol{f} = \mathcal{O}(\boldsymbol{1})$, then the entries in the jth column of B are all $\mathcal{O}\left(\|\hat{A}^{j-1}\|\right)$, where B is again the matrix (6.4.2) associated with the collocation system (6.4.1): $B = \mathcal{P}[\Psi'] + \mathcal{P}\left[A^\top\Psi\right]$. We now want to select all the terms B that are of maximum order, thus let G equal all the terms of BW^{-1} that behave like $\mathcal{O}(\boldsymbol{1})$. The following theorem states that under this choice of basis, a Levin-type method will have a higher asymptotic order.

Theorem 6.5.1 *Suppose that $\boldsymbol{f} = \mathcal{O}(\boldsymbol{1})$, $\hat{A}^{(k+1)\top}\tilde{\boldsymbol{f}} = \mathcal{O}\left(\hat{A}^{k\top}\tilde{\boldsymbol{f}}\right)$, and that G is nonsingular with $G^{-1} = \mathcal{O}(\boldsymbol{1})$. Then*

$$I[\boldsymbol{f}] - Q^B[\boldsymbol{f}] = \mathcal{O}\left(\|\hat{A}^n\|\boldsymbol{1}^\top \hat{A}^{s+1}\tilde{\boldsymbol{y}}\right),$$

where $Q^B[\boldsymbol{f}]$ is a Levin-type method using the asymptotic basis and $s = \min\{m_1, m_\nu\}$.

Proof:

We will show that $\mathcal{L}[\boldsymbol{v}] - \boldsymbol{f} = \mathcal{O}\left(\|\hat{A}^n\|\boldsymbol{1}\right)$. First we find that

$$\mathcal{L}[\boldsymbol{v}] - \boldsymbol{f} = \sum_{k=1}^n c_k \mathcal{L}[\boldsymbol{\psi}_k] - \boldsymbol{f} = \sum_{k=1}^n c_k \left(\boldsymbol{\psi}_k' + A^\top \boldsymbol{\psi}_k\right) - \boldsymbol{f}$$

$$= \sum_{k=1}^n c_k \left(A^\top \boldsymbol{\psi}_{k+1} + A^\top \boldsymbol{\psi}_k\right) - A^\top \boldsymbol{\psi}_1$$

$$= A^\top\left[(c_1 - 1)\boldsymbol{\psi}_1 + \sum_{k=2}^n (c_{k-1} + c_k)\boldsymbol{\psi}_k + c_n \boldsymbol{\psi}_{n+1}\right]$$

$$= \frac{A^\top}{\det B}\left[(\det B_1 - \det B)\boldsymbol{\psi}_1 + \sum_{k=2}^n (\det B_{k-1} + \det B_k)\boldsymbol{\psi}_k + \det B_n \boldsymbol{\psi}_{n+1}\right], \quad (6.5.1)$$

where the matrix B_k is the matrix B with its kth column replaced by $\boldsymbol{\varphi} = \mathcal{P}[\boldsymbol{f}]$, cf. Cramer's rule. If b_{ij} is the ijth entry of $B = \mathcal{P}\left[\Psi' + A^\top\Psi\right]$, then $b_{ij} = \mathcal{O}\left(\|\hat{A}^{j-1}\|\right)$, hence the ijth entry of BW^{-1} is $\frac{b_{ij}}{\|\hat{A}^{j-1}\|} = \mathcal{O}(1)$. It follows that $BW^{-1} - G = \operatorname{o}(\boldsymbol{1})$, as all terms of order $\mathcal{O}(\boldsymbol{1})$ are within G. Since G is nonsingular, Theorem 6.1.1 states that $(BW^{-1})^{-1} = \mathcal{O}(\boldsymbol{1})$. Thus we obtain

$$(\det B)^{-1} = \det B^{-1} = \det(BW^{-1}W)^{-1} = \det \mathcal{O}(\boldsymbol{1}) \det W^{-1}$$

$$= \mathcal{O}(1) \left(\prod_{j=0}^{n-1} \|\hat{A}^j\| \right)^{-1} = \mathcal{O}\left(\prod_{j=0}^{n-1} \|\hat{A}^j\|^{-1} \right).$$

We now wish to show that the term multiplied by ψ_k in (6.5.1), namely $\det B_1 - \det B$, $\det B_{k-1} + \det B_k$ or $\det B_n$, is of order $\mathcal{O}\left(\prod_{\substack{j=0 \\ j \neq k-1}}^{n} \|\hat{A}^j\| \right)$. Note that,

$$\det\left(\ldots, \mathcal{P}\left[A^\top \psi_k\right], \ldots, \mathcal{P}\left[A^\top (\psi_{k+1} + \psi_k)\right], \ldots\right) = \det\left(\ldots, \mathcal{P}\left[A^\top \psi_k\right], \ldots, \mathcal{P}\left[A^\top \psi_{k+1}\right], \ldots\right)$$

which follows since we can add the multiple of one column to another without altering a determinant. Using this fact, along with determinant manipulations *à la* Theorem 5.3.2, we obtain

$$
\begin{aligned}
\det B_1 - \det B &= \det\left(\mathcal{P}\left[A^\top \psi_1\right], \mathcal{P}\left[A^\top (\psi_3 + \psi_2)\right], \ldots, \mathcal{P}\left[A^\top (\psi_{n+1} + \psi_n)\right] \right) \\
&\quad - \det[\mathcal{P}\left[A^\top (\psi_2 + \psi_1)\right], \mathcal{P}\left[A^\top (\psi_3 + \psi_2)\right], \ldots, \mathcal{P}\left[A^\top (\psi_{n+1} + \psi_n)\right]] \\
&= -\det\left(\mathcal{P}\left[A^\top \psi_2\right], \mathcal{P}\left[A^\top (\psi_3 + \psi_2)\right], \ldots, \mathcal{P}\left[A^\top (\psi_{n+1} + \psi_n)\right] \right) \\
&= -\det\left(\mathcal{P}\left[A^\top \psi_2\right], \mathcal{P}\left[A^\top \psi_3\right], \ldots, \mathcal{P}\left[A^\top \psi_{n+1}\right] \right) \\
&= -\det\left(\mathcal{P}\left[\psi_1'\right], \mathcal{P}\left[\psi_2'\right], \ldots, \mathcal{P}\left[\psi_n'\right] \right).
\end{aligned}
$$

Since $\mathcal{P}[\psi_k'] = O\left(\|\hat{A}^k\|, \ldots, \|\hat{A}^k\| \right)^\top$, the kth column in this determinant is composed of entries of order $\mathcal{O}\left(\|\hat{A}^k\| \right)$, thus the determinant is of the requisite order $\mathcal{O}\left(\prod_{k=1}^{n} \|\hat{A}^k\| \right)$.

Likewise, writing the kth column of B, $\mathcal{P}[\mathcal{L}[\boldsymbol{\psi}_k]] = \mathcal{P}\big[A^\top(\boldsymbol{\psi}_k + \boldsymbol{\psi}_{k+1})\big]$, as $\boldsymbol{b}_k$,

$$
\begin{aligned}
\det B_{k-1} + \det B_k &= \det\left(\boldsymbol{b}_1, \ldots, \boldsymbol{b}_{k-2}, \mathcal{P}\big[A^\top\boldsymbol{\psi}_1\big], \boldsymbol{b}_k, \boldsymbol{b}_{k+1}, \ldots, \boldsymbol{b}_n\right) \\
&\quad + \det\left(\boldsymbol{b}_1, \ldots, \boldsymbol{b}_{k-2}, \boldsymbol{b}_{k-1}, \mathcal{P}\big[A^\top\boldsymbol{\psi}_1\big], \boldsymbol{b}_{k+1}, \ldots, \boldsymbol{b}_n\right) \\
&= \det\left(\boldsymbol{b}_1, \ldots, \boldsymbol{b}_{k-2}, \mathcal{P}\big[A^\top\boldsymbol{\psi}_1\big], \mathcal{P}\big[A^\top\boldsymbol{\psi}_{k+1}\big], \boldsymbol{b}_{k+1}, \ldots, \boldsymbol{b}_n\right) \\
&\quad + \det\left(\boldsymbol{b}_1, \ldots, \boldsymbol{b}_{k-2}, \mathcal{P}\big[A^\top\boldsymbol{\psi}_1\big], \mathcal{P}\big[A^\top\boldsymbol{\psi}_k\big], \boldsymbol{b}_{k+1}, \ldots, \boldsymbol{b}_n\right) \\
&\quad + \det\left(\boldsymbol{b}_1, \ldots, \boldsymbol{b}_{k-2}, \mathcal{P}\big[A^\top\boldsymbol{\psi}_k\big], \mathcal{P}\big[A^\top\boldsymbol{\psi}_1\big], \boldsymbol{b}_{k+1}, \ldots, \boldsymbol{b}_n\right) \\
&\quad + \det\left(\boldsymbol{b}_1, \ldots, \boldsymbol{b}_{k-2}, \mathcal{P}\big[A^\top\boldsymbol{\psi}_{k-1}\big], \mathcal{P}\big[A^\top\boldsymbol{\psi}_1\big], \boldsymbol{b}_{k+1}, \ldots, \boldsymbol{b}_n\right) \\
&= \det[\mathcal{P}\big[A^\top\boldsymbol{\psi}_2\big], \ldots, \mathcal{P}\big[A^\top\boldsymbol{\psi}_{k-1}\big], \mathcal{P}\big[A^\top\boldsymbol{\psi}_1\big], \mathcal{P}\big[A^\top\boldsymbol{\psi}_{k+1}\big], \\
&\qquad\qquad \mathcal{P}\big[A^\top\boldsymbol{\psi}_{k+2}\big], \ldots, \mathcal{P}\big[A^\top\boldsymbol{\psi}_{n+1}\big]] \\
&\quad + \det[\mathcal{P}\big[A^\top\boldsymbol{\psi}_2\big], \ldots, \mathcal{P}\big[A^\top\boldsymbol{\psi}_{k-1}\big], \mathcal{P}\big[A^\top\boldsymbol{\psi}_{k-1}\big], \mathcal{P}\big[A^\top\boldsymbol{\psi}_1\big], \\
&\qquad\qquad \boldsymbol{b}_{k+1}, \ldots, \boldsymbol{b}_n] \\
&= \det\left(\mathcal{P}\big[\boldsymbol{\psi}_1'\big], \ldots, \mathcal{P}\big[\boldsymbol{\psi}_{k-2}'\big], \mathcal{P}[\boldsymbol{f}], \mathcal{P}\big[\boldsymbol{\psi}_k'\big], \mathcal{P}\big[\boldsymbol{\psi}_{k+1}'\big], \ldots, \mathcal{P}\big[\boldsymbol{\psi}_n'\big]\right) \\
&= \mathcal{O}\left(\prod_{\substack{j=0 \\ j\neq k-1}}^{n} \|\hat{A}^j\|\right).
\end{aligned}
$$

By similar logic, $\det B_n$ is $\mathcal{O}\big(\prod_{j=0}^{n-1}\|\hat{A}^j\|\big)$. Thus the kth term in (6.5.1)—the term multiplied by $A^\top\boldsymbol{\psi}_k$—is of order $\mathcal{O}\big(\|\hat{A}^n\|/\|\hat{A}^{k-1}\|\big)$. But this term is multiplied by $A^\top\boldsymbol{\psi}_k = \mathcal{O}\big(\hat{A}^{(k-1)\top}\tilde{\boldsymbol{f}}\big)$, hence

$$
\mathcal{L}[\boldsymbol{v}] - \boldsymbol{f} = \sum_{k=1}^{n} \mathcal{O}\left(\frac{\|\hat{A}^n\|}{\|\hat{A}^{k-1}\|}\hat{A}^{(k-1)\top}\tilde{\boldsymbol{f}}\right) = \mathcal{O}\big(\|\hat{A}^n\|\big)\sum_{k=1}^{n}\mathcal{O}\left(\frac{\hat{A}^{(k-1)\top}\tilde{\boldsymbol{f}}}{\|\hat{A}^{k-1}\|}\right) = \mathcal{O}\big(\|\hat{A}^n\|\,\mathbf{1}\big),
$$

and the theorem follows from Corollary 6.2.2.

Q.E.D.

The decomposition to determine the matrix G can be achieved with symbolic algebra in the general case, and by construction in specific cases. As an example, consider the Bessel kernel $(J_0(\omega x), J_1(\omega x))^\top$. Then

$$
A(x) = \begin{pmatrix} 0 & -\omega \\ \omega & -x^{-1} \end{pmatrix} \quad \text{and} \quad W = \mathcal{O}\big(\operatorname{diag}\big(1, \omega^{-1}, \omega^{-2}, \ldots, \omega^{-n+1}\big)\big).
$$
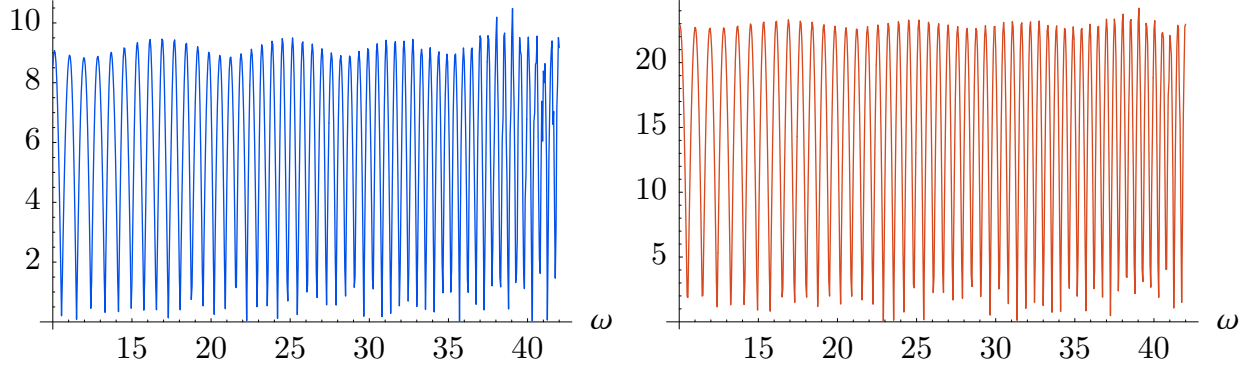
Figure 6.42:   The error scaled by $\omega^{31/4}$ of $Q^B[\boldsymbol{f}]$ with endpoints for nodes and multiplicities both one (left graph), compared to $Q_5^A[\boldsymbol{f}]$ (right graph), for the oscillatory integral $I[f] = \int_1^2 \left[\cos x\,\mathrm{Ai}\,(-\omega x) - \omega\,\mathrm{e}^x\mathrm{Ai}\,'(-\omega x)\right]\,\mathrm{d}x$.

We can write

$$A = A_1 + \omega A_2 \qquad \text{for} \qquad A_2 = \begin{pmatrix} 0 & -1 \\ 1 & 0 \end{pmatrix},$$

where $A^{-1} = -\omega^{-1}A_2 + \mathcal{O}(\omega^{-2}\mathbf{1})$. We want to select only the terms of maximum order. The term of maximum order for $\boldsymbol{\psi}_k$ is $\omega^{-k}\boldsymbol{\phi}_k$, where

$$\boldsymbol{\phi}_1(x) = -A_2^\top \boldsymbol{f}, \qquad \boldsymbol{\phi}_{k+1}(x) = -A_2^\top \boldsymbol{\phi}_k'(x) = (-A_2^\top)^{k+1}\boldsymbol{f}^{(k)}.$$

Thus we obtain the matrix

$$G = \mathcal{P}\left[\left(A_2^\top \boldsymbol{\phi}_1, \ldots, A_2^\top \boldsymbol{\phi}_n\right)\right] = \mathcal{P}\left[\left(\boldsymbol{f}, \ldots, (-A_2^\top)^{n-1}\boldsymbol{f}^{(n-1)}\right)\right].$$

the form of G for other examples can be found by similar logic.

We once again return to the example from Figure 6.37: computing the integral

$$I[f] = \int_1^2 \left[\cos x\,\mathrm{Ai}\,(-\omega x) - \omega\,\mathrm{e}^x\mathrm{Ai}\,'(-\omega x)\right]\,\mathrm{d}x.$$

Consider the case with only the endpoints for nodes and multiplicities both one. Then $n = 4$, i.e., the dimension times the number of nodes, and the theorem predicts an error of order

$$\mathcal{O}\left(\left\|\hat{A}^4\right\|\mathbf{1}^\top \hat{A}^2 \boldsymbol{y}\right) = \mathcal{O}\left(\omega^{-6}\left(\omega^{-3}, \omega^{-3}\right)\begin{pmatrix} \omega^{-1/4} \\ \omega^{5/4} \end{pmatrix}\right) = \mathcal{O}\left(\omega^{-31/4}\right).$$

For comparison, to obtain the same order of error we would have needed to take s equal to five in the asymptotic expansion, or a Levin-type method with multiplicities at least four at the endpoints. This Levin-type method would require solving a much larger system of $4\cdot 2\cdot d = 16$ equations. Figure 6.42 confirms the order of error of the new Levin-type method with asymptotic basis, and compares the error to that of the asymptotic expansion of the

106
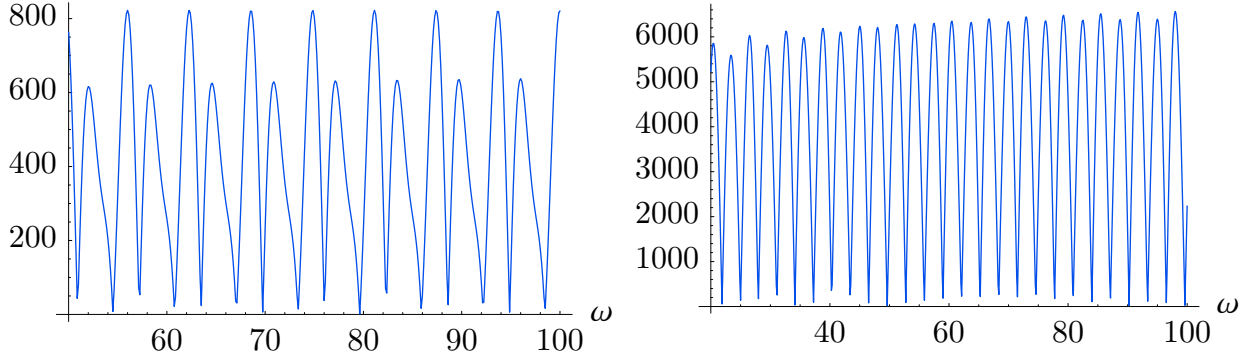
Figure 6.43: The error scaled by $\omega^{13/2}$ of $Q^B[\boldsymbol{f}]$ with endpoints for nodes and multiplicities both one (left graph), compared to the error scaled by $\omega^{17/2}$ of $Q^B[\boldsymbol{f}]$ with an additional node at the midpoint with multiplicity one (right graph), for $\int_1^2 \left[x^{-2} J_2(\omega x) + x^3 J_3(\omega x) \right] \, \mathrm{d}x$.

same order. Note that the method becomes so accurate that it is impractical to extend this graph further: computing the integral with Gauss–Legendre quadrature to sufficient accuracy to make a comparison is extraordinarily expensive.

Figure 6.43 demonstrates that adding a node to $Q^B[\boldsymbol{f}]$ does indeed increase the asymptotic order, using the integral from Figure 6.41

$$ I[f] = \int_1^2 \left[x^{-2} J_2(\omega x) + x^3 J_3(\omega x) \right] \, \mathrm{d}x. $$

In this case, $\|\hat{A}^n\| = \mathcal{O}\!\left(\omega^{-n}\right)$, hence adding a single node increases the order by two. Note that, because of the large difference in the scaling factor, the errors in the right graph are in fact significantly smaller than those in the left graph.

Remark: The derivatives required to find each $\boldsymbol{\psi}_k$ can quickly become unmanageable when either $\boldsymbol{f}$ or A is moderately complicated. This issue can be mitigated since it is possible to show that including the first k of these basis functions, along with any other basis functions of one's choice, results in an error of order $\mathcal{O}\!\left(\left\|\hat{A}^k\right\| \mathbf{1}^\top \hat{A}^{s+1} \boldsymbol{y}\right)$. In short, adding even just the single, trivially computed, basis function $\boldsymbol{\psi}_1 = A^{-\top} \boldsymbol{f}$ to the standard polynomial basis will increase the asymptotic order. It may also be possible to use finite differences in place of derivatives, in a similar vein to Section 3.5, though this idea has not been thoroughly investigated.

Remark: It is obvious how to construct an asymptotic basis for the Levin-type methods of Section 6.3. Indeed, the proof of the asymptotic order should be significantly simpler, being a simple generalization of Theorem 3.3.1. This idea has not yet been investigated in detail.

6.6. Future work

There are still several open questions. The first question is whether similar techniques can be used for multivariate highly oscillatory integrals. It may be possible to combine the techniques from this chapter and Chapter 5—which derived a Levin-type method for integrals of the form

$$\int_\Omega f(\boldsymbol{x}) \mathrm{e}^{\mathrm{i}\omega g(\boldsymbol{x})} \, \mathrm{d}\boldsymbol{x}$$

—to compute integrals whose highly oscillatory component satisfies a partial differential equation. Another open question is quadrature for integrals which contain a turning point, for example

$$\int_0^1 f(x) \operatorname{Ai}(-\omega x) \, \mathrm{d}x. \tag{6.6.1}$$

A turning point is any point ξ where the matrix $A(\xi)$ becomes singular, hence the derivation of the asymptotic expansion is no longer valid over an interval containing such a point. A way to compute (6.6.1) in particular will be presented in Chapter 7, though it cannot be generalized to other kernels containing turning points.

A method for irregular exponential oscillators $\mathrm{e}^{\mathrm{i}\omega g}$ with stationary points was presented in Chapter 4. In this case an interpolation basis was found that could be integrated in closed form, regardless of what the oscillator g was. This basis was constructed by using incomplete Gamma functions [2], where the choice of basis resulted from solving the differential equation

$$v' + (r-1)\mathrm{i}\omega x^{r-1} v = x^k. \tag{6.6.2}$$

It might be possible to find a related ansatz for the vector-valued case. For example, consider the integral

$$\int_{-1}^1 f(x) \, y(x) \, \mathrm{d}x,$$

where y satisfies an Airy-like equation

$$y'' + \omega q y = 0, \qquad \text{where} \qquad q(0) = 0 \quad \text{and} \quad q'(0) \neq 0.$$

Emulating the derivation for the exponential oscillator in (6.6.2) would require finding a solution to the equation

$$v'' + \omega x v = x^k.$$

MATHEMATICA can compute a solution to this differential equation in terms of Airy functions and regularized generalized hypergeometric functions, however hypergeometric functions lack the simplicity of the incomplete Gamma function, and computation is significantly more challenging.

Chapter 7

Unbounded Domains and Infinite Oscillations

As of this chapter, we have only looked at integrals with well-behaved integrands. We now look at two cases that contain singularities. The first situation is when the interval of integration is unbounded. The canonical example is

$$\int_1^\infty \frac{e^{i\omega x}}{x}\, dx,$$

which is related to the exponential, sine and cosine integrals [2]. This integral does not converge absolutely, however it does exist as an improper integral:

$$\int_1^\infty \frac{e^{i\omega x}}{x}\, dx = \lim_{b\to\infty} \int_1^b \frac{e^{i\omega x}}{x}\, dx.$$

Another situation which we will investigate is when the kernel has an infinite number of oscillations within the integration interval, or in other words, for the integral

$$\int_a^b f(x)e^{i\omega g(x)}\, dx,$$

the oscillator $g(x)$ has a singularity. An example of such an integral is

$$\int_0^1 e^{i\omega x^{-1}}\, dx.$$

Despite the apparent intractability of these two problems, a Levin-type method with an appropriate collocation basis is still an extraordinarily effective quadrature scheme.

In Section 7.1, we analyse oscillatory integrals over unbounded intervals. This proceeds as usual: we first derive an asymptotic expansion, which is used in the proof of order for associated Levin-type methods. This methodology again proves successful for integrals with infinite oscillations, in Section 7.2. In Section 7.3, we see that the same ideas can be utilized for other oscillators, in particular integrals involving Airy functions over unbounded intervals. In Section 1.3 it was noted that a useful application for oscillatory integration was the computation of special functions. We finally have the tools necessary for computing special functions using their oscillatory integral representations, which we use for the Airy function in Section 7.4.

Remark: This chapter consists of as-of-yet unpublished original research, though the asymptotic expansions derived are similar to expansions found in [74].

7.1. Unbounded integration domains

In this section we investigate the case where the interval of integration is unbounded, for example integrating over (a, ∞). Consider the integral

$$E_1(-\mathrm{i}\omega) = \int_1^\infty \frac{\mathrm{e}^{\mathrm{i}\omega x}}{x} \, \mathrm{d}x,$$

where E_1 is the exponential integral [**2**]. This function is important since we can derive the cosine integral Ci and sine integral Si from its real and imaginary parts. As before, we begin by deriving an asymptotic expansion:

Theorem 7.1.1 *Suppose that $1/g'$ and its derivatives are bounded in $[a, \infty)$, $f(x) \to 0$ as $x \to \infty$ and $\frac{\mathrm{d}}{\mathrm{d}x}\left[\frac{f(x)}{g'(x)}\right] \sim x^\alpha u(x)$, for a smooth function u such that it and its derivatives are bounded, and this relationship holds under differentiation. If $\alpha < -1$, then*

$$I[f] \sim \sum_{k=1}^\infty \frac{1}{(-\mathrm{i}\omega)^k} \sigma_k(a) \mathrm{e}^{\mathrm{i}\omega g(a)},$$

where, as before,

$$\sigma_1 = \frac{f}{g'}, \qquad \sigma_{k+1} = \frac{\sigma_k'}{g'}, \qquad k \geq 1.$$

Proof: Expanding out the first term of the asymptotic expansion we have

$$\int_a^M f \mathrm{e}^{\mathrm{i}\omega g} \, \mathrm{d}x = \frac{1}{\mathrm{i}\omega}\left[\frac{f}{g'}\mathrm{e}^{\mathrm{i}\omega g}\right]_a^M - \frac{1}{\mathrm{i}\omega}\int_a^M \left(\frac{f(x)}{g'(x)}\right)' \mathrm{e}^{\mathrm{i}\omega g} \, \mathrm{d}x.$$

We know that $\frac{f(M)}{g'(M)}\mathrm{e}^{\mathrm{i}\omega g(M)} \to 0$ as $M \to \infty$, since g' does not approach zero. Furthermore, the integral $I\left[\left(\frac{f}{g}\right)'\right]$ converges absolutely, since the integrand decays faster than x^{-1}. Finally, we obtain

$$\left(\frac{\sigma_1'(x)}{g'(x)}\right)' \sim \left(\frac{x^\alpha u(x)}{g'(x)}\right)' = x^\alpha \left(\frac{u'(x)}{g'(x)} + \alpha\frac{u(x)}{xg'(x)} - \frac{u(x)g''(x)}{g'(x)^2}\right).$$

It is not hard to see that $\frac{u'(x)}{g'(x)} + \alpha\frac{u(x)}{xg'(x)} - \frac{u(x)g''(x)}{g'(x)^2}$ is smooth and it and its derivatives are bounded, thus $\sigma_1'(x)$ satisfies the conditions on f, and the theorem follows by induction.

Q.E.D.

A version of Corollary 3.1.1 follows immediately, where now f only depends on the endpoint a. We cannot, however, use this corollary to derive a Filon-type method, since polynomials do not decay at infinity. We can show that Levin-type methods do work with any basis:

Theorem 7.1.2 *Suppose that f and g satisfy the requirements of Theorem 7.1.1. Then, using the notation of Theorem 3.2.1,*

$$Q^L[f] - I[f] = \mathcal{O}\!\left(\omega^{-s-1}\right),$$

where $s = m_0$ and

$$Q^L[f] = -v(a)\mathrm{e}^{\mathrm{i}\omega g(a)}.$$

Proof: Suppose each function in the basis $\{\psi_1, \ldots, \psi_n\}$ satisfies the conditions on f in Theorem 7.1.1. Then the proof of this theorem is unaltered from Theorem 3.2.1, since $I[\mathcal{L}[v]] = Q^L[f]$. If the basis $\{\psi_1, \ldots, \psi_n\}$ does not satisfy the conditions, we replace it by a basis $\left\{\tilde{\psi}_0, \ldots, \tilde{\psi}_n\right\}$ that does satisfy these properties. Define $\tilde{\psi}_k(x)$ so that it equals $\psi_k(x)$ for all $x_0 \leq x \leq x_\nu$, goes to zero smoothly in $x_\nu < x < N < \infty$ for some fixed constant $N > x_\nu$ and $\tilde{\psi}_k(x) \equiv 0$ for $N \leq x < \infty$. The collocation system (3.2.1) with this new basis is unchanged from the original collocation system, hence $Q^L[f]$ is also unchanged. However, $\tilde{\psi}_k$ now satisfies the requisite properties, and the theorem follows.

Q.E.D.

Returning to the E_1 case, we obtain an asymptotic expansion

$$E_1(-\mathrm{i}\omega) \sim \mathrm{e}^{\mathrm{i}\omega} \sum_{k=1}^{\infty} \frac{(-1)^{k-1}(k-1)!}{(-\mathrm{i}\omega)^k}.$$

It should come as no surprise that this is equivalent to the expansion in [**2**]. We can use the asymptotic basis with a Levin-type method—this time without a constant function in the basis—to derive an approximation. Consider the case of arbitrarily chosen nodes $\{1, 5, 10, 20\}$ with multiplicities all one. This has an order of error $\mathcal{O}\!\left(\omega^{-6}\right)$, thus we compare it to the asymptotic expansion of order $\mathcal{O}\!\left(\omega^{-6}\right)$ in the left side of Figure 7.44. Even with arbitrarily chosen nodes, $Q^B[f]$ is substantially more accurate than the asymptotic expansion; in this case it has less than a tenth of the error. We can also compare the real parts of each approximation to $-\mathrm{Ci}\,(\omega)$, where Ci is the cosine integral as defined in [**2**]. This results in the right side of Figure 7.44.

We can also use this method to compute

$$E_n(-\mathrm{i}\omega) = \int_1^{\infty} \frac{\mathrm{e}^{\mathrm{i}\omega t}}{t^n}\, dt.$$

With this approximation in hand, we can successfully compute the incomplete Gamma function

$$\Gamma(a, -\mathrm{i}\omega) = (-\mathrm{i}\omega)^a E_{1-a}(-\mathrm{i}\omega),$$

111
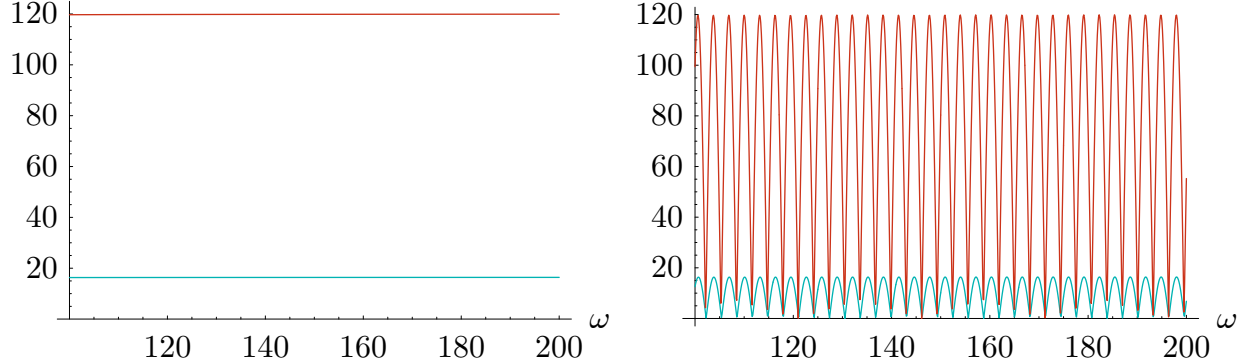
Figure 7.44: On the left, the error scaled by ω^6 of the asymptotic expansion (top) and $Q^B[f]$ with nodes $\{1, 5, 10, 20\}$ and multiplicities all one (bottom) for $I[f] = \int_1^\infty \frac{1}{x} e^{i\omega x} \, dx$ compared to $E_1(-i\omega)$. On the right, the real parts of the same approximations compared to $-\mathrm{Ci}(\omega)$.

whenever $a < 1$. When $a \geq 1$, $\Gamma(a, -i\omega)$ can be computed by the recursive formula

$$\Gamma(a, x) = (a - 1)\Gamma(a - 1, x) + x^{a-1}e^{-x}.$$

This approximation for the incomplete Gamma functions can then be used in conjunction with a Moment-free Filon-type method, to obtain an approximation scheme in terms of only elementary operations.

7.2. Infinite oscillations

Another potential issue is when there are an infinite number of oscillations within the interval of integration. For example, consider the integral

$$\int_0^1 e^{i\omega x^{-1}} \, dx.$$

The convergence of such integrals follows from the definition of a Riemann integral. Assuming g' goes to infinity at a sufficiently fast rate, we can indeed derive an asymptotic expansion:

Theorem 7.2.1 *Suppose that g is smooth, g' is nonzero in $[a, b)$, $1/g'(x) \sim (x - b)^\alpha u(x)$ as $x \to b$, and $f(x) \sim (x - b)^\beta v(x)$, where $\alpha \geq 1$ and both $\sim$ relationships are differentiable. Suppose further that u, v and their derivatives are bounded. If $\alpha + \beta \geq 1$, then*

$$I[f] \sim \sum_{k=1}^{\infty} \frac{1}{(-i\omega)^k} \sigma_k(a) e^{i\omega g(a)}.$$

Proof: Let $M \in (a, b)$ and note that

$$\int_a^M f \mathrm{e}^{\mathrm{i}\omega g} \, \mathrm{d}x = \frac{1}{\mathrm{i}\omega} \left[\frac{f}{g'} \mathrm{e}^{\mathrm{i}\omega g} \right]_a^M - \frac{1}{\mathrm{i}\omega} \int_a^M \left(\frac{f}{g'} \right)' \mathrm{e}^{\mathrm{i}\omega g} \, \mathrm{d}x$$

$$\sim \frac{1}{\mathrm{i}\omega} \left[(x - b)^{\alpha+\beta} uv \mathrm{e}^{\mathrm{i}\omega g} \right]_a^M - \frac{1}{\mathrm{i}\omega} \int_a^M \tilde{v} \mathrm{e}^{\mathrm{i}\omega g} \, \mathrm{d}x,$$

where $\tilde{v} \sim (x-b)^{\alpha+\beta-1} [(\alpha + \beta)uv + (x - b)(uv)']$, which satisfies the conditions on v. Since $\alpha + \beta \geq 1 > 0$, we know that $(x - b)^{\alpha+\beta} \to 0$ as $M \to b$. Furthermore, $\tilde{\beta} = \alpha + \beta - 1 > 0$, hence the integrand is bounded. Thus we let $M \to b$ to obtain

$$I[f] = -\frac{1}{\mathrm{i}\omega} \frac{f(a)}{g'(a)} \mathrm{e}^{\mathrm{i}\omega g(a)} - \frac{1}{\mathrm{i}\omega} \int_a^b \tilde{v} \mathrm{e}^{\mathrm{i}\omega g} \, \mathrm{d}x.$$

Since $\alpha + \tilde{\beta} = 2\alpha + \beta - 1 \geq \alpha \geq 1$, we can repeat the process with $\tilde{v}$ in place of f and $\tilde{\beta}$ in place of β. The asymptotic expansion follows by induction.

<div align="right">Q.E.D.</div>

An equivalent theorem holds over unbounded intervals:

Corollary 7.2.2 *Assume that $a > 0$. Consider the integral over (a, ∞), where $\frac{1}{g'(x)} \sim x^\alpha u(x)$, $f(x) \sim x^\beta v(x)$, again both $\sim$ relationships are differentiable, and $\alpha < 0$. If $\alpha + \beta < 0$, then*

$$I[f] \sim \sum_{k=1}^\infty \frac{1}{(-\mathrm{i}\omega)^k} \sigma_k(a) \mathrm{e}^{\mathrm{i}\omega g(a)}.$$

Proof: The proof to this corollary is similar to Theorem 7.2.1. Let s be an integer large enough so that $s\alpha + \beta \leq -2$. Then the s-term expansion over (a, M) is

$$-\sum_{k=1}^s \frac{1}{(-\mathrm{i}\omega)^k} \{\sigma_k(M) - \sigma_k(a)\} + \frac{1}{(-\mathrm{i}\omega)^s} \int_a^M \sigma_s' \mathrm{e}^{\mathrm{i}\omega g} \, \mathrm{d}x.$$

Note that $\sigma_1(x) \sim x^{\alpha+\beta} u(x)v(x)$ and $\sigma_1'(x) \sim x^{\alpha+\beta} \left[(\alpha + \beta)x^{-1} u(x)v(x) + (u(x)v(x)) \right]'$. Hence $\sigma_k(x) = x^{k\alpha+\beta} \tilde{v}$ for some smooth function $\tilde{v}$, where $\tilde{v} = \mathcal{O}(1)$. It follows that the terms evaluated at M of the expansion vanish as $M \to \infty$. Furthermore the integral $I[\sigma_s']$ converges absolutely, since $|\sigma_s'(x)| \leq C x^{s\alpha+\beta} \leq C' x^{-2}$.

<div align="right">Q.E.D.</div>

A Filon-type method for the bounded interval case follows immediately, where now the order of the method depends only on the multiplicity at a. Finding a Levin-type method is
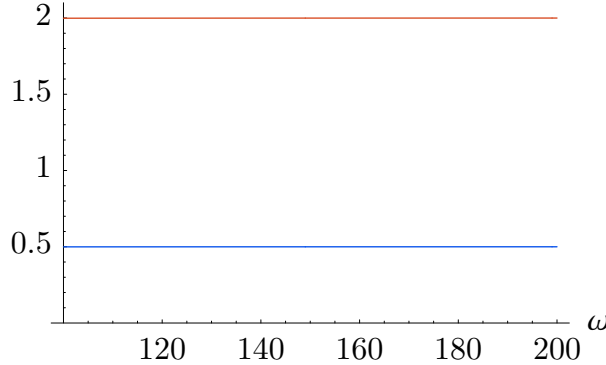
Figure 7.45:   Errors scaled by ω^2 of the one-term asymptotic expansion (top) compared to a Levin-type method collocating at $\{1/2, 1\}$ with multiplicities both one, for $I[f] = \int_0^1 e^{i\omega x^{-1}}\, dx$.

more difficult. We derive it for the finite-interval case, though the infinite-interval case can be handled in the same manner. Note that

$$\int_a^M \mathcal{L}[v]\, e^{i\omega g}\, dx = v(M)e^{i\omega g(M)} - v(a)e^{i\omega g(a)}.$$

In order for this to converge as $M \to b$, $v(M)$ must go to zero. Hence assume that the collocation basis satisfies $\psi_k(b) = 0$. In this case, we define

$$Q^L[f] = I[\mathcal{L}[v]] = -v(a)e^{i\omega g(a)}.$$

The behaviour of $\mathcal{L}[v] = v' + i\omega g'v$ at b depends on the order of the zeros of ψ_k at b: if the order of the pole of g' is greater than that of the zeros, then $L[v]$ will be unbounded at b. Thus we ensure that the order of the zeros of each ψ_k are at least that of the order of the pole of g'. Assuming that b is not a collocation point, we can, for any basis, replace ψ_k by some smooth $\tilde{\psi}_k$ such that $\tilde{\psi}_k(x) = \psi_k(x)$ for all $a \leq x \leq x_\nu$, $\tilde{\psi}_k(x)$ goes to zero in $x_\nu \leq x \leq N < b$ and $\tilde{\psi}_k(x) \equiv 0$ for $N \leq x \leq b$, where N is some constant. As in Theorem 7.1.2, this does not effect the collocation system at all, meaning that replacing ψ_k by $\tilde{\psi}_k$ has no effect on $Q^L[f]$. Hence the requirements on the basis are effectively unchanged.

Theorem 7.2.3 *Suppose that f satisfies the requirements of Theorem 7.2.1 or Corollary 7.2.2, and b is not a collocation point. Then*

$$Q^L[f] - I[f] = \mathcal{O}\left(\omega^{-s-1}\right),$$

where $s = m_0$ and $Q^L[f] = -v(a)e^{i\omega g(a)}$.

As a numerical example, consider the integral $I[f] = \int_0^1 e^{i\omega x^{-1}}\, dx$. Figure 7.45 compares a Levin-type method with the polynomial basis to the asymptotic expansion. In Figure 7.46,
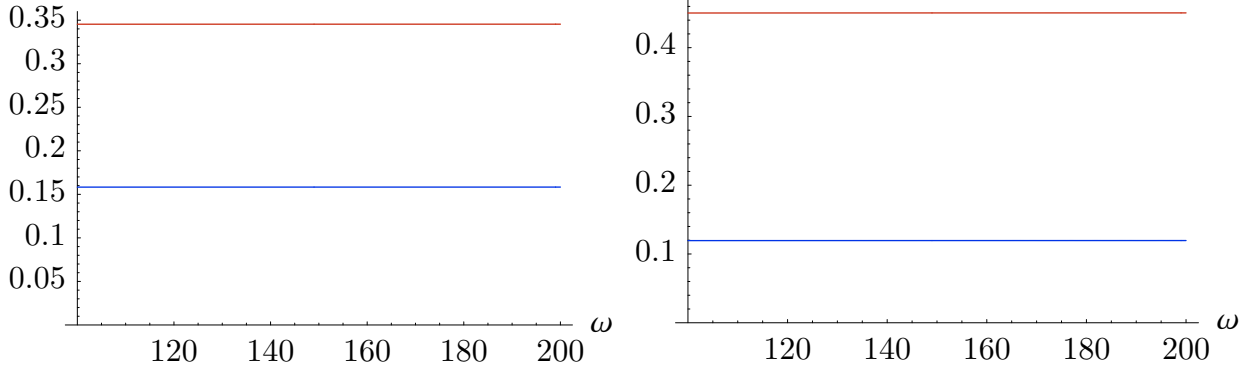
Figure 7.46: Errors scaled by ω^2 of the one-term asymptotic expansion (left graph, top) compared to a Levin-type method collocating at $\{1, 2\}$ with multiplicities both one (left graph, bottom), and errors scaled by ω^3 of the two-term asymptotic expansion (right graph, top) compared to a Levin-type method collocating at $\{1, 2\}$ with multiplicities $\{2, 1\}$ (right graph, bottom), for $I[f] = \int_1^\infty \cos x \, e^{i\omega x^2} \, dx$.

we consider the unbounded integral $\int_1^\infty \cos x \, e^{i\omega x^2} \, dx$, and compare two Levin-type methods to the asymptotic expansion: the first Levin-type method of order $\mathcal{O}(\omega^{-2})$ and the second Levin-type method of order $\mathcal{O}(\omega^{-3})$. In all three diagrams, Levin-type methods are a clear improvement over the asymptotic expansion of the same order.

7.3. Higher order oscillators

We can also generalize the techniques of this chapter for higher order oscillators. For simplicity, we will focus on the case $y_\omega(x) = \text{Ai}(-\omega x)$, over the interval (a, ∞) for $a > 0$:

$$I[f] = \int_a^\infty f(x)\text{Ai}(-\omega x) \, dx.$$

Assume that f and its derivatives are bounded. This integral has both an infinite domain, and an increasingly large frequency of oscillations at ∞. The convergence of the integral will follow from the proof of the asymptotic expansion. We obtain the first term of the expansion over a finite interval via integration by parts:

$$I_M[f] = \int_a^M f y_\omega \, dx = -\frac{1}{\omega^3} \left[\frac{f(x)}{x} y_\omega'(x) + \left(\frac{f(x)}{x} \right)' y_\omega(x) \right]_a^M - \frac{1}{\omega^3} I_M \left[\left(\frac{f(x)}{x} \right)'' \right]$$

As $M \to \infty$, the contributions from that endpoint in the first term go to zero. Moreover, note that:

$$I_M \left[\left(\frac{f}{x} \right)'' \right] = 2 I_M \left[\frac{f}{x^3} \right] - 2 I_M \left[\frac{f'}{x^2} \right] + I_M \left[\frac{f''}{x} \right].$$

115
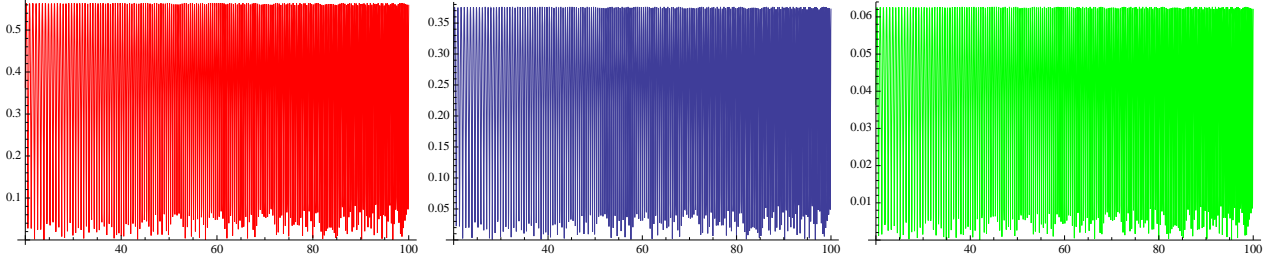
Figure 7.47: The error scaled by $\omega^{13/4}$ of the one-term asymptotic expansion (left graph) compared to a Levin-type method collocating at $\{1, 3\}$ with multiplicities all one (middle graph) and a Levin-type method collocating at $\left\{1, \frac{3}{2}, 2, 3\right\}$ again with multiplicities all one (right graph), for $I[f] = \int_1^\infty \text{Ai}\,(-\omega x)\,\mathrm{d}x$.

The first two of these integrals converge absolutely as $M \to \infty$. To prove that the last integral converges, we integrate it by parts once more. The nonintegral terms evaluated at M go to zero. The remaining integral term can be written as:

$$I_M\left[\left(\frac{f''}{x^2}\right)''\right] = 6I_M\left[\frac{f''}{x^4}\right] - 4I_M\left[\frac{f^{(3)}}{x^3}\right] + I_M\left[\frac{f^{(4)}}{x^2}\right].$$

All three of these integrals converge absolutely. Thus it follows that we can let $M \to \infty$ to obtain

$$I[f] = \int_a^\infty fy_\omega\,\mathrm{d}x = \frac{1}{\omega^3}\left[\frac{f(a)}{a}y_\omega'(a) + \left(\frac{f(a)}{a}\right)' y_\omega(a)\right] - \frac{1}{\omega^3}I\left[\left(\frac{f(x)}{x}\right)''\right].$$

Using induction we derive an asymptotic expansion:

Theorem 7.3.1 *Suppose that f and its derivatives are bounded in (a, ∞). Then*

$$\int_a^\infty f(x)\text{Ai}\,(-\omega x)\,\mathrm{d}x \sim -\sum_{k=1}^\infty \frac{1}{\omega^{3k-1}}\left\{\frac{\sigma_k(a)}{a}\text{Ai}\,'(-\omega a) - \frac{1}{\omega}\left(\frac{\sigma_k(a)}{a}\right)' \text{Ai}\,(-\omega a)\right\},$$

for $\sigma_1(x) = f(x)$ and $\sigma_{k+1}(x) = \left(\frac{\sigma_k(x)}{x}\right)''$.

The asymptotic error for Levin-type methods can be proved similarly to Theorem 6.4.1, where now

$$Q^L[f] = -\boldsymbol{v}(a)^\top \boldsymbol{y}(a) = -v_1(a)y(a) - v_2(a)y'(a).$$

Figure 7.47 compares the asymptotic expansion to two Levin-type methods for the first moment over the interval $(1, \infty)$, which do indeed exhibit an increase of accuracy over the asymptotic expansion, whilst maintaining the asymptotic order. An application of this theorem will appear in the next section.

We can utilize the approximation over the interval (a, ∞) to obtain an approximation for the case of integrating the Airy function $\mathrm{Ai}(-\omega x)$ in a domain which contains the turning point $x = 0$. When $a < 0$, computing the integral over the interval $(a, 0)$ is numerically trivial: the integrand is nonoscillatory, and the value of the integral itself goes to $\frac{1}{3}$ exponentially fast as $\omega \to \infty$ [2]. Thus assume that $a = 0$. From [2], we know that

$$\int_0^\infty \mathrm{Ai}(-\omega x)\ \mathrm{d}x = \frac{2}{3\,\omega},$$

hence we can write

$$I[f] = \int_0^b \mathrm{Ai}(-\omega x)\ \mathrm{d}x = \frac{2}{3\,\omega} - \int_b^\infty \mathrm{Ai}(-\omega x)\ \mathrm{d}x.$$

We know how to approximate the integral $\int_b^\infty \mathrm{Ai}(-\omega x)\ \mathrm{d}x$, thus we have found a way of approximating $\int_0^b \mathrm{Ai}(-\omega x)\ \mathrm{d}x$. All other moments can be expressed explicitly in terms of Ai, Ai$'$, and the first moment, by using the recurrence relationships from [2]:

$$\int x\mathrm{Ai}(x)\ \mathrm{d}x = \mathrm{Ai}'(x),$$

$$\int x^2\mathrm{Ai}(x)\ \mathrm{d}x = x\mathrm{Ai}'(x) - \mathrm{Ai}(x),$$

$$\int x^{k+3}\mathrm{Ai}(x)\ \mathrm{d}x = x^{k+2}\mathrm{Ai}'(x) - x^{k+1}\mathrm{Ai}(x) + (n+1)(n+2)\int x^n\mathrm{Ai}(x)\ \mathrm{d}x.$$

Thus Filon-type methods are a viable option for the Airy kernel. The error in approximation for the first moment is exactly same as in Figure 7.47.

7.4. Computing the Airy function

We now use the tools we have developed throughout this thesis to compute the Airy function $\mathrm{Ai}(x)$, in particular when x is negative and the Airy function is oscillatory. We utilize the integral representation

$$\mathrm{Ai}(x) = \frac{1}{\pi}\int_0^\infty \cos\left(\frac{t^3}{3} + xt\right)\ dt.$$

We can transform this expression into a form more conducive to the methods developed with a change of variables, giving us

$$\mathrm{Ai}(x) = \frac{\sqrt{-x}\,\mathrm{e}^{-\mathrm{i}\frac{2}{3}(-x)^{3/2}}}{\pi}\mathrm{Re}\int_0^\infty \mathrm{e}^{\mathrm{i}(-x)^{3/2}\left(\frac{t^3}{3} - t + \frac{2}{3}\right)}\ dt.$$

This integral contains both a stationary point of order two at $t = 1$ and an infinite number of oscillations at ∞. We thus use a Moment-free Filon-type method from Chapter 4 over the
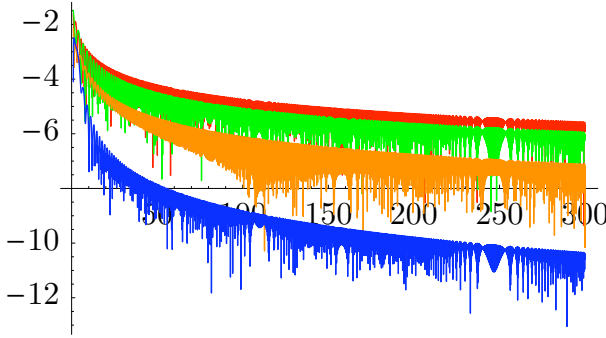
Figure 7.48: Base-10 errors in computing $\text{Ai}(-x)$ by $\tilde{\text{Ai}}(-x)$, for the one-term asymptotic expansion (top), approximation with nodes $\{0, 1, 2\}$ with multiplicities all one (second), nodes $\left\{0, \frac{1}{2}, 1, \frac{3}{2}, 2, 3\right\}$ with multiplicities all one (third) and nodes $\{0, 1, 2\}$ with multiplicities $\{2, 3, 2\}$.

interval $(0, 2)$ and a Levin-type method with asymptotic basis over $(2, \infty)$. Suppose we are given an increasing sequence of nodes $\{x_1, \ldots, x_\nu\}$ with multiplicities $\{m_1, \ldots, m_\nu\}$, where $x_\rho = 2$, for some $\rho \leq \nu$. Then, for

$$g(t) = \frac{t^3}{3} - t + \frac{2}{3},$$

define $Q_g^F[1, (0, 2)]$ as the Moment-free Filon-type method interpolating at the first ρ nodes $\{x_1, \ldots, x_\rho\}$ with multiplicities $\{m_1, \ldots, m_\rho\}$. Furthermore, define $Q_g^B[1, (2, \infty)]$ as the Levin-type method with asymptotic basis, collocating at the nodes $\{x_\rho, \ldots, x_\nu\}$ and multiplicities $\{m_\rho, \ldots, m_\nu\}$. Then we obtain an approximation

$$\tilde{\text{Ai}}(x) = \frac{\sqrt{-x}e^{-i\frac{2}{3}(-x)^{3/2}}}{\pi}\text{Re}\left\{Q_g^F[1, (0, 2)] + Q_g^B[1, (2, \infty)]\right\}$$

In Figure 7.48, we compare four methods for computing the Airy function for negative x of large magnitude: the standard one-term asymptotic expansion, found in [2], our new approximation $\tilde{\text{Ai}}$ with nodes $\{0, 1, 2\}$ and multiplicities all one, nodes $\left\{0, \frac{1}{2}, 1, \frac{3}{2}, 2, 3\right\}$ with multiplicities all one and finally $\tilde{\text{Ai}}$ with nodes $\{0, 1, 2\}$ and multiplicities $\{2, 3, 2\}$. This figure demonstrates that we can indeed improve the accuracy over the asymptotic expansion by orders of magnitude. It should be emphasized that we have not proved that this approximation scheme is guaranteed to converge with the addition of nodes, nor determined what the optimum placement is for the nodes and multiplicities.

There exist many alternative methods for approximating Airy functions for large $|x|$, mostly based on deformation to the complex plane and integrating along the path of steepest descent. A comprehensive list of algorithms was compiled in [67]. In [34], Gauss–Laguerre

quadrature is utilized along the path of steepest descent, though the error is never compared to the asymptotic expansion, and it is unclear whether high asymptotic orders are achieved. It is instead suggested to switch to the asymptotic expansion whenever $|x|$ is large, for example $|x| \geq 15$.

Chapter 8

Asymptotic Least Squares Approximation

In the study of ordinary differential equations, very accurate results can be achieved efficiently when the solution is nonoscillatory. At the same time, when the solution oscillates rapidly, asymptotic results such as the *Wentzel–Kramers–Brillouin approximation* (WKB approximation, also known as the Liouville–Green approximation) [**74**] can be used to approximate the solution to the differential equation, where the accuracy actually improves as the frequency of oscillations increases. Unfortunately, there is a limit to the accuracy of this expansion, meaning that for moderate oscillations this expansion is not appropriate as an approximation scheme. In this chapter we present a method which has the same asymptotic behaviour as the asymptotic expansion, whilst being incredibly more accurate, and in fact appears to converge to the exact solution, even for small frequencies.

In Section 3.3, Section 5.3 and Section 6.5, we used the asymptotic expansion in a collocation system to approximate a particular solution to the Levin differential equation. This approach successfully captured the asymptotic decay of the expansion, while significantly improving the accuracy. Indeed, it was noted in Figure 3.10 that this approximation scheme appeared to converge to the solution for fixed frequency at an exponentially fast rate as collocation points were added. The motivation behind this chapter is to prove this observation, and to generalize the method to other oscillatory differential equations. In place of collocation, we use a least squares system, as intuition suggests that the errors of both methods are related, and proving convergence for least squares should be significantly easier. Though we find an explicit, computable formula for the error in norm, we unfortunately fail to find simple conditions for which this expression goes to zero. We hence leave the final step in the proof of convergence as an open problem.

We analyse the asymptotic behaviour of differential equations with respect to a parameter $\omega \to \infty$, over a finite interval. In other words, we wish to solve the differential equation

$$\mathcal{L}_\omega[v](x) = f(x), \qquad a \le x \le b, \tag{8.0.1}$$

where $\mathcal{L}_\omega[v](x)$ is a linear differential operator. Of course, a unique solution to such an equation only exists if suitable initial or boundary value conditions are imposed. We however search merely for a particular solution: if the equation is inhomogenous, then this allows us to convert the equation into its homogenous form; otherwise, we exploit the fact that the equation is an ODE and find linearly independent particular solutions, which will span the solution space. By accurately approximating the linearly independent solutions and taking

an appropriate linear combination, we immediately obtain an approximation to (8.0.1) with boundary conditions imposed.

An example is the Airy equation, where $\mathcal{L}_\omega[v](x) = v''(x) + \omega x v(x)$ and $f(x)$ is zero. The idea is that ω represents the "frequency" of oscillations, and hence as ω increases the solution to the differential equation becomes more and more oscillatory. Using traditional approximation methods, such as the Runge–Kutta method or finite elements, would necessitate decreasing the step-size in order to compensate for the oscillations. As ω increases this becomes a monumental task, hence it is necessary to search for alternative approximation schemes.

We assume that the we know the asymptotic behaviour of the particular solution we wish to approximate. This means, for a solution v to (8.0.1), we know functions ψ_k such that

$$v(x) \sim \sum_{k=1}^{\infty} \frac{d_k}{\omega^{k+s}} \psi_k(x),$$

where d_k are some constants which we need not know. Applying $\mathcal{L}_\omega[v]$ to both sides of the preceding equation, we obtain an asymptotic expansion for f:

$$f(x) \sim \sum_{k=1}^{\infty} \frac{d_k}{\omega^{k+s}} \mathcal{L}_\omega[\psi_k](x).$$

In Section 8.1, we develop an approximation $v_{n,\omega}^{\mathrm{LS}}$ that is asymptotically close to v, in particular, $\left\| \mathcal{L}_\omega\left[v_{n,\omega}^{\mathrm{LS}}\right] - f \right\|_2 = \mathcal{O}\left(\omega^{-n-s-1}\right)$. Furthermore, we guarantee that the accuracy always improves as n increases, and as n goes to infinity $\left\| \mathcal{L}_\omega\left[v_{n,\omega}^{\mathrm{LS}}\right] - f \right\|_2$ becomes exponentially small. Furthermore, we find a criterion—which is satisfied in all our examples—to determine a simple expression for the exact L_2 error of the method. This expression appears to lend itself to a proof of convergence, though the proof is not completed.

With this approximation in hand, we then turn our attention to two important examples. First we revisit the approximation of highly oscillatory integrals, in Section 8.2. This is essentially the asymptotic basis utilized in Section 3.3, with least squares in place of collocation. Then, in Section 8.3, we investigate second order ODEs, particularly those for which the WKB approximation is known. In both cases, we demonstrate numerically that the approximation appears to converge exponentially fast for fixed ω, as $n \to \infty$. We follow this with a brief discussion on numerical issues with the approximation scheme in Section 8.4. Here we compare numerically least squares to collocation, a comparison which suggests that the errors of the two methods are indeed related. We also present an alternative to the asymptotic basis which uses finite differences in place of derivatives. Finally, we comment on other applications that this method might have in Section 8.5.

Remark: This chapter consists of as-of-yet unpublished original research.

8.1. Asymptotic least squares approximation

While an explicit solution to the differential equation (8.0.1) is not typically available, often an asymptotically accurate approximation is known; in other words a function v is known such that $\mathcal{L}_\omega[v] \to f$ as $\omega \to \infty$. In many circumstances, we have a whole expansion, where taking more terms in the expansion causes $\mathcal{L}_\omega[v]$ to converge faster to f as ω increases. Unfortunately, when the parameter ω is fixed this expansion does not in general converge, and for small ω the expansion is not an accurate approximation whatsoever.

The asymptotic expansion has the form

$$v(x) \sim \sum_{k=1}^{\infty} \frac{d_k}{\omega^{k+s}} \psi_k(x),$$

for some set of functions $\{\psi_k\}$, where the coefficients d_k are given. The idea behind the method is to treat the constants d_k as unknowns, determined not by the usual methods but by minimizing the norm $\|f - \mathcal{L}_\omega[v]\|$, where the norm results from a related complex-valued inner product $\langle \cdot, \cdot \rangle$. We prove the results for a general inner product, however, in all examples below we use the standard L_2 inner product

$$\langle f, g \rangle = \int_a^b f(x) \bar{g}(x) \, \mathrm{d}x.$$

Though the expansion itself can actually become less accurate as terms are added, this cannot happen when we minimize the norm. Furthermore, we will prove that this approximation has the same asymptotic decay as the original expansion, for increasing ω.

Theorem 8.1.1 *Suppose that*

$$\left\| f - \sum_{k=1}^{n} \frac{d_k}{\omega^{k+s}} \mathcal{L}_\omega[\psi_k] \right\| = \mathcal{O}\left(\omega^{-n-s}\right), \qquad \omega \to \infty, \tag{8.1.1}$$

for some coefficients d_k. Let $v_{n,\omega}^{\mathrm{LS}}(x) = \sum_{k=1}^{n} c_k \psi_k(x)$, where the coefficients c_k are chosen to minimize

$$\left\| f - \mathcal{L}_\omega\left[v_{n,\omega}^{\mathrm{LS}} \right] \right\|.$$

Then

$$\left\| f - \mathcal{L}_\omega\left[v_{n,\omega}^{\mathrm{LS}} \right] \right\| = \mathcal{O}\left(\omega^{-n-s}\right).$$

Proof: We know for $c_k = d_k/\omega^{k+s}$ that $\left\| f - \mathcal{L}_\omega\left[v_{n,\omega}^{\mathrm{LS}} \right] \right\| = \mathcal{O}\left(\omega^{-n-s}\right)$. Thus, as the error for the minimizer is less than or equal to this, the theorem follows.

<div align="right">Q.E.D.</div>

We call this method *asymptotic least squares*. In our examples,

$$f(x) = \sum_{k=1}^{n} \frac{d_k}{\omega^{k+s}} \mathcal{L}_\omega[\psi_k](x) + \mathcal{O}\left(\omega^{-n-s}\right)$$

holds true uniformly pointwise, thus (8.1.1) holds true for the L_2 norm. As n increases, we know that $\left\| f - \mathcal{L}_\omega\left[v_{n,\omega}^{\mathrm{LS}}\right] \right\|$ has no choice but to decrease, until it converges. The error of its limit must decay faster for increasing ω than any finite choice of n, as it is by necessity smaller. Hence we obtain the following corollary:

Corollary 8.1.2 *Let* $v^\star = \lim_{n\to\infty} v_{n,\omega}^{\mathrm{LS}}$. *Then* $\left\| f - \mathcal{L}_\omega[v^\star] \right\|$ *decays exponentially fast as* $\omega \to \infty$.

Minimizing the norm is accomplished by finding the minimum to the associated quadratic function

$$\left\| f - \mathcal{L}_\omega\left[v_{n,\omega}^{\mathrm{LS}}\right] \right\|^2 = \langle f, f \rangle - \sum \bar{c}_k \left(\langle f, \mathcal{L}_\omega[\psi_k] \rangle + \langle \mathcal{L}_\omega[\psi_k], f \rangle \right) + \sum c_j \bar{c}_k \langle \mathcal{L}_\omega[\psi_j], \mathcal{L}_\omega[\psi_k] \rangle$$
$$= \boldsymbol{c}^\star A \boldsymbol{c} - (\boldsymbol{b} + \bar{\boldsymbol{b}})\boldsymbol{c} + \|f\|^2,$$

where

$$A = \begin{pmatrix} \langle \mathcal{L}_\omega[\psi_1], \mathcal{L}_\omega[\psi_1] \rangle & \cdots & \langle \mathcal{L}_\omega[\psi_n], \mathcal{L}_\omega[\psi_1] \rangle \\ \vdots & \ddots & \vdots \\ \langle \mathcal{L}_\omega[\psi_1], \mathcal{L}_\omega[\psi_n] \rangle & \cdots & \langle \mathcal{L}_\omega[\psi_n], \mathcal{L}_\omega[\psi_n] \rangle \end{pmatrix} \quad \text{and} \quad \boldsymbol{b} = \begin{pmatrix} \langle f, \mathcal{L}_\omega[\psi_1] \rangle \\ \vdots \\ \langle f, \mathcal{L}_\omega[\psi_n] \rangle \end{pmatrix}.$$

(8.1.2)

It is well known that a minimum of this linear system is $\boldsymbol{c} = A^+ \boldsymbol{b}$ whenever A is positive definite, where A^+ is the pseudoinverse (which is equivalent to A^{-1} when A is nonsingular). Since A is a Gram matrix, it is positive definite whenever it is nonsingular, or equivalently whenever the basis $\{\mathcal{L}_\omega[\psi_1], \ldots, \mathcal{L}_\omega[\psi_n]\}$ is linearly independent. If the basis is linearly dependent, the minimum can still be determined by using singular value decomposition.

The fact that the approximation converges to something exponentially small is insufficient for a numerical approximation, as ω is fixed and the constant in front of the exponentially decreasing term is unknown. In our examples, however, the approximation appears to converge to the exact solution at an exponentially fast rate. The following theorem gives us a computable expression for the error in approximation:

Theorem 8.1.3 *Fix the frequency* ω. *Suppose that we can find find functions* $\{\phi_1, \ldots, \phi_n\}$ *such that* $\mathcal{L}_\omega[\psi_k] = \phi_{k+1} + \omega \phi_k$, *where* $\phi_1 = f$. *If the functions* $\{\phi_1, \ldots, \phi_{n+1}\}$ *are linearly dependent, then* $f = \mathcal{L}_\omega\left[v_{n,\omega}^{\mathrm{LS}}\right]$ *for* ω *large enough. Otherwise,*

$$\|f - \mathcal{L}_\omega[v_n]\|^2 = \frac{1}{\boldsymbol{\xi}_\omega^\star G_{n+1}^{-1} \boldsymbol{\xi}_\omega},$$

where $\star$ is the conjugate transpose, G_n is the Gram matrix associated with $\{\phi_1, \ldots, \phi_n\}$,

$$G_n = \begin{pmatrix} \langle \phi_1, \phi_1 \rangle & \cdots & \langle \phi_1, \phi_n \rangle \\ \vdots & \ddots & \vdots \\ \langle \phi_n, \phi_1 \rangle & \cdots & \langle \phi_n, \phi_n \rangle \end{pmatrix} \quad \text{and} \quad \boldsymbol{\xi}_\omega = \begin{pmatrix} 1 \\ -\omega \\ \omega^2 \\ \vdots \\ (-\omega)^n \end{pmatrix}.$$

Proof:

As a shorthand, we will write

$$\langle \boldsymbol{q} \otimes \boldsymbol{r} \rangle = \begin{pmatrix} \langle q_1, r_1 \rangle & \cdots & \langle q_n, r_1 \rangle \\ \vdots & \ddots & \vdots \\ \langle q_1, r_m \rangle & \cdots & \langle q_n, r_m \rangle \end{pmatrix} \quad \text{for} \quad \boldsymbol{q} = \begin{pmatrix} q_1 \\ \vdots \\ q_n \end{pmatrix} \quad \text{and} \quad \boldsymbol{r} = \begin{pmatrix} r_1 \\ \vdots \\ r_n \end{pmatrix}.$$

We also define

$$\boldsymbol{\psi} = \begin{pmatrix} \psi_1 \\ \vdots \\ \psi_n \end{pmatrix} \quad \text{hence} \quad \mathcal{L}_\omega[\boldsymbol{\psi}] = \begin{pmatrix} \mathcal{L}_\omega[\psi_1] \\ \vdots \\ \mathcal{L}_\omega[\psi_n] \end{pmatrix} = \begin{pmatrix} \phi_2 + \omega \phi_1 \\ \vdots \\ \phi_{n+1} + \omega \phi_n \end{pmatrix}.$$

Furthermore, let $\tilde{\boldsymbol{\phi}}_k = (\phi_1, \ldots, \phi_{k-1}, \phi_{k+1}, \ldots, \phi_{n+1})^\top$.

Assume that $\{\phi_1, \ldots, \phi_{n+1}\}$ are linearly independent, which means that the functions $\{\mathcal{L}_\omega[\psi_1], \ldots, \mathcal{L}_\omega[\psi_n]\}$ are also linearly independent, since

$$\sum_{k=1}^{n} c_k \mathcal{L}_\omega[\psi_k] = \omega c_1 \phi_1 + \sum_{k=2}^{n} (\omega c_k + c_{k-1}) \phi_k + c_n \phi_{n+1} \neq 0.$$

We can rearrange the terms in the error of the approximation, using the fact that $f - \mathcal{L}_\omega\left[v_{n,\omega}^{\mathrm{LS}}\right]$ is orthogonal to every $\mathcal{L}_\omega[\psi_k]$, hence orthogonal to $\mathcal{L}_\omega\left[v_{n,\omega}^{\mathrm{LS}}\right]$:

$$\left\| f - \mathcal{L}_\omega\left[v_{n,\omega}^{\mathrm{LS}}\right] \right\|^2 = \left\langle f - \mathcal{L}_\omega\left[v_{n,\omega}^{\mathrm{LS}}\right], f - \mathcal{L}_\omega\left[v_{n,\omega}^{\mathrm{LS}}\right] \right\rangle = \left\langle f - \mathcal{L}_\omega\left[v_{n,\omega}^{\mathrm{LS}}\right], f \right\rangle$$

$$= \|f\|^2 - \sum_{k=1}^{n} c_k \langle \phi_{k+1} + \omega \phi_k, f \rangle$$

$$= (1 - \omega c_1) \|f\|^2 - \sum_{k=2}^{n} (c_{k-1} + \omega c_k) \langle \phi_k, f \rangle - c_n \langle \phi_{n+1}, f \rangle$$

$$= -\frac{1}{\det A}\Bigg[(\omega A_1 - \det A) \|f\|^2 + \sum_{k=2}^{n} (A_{k-1} + \omega A_k) \langle \phi_k, f \rangle$$

$$+ A_n \langle \phi_{n+1}, f \rangle \Bigg], \tag{8.1.3}$$

124

where A_k is the determinant of the matrix A with the kth row replaced with $\boldsymbol{b} = \langle f, \mathcal{L}_\omega[\boldsymbol{\psi}]\rangle$, as in Cramer's rule.

We now show that the sum within the brackets of (8.1.3) is equal to $-\det G_{n+1}$. With a similar procedure to the proof of Theorem 5.3.2, the first term is

$$
\begin{aligned}
\omega A_1 - \det A &= \omega \det \langle (\phi_1, \phi_3 + \omega\phi_2, \ldots, \phi_{n+1} + \omega\phi_n) \otimes \mathcal{L}_\omega[\boldsymbol{\psi}]\rangle \\
&\quad - \det \langle (\phi_2 + \omega\phi_1, \phi_3 + \omega\phi_2, \ldots, \phi_{n+1} + \omega\phi_n) \otimes \mathcal{L}_\omega[\boldsymbol{\psi}]\rangle \\
&= -\det \langle (\phi_2, \phi_3 + \omega\phi_2, \ldots, \phi_{n+1} + \omega\phi_n) \otimes \mathcal{L}_\omega[\boldsymbol{\psi}]\rangle \\
&= -\det \langle (\phi_2, \phi_3, \ldots, \phi_{n+1}) \otimes \mathcal{L}_\omega[\boldsymbol{\psi}]\rangle \\
&= -\det \left\langle \tilde{\boldsymbol{\phi}}_1 \otimes \mathcal{L}_\omega[\boldsymbol{\psi}]\right\rangle.
\end{aligned}
$$

Similarly

$$
\begin{aligned}
A_{k-1} &+ \omega A_k \\
&= \det \langle (\mathcal{L}_\omega[\psi_1], \ldots, \mathcal{L}_\omega[\psi_{k-2}], f, \phi_{k+1} + \omega\phi_k, \mathcal{L}_\omega[\psi_{k+1}], \ldots, \mathcal{L}_\omega[\psi_n]) \otimes \mathcal{L}_\omega[\boldsymbol{\psi}]\rangle \\
&\quad + \omega \det \langle (\mathcal{L}_\omega[\psi_1], \ldots, \mathcal{L}_\omega[\psi_{k-2}], \phi_k + \omega\phi_{k-1}, f, \mathcal{L}_\omega[\psi_{k+1}], \ldots, \mathcal{L}_\omega[\psi_n]) \otimes \mathcal{L}_\omega[\boldsymbol{\psi}]\rangle \\
&= \det \langle (\phi_2, \ldots, \phi_{k-1}, f, \phi_{k+1} + \omega\phi_k, \mathcal{L}_\omega[\psi_{k+1}], \ldots, \mathcal{L}_\omega[\psi_n]) \otimes \mathcal{L}_\omega[\boldsymbol{\psi}]\rangle \\
&\quad - \det \langle (\phi_2, \ldots, \phi_{k-1}, f, \omega\phi_k, \mathcal{L}_\omega[\psi_{k+1}], \ldots, \mathcal{L}_\omega[\psi_n]) \otimes \mathcal{L}_\omega[\boldsymbol{\psi}]\rangle \\
&= \det \langle (\phi_2, \ldots, \phi_{k-1}, f, \phi_{k+1}, \phi_{k+2}, \ldots, \phi_{n+1}) \otimes \mathcal{L}_\omega[\boldsymbol{\psi}]\rangle \\
&= (-1)^k \det \langle (\phi_1, \ldots, \phi_{k-1}, \phi_{k+1}, \ldots, \phi_{n+1}) \otimes \mathcal{L}_\omega[\boldsymbol{\psi}]\rangle = (-1)^k \det \left\langle \tilde{\boldsymbol{\phi}}_k \otimes \mathcal{L}_\omega[\boldsymbol{\psi}]\right\rangle.
\end{aligned}
$$

Finally,

$$
\begin{aligned}
A_n &= \det \langle (\phi_2 + \omega\phi_1, \ldots, \phi_n + \omega\phi_{n-1}, f) \otimes \mathcal{L}_\omega[\boldsymbol{\psi}]\rangle = (-1)^n \det \langle (\phi_1, \ldots, \phi_n) \otimes \mathcal{L}_\omega[\boldsymbol{\psi}]\rangle \\
&= (-1)^n \det \left\langle \tilde{\boldsymbol{\phi}}_{n+1} \otimes \mathcal{L}_\omega[\boldsymbol{\psi}]\right\rangle.
\end{aligned}
$$

Thus it follows that the sum in the bracket of (8.1.3) is equal to

$$
\sum_{k=1}^{n+1} (-1)^k \langle \phi_k, \phi_1 \rangle \det \left\langle \tilde{\boldsymbol{\phi}}_k \otimes \mathcal{L}_\omega[\boldsymbol{\psi}]\right\rangle
$$

$$
= -\det \begin{pmatrix} \langle \phi_1, \phi_1 \rangle & \langle \phi_2, \phi_1 \rangle & \cdots & \langle \phi_{n+1}, \phi_1 \rangle \\ \langle \phi_1, \phi_2 + \omega\phi_1 \rangle & \langle \phi_2, \phi_2 + \omega\phi_1 \rangle & \cdots & \langle \phi_{n+1}, \phi_2 + \omega\phi_1 \rangle \\ \vdots & \vdots & \ddots & \vdots \\ \langle \phi_1, \phi_{n+1} + \omega\phi_n \rangle & \langle \phi_2, \phi_{n+1} + \omega\phi_n \rangle & \cdots & \langle \phi_{n+1}, \phi_{n+1} + \omega\phi_n \rangle \end{pmatrix}
$$

$$
= -\det \begin{pmatrix} \langle \phi_1, \phi_1 \rangle & \langle \phi_2, \phi_1 \rangle & \cdots & \langle \phi_{n+1}, \phi_1 \rangle \\ \langle \phi_1, \phi_2 \rangle & \langle \phi_2, \phi_2 \rangle & \cdots & \langle \phi_{n+1}, \phi_2 \rangle \\ \vdots & \vdots & \ddots & \vdots \\ \langle \phi_1, \phi_{n+1} \rangle & \langle \phi_2, \phi_{n+1} \rangle & \cdots & \langle \phi_{n+1}, \phi_{n+1} \rangle \end{pmatrix} = -\det G_{n+1},
$$

after determinant manipulations.

We next show that

$$\det A = \boldsymbol{\xi}_\omega^\star \operatorname{adj} G_{n+1} \, \boldsymbol{\xi}_\omega,$$

where $\operatorname{adj} G_{n+1}$ is the adjugate matrix of G_{n+1}:

$$\operatorname{adj} G_{n+1} = \begin{pmatrix} \det \left\langle \tilde{\boldsymbol{\phi}}_1 \otimes \tilde{\boldsymbol{\phi}}_1 \right\rangle & \cdots & \det \left\langle \tilde{\boldsymbol{\phi}}_n \otimes \tilde{\boldsymbol{\phi}}_1 \right\rangle \\ \vdots & \ddots & \vdots \\ \det \left\langle \tilde{\boldsymbol{\phi}}_1 \otimes \tilde{\boldsymbol{\phi}}_n \right\rangle & \cdots & \det \left\langle \tilde{\boldsymbol{\phi}}_n \otimes \tilde{\boldsymbol{\phi}}_n \right\rangle \end{pmatrix}.$$

Exploiting the multilinear nature of determinants, we find that

$$\det A = \det \left\langle (\phi_2 + \omega\phi_1, \cdots, \phi_{n+1} + \omega\phi_n) \otimes \mathcal{L}_\omega[\boldsymbol{\psi}] \right\rangle = \sum_{k=1}^{n+1} \omega^k \left\langle \tilde{\boldsymbol{\phi}}_k \otimes \mathcal{L}_\omega[\boldsymbol{\psi}] \right\rangle.$$

But

$$\det \left\langle \boldsymbol{u} \otimes \mathcal{L}_\omega[\boldsymbol{\psi}] \right\rangle = \det \begin{pmatrix} \left\langle \boldsymbol{u} \otimes \phi_2 + \omega\phi_1 \right\rangle \\ \vdots \\ \left\langle \boldsymbol{u} \otimes \phi_{n+1} + \omega\phi_n \right\rangle \end{pmatrix} = \sum_{k=1}^{n+1} \bar{\omega}^{k-1} \det \left\langle \boldsymbol{u} \otimes \tilde{\boldsymbol{\phi}}_k \right\rangle.$$

Thus

$$\det A = \sum_{j,k=1}^{n+1} \omega^{j-1} \bar{\omega}^{k-1} \det \left\langle \tilde{\boldsymbol{\phi}}_j \otimes \tilde{\boldsymbol{\phi}}_k \right\rangle = \boldsymbol{\xi}_\omega^\star \operatorname{adj} G_{n+1} \, \boldsymbol{\xi}_\omega.$$

Hence we have found that

$$\left\| f - \mathcal{L}_\omega \left[v_{n,\omega}^{\mathrm{LS}} \right] \right\|^2 = \frac{\det G_{n+1}}{\boldsymbol{\xi}_\omega^\star \operatorname{adj} G_{n+1} \, \boldsymbol{\xi}_\omega} = \frac{1}{\boldsymbol{\xi}_\omega^\star G_{n+1}^{-1} \boldsymbol{\xi}_\omega}.$$

We still need to handle the situation where the functions $\{\phi_1, \ldots, \phi_{n+1}\}$ are linearly dependent. If the basis $\{\mathcal{L}_\omega[\psi_1], \ldots, \mathcal{L}_\omega[\psi_n]\}$ is still linearly independent, then the error is zero since

$$\|f - \mathcal{L}_\omega[v]\|^2 = \frac{\det G_{n+1}}{\det A} = 0.$$

Thus we can assume $\{\mathcal{L}_\omega[\psi_1], \ldots, \mathcal{L}_\omega[\psi_n]\}$ are also linearly dependent. Let $j \leq n$ be the smallest integer such that $\phi_{j+1} = \sum_{k=1}^j a_k \phi_k$. Then, letting $\tilde{v} = \sum_{k=1}^j c_k \phi_k$,

$$\mathcal{L}_\omega[\tilde{v}] = \omega c_1 \phi_1 + \sum_{k=2}^j (\omega c_k + c_{k-1}) \phi_k + c_j \phi_{j+1} = (a_1 c_j + \omega c_1) \phi_1 + \sum_{k=2}^j (\omega c_k + c_{k-1} + a_k c_j) \phi_k.$$

We want to show that

$$\begin{pmatrix} \omega & & & a_1 \\ 1 & \omega & & a_2 \\ & \ddots & \ddots & \vdots \\ & & 1 & \omega + a_j \end{pmatrix} \boldsymbol{c} = \begin{pmatrix} 1 \\ 0 \\ \vdots \\ 0 \end{pmatrix}$$

126

has a solution. From the theory of companion matrices [**86**], we know that the determinant of the matrix in this equality is equal to the polynomial

$$(-\omega)^j - a_j(-\omega)^{j-1} + \cdots + a_2\omega - a_1.$$

Large ω ensures that this polynomial is nonzero.

<div align="right">Q.E.D.</div>

This theorem tells us exactly the error of approximation using only information needed in computing the approximation, except in the exceptional case where ϕ_k are linearly dependent and an unfortunate choice of ω is used. An example of a situation when this method fails is solving the differential equation

$$v' + \omega v = \mathrm{e}^{-x}$$

with $\omega = 1$. In this case $\psi_k = f^{(k)} = (-1)^k f$ for $f(x) = \mathrm{e}^{-x}$, thus

$$\mathcal{L}_\omega[\psi_k] = \psi_{k+1} + \psi_k = (-1)^k(f - f) = 0,$$

hence every choice of coefficients minimizes the norm $\left\| f - \mathcal{L}_\omega\left[v_{n,\omega}^{\mathrm{LS}}\right] \right\| = \|f\|$. In this example, the exact solution is

$$v_\omega(x) = \begin{cases} \frac{\mathrm{e}^{-x}}{\omega-1} + C\mathrm{e}^{-\omega x} & \omega \neq 1, \\ x\mathrm{e}^{-x} + C\mathrm{e}^{-x} & \text{otherwise.} \end{cases}$$

Thus $\omega = 1$ corresponds to a pole in the ω plane: the solution is continuous with respect to ω everywhere else. Thus it is not a relic of the approximation, but rather due to a fundamental property of the differential equation. Because of the nature of the problem, and the fact that even a slight perturbation of ω rectifies it, we will not dwell further on this issue. In all our examples ϕ_k are linearly independent, hence we are not affected by this problem.

8.2. Highly oscillatory integrals

In the next two sections, we will investigate how asymptotic least squares can be used in practice. In both cases, we use it to find very accurate solutions to highly oscillatory differential equations. We return to the highly oscillatory integral without stationary points

$$I[f] = \int_a^b f(x)\mathrm{e}^{\mathrm{i}\omega g(x)}\,\mathrm{d}x, \qquad g'(x) \neq 0.$$

In this section we use asymptotic least squares to find an alternate approximation which appears to converge exponentially fast to the integral in question.

In a spirit similar to the Levin collocation method and Levin-type methods, we rewrite this integral as a differential equation:

$$\mathcal{L}_\omega[v] = v' + \mathrm{i}\omega g'v = f. \tag{8.2.1}$$

As in Section 2.8, if we approximate a solution to this differential equation then we automatically obtain an approximation to the integral, because

$$\int_a^b f e^{i\omega g}\,dx \approx \int_a^b \mathcal{L}_\omega[v]\,e^{i\omega g}\,dx = \int_a^b (v e^{i\omega g})'\,dx = v(b)e^{i\omega g(b)} - v(a)e^{i\omega g(a)}.$$

Since we are using definite integration, the constant of integration is irrelevant. In other words, we do not care which particular solution to (8.2.1) is approximated, only that the residual $\mathcal{L}_\omega[v] - f$ is small. Thus we do not need to impose any boundary or initial value conditions.

Typically the asymptotic expansion for such integrals is determined by partial integration, as in Section 2.2. Instead, we wish to find an expansion not for the integral, but for the associated differential equation. The derivation of the asymptotic expansion is accomplished in a straightforward manner, the first term follows from choosing v_1^{A} so that $i\omega g' v_1^{\mathrm{A}} = f$, or in other words,

$$v_1^{\mathrm{A}} = \frac{f}{i\omega g'} \qquad \text{resulting in} \qquad \mathcal{L}_\omega\!\left[v_1^{\mathrm{A}}\right] - f = \frac{1}{i\omega}\frac{\mathrm{d}}{\mathrm{d}x}\frac{f}{g'}.$$

The next term is chosen so that this error term is cancelled:

$$v_2^{\mathrm{A}} = v_1^{\mathrm{A}} - \frac{1}{(i\omega)^2 g'}\frac{\mathrm{d}}{\mathrm{d}x}\frac{f}{g'} = \frac{f}{i\omega g'} - \frac{1}{(i\omega)^2 g'}\frac{\mathrm{d}}{\mathrm{d}x}\frac{f}{g'} \qquad \Rightarrow \qquad \mathcal{L}_\omega\!\left[v_2^{\mathrm{A}}\right] - f = -\frac{1}{(i\omega)^2}\frac{\mathrm{d}}{\mathrm{d}x}\frac{1}{g'}\frac{\mathrm{d}}{\mathrm{d}x}\frac{f}{g'}.$$

Iterating this process results in the following expansion:

Lemma 8.2.1 *Suppose that $g' \neq 0$ within $[a,b]$. Define*

$$\psi_1 = \frac{f}{g'}, \qquad \psi_{k+1} = \frac{\psi_k'}{g'}.$$

Then

$$\left\|\mathcal{L}_\omega\!\left[v_{n,\omega}^{\mathrm{A}}\right] - f\right\| = \mathcal{O}\!\left(\omega^{-n}\right) \qquad \text{for} \qquad v_{n,\omega}^{\mathrm{A}} = -\sum_{k=1}^n (-i\omega)^{-k}\psi_k.$$

Though in general the solutions to this differential equation are oscillatory, the terms in this expansion are not. This results from not imposing any boundary conditions: we are picking out a single nonoscillatory solution to the equation. The existence of such a solution was proved in [**60**], however, this fact is not needed in the proofs of this section. Thus, strictly speaking, we are not solving a highly oscillatory differential equation, but rather, we are solving the oscillatory differential equation

$$F' = f(x)e^{i\omega g(x)}$$

by removing the oscillatory component.

With an asymptotic expansion in hand, we can employ asymptotic least squares to approximate a solution to (8.2.1), and obtain the approximation

$$Q^B[f] = v_{n,\omega}^{\mathrm{LS}}(b)\mathrm{e}^{\mathrm{i}\omega g(b)} - v_{n,\omega}^{\mathrm{LS}}(a)\mathrm{e}^{\mathrm{i}\omega g(a)}.$$

This is closely related to collocation by the asymptotic basis which was presented in Section 3.3. Note that collocation is equivalent to minimizing an l_2 norm at the given collocation points. So essentially we merely replace the discrete l_2 norm with the continuous L_2 norm. Doing so has several benefits:

- We are now guaranteed to converge to something close to the solution, whereas in the l_2 case adding additional points presented the possibility of divergence. This is similar to Runge's phenomenon with polynomial interpolation, but without the wealth of knowledge known about the basis that can be used in choosing collocation points.

- As originally presented, an additional criterion known as the regularity condition was needed, requiring that the basis $\{\psi_k\}$ could interpolate at the given nodes.

There are, however, some disadvantages. The most obvious is that we need to compute nonoscillatory integrals in order to determine the inner products, whereas collocation requires significantly less computation. Furthermore, when we use collocation we can ensure that the approximant $\mathcal{L}_\omega[v]$ is equal to f at the boundary points, resulting in an order of error $\mathcal{O}(\omega^{-n-2})$ versus $\mathcal{O}(\omega^{-n-1})$.

From Theorem 8.1.1 and the fact that

$$\left|I[f] - Q^{\mathrm{LS}}[f]\right| = \left|I\left[f - \mathcal{L}_\omega\left[v_{n,\omega}^{\mathrm{LS}}\right]\right]\right| \le \sqrt{b-a}\left\|f - \mathcal{L}_\omega\left[v_{n,\omega}^{\mathrm{LS}}\right]\right\|_2 = \mathcal{O}(\omega^{-n}),$$

we know immediately that asymptotic least squares approximates the integral with an asymptotic error $\mathcal{O}(\omega^{-n})$. But the highly oscillatory component in the integral increases the asymptotic order even further:

Theorem 8.2.2 *Define*

$$Q^{\mathrm{LS}}[f] = v_{n,\omega}^{\mathrm{LS}}(b)\mathrm{e}^{\mathrm{i}\omega g(b)} - v_{n,\omega}^{\mathrm{LS}}(a)\mathrm{e}^{\mathrm{i}\omega g(a)}.$$

Then

$$I[f] - Q^{\mathrm{LS}}[f] = \mathcal{O}(\omega^{-n-1}).$$

Proof:

If $\{\mathcal{L}_\omega[\psi_1], \ldots, \mathcal{L}_\omega[\psi_n]\}$ are linear dependent, then $\{\phi_1, \ldots, \phi_{n+1}\}$ in Theorem 8.1.3 are linearly dependent, and the theorem informs us that $Q^{\mathrm{LS}}[f]$ is exact for large enough ω.
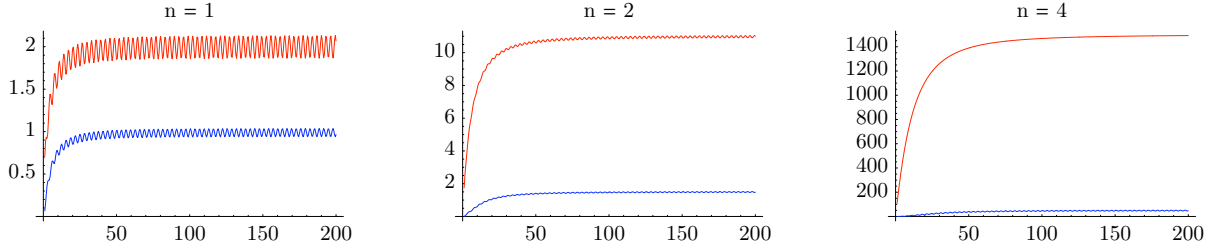
Figure 8.49: Errors in approximating $\int_0^1 \cos x \, \mathrm{e}^{\mathrm{i}\omega(x^2+x)} \, \mathrm{d}x$. The error scaled by ω^{n+1} for the n-term asymptotic expansion (top) and $Q^{\mathrm{LS}}[f]$ (bottom), for $n = 1, 2$ and 4.

Otherwise, in a similar manner to the proof of Theorem 8.1.3, we determine that

$$f - \mathcal{L}_\omega[v] = -\frac{1}{\det A} \left[(\omega A_1 - \det A)f + \sum_{k=2}^n (A_k + \omega A_{k+1})\phi_k + A_n \phi_{n+1} \right], \qquad (8.2.2)$$

where A and A_k are subject to the same definitions as in (8.1.2) and (8.1.3). We cannot combine this sum into one determinant, but each term is $\mathcal{O}(\omega^n)$. Furthermore, it is clear from Theorem 8.1.3 that $\frac{1}{\det A} = \mathcal{O}(\omega^{-2n})$. Thus we obtain $f - \mathcal{L}_\omega[v] = \mathcal{O}(\omega^{-n})$, which holds pointwise. This relationship can be differentiated: the asymptotic order is contained within the coefficients of (8.2.2). Thus the theorem is proved via integration by parts:

$$\begin{aligned}
I[f] - Q^{\mathrm{LS}}[f] &= \int_a^b (f - \mathcal{L}_\omega[v_{n,\omega}^{\mathrm{LS}}]) \mathrm{e}^{\mathrm{i}\omega g} \, \mathrm{d}x \\
&= \frac{1}{\mathrm{i}\omega} \left[\left\{ f(b) - \mathcal{L}_\omega[v_{n,\omega}^{\mathrm{LS}}](b) \right\} \mathrm{e}^{\mathrm{i}\omega g(b)} - \left\{ f(a) - \mathcal{L}_\omega[v_{n,\omega}^{\mathrm{LS}}](a) \right\} \mathrm{e}^{\mathrm{i}\omega g(a)} \right] \\
&\quad - \frac{1}{\mathrm{i}\omega} \int_a^b \left(\frac{f - \mathcal{L}_\omega[v_{n,\omega}^{\mathrm{LS}}]}{g'} \right)' \mathrm{e}^{\mathrm{i}\omega g} \, \mathrm{d}x \\
&= \mathcal{O}(\omega^{-n-1}).
\end{aligned}$$

Q.E.D.

As an example, consider the integral

$$\int_0^1 \cos x \, \mathrm{e}^{\mathrm{i}\omega(x^2+x)} \, \mathrm{d}x.$$

In Figure 8.49 we compare the error in approximating $I[f]$ by $Q^{\mathrm{LS}}[f]$ to that of the asymptotic expansion of the same order, for $n = 1$, $n = 2$ and $n = 4$. As can be seen, a dramatic increase in accuracy is obtained, with the increase becoming more significant as the asymptotic order increases.

130
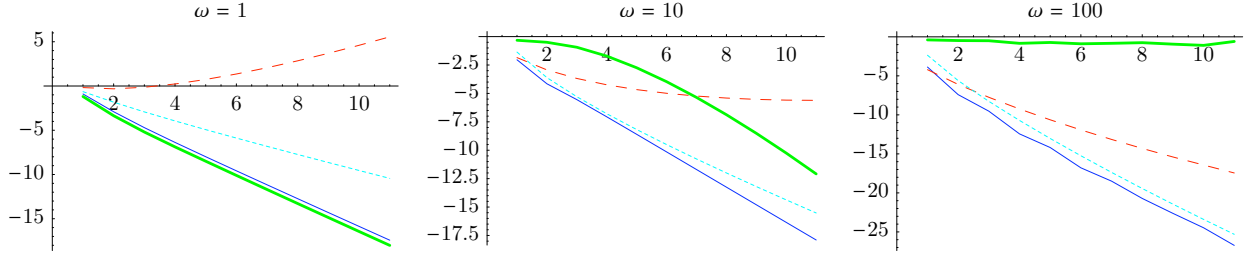
Figure 8.50: The base-10 logarithm of the errors in approximating $\int_0^1 \log(x+1)\mathrm{e}^{\mathrm{i}\omega x}\,\mathrm{d}x$, for three choices of ω. We compare $\left\| f - \mathcal{L}_\omega\left[v_{n,\omega}^{\mathrm{LS}}\right] \right\|$ (dotted line), $Q^{\mathrm{LS}}[f]$ (solid line), the n-term asymptotic expansion (dashed line) and Gauss–Legendre quadrature with n points (thick line).

Perhaps the more interesting question is how the approximation behaves as we increase n, with respect to a fixed frequency ω. Returning to an example first presented in Section 3.3, consider the intergral

$$\int_0^1 \log(x+1)\,\mathrm{e}^{\mathrm{i}\omega x}\,\mathrm{d}x.$$

In this case, the basis is equivalent to

$$\psi_1(x) = \log(x+1), \qquad \psi_k(x) = (x+1)^{-k-1},$$

and we can easily compute the inner products in closed form. In Figure 8.50, we compare asymptotic least squares with its computable bound

$$\left| I[f] - Q^{\mathrm{LS}}[f] \right| \leq \left\| f - \mathcal{L}_\omega\left[v_{n,\omega}^{\mathrm{LS}}\right] \right\| = \sqrt{\frac{1}{\boldsymbol{\xi}_\omega^\star G_{n+1}\boldsymbol{\xi}_\omega}},$$

the asymptotic expansion of the same order and the Gauss–Legendre quadrature scheme with n nodes. In the first graph, we see that even for small frequencies, the method is very powerful: we obtain machine precision accuracy by solving an 11×11 system, though the bound is noticeably less optimistic. Interestingly, the error is almost exactly the same as Gauss–Legendre quadrature. As ω increases, the bound becomes more accurate, as does the asymptotic expansion. Furthermore $Q^{\mathrm{LS}}[f]$ becomes even more efficient: when ω is 100 we obtain machine precision accuracy by solving a 5×5 system. On the other hand, Gauss–Legendre quadrature becomes less and less effective, where by $\omega = 100$ it is completely useless with ten function samplings. Of course this is an unfair comparison: if we did not know the inner products explicitly, we would have had to employ Gauss–Legendre quadrature to compute them. Hence it must be emphasized that we present the error in Gauss–Legendre quadrature as a reference, not as a valid comparison. A more appropriate comparison is presented in Section 8.4, where we compare Gauss–Legendre quadrature to the method that uses collocation.

Both the examples so far presented have had well-behaved integrands, besides the oscillations. The next example involves an integral whose amplitude suffers from Runge's
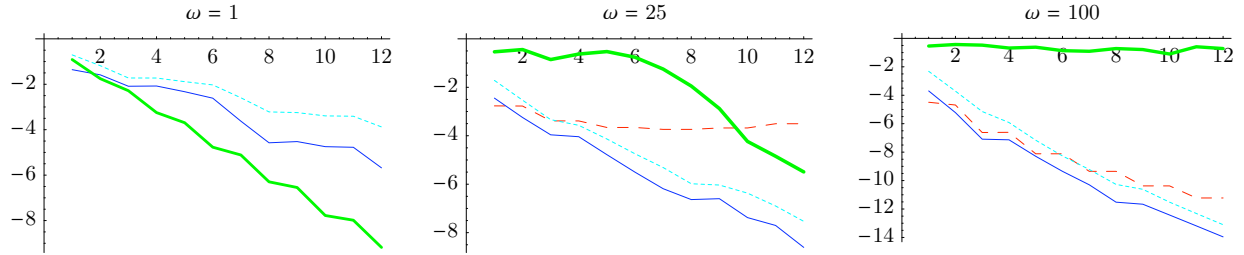
Figure 8.51: The base-10 logarithm of the errors in approximating $\int_0^1 \frac{1}{10x^2+1}e^{i\omega x}\,dx$, for three choices of ω. We compare $\left\|f - \mathcal{L}_\omega\left[v_{n,\omega}^{\mathrm{LS}}\right]\right\|$ (dotted line), $Q^{\mathrm{LS}}[f]$ (solid line) and the n-term asymptotic expansion (dashed line).
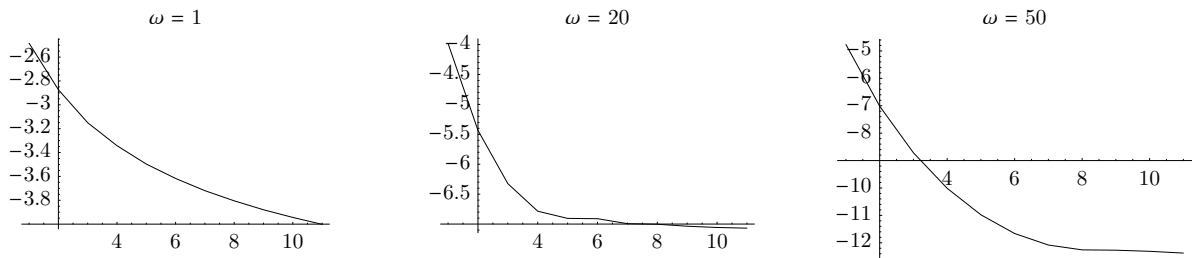
Figure 8.52: The base-10 logarithm of the error in approximating $\int_0^1 e^{-\frac{1}{x^2}+i\omega x}\,dx$, for three choices of ω.

phenomenon [82]: in particular we approximate the integral

$$\int_0^1 \frac{1}{10x^2+1}e^{i\omega x}\,dx.$$

The derivatives of f grow incredibly fast. Yet surprisingly, exponential convergence rate appears to be maintained, though the method does not converge quite as astoundingly quick as in the preceding example. This is demonstrated numerically in Figure 8.51. In the first graph we do not plot the asymptotic expansion, as ω is so small that this expansion never achieves even one digit of accuracy, and the error grows exponentially. From these graphs we can gather that the bound is off by a factor of 100, but appears to capture the behaviour of the decay of error. Furthermore, though in all of the graphs convergence appears to be exponential, increasing ω causes the convergence rate to increase drastically. Finally, it is worth noting that in one point of the last graph the asymptotic expansion is more accurate: this is since we are minimizing the norm $\left\|f - \mathcal{L}_\omega\left[v_{n,\omega}^{\mathrm{LS}}\right]\right\|$, rather than the error $\left|I[f] - Q^{\mathrm{LS}}[f]\right|$. Thus this is merely due to happenstance, rather than to any inherent property of these approximation schemes.

Both examples so far have utilized analytic functions, and seem to roughly achieve exponential convergence. In fact, many other examples not pictured also exhibit such convergent

behaviour, including the following amplitude functions with $g(x) = x$:

$$\cos 10(x^2 + x), \qquad \cos 10x^2, \qquad \mathrm{Ai}\left(3(x-1)\right),$$
$$\mathrm{Ai}\left(3(x^2-1)\right), \qquad \Gamma(x+2) \qquad \text{and} \qquad \mathrm{e}^{-x^2}.$$

On the other hand, if f is only C^r, convergence is impossible: the asymptotic basis depends on derivatives and is no longer well-defined (unless a clever construction utilizing generalized functions is possible, though retaining convergence seems highly unlikely). This leaves one other possible set of functions f that we can use this approximation method for: functions which are C^∞ but not analytic. Thus consider the integral

$$\int_0^1 \mathrm{e}^{-\frac{1}{x^2}+\mathrm{i}\omega x}\,\mathrm{d}x.$$

This has a single point where analyticity is lost: at $x = 0$. Unfortunately, it seems in Figure 8.52 that convergence to the exact solution is no longer achieved, though the asymptotic decay rate is still maintained due to Theorem 8.1.1. If we choose an integration range that does not contain 0, then exponential convergence appears to be achieved again.

8.3. Highly oscillatory ordinary differential equations

In the preceding section, we found a particular solution to a first order differential equation. In this section, we take the next step and investigate second order differential equations. In particular, we focus on the Airy-type differential equation

$$\mathcal{L}_\omega[v] = f \qquad \text{for} \qquad \mathcal{L}_\omega[v]\,(x) = v''(x) + \omega^2 q(x)v(x),$$

where we assume that $q(x) > 0$ for $a \le x \le b$. Since we are no longer focused on integration, which particular solution is approximated is important, hence we will find approximations for all of the basis functions which span the entire solution space.

As it is more in line with the method presented in the preceding section, we first consider the inhomogenous case $\mathcal{L}_\omega[v] = f$ for f not identically zero. Finding a particular solution allows us to convert the problem into a homogenous differential equation. Our first task, then, is to find an asymptotic expansion for any particular solution. Like before, the first term is determined by choosing v_1^{A} so that $\omega^2 q v_1^{\mathrm{A}} = f$, or in other words

$$v_1^{\mathrm{A}} = \frac{f}{\omega^2 q} \qquad \text{resulting in} \qquad \mathcal{L}_\omega\left[v_1^{\mathrm{A}}\right] - f = -\frac{1}{\omega^2}\left(\frac{f}{q}\right)''.$$

Iterating this procedure, in analogue to Lemma 8.2.1, we obtain the following asymptotic expansion:
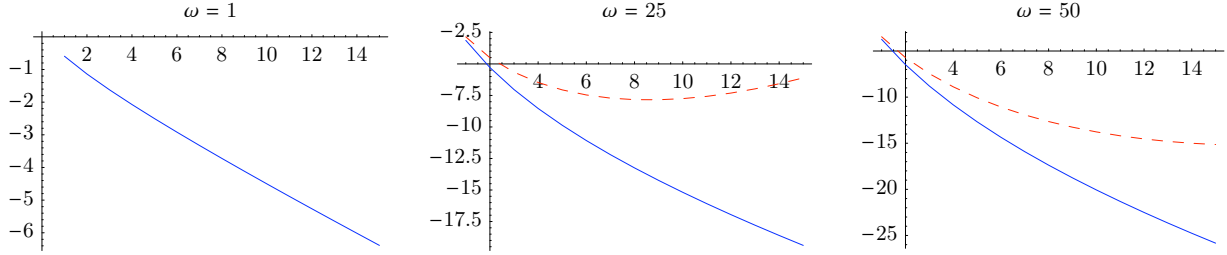
Figure 8.53: The base-10 logarithm of the error in the residual $\left\|\mathcal{L}_\omega\left[v_{n,\omega}^{\mathrm{LS}}\right] - f\right\|$ (solid line) and the residual $\left\|\mathcal{L}_\omega\left[v_{n,\omega}^{\mathrm{A}}\right] - f\right\|$ (dashed line), for $\omega = 1$, 25 and 100.

Lemma 8.3.1 *Define*

$$\psi_1 = \frac{f}{q}, \qquad \psi_{k+1} = -\frac{\psi_k''}{q} \qquad \text{and} \qquad v_{n,\omega}^{\mathrm{A}} = \sum_{k=1}^n (\omega)^{-2k} \psi_k.$$

Then

$$\left\|\mathcal{L}_\omega\left[v_{n,\omega}^{\mathrm{A}}\right] - f\right\| = \mathcal{O}\left(\omega^{-2n}\right).$$

Using the basis ψ_k in a least squares system, we obtain an approximation $v_{n,\omega}^{\mathrm{LS}}$ to some particular solution v of the differential equation. The conditions of Theorem 8.1.1 and Theorem 8.1.3 are both satisfied, thus we know, for $\phi_k(x) = q(x)\sigma_k(x)$ and replacing ω with ω^2 in the definition of $\boldsymbol{\xi}$, that

$$\left\|\mathcal{L}_\omega\left[v_{n,\omega}^{\mathrm{LS}}\right] - f\right\|^2 = \frac{1}{\boldsymbol{\xi}^\star G_{n+1}\boldsymbol{\xi}} = \mathcal{O}\left(\omega^{-4n}\right).$$

As an example, consider the inhomogenous Airy equation

$$v''(x) + \omega^2 x v(x) = 1.$$

From [**74**], we know that it has a particular solution

$$\frac{\mathrm{Wi}\left(-\omega^{2/3}x\right)}{\omega^{4/3}} \qquad \text{for} \qquad \mathrm{Wi}\left(x\right) = \pi\left[\mathrm{Bi}\left(x\right)\int_0^x \mathrm{Ai}\left(t\right)\,dt - \mathrm{Ai}\left(x\right)\int_0^x \mathrm{Bi}\left(t\right)\,dt\right].$$

However, this specific particular solution is different from the one which we will approximate: it becomes oscillatory as ω increases whereas our approximating basis is nonoscillatory. Figure 8.53 compares the error in residual of asymptotic least squares to the asymptotic expansion.

Finding particular solutions to the homogenous equation

$$\mathcal{L}_\omega[v]\left(x\right) = 0, \qquad a \leq x \leq b,$$

requires a bit more finesse; applying the previous technique without change results in finding a particular solution that satisfies the differential equation exactly, but is completely useless:

134

$v(x) \equiv 0$. Because of the form of the differential equation, WKB analysis gives us asymptotic expansions for the two independent solutions [74]. We now present a formal derivation of this asymptotic expansion, based loosely on the derivation found in [55]. The idea is to assume that the oscillations are exponential in nature with period ω, which suggests using the ansatz $v = h e^{i\omega g}$. We then obtain

$$\mathcal{L}_\omega[v] = (h'' + i\omega[2g'h' + hg''] + \omega^2 h[q - g'^2])e^{i\omega g}.$$

Cancelling out the ω^2 term involves choosing g so that $g'^2 = q$, in other words:

$$g = \pm \int q^{1/2} \, dx.$$

The choice of plus or minus determines which of the two independent solutions the expansion approximates. We obtain the alternate differential equations

$$\tilde{\mathcal{L}}_\omega^\pm[h] = 0 \qquad \text{for} \qquad \tilde{\mathcal{L}}_\omega^\pm[h] = h'' \pm i\omega(2g'h' + hg'') = h'' \pm \frac{i\omega}{2\sqrt{q}}\left[4qh' + q'h\right].$$

The $\pm$ can be subsumed into the parameter ω, meaning that $\tilde{\mathcal{L}}_\omega^\pm = \tilde{\mathcal{L}}_{\pm\omega}$. Hence we can focus on the single differential equation $\tilde{\mathcal{L}}_\omega = \tilde{\mathcal{L}}_\omega^+$, keeping in mind that ω can be either positive or negative.

To find the asymptotic expansion for this new differential equation, we begin by choosing h so that $4qh' + q'h = 0$, thus cancelling the term which grows with ω. This is equivalent to solving

$$\frac{4}{h} \, dh = -\frac{q'}{q} \, dx, \qquad \text{or in other words} \qquad \sigma_0 = h = q^{-1/4}.$$

This has an error

$$\tilde{\mathcal{L}}_\omega[\sigma_0] = \sigma_0'' = \frac{4qq'' - 3q'^2}{16q^{7/4}}.$$

To continue the derivation of the expansion, we need to find a solution to the equation

$$\frac{1}{2\sqrt{q}}\left[4qh' + q'h\right] = \sigma,$$

where σ is a general function. We can rewrite this as

$$4q\frac{dh}{dx} + q'h = 2\sqrt{q}\sigma,$$

which has a solution

$$h = q^{-1/4}\int \sigma q^{-1/4} \, dx.$$

Thus by induction we obtain the following theorem:

Theorem 8.3.2 *Define*

$$\sigma_0 = q^{-1/4}, \qquad \sigma_{k+1} = q^{-1/4} \int \sigma_k'' q^{-1/4} \, dx$$

and

$$v_{n,\omega}^{\mathrm{A}} = e^{i\omega \int q^{1/2} dx} \sum_{k=0}^{n} (-i\omega)^{-k} \sigma_k.$$

Then

$$\left\| \mathcal{L}_\omega \left[v_{n,\pm\omega}^{\mathrm{A}} \right] \right\| = \mathcal{O}\left(\omega^{-n} \right).$$

With this asymptotic expansion in hand, we can employ asymptotic least squares. Note that

$$\left\| \mathcal{L}_\omega \left[e^{\pm i\omega g} h \right] \right\| = \left\| e^{\pm i\omega g} \tilde{\mathcal{L}}_\omega^{\pm}[h] \right\| = \left\| \tilde{\mathcal{L}}_{\pm\omega}[h] \right\|,$$

hence if we minimize the norm for the residual of the alternate differential operator $\tilde{\mathcal{L}}_\omega$, we automatically do so for the original operator $\mathcal{L}$. Unfortunately, as touched on before, we can easily minimize the residual with the solution $v(x) \equiv 0$, which is not especially useful. To prevent this, we force it to approximate a nonzero particular solution by insisting that the first coefficient in the expansion is one, or in other words, we actually approximate a particular solution to the equation $\tilde{\mathcal{L}}_\omega[v] = \sigma_0''$. If $\tilde{v}_{n,\omega}^{\mathrm{LS}}$ is the approximation for the alternate differential equation, then we can define the approximation

$$v_{n,\omega}^{\mathrm{LS}} = e^{i\omega \int \sqrt{q} \, dx} \left[\sigma_0 - \tilde{v}_{n,\omega}^{\mathrm{LS}} \right]$$

The two linear independent solutions are thus $v_{n,\pm w}^{\mathrm{LS}}$. The requirements of Theorem 8.1.1 and Theorem 8.1.3 are again satisfied: in this case $\phi_k = \frac{1}{2\sqrt{q}} \left[4q\sigma_k' + q'\sigma_k \right]$.

As an example, consider the canonical case of the Airy equation; where $q(x) = x$, and we assume that $0 < a < b$. Then

$$\int q^{1/2} \, dx = \frac{2}{3} x^{\frac{3}{2}}.$$

Furthermore, it can be computed that

$$\sigma_0(x) = x^{-1/4}, \sigma_1(x) = -\frac{5}{48} x^{-7/4}, \sigma_2(x) = \frac{385}{4608} x^{-13/4}, \dots.$$

The coefficients in this expansion are immaterial as far as asymptotic least squares is concerned, thus we use the basis

$$\psi_k(x) = x^{-\frac{1}{4} - \frac{3}{2}k}.$$

Even for this simple case, computation for high frequencies is still very much an important problem. The standard computational implementation of the Airy function is to use the asymptotic expansion whenever the required precision can be achieved, while reverting to
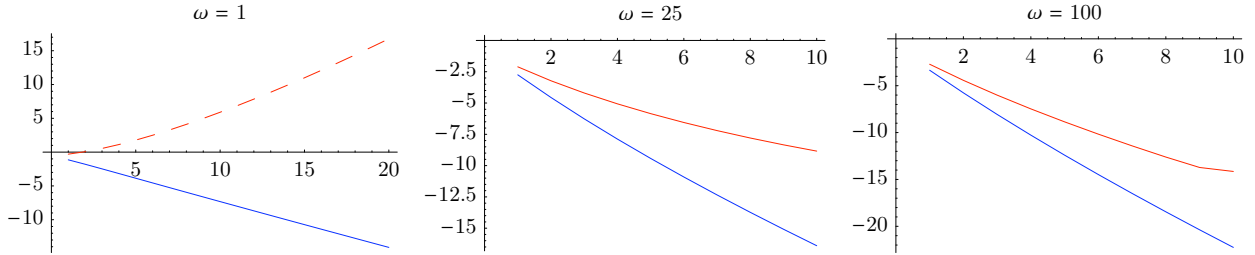
Figure 8.54: The base-10 logarithm of the residual errors $\left\|\mathcal{L}_\omega\left[v_{n,\omega}^{\text{LS}}\right]\right\|$ (bottom) and $\left\|\mathcal{L}_\omega\left[v_{n,\omega}^{\text{A}}\right]\right\|$ (top) for $\omega = 1$, 25 and 100.
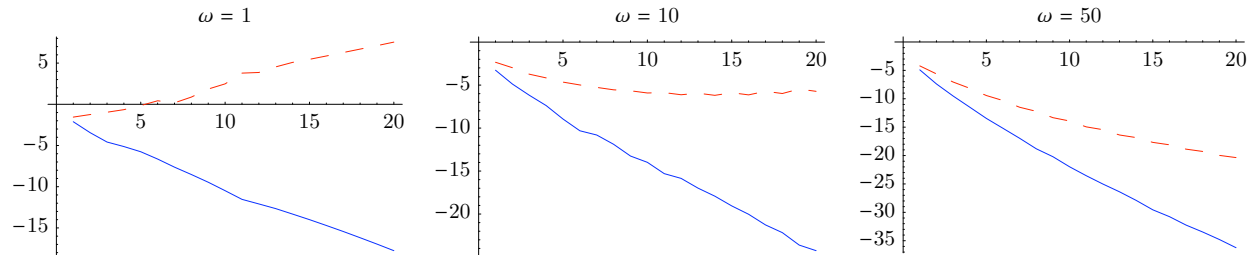
Figure 8.55: The base-10 logarithm of the error $\left\|v_{n,\omega}^{\text{LSBC}} - v\right\|_\infty$ (solid line) versus the error $\left\|v_{n,\omega}^{\text{ABC}} - v\right\|_\infty$ (dashed line) for the boundary value problem $v(1) = 1$ and $v(2) = 2$.

other computational methods—e.g., power series or Gauss–Legendre quadrature—when the precision needed is too fine for the asymptotic expansion [28]. Thus improving upon the asymptotic expansion whilst maintaining its asymptotic properties is extremely useful. This is not to suggest that no other methods exist for the asymptotic regime: indeed, [35] computes such integrals by using the path of steepest descent to transform the Airy function's integral representation into an exponential decaying integral, for which traditional quadrature methods are effective. We also derived another asymptotically accurate approximation to the Airy equation in Section 7.4.

Figure 8.54 compares the error in residual $\left\|\mathcal{L}_\omega\left[v_{n,\omega}^{\text{LS}}\right]\right\|$ to the error in residual for the n-step asymptotic expansion, for ω equal to 1, 25 and 100. The residual $\left\|\mathcal{L}_\omega\left[v_{n,\omega}^{\text{A}}\right]\right\|$ can be found exactly in terms of the inner products used in computing $v_{n,\omega}^{\text{LS}}$. As predicted, asymptotic least squares beats the asymptotic expansion in all three graphs. Indeed, for $\omega = 1$ the asymptotic expansions error steadily increases, while asymptotic least squares appears to converge exponentially fast. Increasing the frequency causes the rate of convergence to increase.

Though it is important that the residual is small, it is almost certainly more important that we approach the solution we are trying to approximate. This is where we truly diverge from the development of highly oscillatory integrals, where any particular solution was ac-
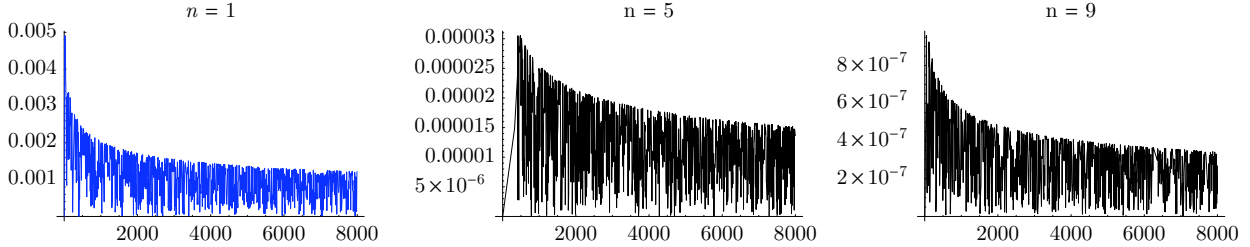
Figure 8.56: The error $\left|\text{Ai}\left(-x\right) - v_n^{\text{LSIC}}(x)\right|$ for $n = 1, 4, 9$ and $1 \leq x \leq 8000$.

ceptable. Thus we now consider the boundary value problem where $v(a) = 1$ and $v(b) = 2$. The exact solution has the form

$$v(x) = A\text{Ai}\left(-\omega^{2/3}x\right) + B\text{Bi}\left(-\omega^{2/3}x\right),$$

where Ai and Bi are Airy functions [2], and A and B are found so that v satisfies the boundary conditions. We thus approximate the solution by

$$v_{n,\omega}^{\text{LSBC}}(x) = A^{\text{BC}}v_{n,\omega}^{\text{LS}}(x) + B^{\text{BC}}v_{n,-\omega}^{\text{LS}}(x),$$

where we determine the coefficients A^{BC} and B^{BC} so that the boundary conditions are satisfied: $v_{n,\omega}^{\text{LSBC}}(1) = 1$ and $v_{n,\omega}^{\text{LSBC}}(2) = 2$. Alternatively, we could also approximate the solution with a linear combination of the asymptotic expansions, defining $v_{n,\omega}^{\text{ABC}}$ with $v_{n,\pm\omega}^{\text{A}}$ in place of $v_{n,\pm w}^{\text{LS}}$. In Figure 8.55, we compare the base-10 logarithm of the L_∞ error in approximating v by $v_{n,\omega}^{\text{LSBC}}$ and $v_{n,\omega}^{\text{ABC}}$, for three values of ω. As can be seen, the method remains very accurate for boundary value problems, and amazingly, appears to converge uniformly to the solution at an exponential rate.

Remark: We do not actually compute the L_∞ error, rather we take the maximum of the error evaluated at 40 evenly spaced points within the interval. No noticeable difference in the approximation error was seen when moving from 20 to 40 points.

The fact that the method is accurate when $\omega = 1$ suggests an interesting possibility: using the method to compute the standard Airy equation for an initial value problem, rather than a boundary value problem. To avoid the turning point, we begin at $a = 1$ and wish to minimize the norm up to $b = \infty$. We can compute the inner products needed in closed form, so there is no issue with having an unbounded interval. We approximate the solution to the initial value problem

$$v''(x) + xv(x) = 0, \qquad v(1) = \text{Ai}\left(-1\right), \qquad v'(1) = -\text{Ai}'(-1),$$

whose exact solution is simply $v(x) = \text{Ai}\left(-x\right)$. We approximate it by

$$v_n^{\text{LSIC}}(x) = A^{\text{IC}}v_{n,\omega}^{\text{LS}}(x) + B^{\text{IC}}v_{n,-\omega}^{\text{LS}}(x),$$

138

where A^{IC} and B^{IC} are now chosen so that $v_n^{\mathrm{LSIC}}(1) = \mathrm{Ai}(-1)$ and $v_n^{\mathrm{LSIC}'}(1) = -\mathrm{Ai}'(-1)$. Figure 8.56 shows the error of this method for three choices of n: $n = 1, 4$ and 9. We can infer from this figure that the error quickly reaches a maximum, and then decreases at the same rate as the solution, namely like $\mathcal{O}(x^{-1/4})$. Moreover, adding additional basis functions appears to cause this approximation to converge uniformly, over infinite time! Thus with very little computational work at all—we only needed to solve a 9×9 linear system—we have obtained an approximation to the Airy function accurate to seven digits throughout $(-\infty, -1)$. When this is increased to a 40×40 system we achieve machine precision throughout the line segment.

Alternatively to this approximation, we could have just expanded the Airy function into its known asymptotic expansion. In that case, the error in approximation would have decayed arbitrarily quickly for increasing x, however the expansion would not satisfy the initial value conditions. For other oscillatory differential equations we do not have this luxury: though we can find two linearly independent asymptotic expansions, there is no way to know which linear combination is asymptotic to the solution for any particular initial value problem.

8.4. Numerical issues

There are several issues preventing this method from reaching its full potential: the requirement to compute derivatives, computation of inner products, need for the asymptotic expansion and solving linear systems with ill conditioned matrices. In this section we explain how these issues affect the approximation, and develop some potential workarounds for the problems. Though we do study these workarounds numerically, we do not prove any theorems about their accuracy.

A very simple, yet powerful alternative to using derivatives is motivated by results from [47]. We return to the case of highly oscillatory integrals, where for simplicity we assume that we have an integral over $[0, 1]$ with the Fourier oscillator $g(x) = x$:

$$I[f] = \int_0^1 f(x)\mathrm{e}^{\mathrm{i}\omega x}\,\mathrm{d}x.$$

Filon-type methods were developed in Section 3.1, where Hermite interpolation was used with derivatives at the endpoints to obtain high order approximations. Then in Section 3.5, it was noted that a derivative could be replaced by interpolation near the endpoints. In particular, interpolating at the points $\left\{0, \frac{1}{\omega}, 1 - \frac{1}{\omega}, 1\right\}$ had the same asymptotic order as interpolating the function and its derivative at the endpoints 0 and 1. This suggests that the first two terms of our basis can be $f(x)$ and $f(x + \frac{1}{\omega})$ instead of $f(x)$ and $f'(x)$. In the framework of this chapter, we require an asymptotic expansion in terms of our basis. The first term of such an expansion is determined in exactly the same manner as in Section 8.2, namely $\frac{f(x)}{\mathrm{i}\omega}$, so that $\mathcal{L}_\omega[v] = f(x) + \mathcal{O}(\omega^{-1})$. We now wish to cancel out the remainder term
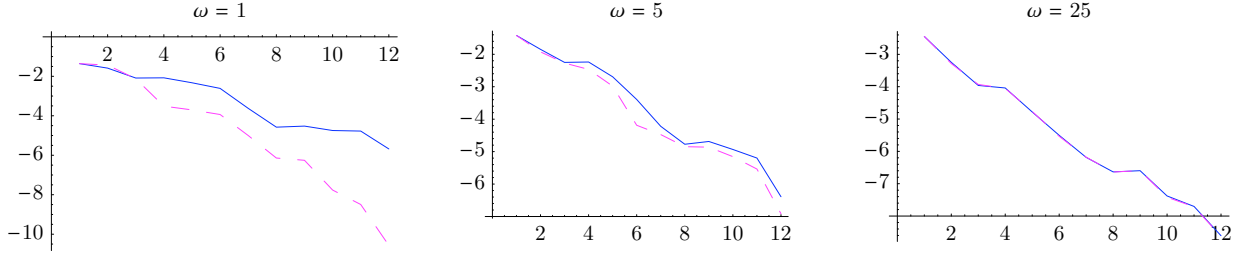
Figure 8.57: The base-10 logarithm of the errors in approximating $\int_0^1 \frac{1}{10x^2+1}e^{i\omega x}\,dx$, for three choices of ω. We compare $Q^{LS}[f]$ (solid line) to the finite difference basis (dotted line).

$\frac{f'(x)}{i\omega}$ with finite differences, which can be accomplished with the basis element $\frac{f(x+\frac{1}{\omega})-f(x)}{\omega}$. Thus we obtain

$$\mathcal{L}_\omega\left[\frac{f(x)}{i\omega}+\frac{f(x+\frac{1}{\omega})-f(x)}{\omega}\right]=f(x)+\frac{f'(x)-\omega\left[f(x+\frac{1}{\omega})-f(x)\right]}{i\omega}+\frac{f'(x+\frac{1}{\omega})-f'(x)}{\omega}$$

$$=f(x)+\mathcal{O}\left(\omega^{-2}\right).$$

This derivation can be extended, suggesting the basis

$$f(x),f\left(x+\frac{1}{\omega}\right),f\left(x-\frac{1}{\omega}\right),f\left(x+\frac{1}{2\omega}\right),\ldots,f\left(x\pm\frac{1}{k\omega}\right),\ldots.$$

This basis is of course numerically unsuitable—the basis becomes almost linearly dependent as ω and k increase, which leads to very ill-conditioned matrices—but the basis can be altered, say by using finite differences or by applying the Gram–Schmidt procedure. We also require the first derivative $f'(x\pm\frac{1}{k\omega})$, as we seed the functions in this basis into the operator $\mathcal{L}_\omega[v]=v'+i\omega v$. Finally, though the derivatives of f do in fact lie in the closed span of the basis, it is unclear whether the rate of decay is maintained. Figure 8.57 suggests it is, where we employ this basis for the Runge example $f(x)=\frac{1}{10x^2+1}$, with three choices of ω. Unexpectedly, the finite difference basis outperforms the asymptotic basis for low frequencies, though asymptotically they are equivalent. Whether the accuracy at low frequencies is an inherent property of the finite difference basis or simply due to the choice of f requires further investigation.

As touched on briefly in Section 8.2, numerical difficulties in the computation of inner products might be alleviated by replacing a least squares system with a collocation system. This means that we determine the coefficients in $v_{n,\omega}^C(x)=\sum_{k=1}^n c_k\psi_k(x)$ by solving the system

$$\mathcal{L}_\omega\left[v_{n,\omega}^C\right](x_1)=f(x_1),\ldots,\mathcal{L}_\omega\left[v_{n,\omega}^C\right](x_n)=f(x_n).$$
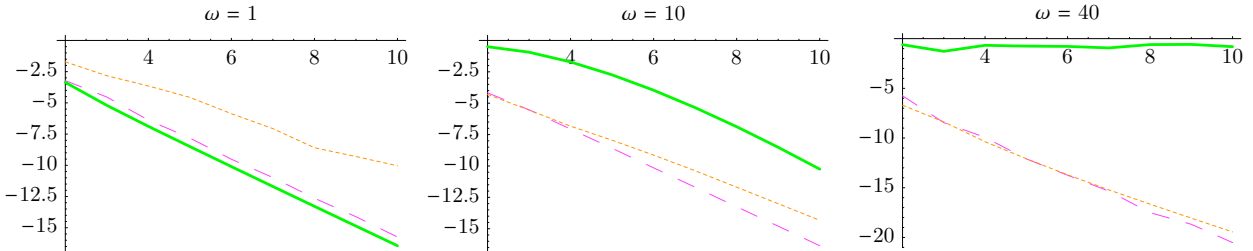
Figure 8.58: The base-10 logarithm of the errors in approximating $\int_0^1 \log(x+1)e^{i\omega x}\,dx$ for three choices of ω. We compare asymptotic least squares with finite difference basis (dashed line), collocation with finite difference basis (dotted line) and n-point Gauss–Legendre quadrature (thick line).

For oscillatory integrals, we obtain the approximation

$$Q^B[f] = v_{n,\omega}^{\mathrm{C}}(b)e^{i\omega g(b)} - v_{n,\omega}^{\mathrm{C}}(a)e^{i\omega g(a)}.$$

This is equivalent to the construction in Section 3.3, which also proved that as long as the basis ψ_k can interpolate at the given collocation points and the endpoints of the interval are included as collocation points, we obtain the asymptotic order

$$I[f] - Q^B[f] \sim \mathcal{O}\!\left(\omega^{-n-2}\right).$$

In this section we do not include the constant function in the collocation basis. Figure 3.10 and Table 3.1 suggest that the exponential convergence rate is retained, however this conjecture is not proved. If we are able to prove the convergence rate for the asymptotic least squares—say, via Theorem 8.1.3—then we may have the tools needed in order to prove the convergence rate for $Q^B[f]$, *à la* the proof of convergence when interpolating at Chebyshev points.

We can also combine collocation with the finite difference basis, as seen in Figure 8.58. For the collocation method in this graph we use Lobatto quadrature points. There is no particular reason known to use such collocation points, other than we want to include the endpoints and Lobatto points seem to result in more accurate results than evenly spaced points. This is the first figure in which the comparison with Gauss–Legendre quadrature is almost fair: the number of sample points is exactly the same for each quadrature scheme, however, the collocation method requires the value of f' at the collocation points in addition to the value of f. Though for low frequencies Gauss–Legendre quadrature beats the new methods presented, it quickly loses its lustre. Not pictured are the other two methods we have discussed in this chapter: the original asymptotic least squares and collocation with the asymptotic basis. Interestingly, both of these methods have almost the same error as their finite difference counterparts. This picture also suggests that all these asymptotic methods are roughly equivalent as the frequency increases, thus when the frequency is large, it probably makes the most sense to use collocation with a finite difference basis.

As for the requirement of the terms in an asymptotic expansion, the need for it may indeed be a red-herring. Consider all the figures in which we took $\omega = 1$. In this case we still seem to achieve exponential convergence, despite the fact that the asymptotic expansion has no meaning whatsoever for this fixed choice of ω. This suggests that the more fundamental property used is the form of Theorem 8.1.3; the fact that the basis is also an asymptotic expansion is only relevant in the asymptotic regime. If this is indeed the case, a possible approximation scheme to any nonsingular vector-valued differential equation

$$\boldsymbol{y}' + A\boldsymbol{y} = \boldsymbol{f}$$

would be a least squares approximation with the basis $\boldsymbol{\psi}_1 = A^{-1}\boldsymbol{f}$, $\boldsymbol{\psi}_{k+1} = A^{-1}\boldsymbol{\psi}'_k$. This is in fact the asymptotic basis presented in Section 6.5. Whether this method can compete with traditional ODE methods in the nonoscillatory regime is doubtful.

In all the examples presented so far, we have used significantly more digits than specified by IEEE arithmetic. This has partly been necessitated by our use of less than optimal bases: in many of our examples the derivatives grow extraordinarily quickly, hence the norm of the basis elements also grows. In addition, the finite difference basis becomes closer to being singular as ω and k increase. These factors can be negated by normalizing the basis or reordering the terms. Even with these tricks, there is a limit to the accuracy of the methods; with machine precision accuracy, the error for the examples presented levels off at approximately ten digits of accuracy. Ten digits is usually more than any application actually needs [12], however it should be investigated why we achieve ten digits rather than, say, 15 digits or five digits.

A least squares system typically leads to a badly conditioned matrix: even with moderate values of n, the eigenvalues of such systems can easily be less than machine precision. This results in a system, though analytically positive definite, numerically behaving as if it were only positive semidefinite. Since we only need to solve very small systems to achieve high accuracy approximation methods—the largest matrix in this entire chapter is 12×12—this problem is tractable, and the built-in linear solvers of modern mathematical packages (e.g., MAPLE, MATHEMATICA and MATLAB) should easily be able to circumvent this issue.

8.5. Future work

When deriving an asymptotic expansion throughout the complex plane, different sectors require different asymptotic bases. In choosing which terms of the expansion are included, one must take into account Stokes' phenomenon, where exponentially small remainder terms contribute significantly to the error of expansion [10]. This suggest an intriguing possibility: unlike an asymptotic expansion, a least squares system has no choice but to improve when additional basis elements are added. Thus it might be possible to achieve an approximation that is valid throughout the complex plane by including the bases from the asymptotic expansion in all sectors, and this should automatically remain valid across Stokes' lines.

For the differential equations in Section 8.3, an alternate accurate approximation scheme exists based on highly oscillatory integrals, using the modified Magnus expansion [**44**]. In this method the differential equation is modified, then the Magnus expansion is used to write the solution to it as the matrix exponential of a sum of oscillatory integrals. An in depth comparison between the method presented in this chapter and modified Magnus expansion, discussed briefly in Section 1.1, would be interesting. These two methods are very similar in character: both translate the problem into a numerical quadrature problem. However the modified Magnus expansion depends also on multivariate integration and time-stepping. At the same time, it does not require the terms in the asymptotic expansion.

Finally, there is the question of whether it is possible to generalize this method for partial differential equations and integral equations. The most obvious example is that of the Helmholtz equation

$$\nabla^2 v + \omega^2 v = 0,$$

whose solution can become oscillatory as $|\omega| \to \infty$. In the theorems of Section 8.1, the fact that $\mathcal{L}_\omega[v]$ was an ODE was not used: the univariate structure was hidden in the inner product and norm. Thus given the asymptotics to a PDE, we could immediately approximate the value of a particular solution using the method presented in this chapter. Indeed, numerical results suggest that this can be used with great effectiveness for finding a particular solution to an inhomogenous Helmholtz equation. But it is no longer true that finitely many linearly independent solutions span the solution space, hence boundary conditions can not be so easily disregarded. One might be tempted to find a set of particular solutions, which then are used to approximately satisfy the boundary conditions, say with another least squares system. However in general the solutions to such a PDE will be oscillatory along the boundary—$v(\boldsymbol{x}) = \mathrm{e}^{\mathrm{i}\omega\boldsymbol{\kappa}\cdot\boldsymbol{x}}$ is a particular solution whenever $\boldsymbol{\kappa}$ is a unit vector—thus if the boundary conditions are not oscillatory, this idea is impractical.

Closing Remarks

Several methods exist for approximating highly oscillatory integrals efficiently, where the accuracy improves as the frequency of oscillations increases. When moments are available, we can use a Filon-type method, whilst a Levin-type method uses collocation to provide an approximation whenever there are no stationary points. Moment-free Filon-type methods were developed for oscillatory integrals whose moments are not available, including integrals with stationary points. Both Filon-type and Levin-type methods can be generalized to multivariate integrals, though there are issues with stationary points and resonance points. We can also generalize Levin-type methods to handle oscillatory integrals over unbounded domains, and integrals with an infinite amount of oscillation. Finally, we developed a method which achieves the same asymptotic order as an asymptotic expansion, whilst appearing to converge exponentially fast. In short, a large number of highly oscillatory integrals can be approximated by at least one of the methods discussed in this thesis.

Related to the research of this dissertation is function approximation using the modified Fourier series found in [**51**]. As mentioned in Section 1.4, with a slight modification of the standard Fourier series, we obtain an orthogonal series that can approximate nonperiodic functions efficiently. The coefficients of the resulting series are oscillatory integrals, hence they can be approximated quickly using the methods we have developed. This results in an accurate function approximation scheme. This series' use in spectral methods is being investigated by Ben Adcock [**4**].

Another area of research is applying the techniques presented in this thesis to the numerical computation of highly oscillatory differential equations. We have already seen the usefulness of our methods for linear ordinary differential equations where WKB expansions are known. Another extremely important example is the time-dependent Schrödinger equations. Magnus expansion techniques have been used recently to approximate such equations with numerical success [**37**]. Whether the integrals in such an expansion can be approximated with acceptable asymptotic behaviour remains to be seen. The applications of numerically efficient methods for approximating such equations are wide and numerous.

An aspect of Filon-type methods which has not been emphasized enough is the fact that they maintain accuracy relative to the integral as ω moves throughout the complex plane. Thus, with stark contrast to standard asymptotic theory, we do not need to change the approximation for different sectors of the complex plane. Perhaps Moment-free Filon-type methods can be developed that maintain this property, which could be utilized to determine uniform approximations to special functions. This idea was used in Section 7.4 for negative real values of the Airy function, but many more difficulties are present for complex arguments.

In this case, a complex contour must be used, which must pass through stationary points to avoid areas of exponential increase. The location of such points depends on the argument of the Airy function. Efficient approximations for other special functions are desperately needed, especially hypergeometric functions.

Another possible application is integration of nonoscillatory functions over moderately large dimensional domains. This is a difficult problem, as either the number of sample points required grows exponentially with the dimension, or Monte Carlo or quasi-Monte Carlo methods must be used, which still require a significant number of sample points. On the other hand, using only sample points at the vertices of the domain, we obtain very accurate results for multivariate oscillatory integrals. The number of vertices of a d-dimensional simplex is $d + 1$, which only grows linearly with the dimension. Thus we can accurately integrate oscillatory integrals over simplices without sampling the integrand at exponentially many points, though unfortunately the amount of work needed for Levin-type methods or to compute moments still grows exponentially with the dimension. The work required is still feasible at moderate sized dimensions, say $d = 3, 4$ or 5. It might be possible to apply some of the ideas for oscillatory quadrature to nonoscillatory quadrature, at the very least when the integrand has a known form.

There are most likely myriad other applications for oscillatory integrals. Highly oscillatory waves are omnipresent in physics, which often are integrated in the approximation of differential equations and integral equations. We have already briefly mentioned acoustics and oscillatory Schrödinger equations. Moreover, we have used oscillatory quadrature to approximate the Airy function, which itself originated in an optical physical problem. Conventional wisdom is that oscillatory quadrature is difficult, and making people aware that this is simply untrue is important.

References

[1] Ablowitz, M.J. and Fokas, A.S., *Complex Variables: Introduction and Applications*, Cambridge University Press, Cambridge, 2003.

[2] Abramowitz, M. and Stegun, I., *Handbook of Mathematical Functions*, National Bureau of Standards Appl. Math. Series, #55, U.S. Govt. Printing Office, Washington, D.C., 1970.

[3] Adam, G.H. and Nobile, A., Product integration rules at Clenshaw–Curtis and related points: a robust implementation, *IMA J. Numer. Anal.* **11** (1991), 271–296.

[4] Adcock, B., Spectral methods and modified Fourier series, preprint, DAMTP Tech. Rep. NA2007/08, University of Cambridge, 2007.

[5] Alaylioglu, A., Evans, G.A. and Hyslop, J., The use of Chebyshev series for the evaluation of oscillatory integrals, *Comput. J.* vol. **19** no. **3** (1976), 258–267.

[6] Averbuch, A., Braverman, E., Coifman, R., Israeli, M. and Sidi, A., Efficient computation of oscillatory integrals via adaptive multiscale Local Fourier Bases, *Applied and Computational Harmonic Analysis* **9** (2000), 19–53.

[7] Averbuch, A., Braverman, E., Israeli, M. and Coifman, R. , On efficient computation of multidimensional oscillatory integrals with local Fourier bases, *Nonlinear Analysis* vol. **47** no. **5** (2001), 3491–3502.

[8] Bakhvalov, N.S. and Vasil'eva, L.G., Evaluation of the integrals of oscillating functions by interpolation at nodes of Gaussian quadratures, *USSR Comput. Math. Math. Phys.* **8** (1968), 241–249.

[9] Bateman, H., *Higher Transcendental Functions*, McGraw-Hill, New York, 1953.

[10] Berry, M. V., Asymptotics, superasymptotics, hyperasymptotics, *in*: *Asymptotics beyond all orders*, ed: H Segur and S Tanveer, Plenum, New York 1991, 1–14.

[11] Bleistein, N. and Handelsman, R.,*Asymptotic expansions of integrals*, Holt, Rinehart and Winston, New York, 1975.

[12] Bornemann, F.A., *The SIAM 100-Digit Challenge: A Study in High-Accuracy Numerical Computing*, SIAM, 2004.

[13] Brezinski, C. and Redivo Zaglia, M., *Extrapolation Methods: Theory and Practice*, North-Holland, Amsterdam, 1991.

[14] Bruno, O. P., Fast, high-order, high-frequency integral methods for computational acoustics and electromagnetics, *in*: *Topics in computational wave propagation: direct and inverse problems. Lecture Notes in Computational Science and Engineering no. 31*, Springer 2003, 43–82.

[15] Bruno, O. P., Geuzaine, C.A., Monro, J.A. and Reitich, F., Prescibed error tolerances within fixed computational times for scattering problems of arbitrarily high frequency: the convex case, *Phil. Trans. R. Soc. Lond. A.* vol. **362** no. **1816** (2004), 629–645.

[16] Cheney, W. and Light, W., *A Course in Approximation Theory*, Brooks/Cole Publishing Company, Pacific Grove, CA, 2000.

[17] Chrysos, M., An extension of the Filon method for the accurate numerical integration of rapidly varying functions, *J. Phys. B: At. Mol. Opt. Phys.* **28** (1995), 373–377.

[18] Chung, K. C., Evans, G. A. and Webster, J. R., A method to generate generalized quadrature rules for oscillatory integrals, *Appl. Numer. Maths* **34** (2000), 85–93.

[19] Clendenin, W.W., A method for numerical calculation of Fourier integrals, *Numer. Math.* **8** (1966), 422–436. .

[20] Cody, W. J., *An Overview of Software Development*, Lecture Notes in Mathematics, 506, Numerical Analysis, Dundee G.A. Watson (ed.), Springer-Verlag, Berlin, 1976.

[21] Davis, P.J. and Rabinowitz, P., *Methods of Numerical Integration, Second Edition*, Academic Press, Orlando, 1984.

[22] Evans, G.A., An alternative method for irregular oscillatory integrals over a finite range, *Int. J. Comput. Math.* **53** (1994), 185–193.

[23] Evans, G.A., An expansion method for irregular oscillatory integrals, *Int. J. Comput. Math.* **63** (1997), 137–148.

[24] Evans, G. A. and Chung, K. C., Some theoretical aspects of generalised quadrature methods, *J. Complexity* **19** (2003), 272–285.

[25] Evans, G. A. and Chung, K. C., Evaluating infinite range oscillatory integrals using generalised quadrature methods, *Appl. Numer. Maths* **57** (2007), 73–79.

[26] Evans, G.A. and Webster, J.R., A high order progressive method for the evaluation of irregular oscillatory integrals, *Appl. Num. Maths* **23** (1997), 205–218.

[27] Evans, G.A. and Webster, J.R., A comparison of some methods for the evaluation of highly oscillatory integrals, *J. Comp. Appl. Maths* **112** (1999), 55–69.

[**28**] Fabijonas, B.R., Lozier, D.W. and Olver, F.W.J., Computation of complex Airy functions and their zeros using asymptotics and the differential equation, *ACM Trans. on Math. Soft.* vol. **30** no. **4** (2004), 471–490.

[**29**] Filon, L.N.G., On a quadrature formula for trigonometric integrals, *Proc. Roy. Soc. Edinburgh* **49** (1928), 38–47.

[**30**] Flinn, E.A., A modification of Filon's method of numerical integration, *J. ACM* vol. **9** no. **2** (1960), 181–184.

[**31**] Forrey, R.C., Computing the hypergeometric function, *Journal of Computational Physics* **137** (1997), 79–100.

[**32**] Gasper, G. and Rahman, M., *Basic Hypergeometric Series*, Cambridge University Press, Cambridge, 1990.

[**33**] Gil, A., Segura, J. and Temme, N.M., On non-oscillating integrals for computing inhomogeneous Airy functions, *Math. Comput.* vol. **70** no. **235** (2001), 1183–1194.

[**34**] Gil, A., Segura, J. and Temme, N.M., Computing complex Airy functions by numerical quadrature, *Numer. Algorithms* **30** (2002), 11–23.

[**35**] Gil, A., Segura, J. and Temme, N.M., Computing special functions by using quadrature rules, *Numer. Algorithms* **33** (2003), 265–275.

[**36**] Golub, G.H. and Welsch, J.H., Calculation of Gauss Quadrature Rules, *Maths Comp.* vol. **23** no. **106** (1969), 221–230.

[**37**] Hochbruck, M. and Lubich, C., On Magnus integrators for time-dependent Schrödinger equations, *SIAM J. Num. Anal.* vol. **41** no. **3** (2003), 954–963.

[**38**] Huybrechs, D., *Multiscale and Hybrid Methods for the Solution of Oscillatory Integral Equations*, Ph.D. Thesis, Katholieke Universiteit Leuven, Faculteit Ingenieurswetenschappen Arenbergkasteel, B-3001 Leuven, Belgium, 2006.

[**39**] Huybrechs, D. and Vandewalle, S., The efficient evaluation of highly oscillatory integrals in BEM by analytic continuation, *in: Proceedings of the 5th UK Conference on Boundary Integral Methods (Chen, K., ed.)*, Liverpool University Press, Liverpool, 2005, 20–31.

[**40**] Huybrechs, D. and Vandewalle, S., On the evaluation of highly oscillatory integrals by analytic continuation, *SIAM J. Num. Anal.* vol. **44** no. **3** (2006), 1026–1048.

[**41**] Huybrechs, D. and Vandewalle, S., The construction of cubature rules for multivariate highly oscillatory integrals, *Math. Comp.* vol. **76** no. **260** (2007), 1955–1980.

[42] Huybrechs, D. and Vandewalle, S., A sparse discretisation for integral equation formulations of high frequency scattering problems, *SIAM J. Sci. Comput.* vol. **29** no. **6** (2007), 2305–2328.

[43] Iserles, A., On the global error of discretization methods for highly-oscillatory ordinary differential equations, *BIT* **42** (2002), 561–599.

[44] Iserles, A., On the numerical quadrature of highly-oscillatory integrals I: Fourier transforms, *IMA J. Num. Anal.* **24** (2004), 1110–1123.

[45] Iserles, A., On the numerical quadrature of highly-oscillatory integrals II: Irregular oscillators, *IMA J. Num. Anal.* **25** (2005), 25–44.

[46] Iserles, A., On the numerical analysis of high oscillation, *in*: *Group Theory and Numerical Analysis*, CRM Proceedings 39 (2005) 149–163.

[47] Iserles, A. and Nørsett, S.P., On quadrature methods for highly oscillatory integrals and their implementation, *BIT* **44** (2004), 755–772.

[48] Iserles, A. and Nørsett, S.P., Efficient quadrature of highly oscillatory integrals using derivatives, *Proceedings Royal Soc. A.* **461** (2005), 1383–1399.

[49] Iserles, A. and Nørsett, S.P., Quadrature methods for multivariate highly oscillatory integrals using derivatives, *Maths Comp.* **75** (2006), 1233–1258.

[50] Iserles, A. and Nørsett, S.P., On the computation of highly oscillatory multivariate integrals with critical points, *BIT*, to appear.

[51] Iserles, A. and Nørsett, S.P., From high oscillation to rapid approximation I: Modified Fourier expansions, preprint, DAMTP Tech. Rep. NA2006/05, University of Cambridge, 2006.

[52] Iserles, A. and Nørsett, S.P., From high oscillation to rapid approximation II: Expansions in polyharmonic eigenfunctions, preprint, DAMTP Tech. Rep. NA2006/07, University of Cambridge, 2006.

[53] Iserles, A. and Nørsett, S.P., From high oscillation to rapid approximation III: Multivariate expansions, preprint, DAMTP Tech. Rep. NA2007/01, University of Cambridge, 2007.

[54] Jeffery, G.B., Louis Napoleon George Filon. 1875–1937, *Obituary Notices of Fellows of the Royal Society* vol. **2** no. **7** (1939), 500–509.

[55] Jeffreys, H. and Jeffreys, B.S., *Methods of Mathematical Physics*, 3rd ed. Cambridge University Press, London and New York, 1956.

[56] Kim, K. J., Cools, R. and Ixaru, L. G., Quadrature rules using first derivatives for oscillatory integrands, *J. Comput. Appl. Maths* **140** (2002), 479–497.

[57] Kim, K. J., Cools, R. and Ixaru, L. G., Extended quadrature rules for oscillatory integrands, *Appl. Numer. Maths* **46** (2003), 59–73.

[58] Kopal, Z., *Numerical Analysis: With Emphasis on the Application of Numerical Techniques to Problems of Infinitesimal Calculus in Single Variable*, Chapman & Hall, London, 1955.

[59] Krein, M. G., On a special class of differential operators, *Doklady AN USSR* **2** (1935), 345–349.

[60] Levin, D., Procedures for computing one and two-dimensional integrals of functions with rapid irregular oscillations, *Math. Comp.* **38** (1982), no. 158 531–538.

[61] Levin, D., Fast integration of rapidly oscillatory functions, *J. Comput. Appl. Maths* **67** (1996), 95–101.

[62] Levin, D., Analysis of a collocation method for integrating rapidly oscillatory functions, *J. Comput. Appl. Maths* **78** (1997), 131–138.

[63] Littlewood, R.K. and Zakian, V., Numerical evaluation of Fourier integrals, *J. Inst. Math. Appl.* **18** (1976), 331–339.

[64] Longman, I.M., Note on a method for computing infinite integrals of oscillatory functions, *Proc. Cambridge Phil. Soc.* **52** (1956), 764.

[65] Longman, I.M., Tables for the rapid and accurate numerical evaluation of certain infinite integrals involving Bessel functions, *MTAC* **11** (1957), 166.

[66] Longman, I.M., A method for numerical evaluation of finite integrals of oscillatory functions, *Maths Comp.* vol. **14** no. **69** (1960), 53–59.

[67] Lozier, D.W. and Olver, F.W.J., Numerical evaluation of special functions, *in: AMS Proceedings of Symposia in Applied Mathematics*, ed: W. Gautschi, 1994, 79–125.

[68] Luke, Y.L., On the computation of oscillatory integrals, *Proc. Cambridge Phil. Soc* **50** (1954), 269–277.

[69] Magnus, W., On the exponential solution of differential equations for a linear operator, *Comm. Pure and Appl. Math* **VII** (1954), 649–673.

[70] Melnik, K. N. and Melnik, R. V. N., Optimal-by-order quadrature formulae for fast oscillatory functions with inaccurately given a priori information, *J. Comp. Appl. Maths* **110** (1999), 45–72.

[71] Melnik, K. N. and Melnik, R. V. N., Optimal cubature furmulæ and recovery of fast-oscillating functions from an interpolational class, *BIT* vol. **41** no. **4** (2001), 748–775.

[72] Melnik, K. N. and Melnik, R. V. N., Optimal-by-accuracy and optimal-by-order cubature formulæin interpolational classes, *J. Comput. Appl. Maths* **147**(2002), 233–262.

[73] Muller, K.E., Computing the confluent hypergeometric function, $M(a, b, x)$, *Numer. Math.* **90** (2001), 179–196.

[74] Olver, F.W.J., *Asymptotics and Special Functions*, Academic Press, New York, 1974.

[75] Olver, S., Moment-free numerical integration of highly oscillatory functions, *IMA J. Num. Anal.* **26** (2006), 213–227.

[76] Olver, S., On the quadrature of multivariate highly oscillatory integrals over non-polytope domains, *Numer. Math.* **103** (2006), 643–665.

[77] Olver, S., Numerical approximation of vector-valued highly oscillatory integrals, *BIT* **47** (2007), 637–655.

[78] Olver, S., Moment-free numerical approximation of highly oscillatory integrals with stationary points, *Euro. J. Appl. Maths* **18** (2007), 435–447.

[79] Olver, S., On the convergence rate of a modified Fourier series, preprint, Report no. NA2007/02, DAMTP, University of Cambridge, 2007.

[80] Patterson, T.N.L., On high precision methods for the evaluation of Fourier integrals with finite and infinite limits, *Numer. Math.* **24** (1976), 41–52.

[81] Piessens, R., Gaussian quadrature formulas for the integration of oscillating functions, *ZAMM* **50** (1970), 698–700.

[82] Powell, M.J.D., *Approximation Theory and Methods*, Cambridge University Press, Cambridge, 1981.

[83] Sauter, T., Computation of irregularly oscillating integrals, *Appl. Num. Maths* **35** (2000), 245–264.

[84] Sidi, A., A user-friendly extrapolation method for oscillatory infinite integrals, *Math. Comp.* vol. **51** no. **183** (1988), 249–266.

[85] Stein, E., *Harmonic Analysis: Real-Variable Methods, Orthogonality, and Oscillatory Integrals*, Princeton University Press, Princeton, NJ, 1993.

[86] Trefethen, L.N. and Bau III, D., *Numerical Linear Algebra*, SIAM, 1997, p. 191–192.

[87] Tukey, J.W., *On Numerical Approximation*, Ed. R. E. Langer, Madison, 1959, p. 400.

[**88**] van der Laan, C.G. and Temme, N. M., *Calculation of Special Functions: The Gamma Function, the Exponential Integrals and Error-Like Functions*, CWI Tract, Vol. 10, Stichting Mathematisch Centrum, Centrum voor Wiskunde en Informatica 1984.

[**89**] Wong, R., *Asymptotic Approximations of Integrals*, Academic Press, New York, 1989.

[**90**] Xiang, S., Numerical analysis of a fast integration method for highly oscillatory functions, *BIT* vol. **47** no. **2** (2007), 469–482.

[**91**] Xiang, S., Efficient Filon-type methods for $\int_a^b f(x)\mathrm{e}^{\mathrm{i}\omega g(x)}\,\mathrm{d}x$, *Numer. Math.* vol. **205** no. **4** (2007), 633–658.

[**92**] Zamfirescu, I., An extension of Gauss's method for calculation of improper integrals, *Acad. R.P. Romine Stud. Cerc. Mat* **14** (1963), 615–631.

[**93**] Zotsenko, K. and Melnik, R., Optimal minimax algorithm for integrating fast oscillatory functions in two dimensions, *Engineering Computations: Int. J. Computer-Aided Engineering* vol. **21** no. **8** (2004), 834–847.

Index